

Copyright 2019 Jet Propulsion Laboratory, California Institute of Technology. U.S. Government sponsorship acknowledged.

# Geophysical investigation of minor bodies Vesta and Ceres using gravity and shape data

Jet Propulsion Laboratory  
Post-doc seminar  
15 July 2019

A. I. Ermakov<sup>1</sup> ([anton.ermakov@jpl.nasa.gov](mailto:anton.ermakov@jpl.nasa.gov)), R. S. Park<sup>1</sup>, C. A. Raymond<sup>1</sup>, M. T. Zuber<sup>2</sup>,  
C. T. Russell<sup>3</sup>, R. R. Fu<sup>4</sup>

<sup>1</sup>Jet Propulsion Laboratory, California Institute of Technology

<sup>2</sup>Department of the Earth, Atmospheric and Planetary Sciences, Massachusetts Institute of Technology

<sup>3</sup>University of California Los Angeles

<sup>4</sup>Department of Earth and Planetary Sciences, Harvard University.





# Outline

- **Why do we need to study remnant planetesimals (a.k.a planetary embryos a.k.a protoplanets)?**
- **How do we study them?**
- **Dawn at Vesta**
- **Dawn at Ceres**
- **Future data**



# Outline

- **Why do we need to study remnant planetesimals (a.k.a planetary embryos a.k.a protoplanets)?**
- **How do we study them?**
- **Dawn at Vesta**
- **Dawn at Ceres**
- **Future data**

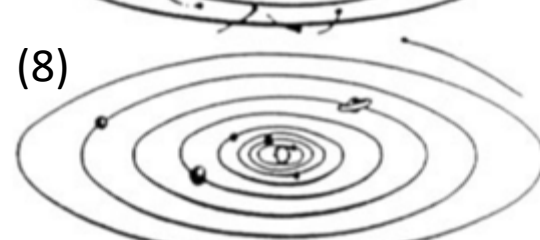
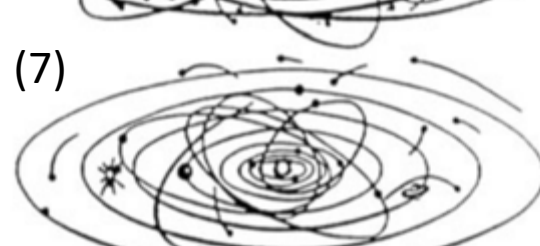
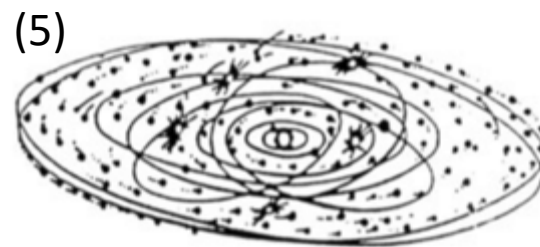
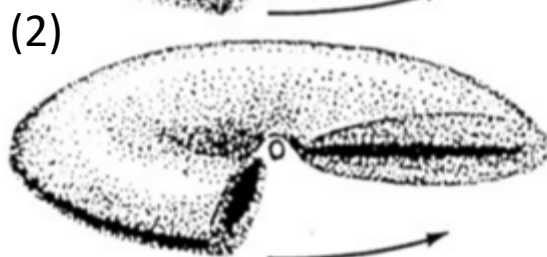


# Outline

- **Why do we need to study remnant planetesimals (a.k.a planetary embryos a.k.a protoplanets)?**
- **How do we study them?**
- **Dawn at Vesta**
- **Dawn at Ceres**
- **Future data**

# Planet formation

- ① Formation of a nebula disk
- ② Settling to mid-plane
- ③ Dust coagulation
- ④ Orderly growth
- ⑤ Run-away growth
- ⑥ Gas dispersal
- ⑦ Late-state mergers
- ⑧ Present state

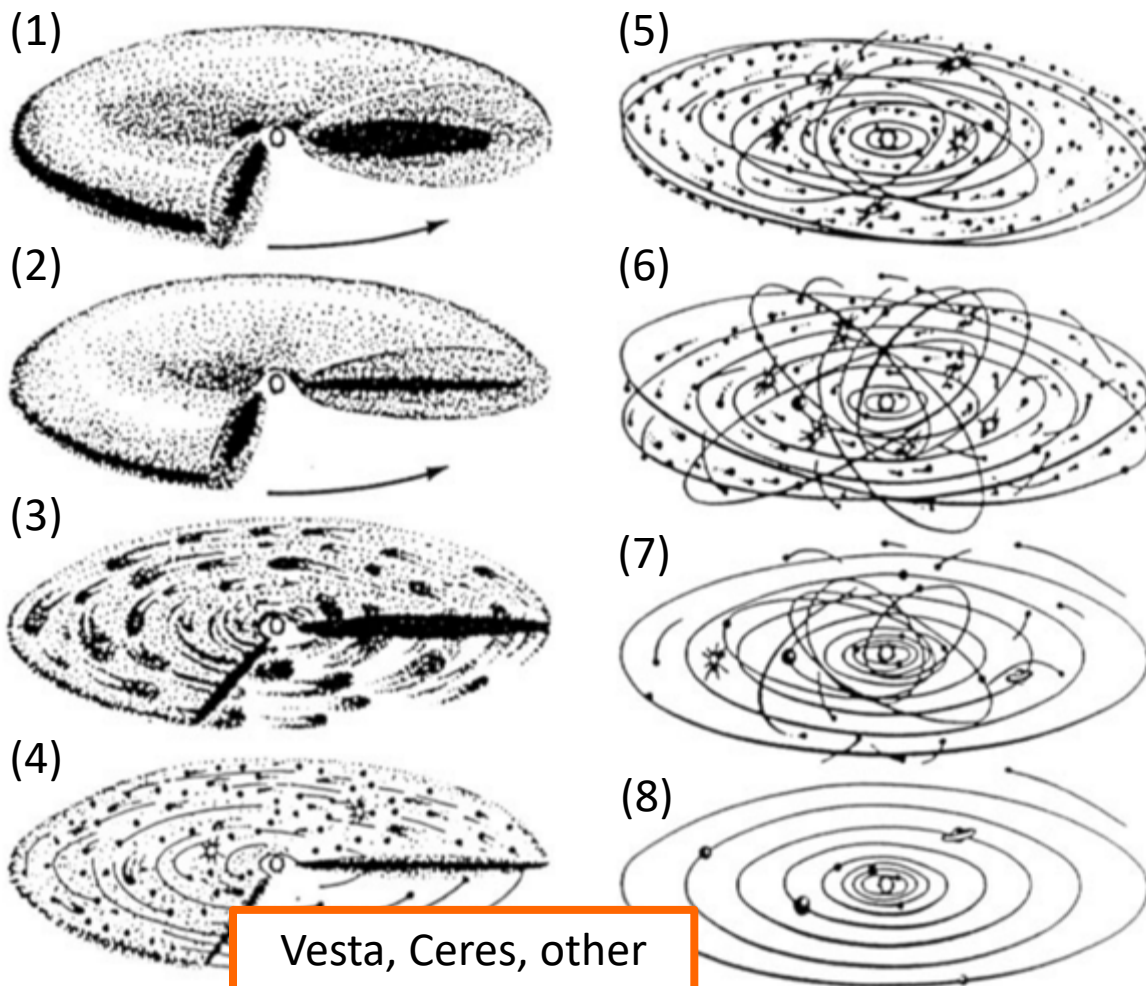


Safronov & Ruskol 1994

JPL post-doc seminar

# Planet formation

- ① Formation of a nebula disk
- ② Settling to mid-plane
- ③ Dust coagulation
- ④ Orderly growth
- ⑤ Run-away growth
- ⑥ Gas dispersal
- ⑦ Late-state mergers
- ⑧ Present state

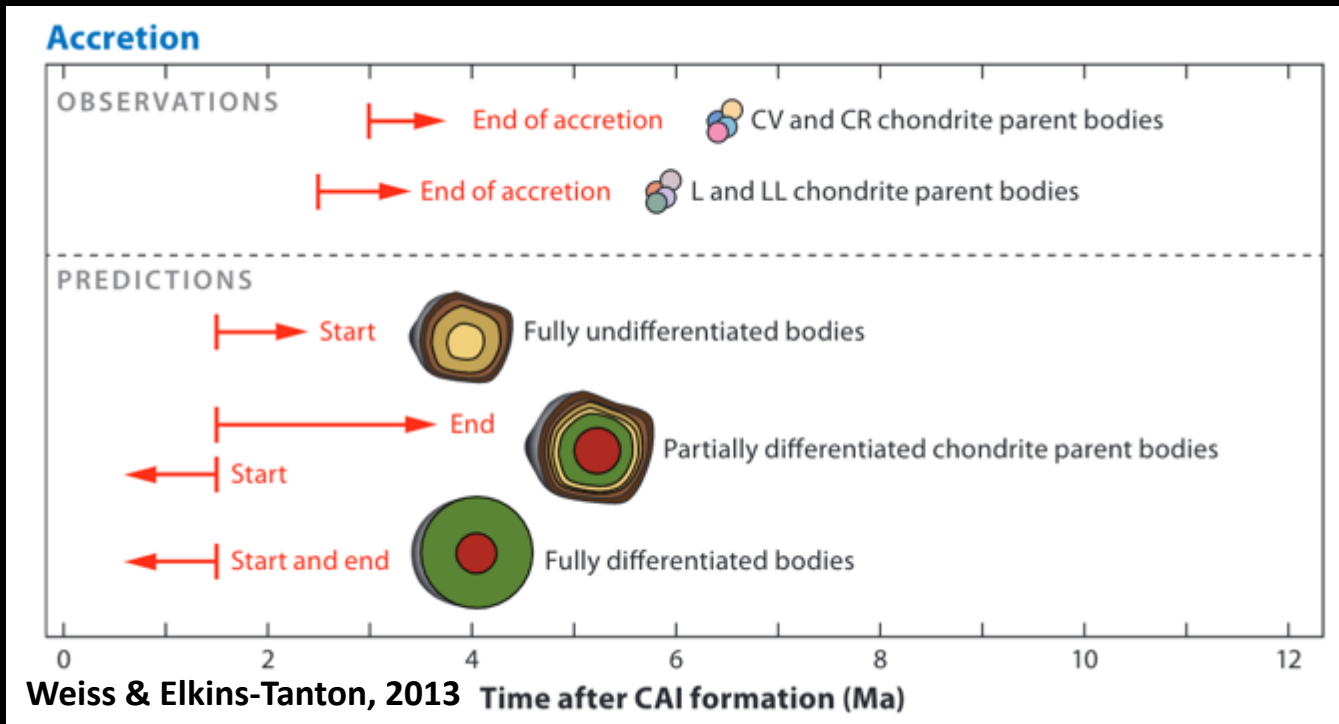


Vesta, Ceres, other  
big asteroids

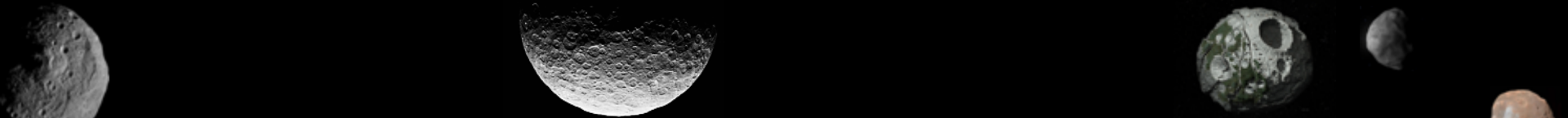
Safronov & Ruskol 1994

JPL post-doc seminar

# A spectrum of protoplanet internal structure

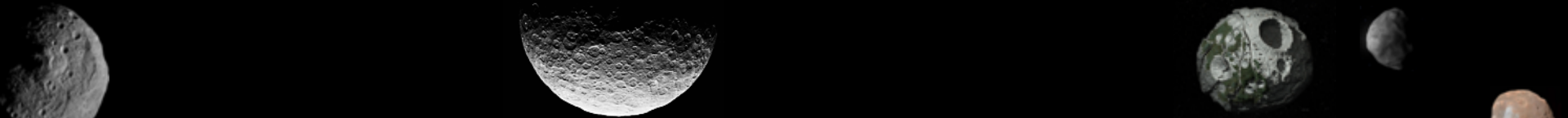


- What was the differentiation state of planetesimals?
  - Differentiated or undifferentiated?
  - How much water?
- What can interior structure tell us about the accretion process?
  - Fast or slow
  - Early or late



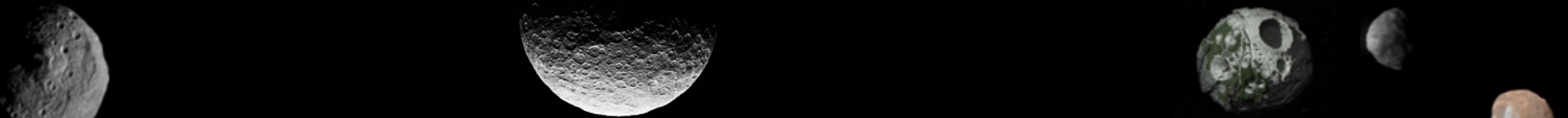
# How do we study a planetary interior with gravity and topography?

- **We study the interior but looking at its response to various forcings such as:**
  - **Rotation**
  - **Tides**
  - **Surface loads**
  - **Subsurface loads**



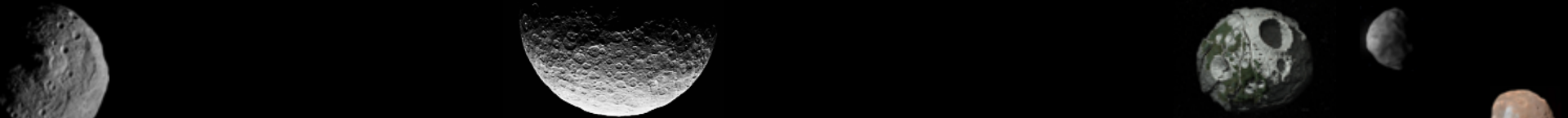
## Hydrostatic equilibrium

- **In hydrostatic equilibrium**
  - Surfaces of constant density, pressure and potential coincide
  - No shear stresses



# Hydrostatic equilibrium

➤ **In** hydrostatic equilibrium



# Hydrostatic equilibrium

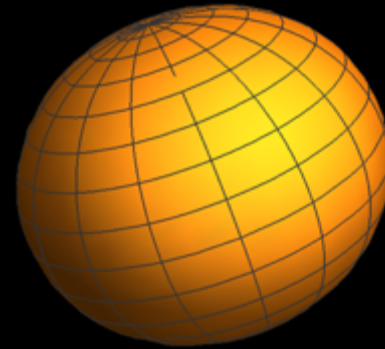
➤ In hydrostatic equilibrium

$$\rho = \rho(r), \omega$$

# Hydrostatic equilibrium

➤ In hydrostatic equilibrium

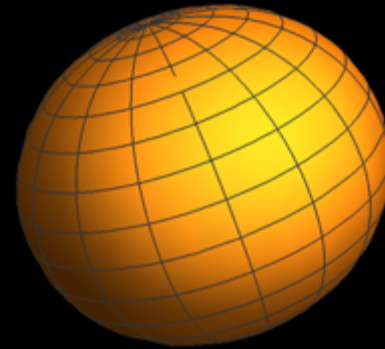
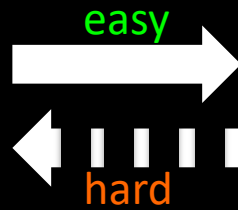
$$\rho = \rho(r), \omega$$



# Hydrostatic equilibrium

➤ In hydrostatic equilibrium

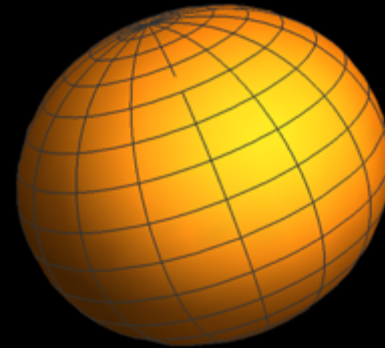
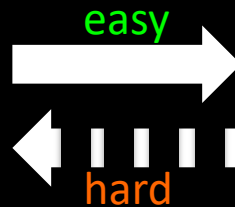
$$\rho = \rho(r), \omega$$



# Hydrostatic equilibrium

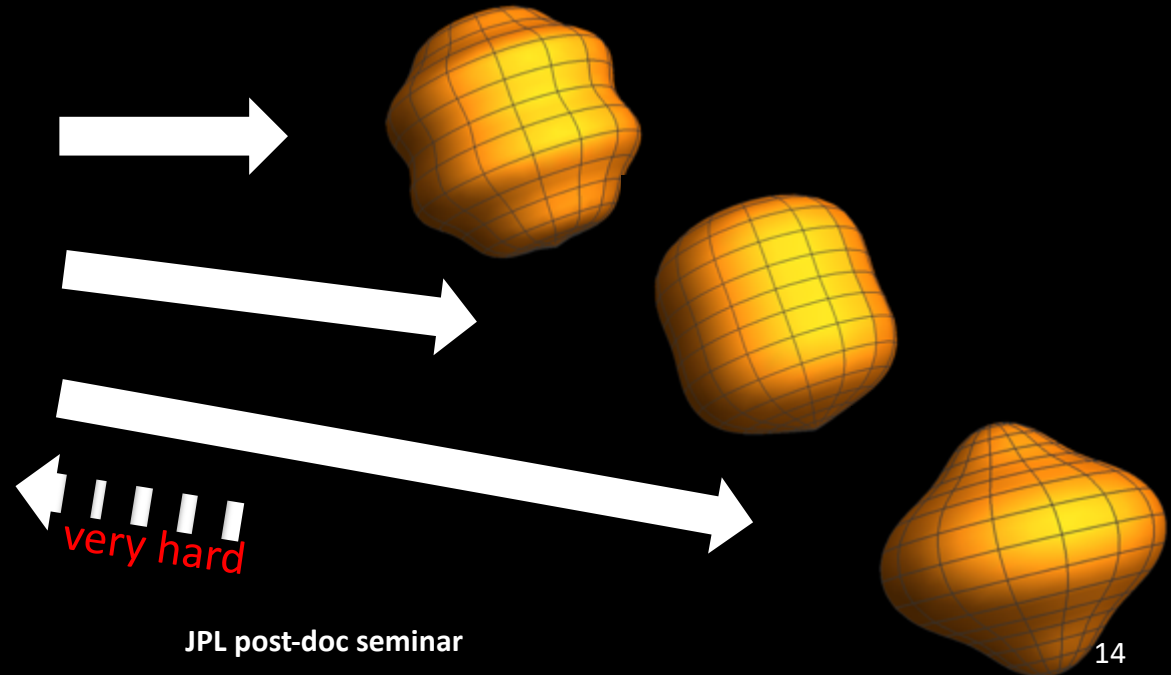
➤ **In** hydrostatic equilibrium

$$\rho = \rho(r), \omega$$



➤ **Not in** hydrostatic equilibrium

$$\rho = \rho(r), \omega$$



# Spherical Harmonics

## ➤ Shape

$$r(\phi, \lambda) = R_0 \sum_{n=0}^{\infty} \sum_{m=-n}^n A_{nm} Y_{nm}(\phi, \lambda)$$

## ➤ Gravitational potential

$$U(r, \phi, \lambda) = \frac{GM}{r} \sum_{n=0}^{\infty} \sum_{m=-n}^n \left( \frac{R_0}{r} \right)^n C_{nm} Y_{nm}(\phi, \lambda)$$

**$U$**  – gravitational potential

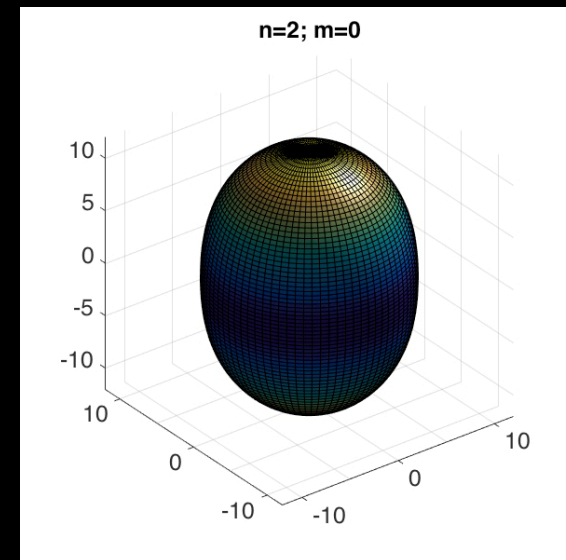
**$\phi$**  – latitude

**$\lambda$**  – longitude

**$r$**  – radial distance

**$n$**  – degree

**$m$**  – order



# Spherical Harmonics

## ➤ Shape

$$r(\phi, \lambda) = R_0 \sum_{n=0}^{\infty} \sum_{m=-n}^n A_{nm} Y_{nm}(\phi, \lambda)$$

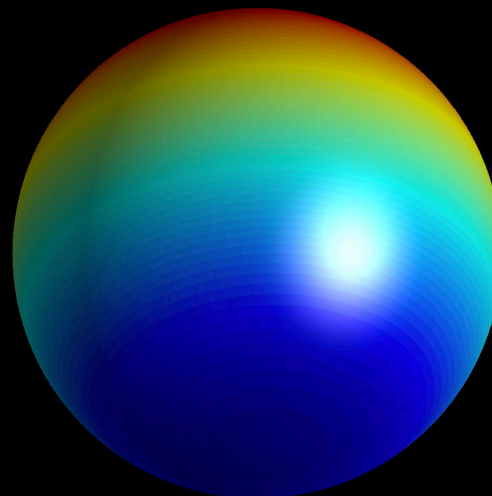
## ➤ Gravitational potential

$$U(r, \phi, \lambda) = \frac{GM}{r} \sum_{n=0}^{\infty} \sum_{m=-n}^n \left( \frac{R_0}{r} \right)^n C_{nm} Y_{nm}(\phi, \lambda)$$

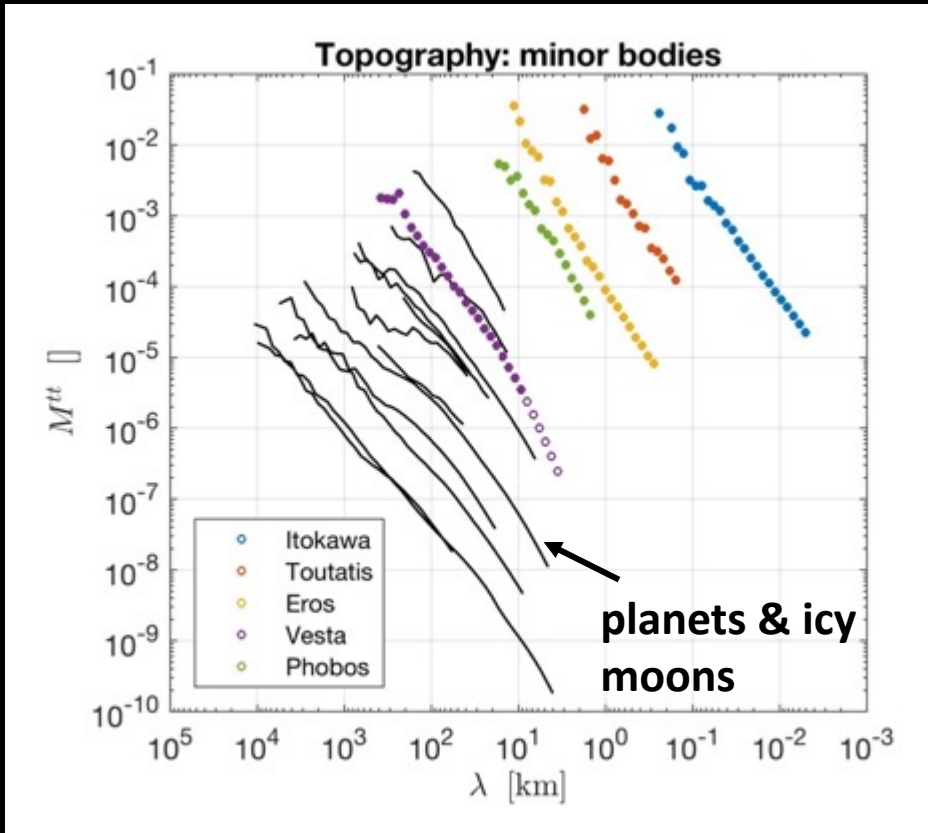
## ➤ RMS spectrum

$$M_n^{gg} = \sqrt{\frac{\sum_{m=-n}^n C_{nm}^2}{2n+1}} \quad \text{gravity}$$

$$M_n^{tt} = \sqrt{\frac{\sum_{m=-n}^n A_{nm}^2}{2n+1}} \quad \text{topography}$$



# Topography power spectrum and Kaula rule



Ermakov et al., 2018a

$$\Delta\sigma = \rho_{crust} g h \quad \text{Stress perturbation due to topography } h$$

$$h = \frac{\Delta\sigma_{max}}{\rho_{crust} g}$$

$$M^{tt} \propto \frac{h}{R} \quad \text{Topography power spectrum}$$

$$M^{tt} \propto \Delta\sigma_{max} \rho_{crust}^{-1} \bar{\rho}^{-1} R^{-2}$$

$$M^{tt} \propto \Delta\sigma_{max} \bar{\rho}^{-2} R^{-2} \lambda^{\alpha}$$

Kaula rule



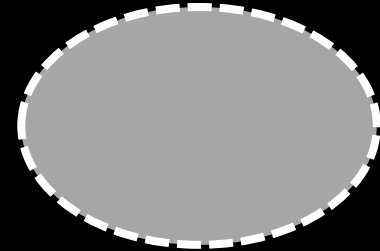
# Gravity anomalies

- Free-air anomaly

$$\sigma_{\text{FA}} = \sigma_{\text{obs}} - \sigma_{\text{model}}$$

$$\sigma_{\text{model}} =$$

gravity of  
hydrostatic figure

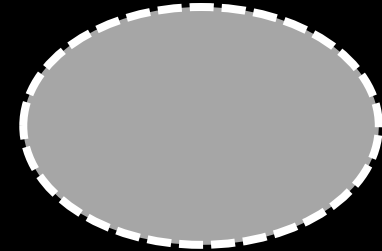


# Gravity anomalies

- Free-air anomaly

$$\sigma_{\text{FA}} = \sigma_{\text{obs}} - \sigma_{\text{model}}$$

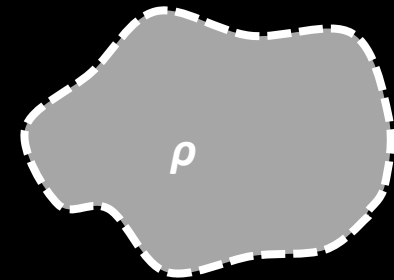
$\sigma_{\text{model}} =$  gravity of hydrostatic figure



- Bouguer anomaly

$$\sigma_{\text{BA}} = \sigma_{\text{obs}} - \sigma_{\text{model}}$$

$\sigma_{\text{model}} =$  gravity of shape assuming  $\rho$

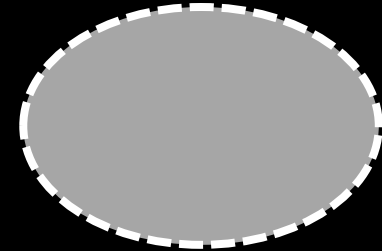


# Gravity anomalies

- Free-air anomaly

$$\sigma_{FA} = \sigma_{obs} - \sigma_{model}$$

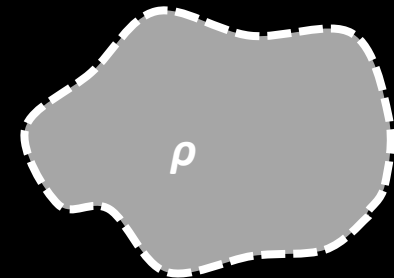
$\sigma_{model} =$  gravity of hydrostatic figure



- Bouguer anomaly

$$\sigma_{BA} = \sigma_{obs} - \sigma_{model}$$

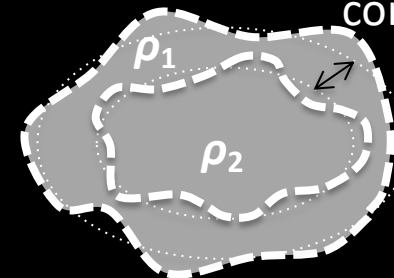
$\sigma_{model} =$  gravity of shape assuming  $\rho$



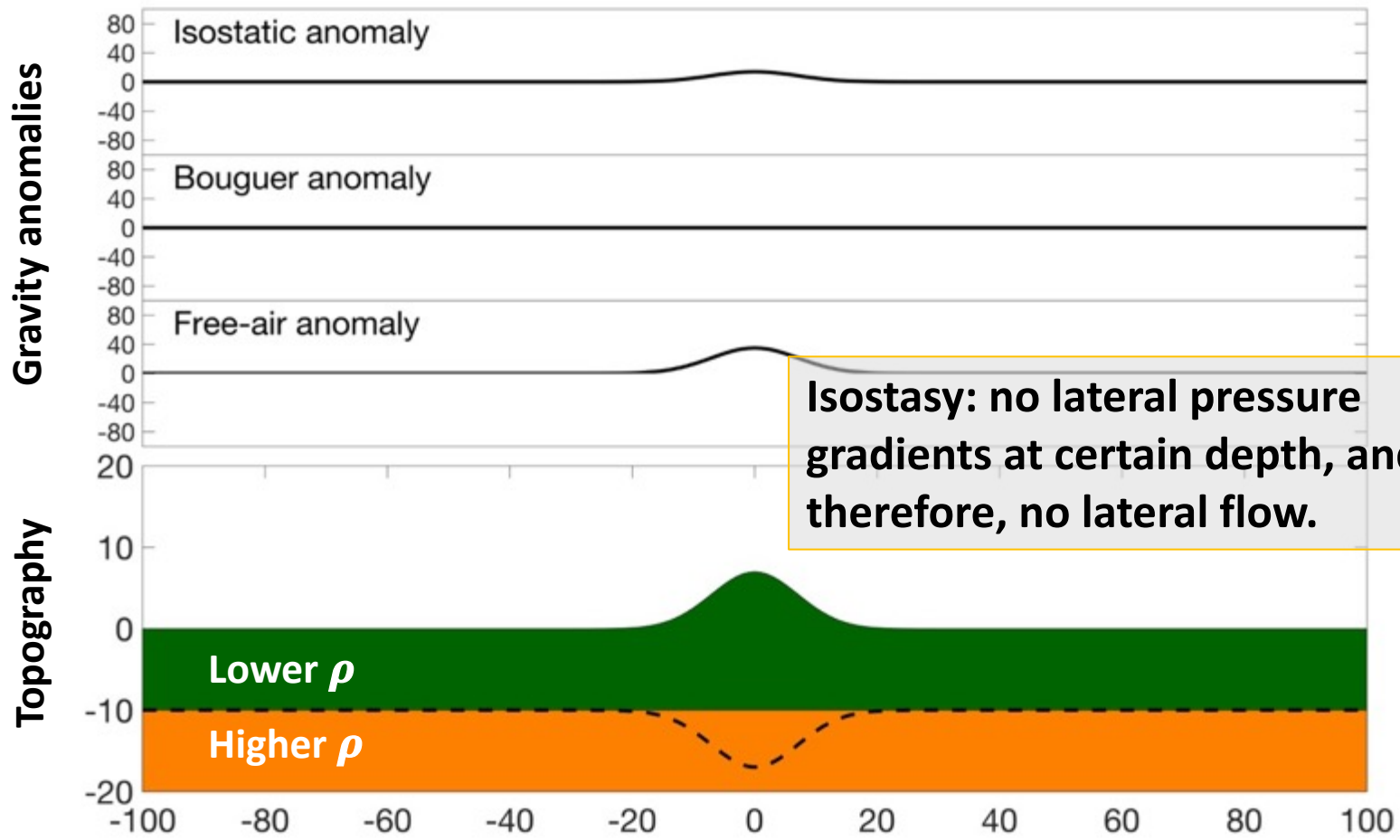
- Isostatic anomaly

$$\sigma_{IA} = \sigma_{obs} - \sigma_{model} \quad h - \text{depth of compensation}$$

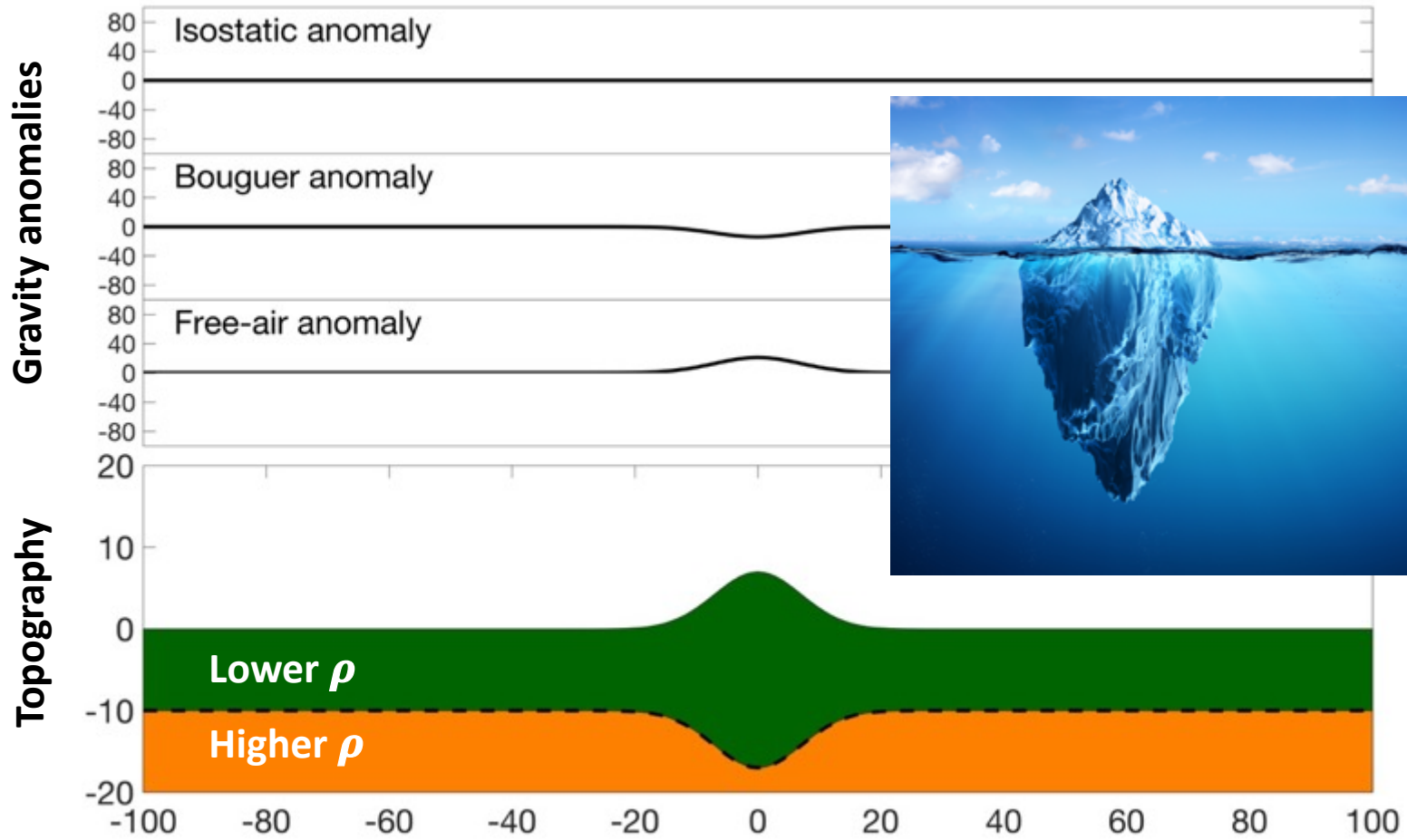
$\sigma_{model} =$  gravity assuming isostasy for  $\rho_1, \rho_2, h$



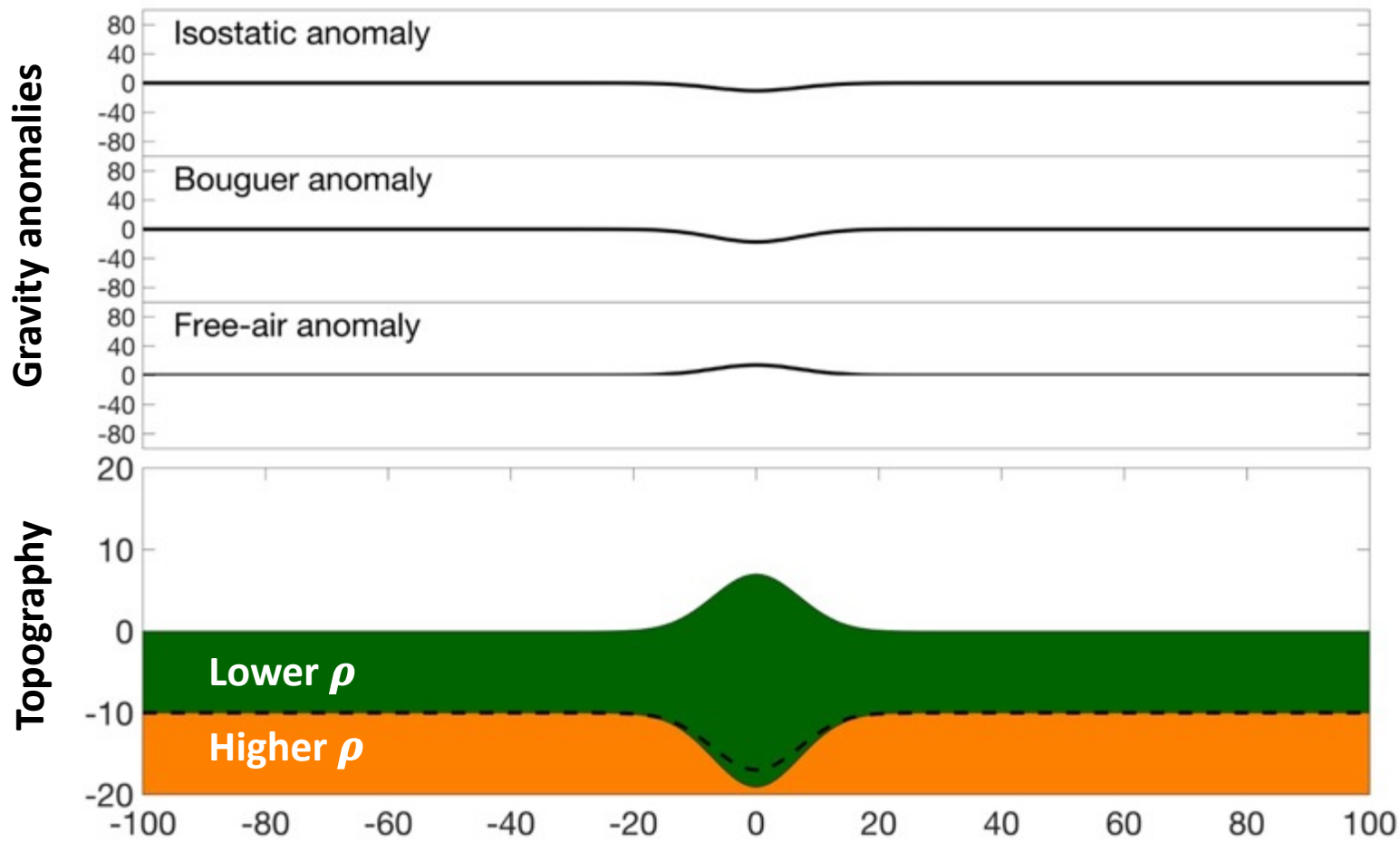
# Example: uncompensated topography



# Example: compensated topography



# Example: supercompensated topography

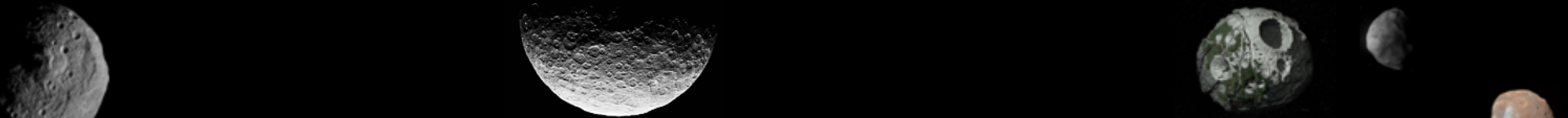




# Admittance

$Z_n$  - gravity-topography admittance

$$Z_n = \frac{\textit{gravity}}{\textit{topography}} \text{ for a given wavelength}$$



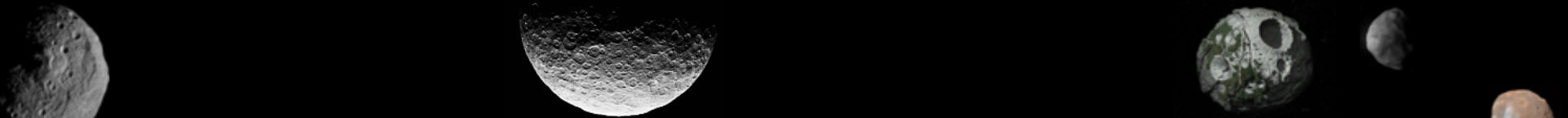
# Admittance

$Z_n$  - gravity-topography admittance

$$Z_n = \frac{\textit{gravity}}{\textit{topography}} \text{ for a given wavelength}$$

**Homogeneous**

$$Z_n = \frac{\overbrace{GM \ 3(n+1)}^{\text{Homogeneous}}}{R^3 \ 2n+1}$$



# Admittance

$Z_n$  - gravity-topography admittance

$$Z_n = \frac{\text{gravity}}{\text{topography}} \text{ for a given wavelength}$$

**Homogeneous**

$$Z_n = \frac{GM}{R^3} \frac{3(n+1)}{2n+1} \frac{\rho_{crust}}{\bar{\rho}}$$

**Two-layer**

# Admittance

$Z_n$  - gravity-topography admittance

$$Z_n = \frac{\text{gravity}}{\text{topography}} \text{ for a given wavelength}$$

**Homogeneous**

$$Z_n = \frac{GM}{R^3} \frac{3(n+1)}{2n+1} \frac{\rho_{crust}}{\bar{\rho}} \left[ 1 - \left( \frac{R - D_{comp}}{R} \right)^{n+2} \right]$$

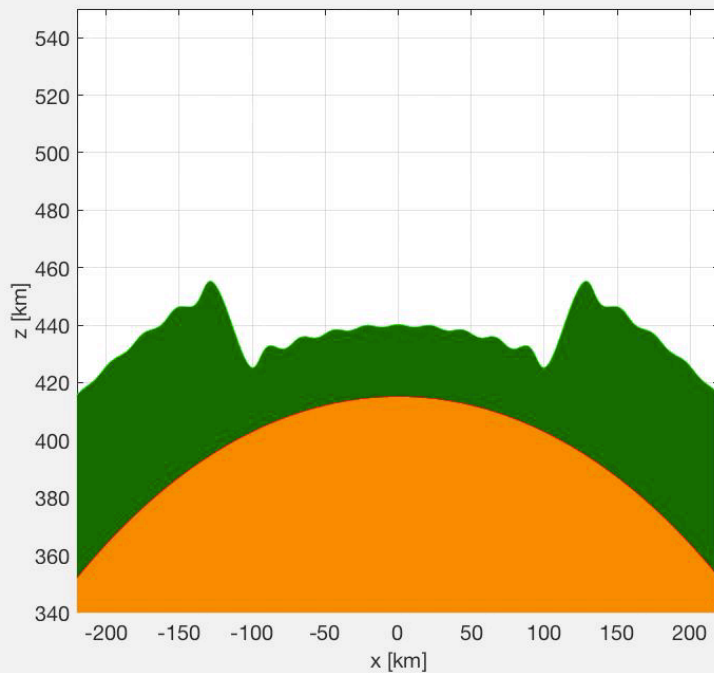
**Two-layer**

**Isostatic**

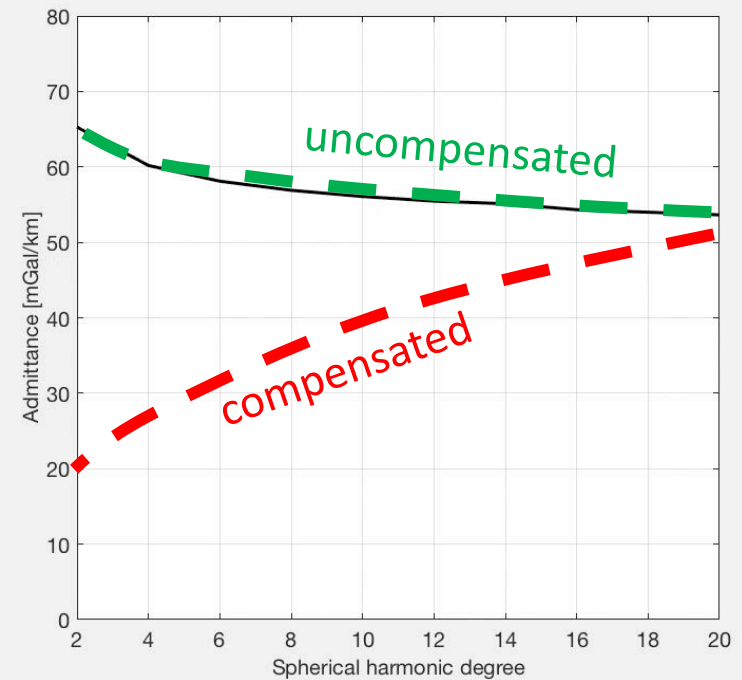
# Isostatic compensation

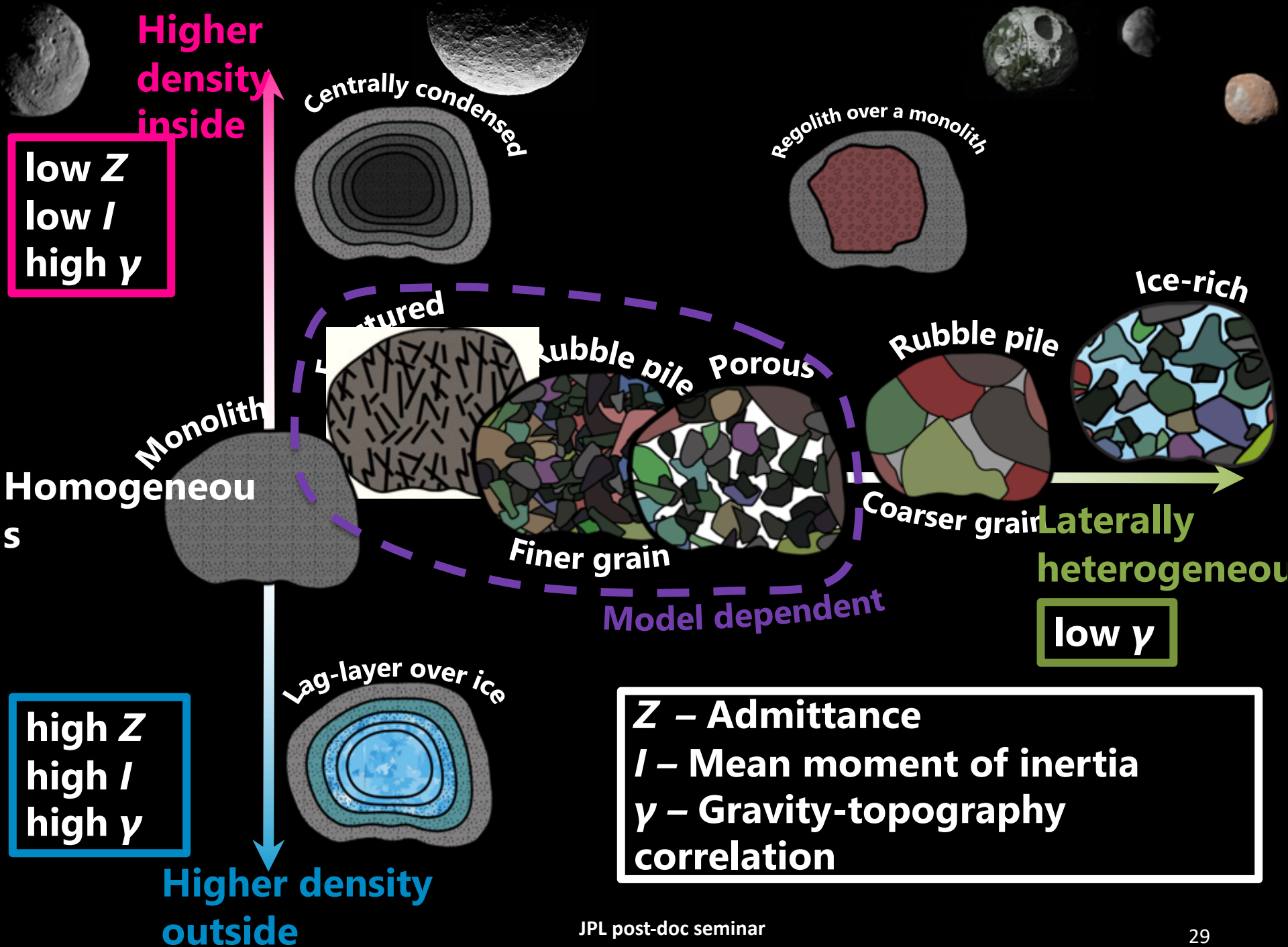
- Example of a spherical cap (depression) relaxation

## Interface evolution



## Admittance evolution



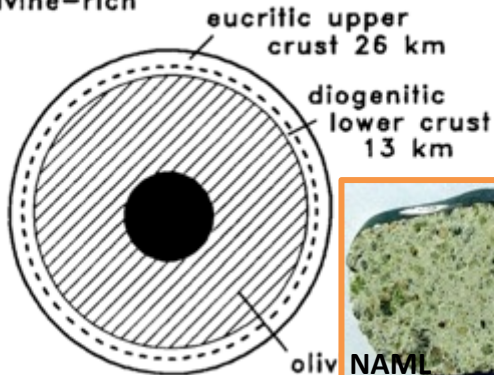


# What did we know before Dawn?

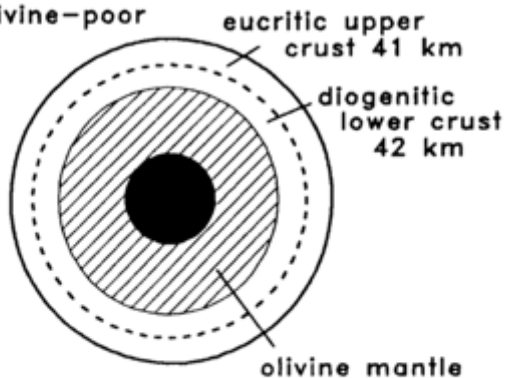
## Vesta



### Vesta olivine-rich



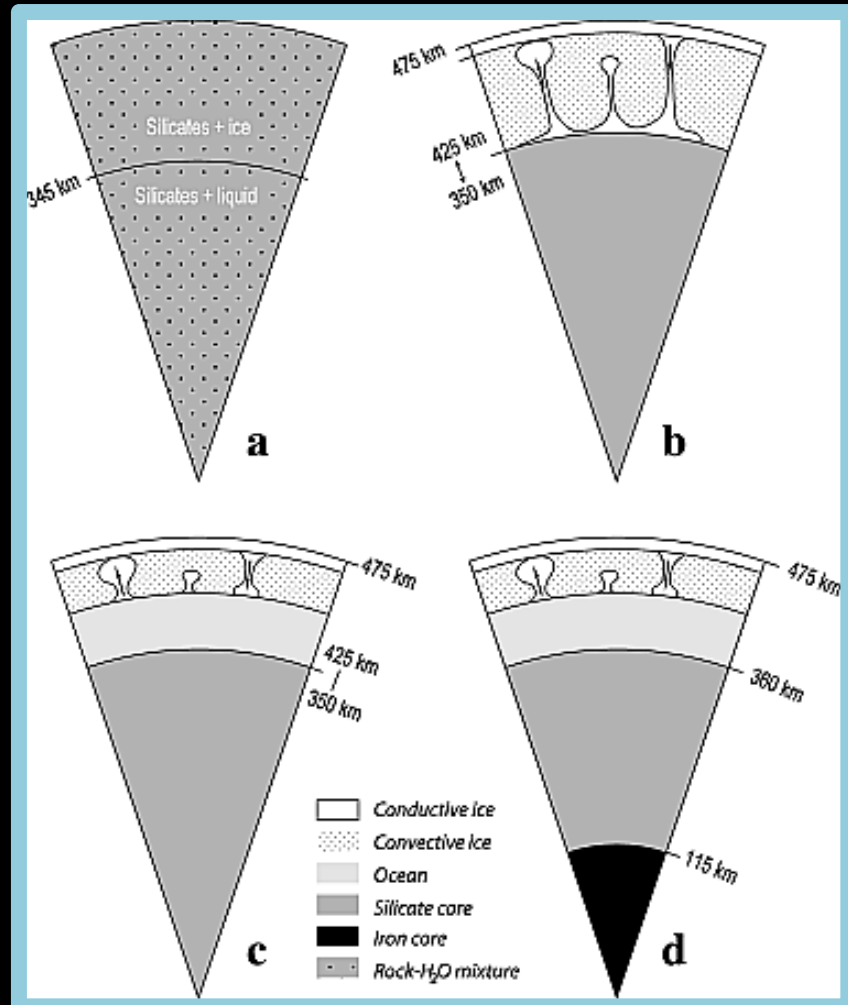
### Vesta olivine-poor



core mass = 5%  
core radius = 75 km  
asteroid radius = 265 km

Ruzicka et al., 1997

## Ceres



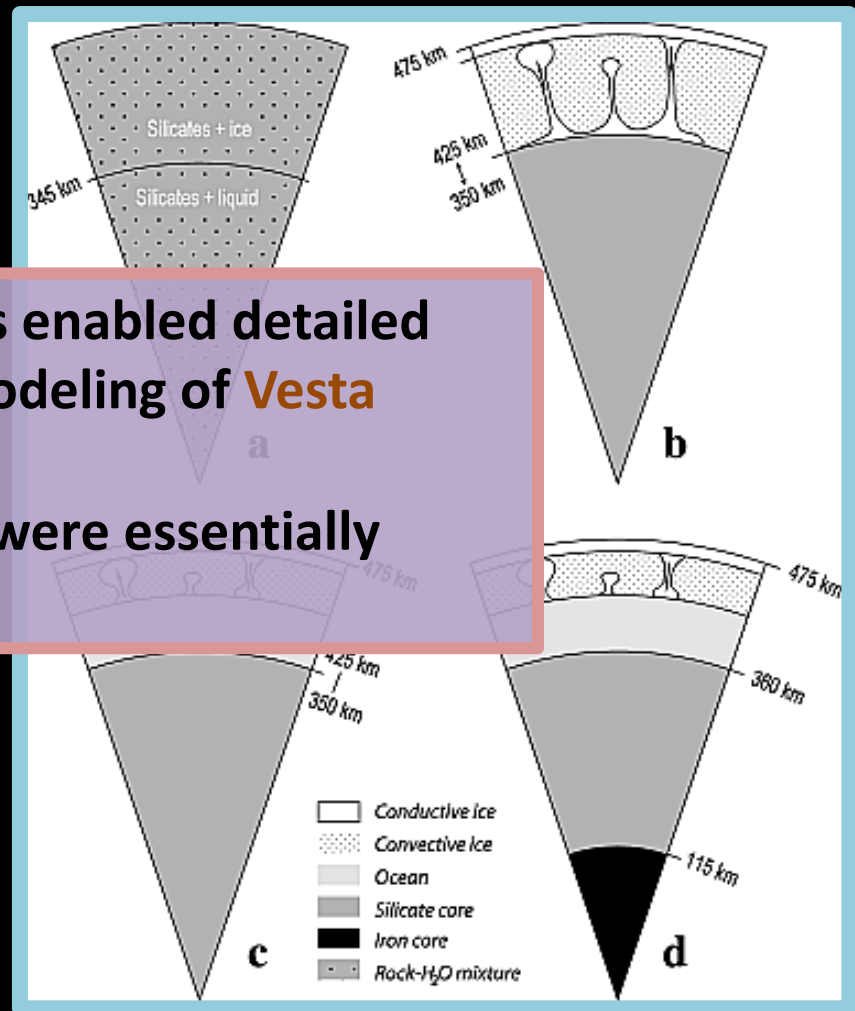
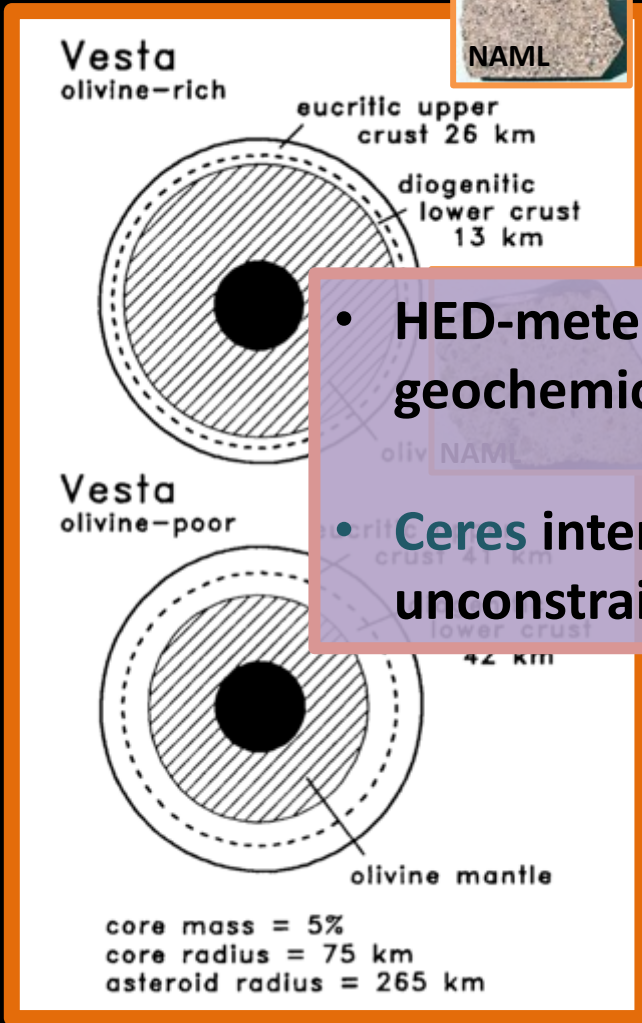
McCord and Sotin, 2005

# What did we know before Dawn?

## Vesta



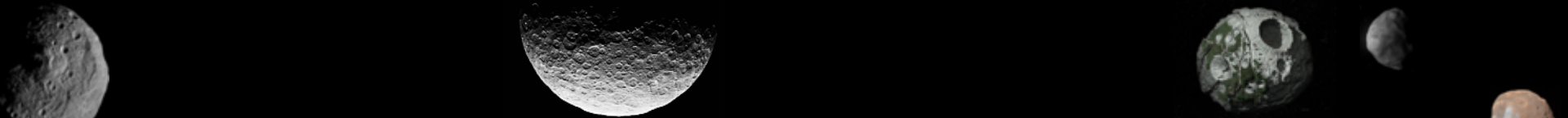
## Ceres



- HED-meteorites enabled detailed geochemical modeling of **Vesta**
- **Ceres** interiors were essentially unconstrained

Ruzicka et al., 1997

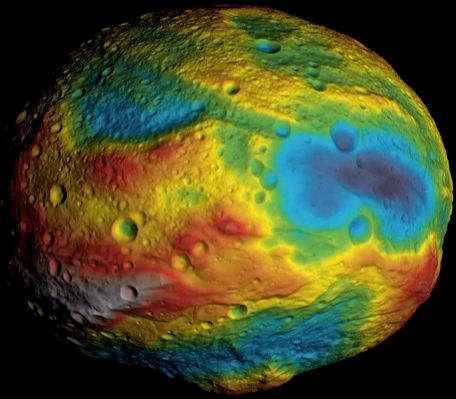
McCord and Sotin, 2005



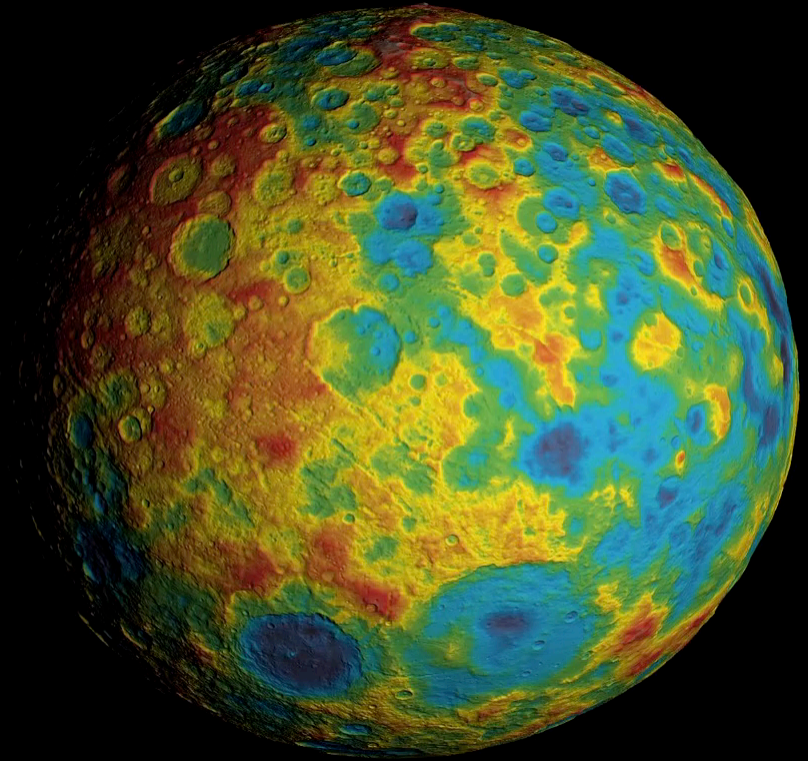
# Dawn geophysical data

- Shape model
  - Stereophotogrammetry (SPG) from DLR
  - Stereophotoclinometry (SPC) from JPL
  - Mutually consistent with the accuracy much better than the spatial resolution of gravity field
- Gravity field
  - Accurate up to  $n = 18$  ( $\lambda=93$  km) for **Vesta** (Konopliv et al., 2014)
  - Accurate up to  $n = 17$  ( $\lambda=174$  km) for **Ceres** (Konopliv et al., 2017)
- Assumptions we have to make:
  - Multilayer model with uniform density layers
  - Range of core densities for **Vesta**
  - Range of crustal densities from HEDs for **Vesta**
  - Can't really assume anything for **Ceres**

# Vesta and Ceres

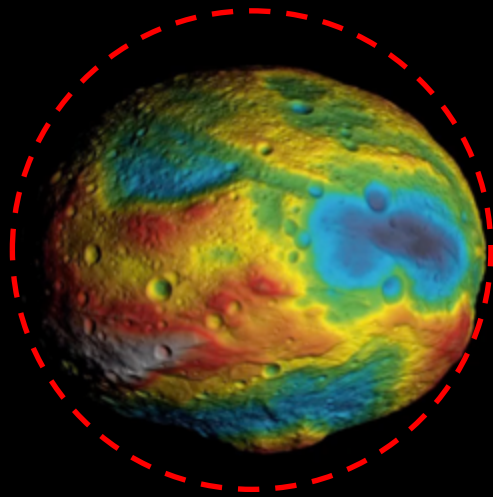


Gaskell, 2012

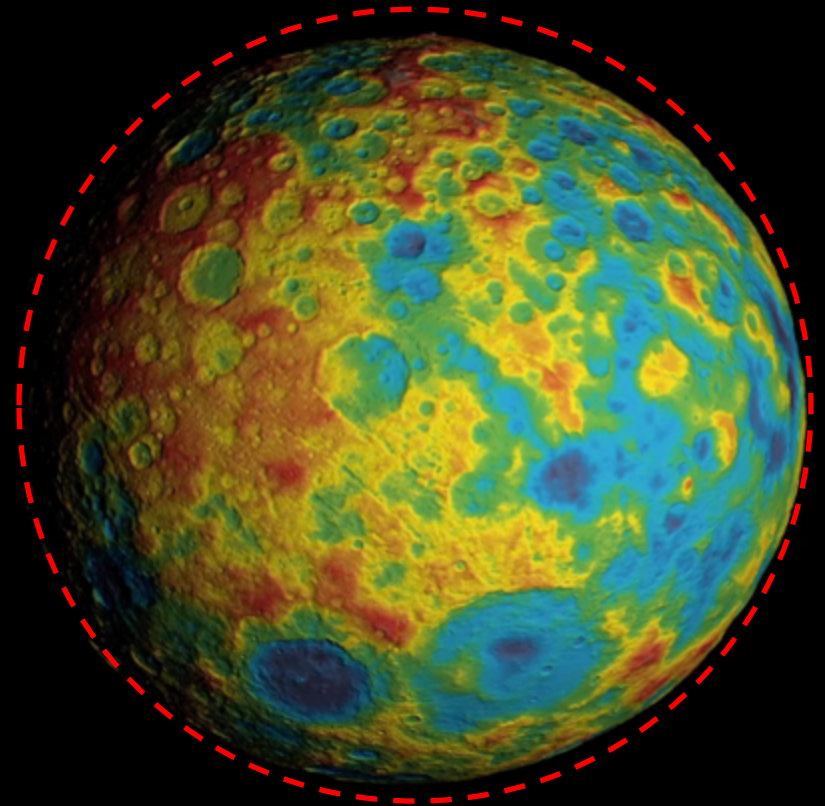


Park et al., 2016

# Vesta and Ceres



Gaskell, 2012



Park et al., 2016

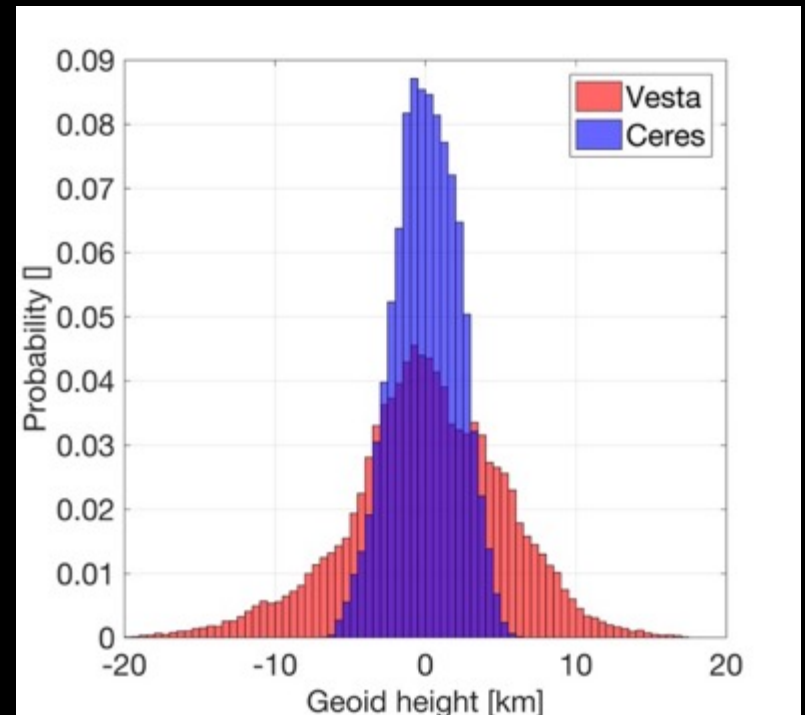
# Vesta and Ceres topography

## Shape statistics

Parameter	Vesta	Ceres
Equatorial flattening	0.0262	0.0043
Geoidal height range (km)	37.9	13.2
Geoidal height RMS (km)	5.2	2.1

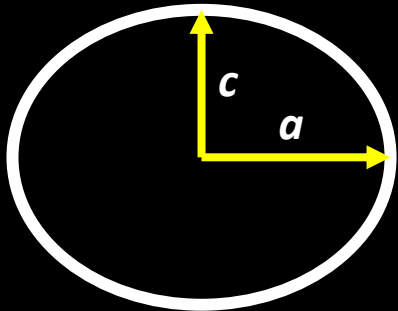
- Ceres is closer to hydrostatic equilibrium than Vesta
- Smoother topography at Ceres

## Hypsograms of Vesta and Ceres



\**Hypsogram* is a fancy word for the “histogram of elevations”

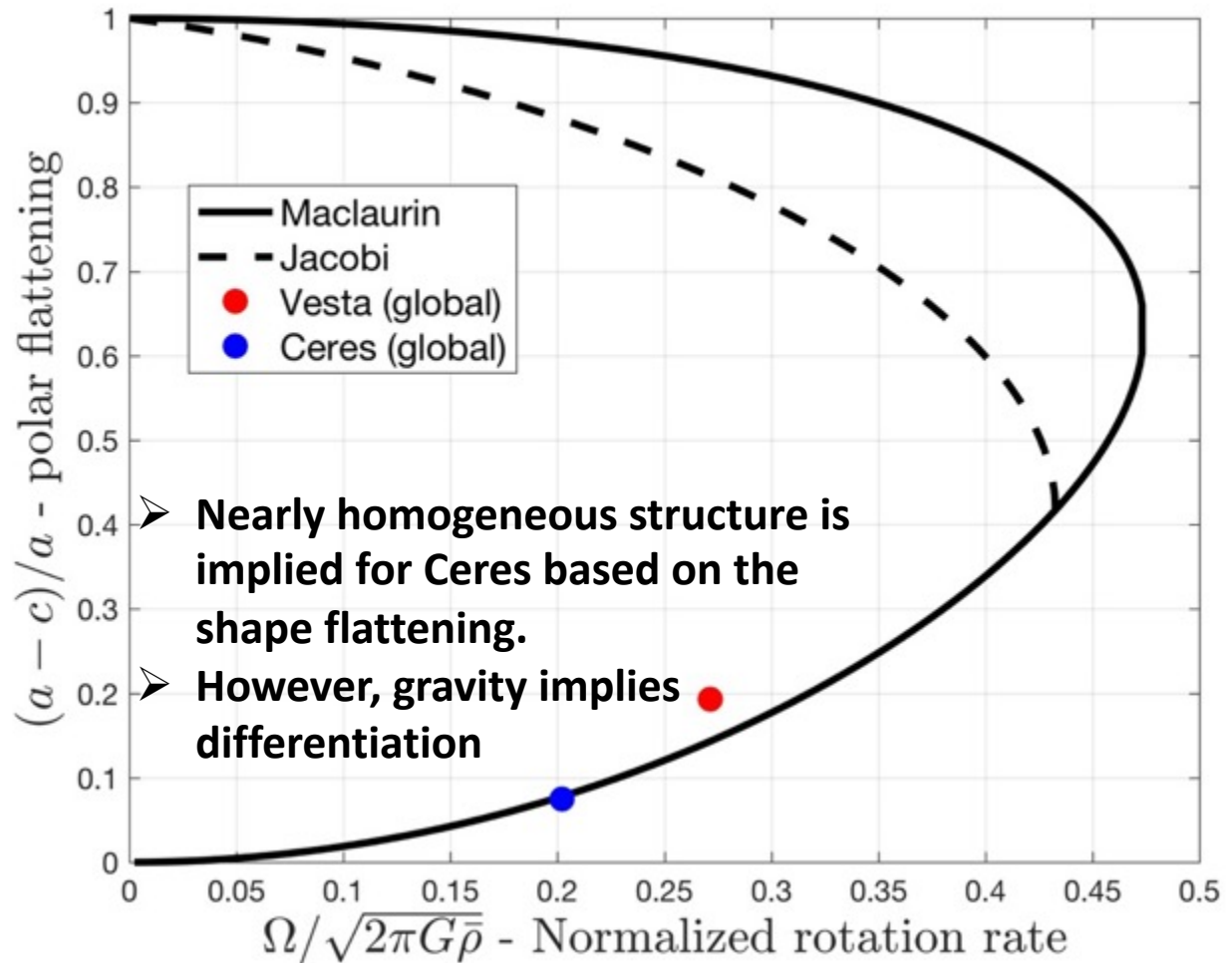
# Flattening vs rotation rate



homogeneous  
more oblate

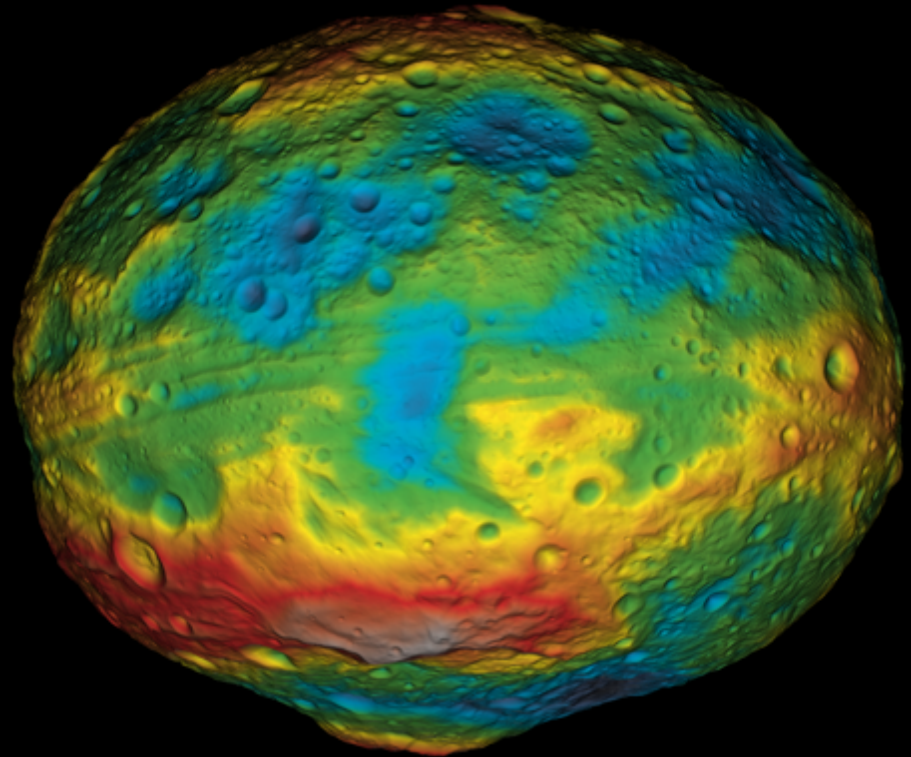
differentiated

less oblate



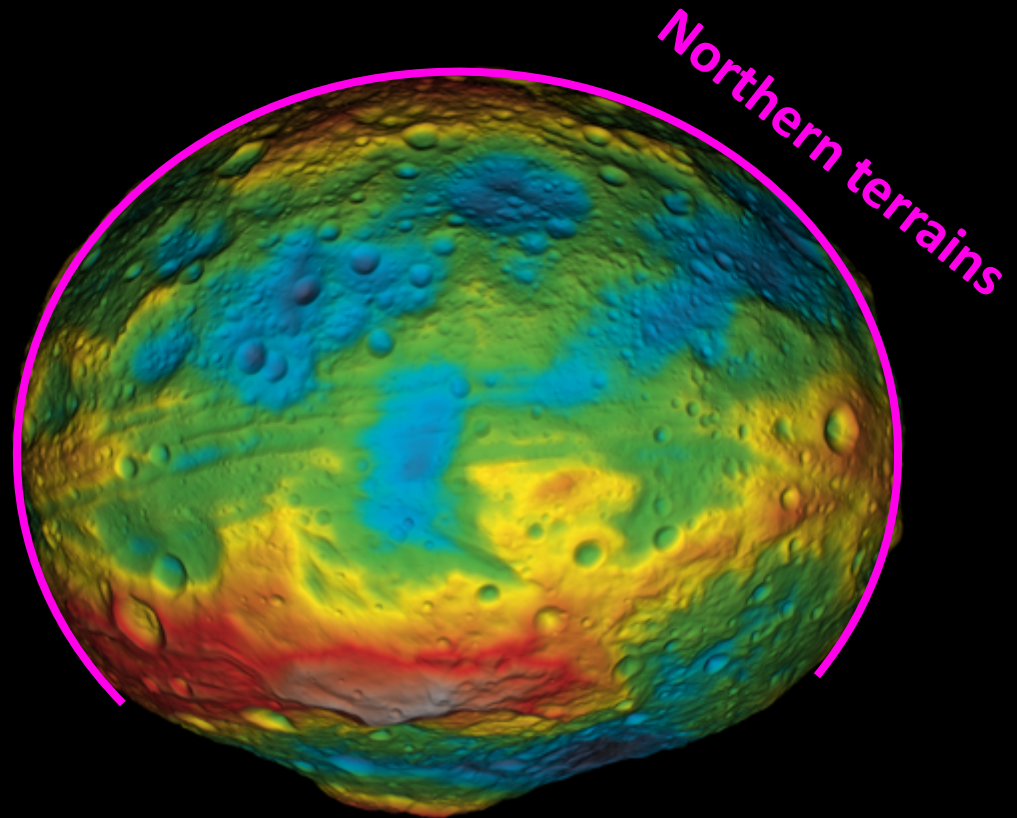
# Early efficient viscous relaxation of Vesta

- Vesta was likely close to hydrostatic equilibrium in its early history (Fu et al., 2014).
- Vesta's northern terrains likely reflect its pre-impact equilibrium shape.
- Major impact occurred when Vesta was effectively non-relaxing leading to uncompensated Rheasilvia and Veneneia basins.



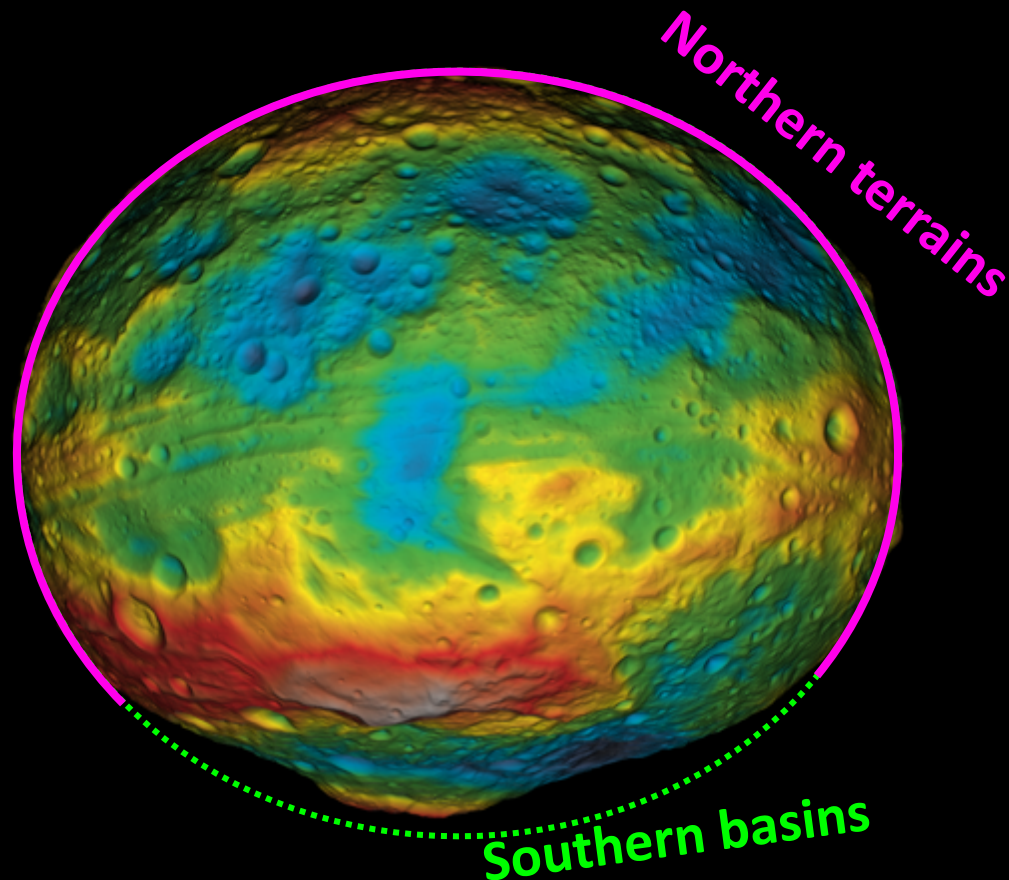
# Early efficient viscous relaxation of Vesta

- Vesta was likely close to hydrostatic equilibrium in its early history (Fu et al., 2014).
- Vesta's northern terrains likely reflect its pre-impact equilibrium shape.
- Major impact occurred when Vesta was effectively non-relaxing leading to uncompensated Rheasilvia and Veneneia basins.

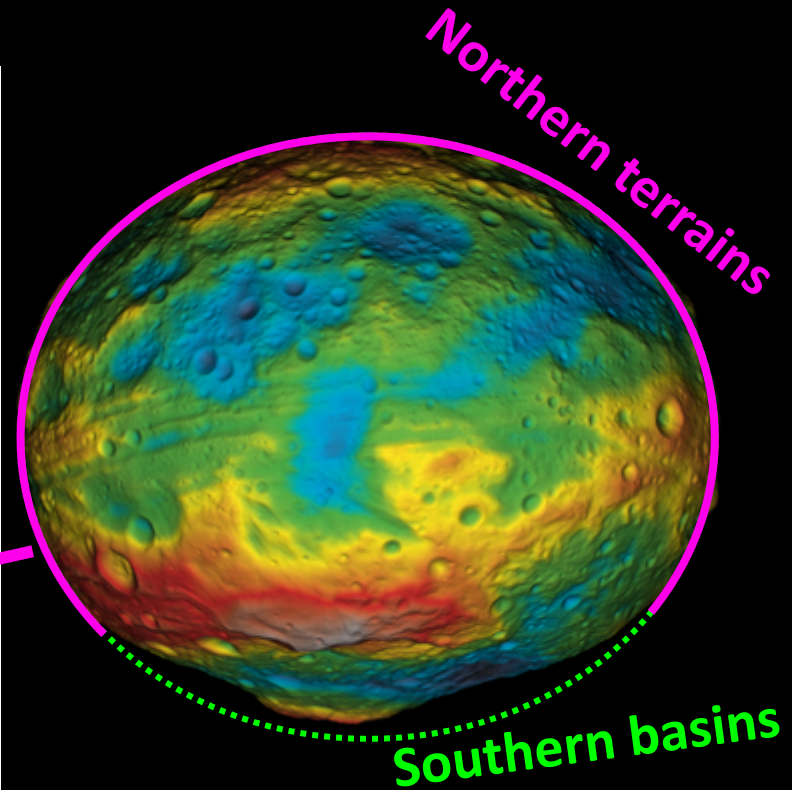
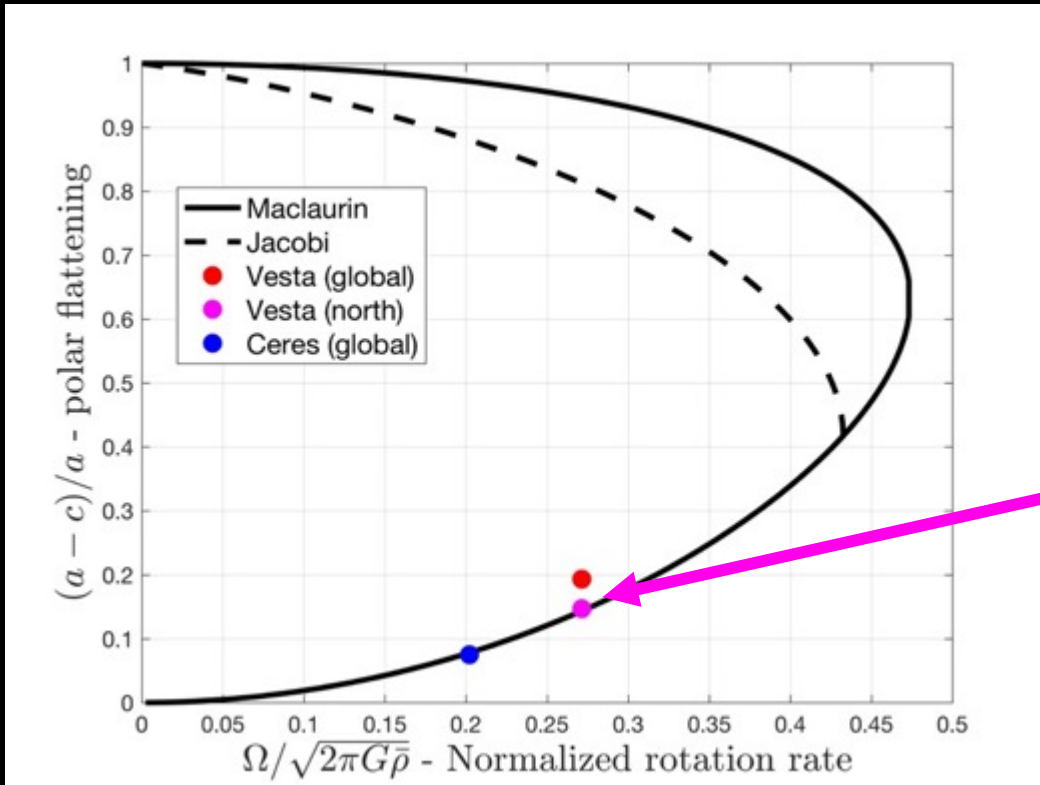


# Early efficient viscous relaxation of Vesta

- Vesta was likely close to hydrostatic equilibrium in its early history (Fu et al., 2014).
- Vesta's northern terrains likely reflect its pre-impact equilibrium shape.
- Major impact occurred when Vesta was effectively non-relaxing leading to uncompensated Rheasilvia and Veneneia basins.

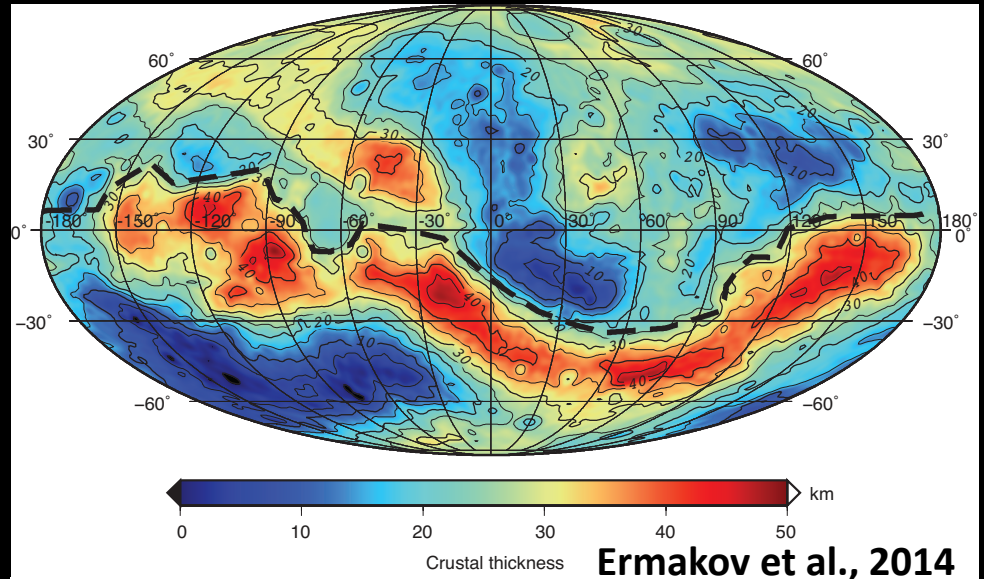


# Early efficient viscous relaxation of Vesta

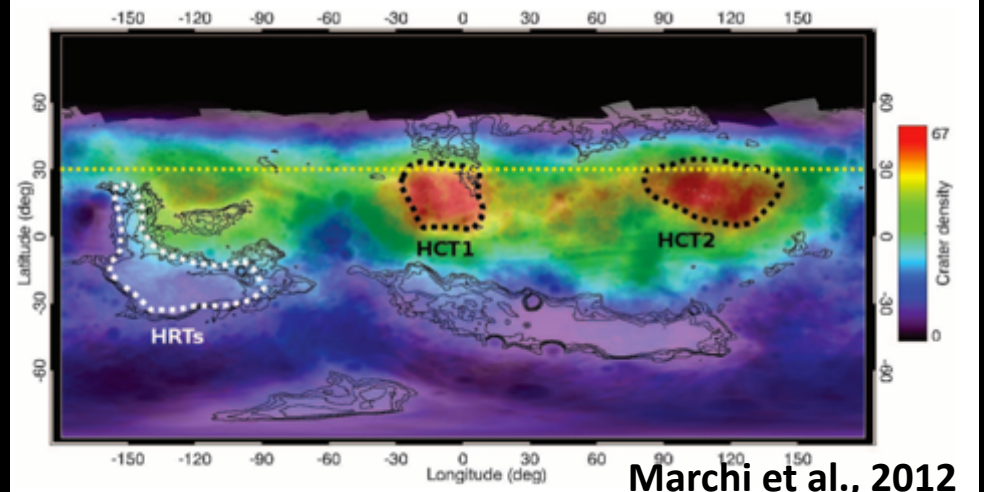


# Vesta Crustal Thickness

➤ Crustal thickness inversion show a belt of thicker crust around the Southern Basins

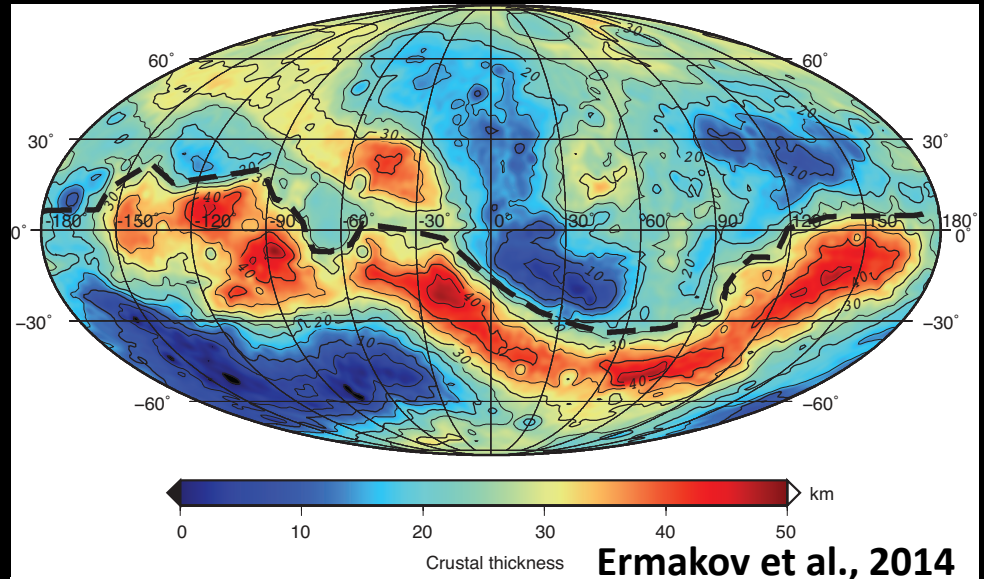


➤ Crater counting reveals that the northern Vesta terrains are old (>3Gy)

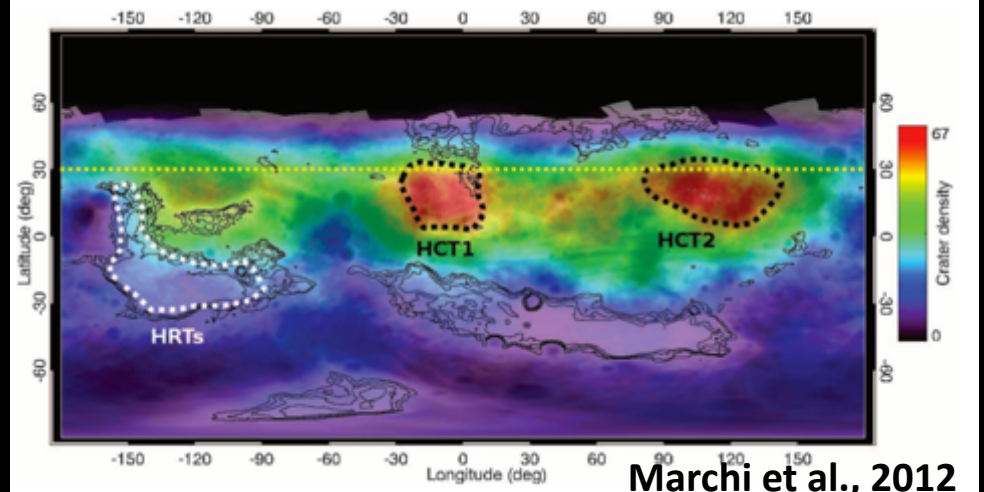


# Vesta Crustal Thickness

➤ Crustal thickness inversion show a belt of thicker crust around the Southern Basins

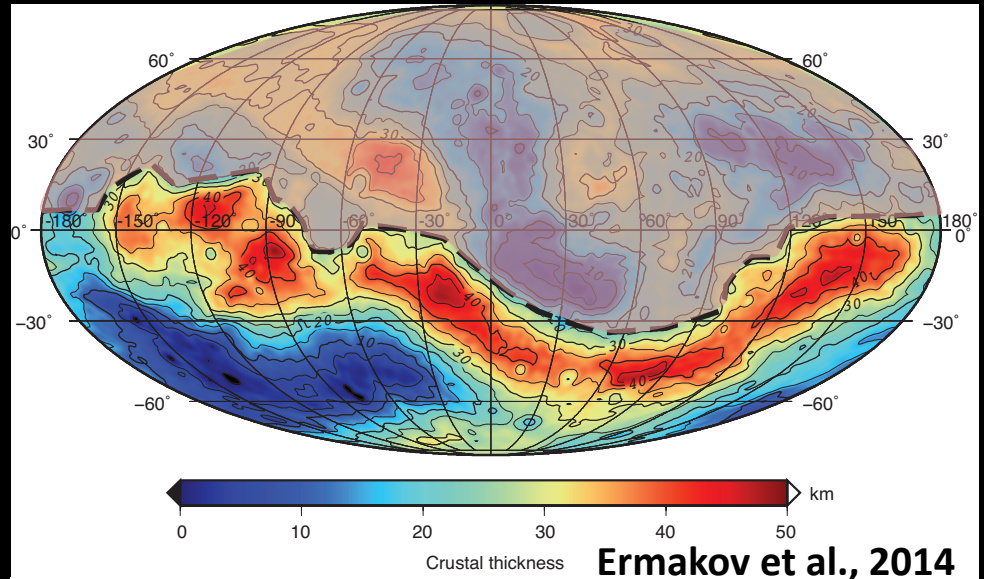


➤ Crater counting reveals that the northern Vesta terrains are old (>3Gy)

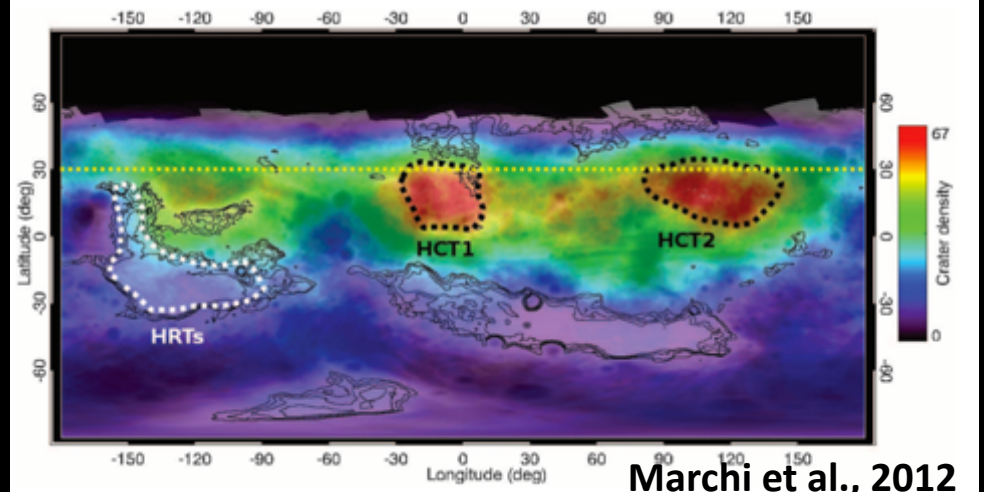


# Vesta Crustal Thickness

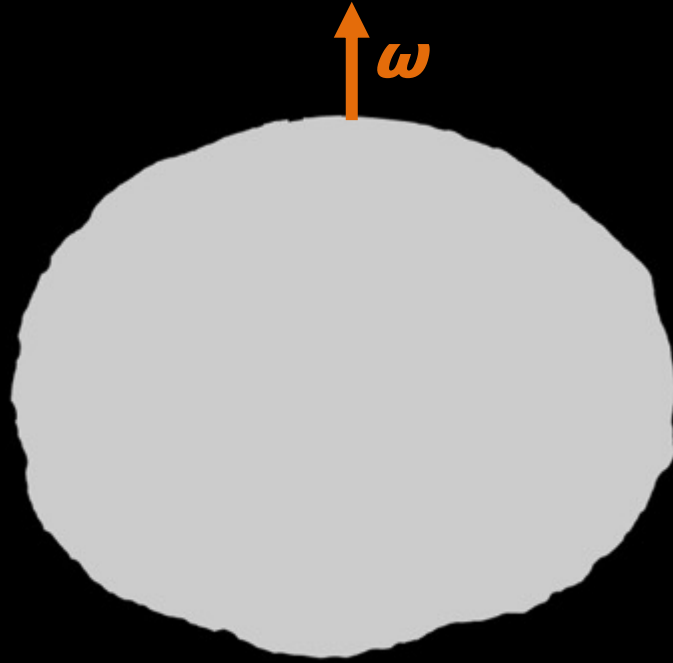
➤ Crustal thickness inversion show a belt of thicker crust around the Southern Basins



➤ Crater counting reveals that the northern Vesta terrains are old (>3Gy)

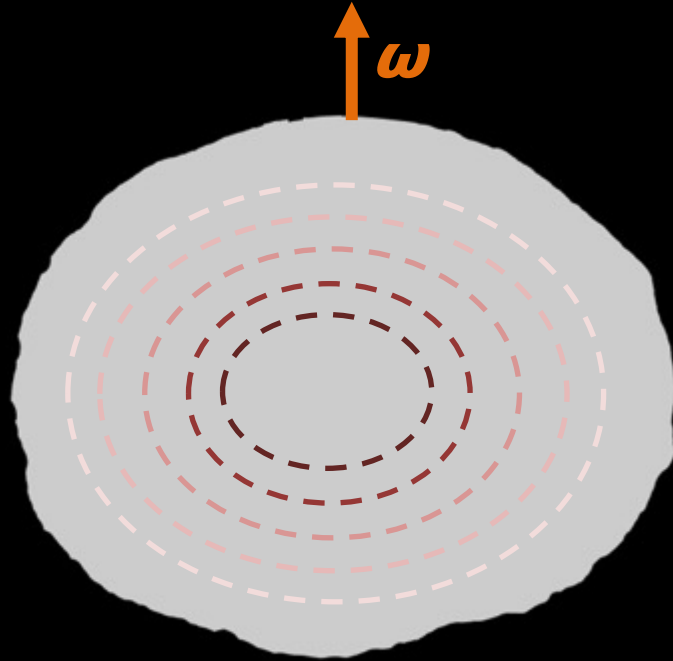


# Solving for Vesta's internal structure



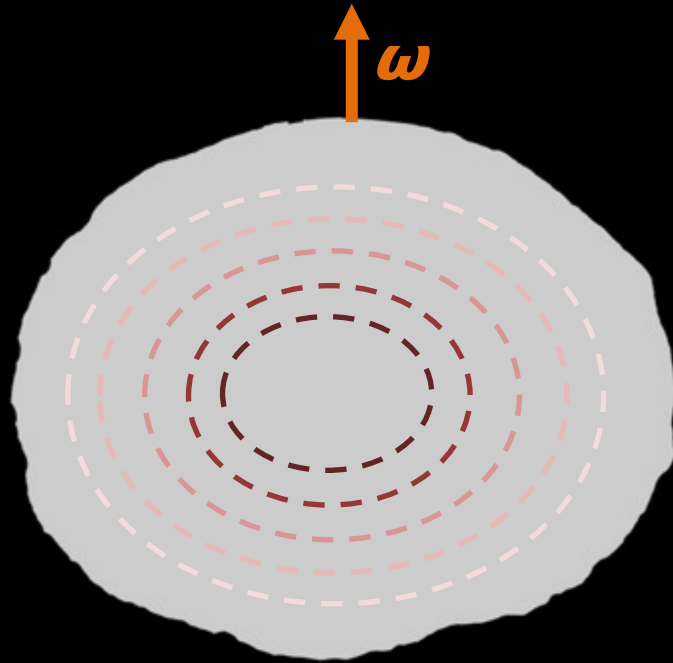
➤ Vary rotation rate

# Solving for Vesta's internal structure



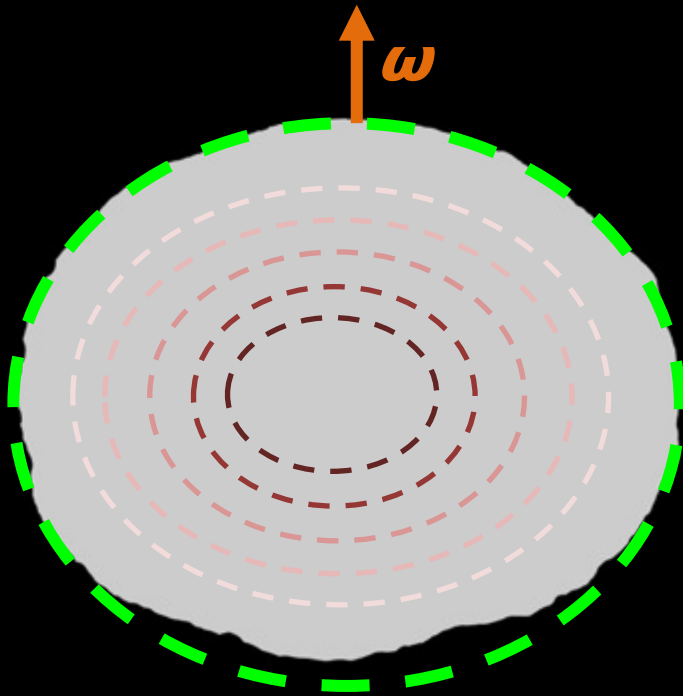
- Vary rotation rate
- Vary core size

# Solving for Vesta's internal structure



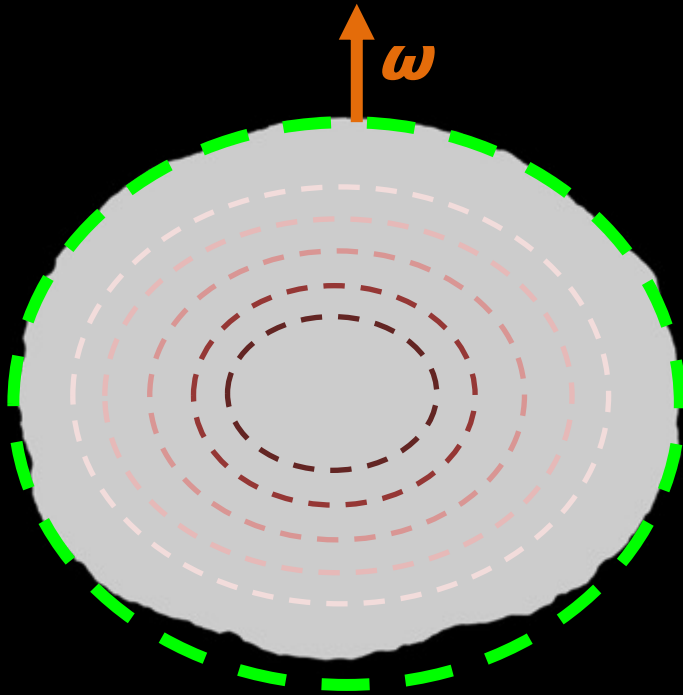
- Vary rotation rate
- Vary core size
  - assuming equilibrium shape

# Solving for Vesta's internal structure



- Vary rotation rate
- Vary core size
  - assuming equilibrium shape
- Match northern shape with the equipotential surface

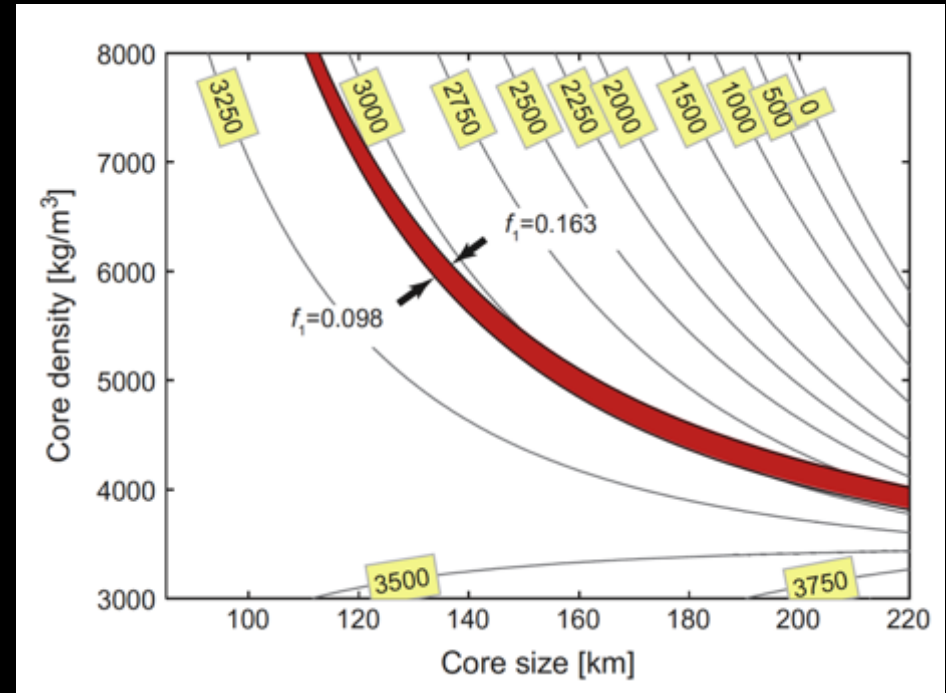
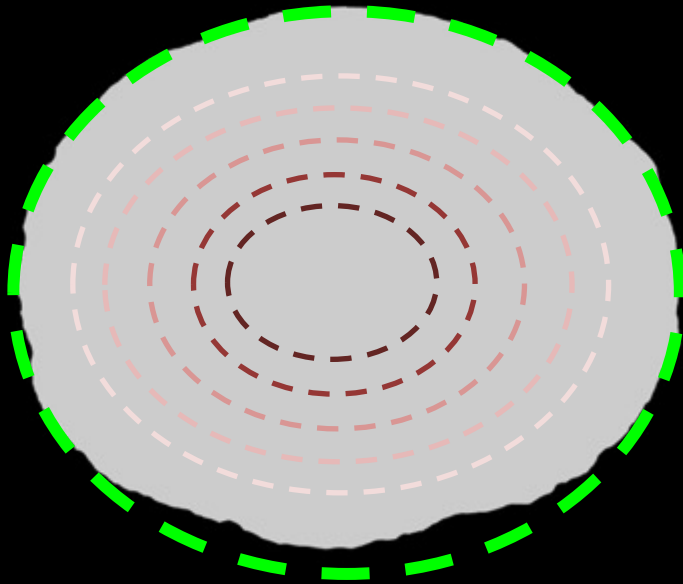
# Solving for Vesta's internal structure



- Vary rotation rate
- Vary core size
  - assuming equilibrium shape
- Match northern shape with the equipotential surface
- Match observed and modeled gravity coefficient  $J_2$

# Solving for Vesta's internal structure

Contours are mantle density [ $\text{kg/m}^3$ ]

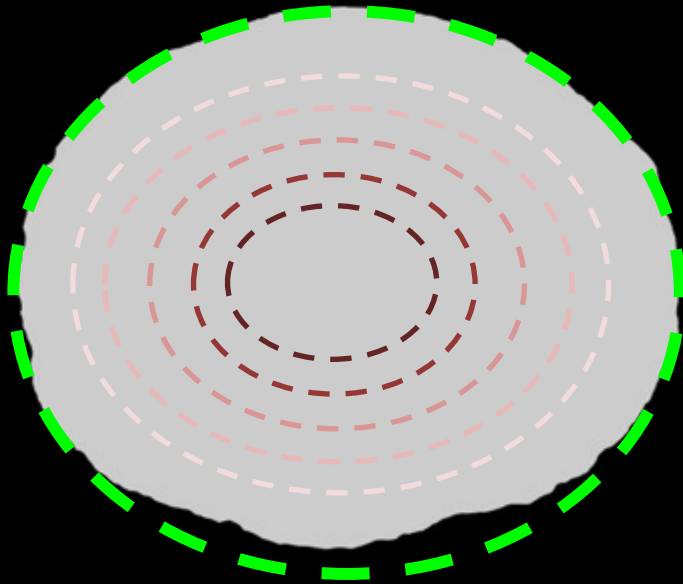


➤ Can find a consistent solution for  $4.83 < T < 4.93$  hours

➤  $T_{\text{present}} = 5.342$

Ermakov et al., 2014

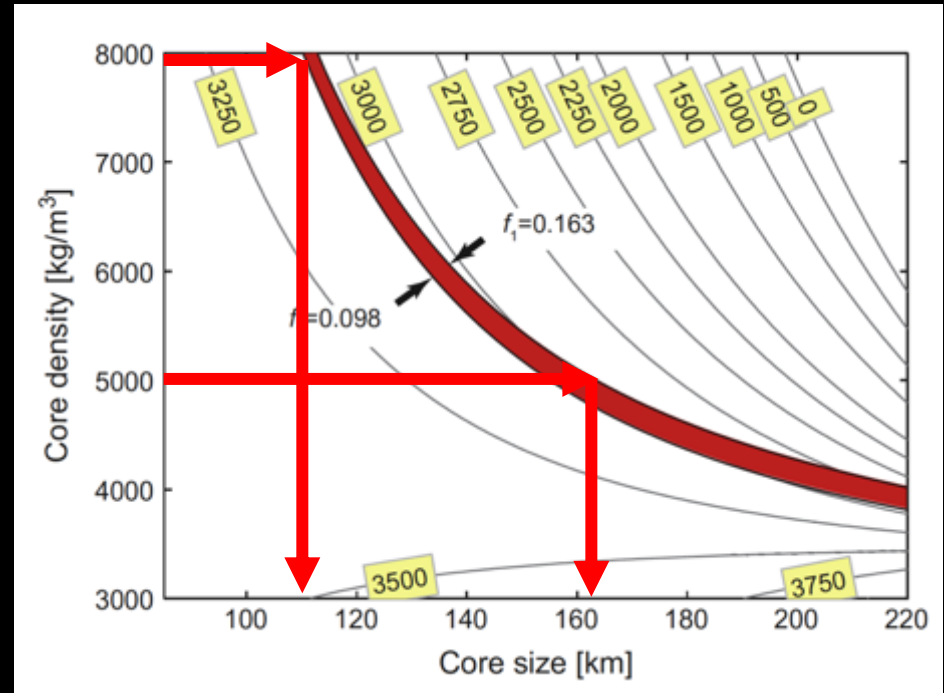
# Solving for Vesta's internal structure



➤ Can find a consistent solution for  $4.83 < T < 4.93$  hours

➤  $T_{\text{present}} = 5.342$

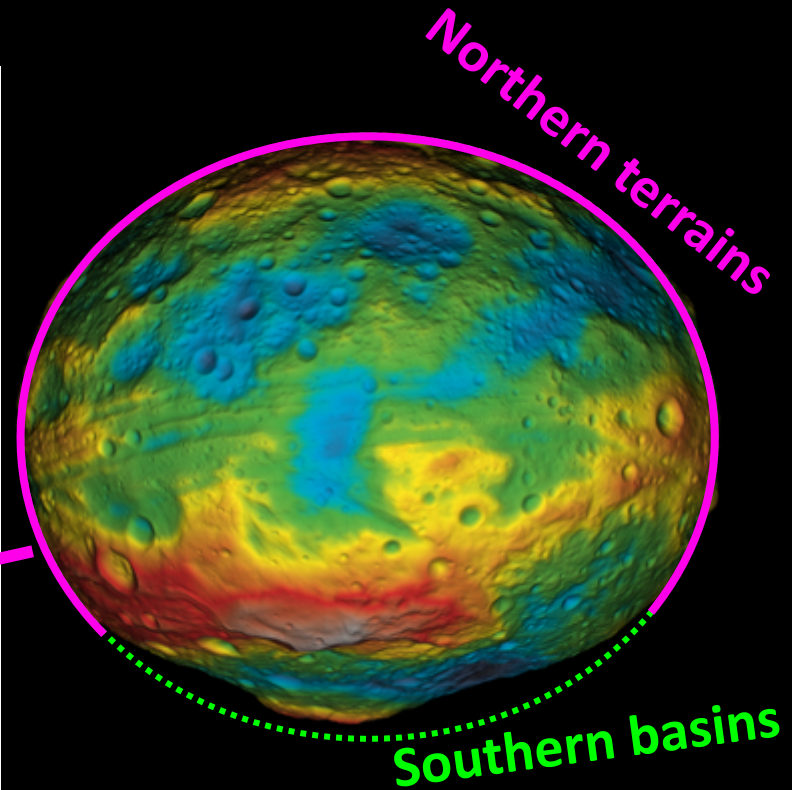
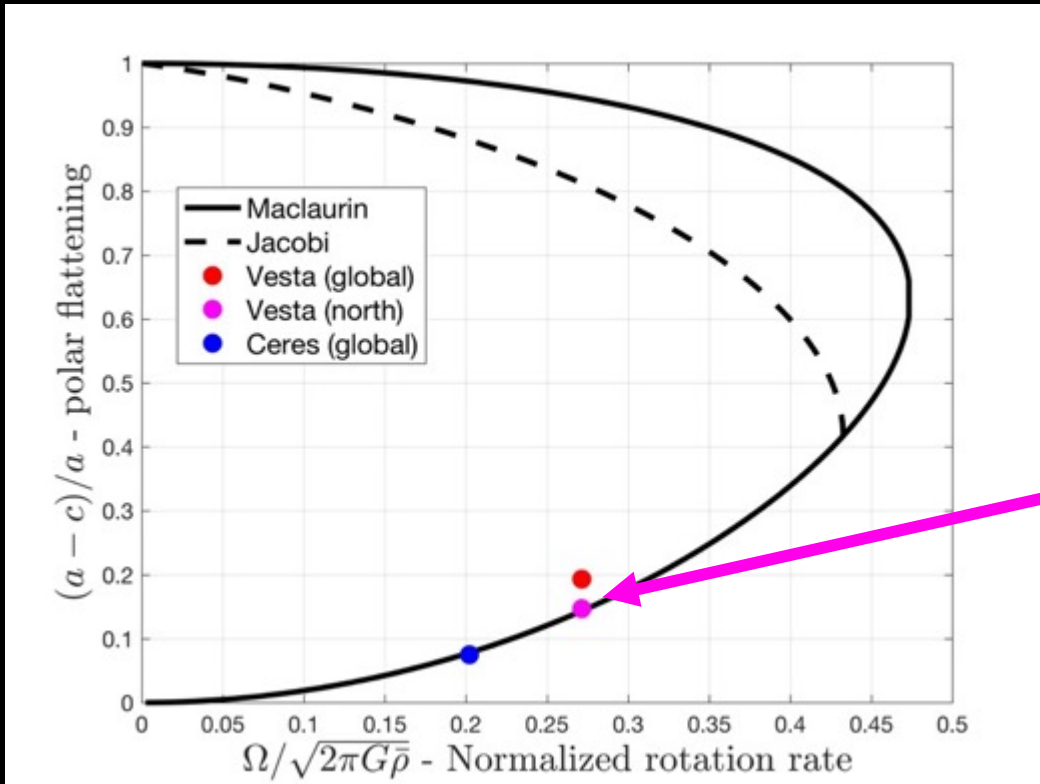
Contours are mantle density [ $\text{kg/m}^3$ ]



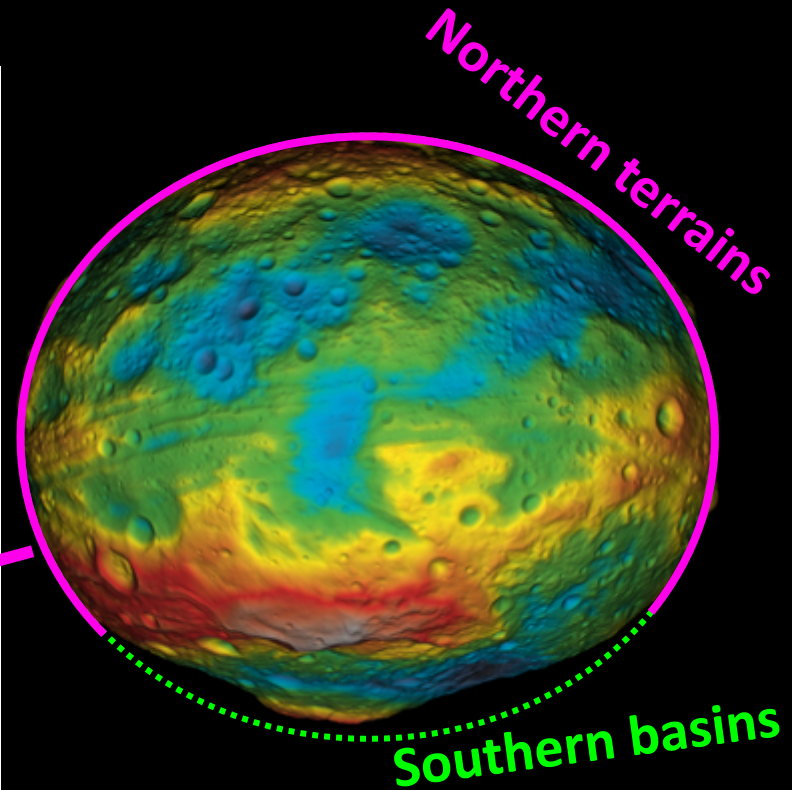
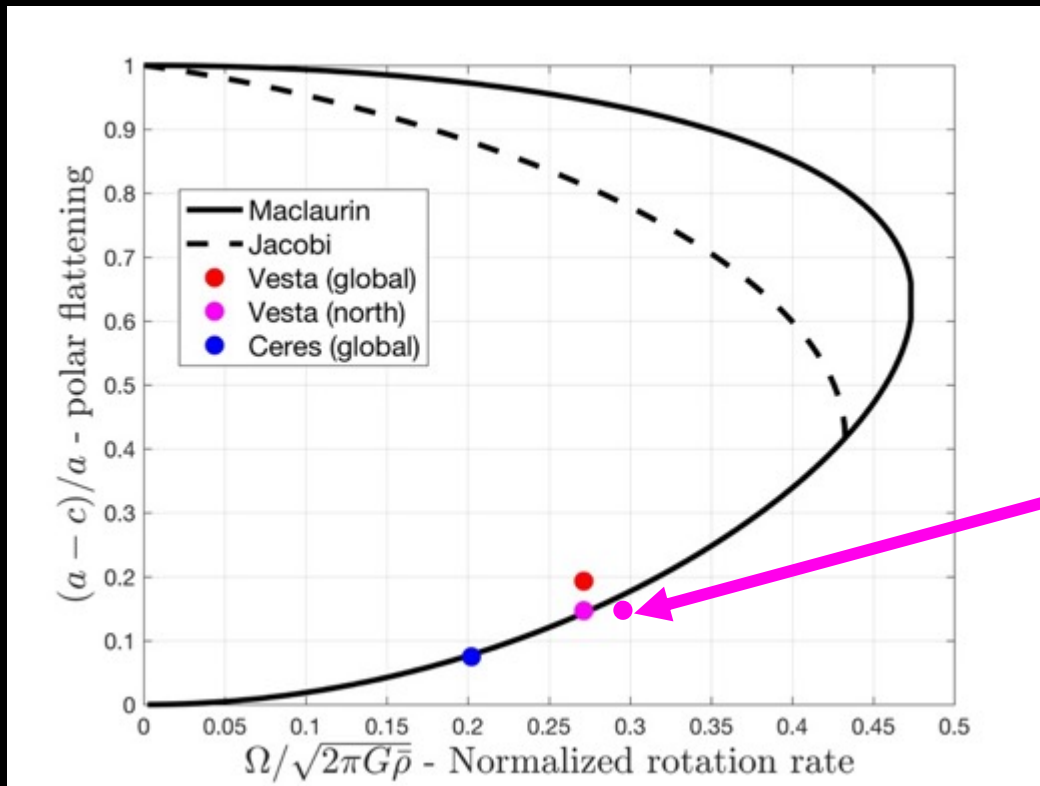
Core radius of 110 to 162 km

Ermakov et al., 2014

# Early efficient viscous relaxation of Vesta



# Early efficient viscous relaxation of Vesta



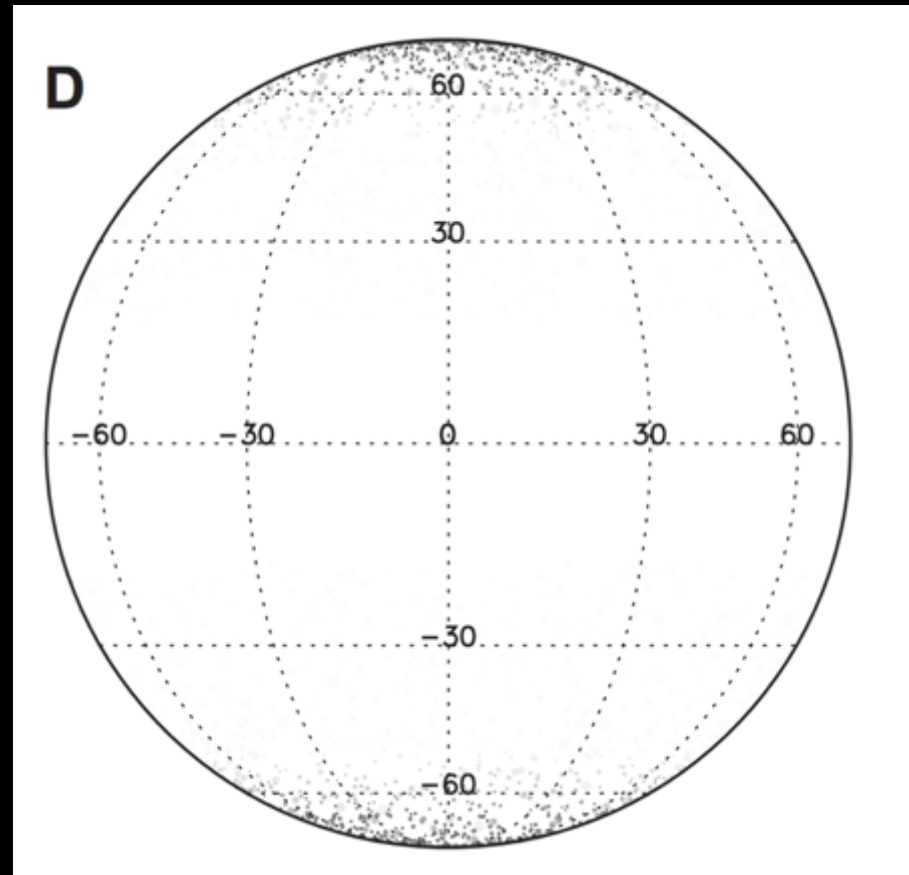
# Summary on Vesta



- Once hot and hydrostatic, **Vesta** is no longer either
- Formed early (< 5 My after CAI)
- Differentiated interior
- Most of topography acquired when **Vesta** was already cool => uncompensated topography
- Combination of gravity/topography data with meteoritic geochemistry data provides constraints on the internal structure

# Ceres expectations

- Bland et al., 2013 predicted that craters on Ceres would quickly relax in an ice-dominated shell
  - Equatorial warmer craters would relax faster than colder polar craters
- Bland et al., 2016 did not find evidence for such relaxation pattern
  - No latitude dependence of crater depth

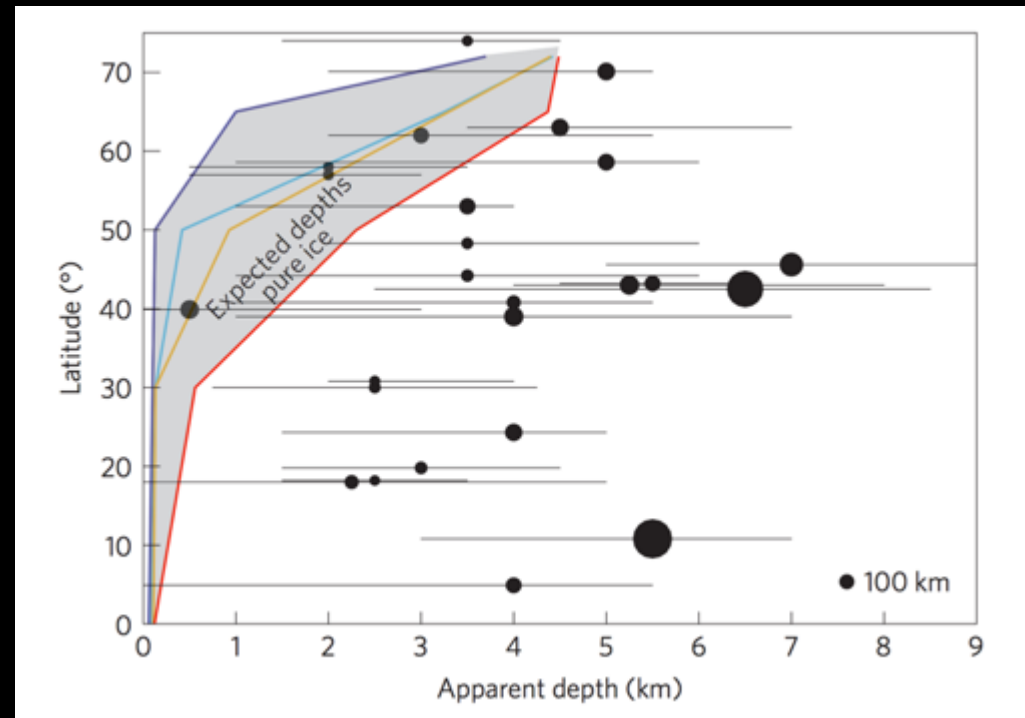


Bland, 2013

# Ceres observation

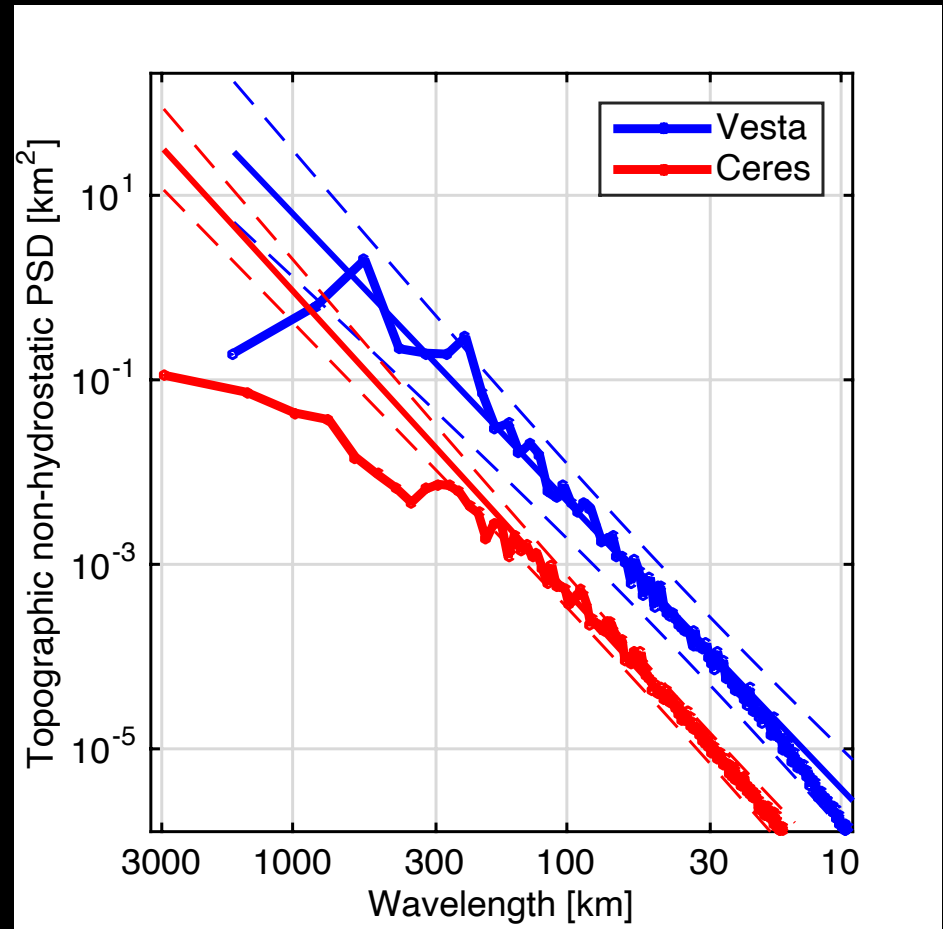
- Bland et al., 2013 predicted that craters on Ceres would quickly relax in an ice-dominated shell
  - Equatorial warmer craters would relax faster than colder polar craters
- Bland et al., 2016 did not find evidence for such relaxation pattern
  - No latitude dependence of crater depth

## Crater depth study



# Evidence for viscous relaxation

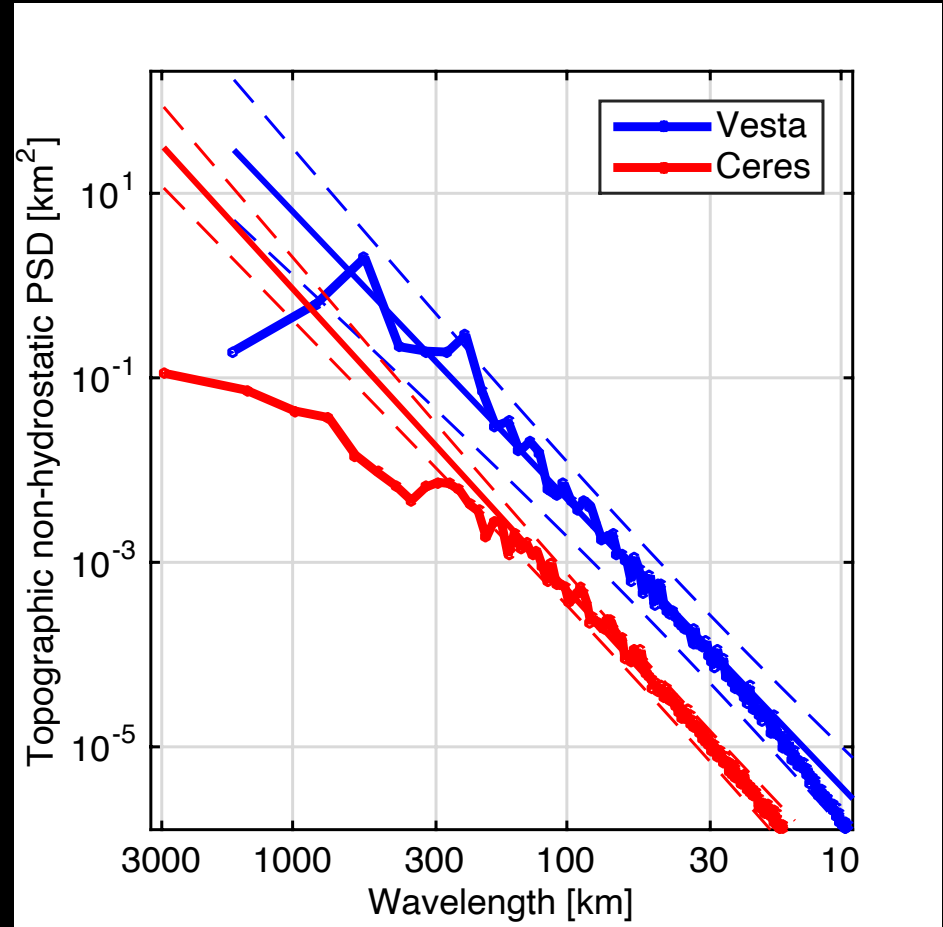
- **More general approach: study topography power spectrum**
- **Power spectra for Vesta closely fits with the power law to the lowest degrees ( $\lambda < 750$  km)**
- **Ceres power spectrum deviates from the power law at  $\lambda > 270$  km**



Ermakov et al., 2017a

# Evidence for viscous relaxation

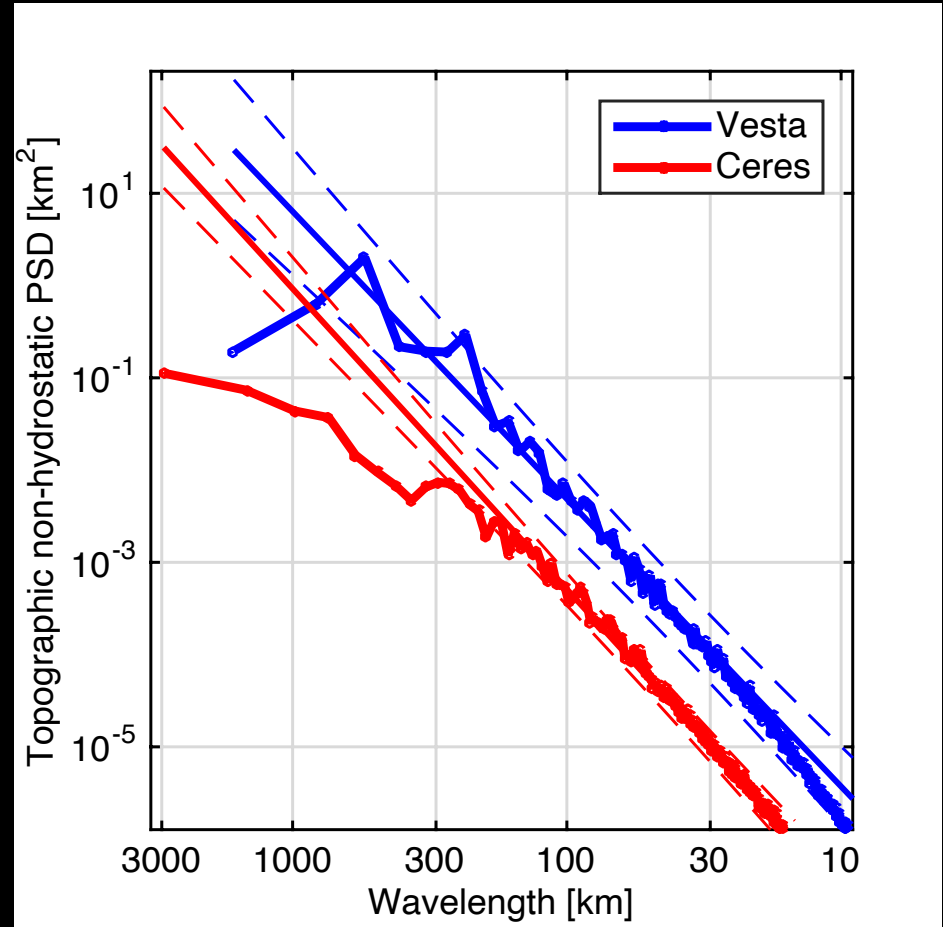
- **More general approach: study topography power spectrum**
- **Power spectra for Vesta closely fits with the power law to the lowest degrees ( $\lambda < 750$  km)**
- **Ceres power spectrum deviates from the power law at  $\lambda > 270$  km**



Ermakov et al., 2017a

# Evidence for viscous relaxation

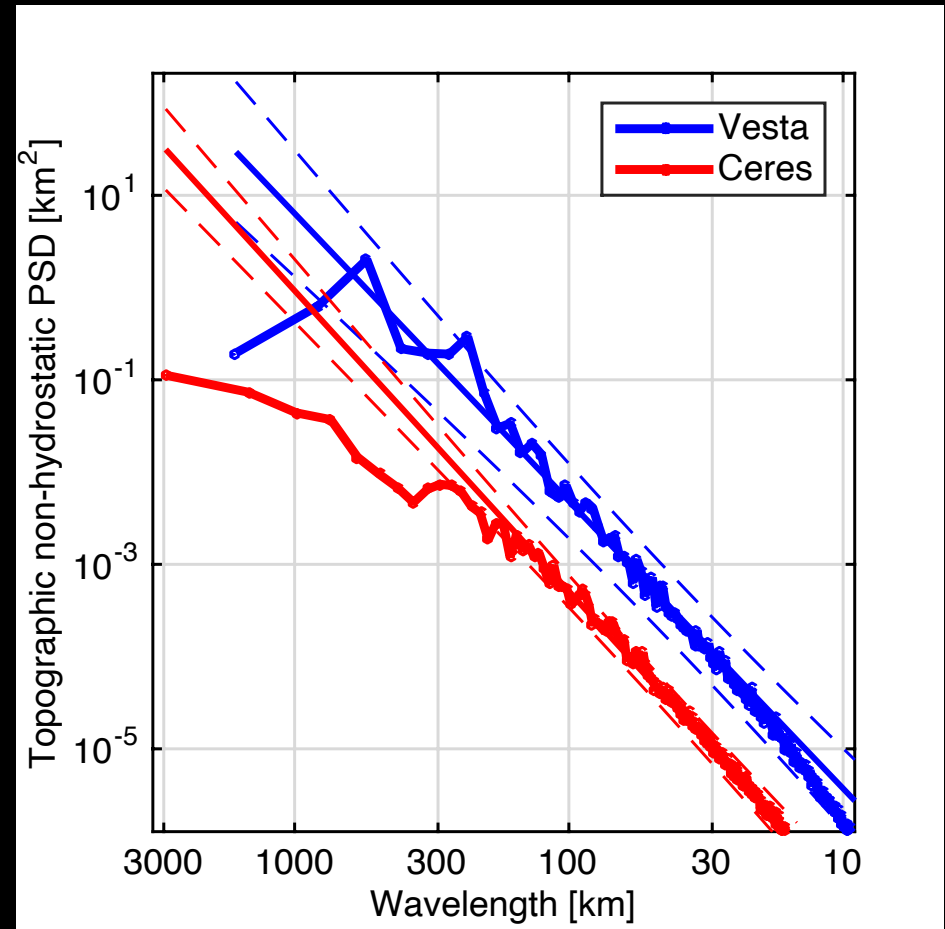
- **More general approach: study topography power spectrum**
- **Power spectra for Vesta closely fits with the power law to the lowest degrees ( $\lambda < 750$  km)**
- **Ceres power spectrum deviates from the power law at  $\lambda > 270$  km**



Ermakov et al., 2017a

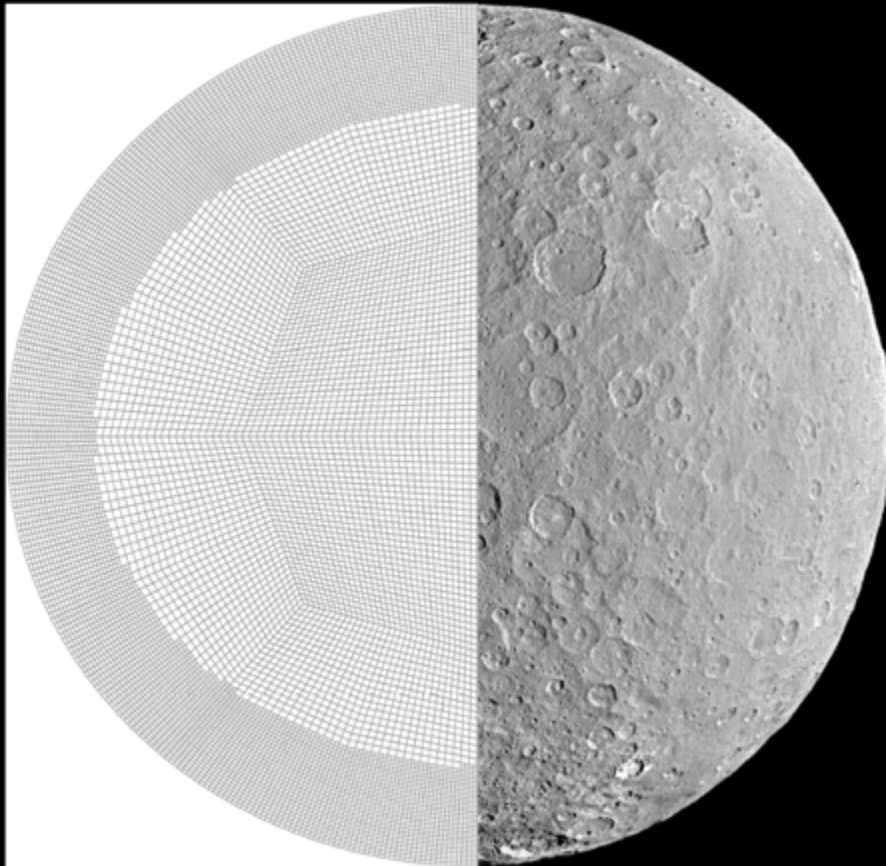
# Evidence for viscous relaxation

- More general approach: study topography power spectrum
- Power spectra for Vesta closely fits with the power law to the lowest degrees ( $\lambda < 750$  km)
- Ceres power spectrum deviates from the power law at  $\lambda > 270$  km



Ermakov et al., 2017a

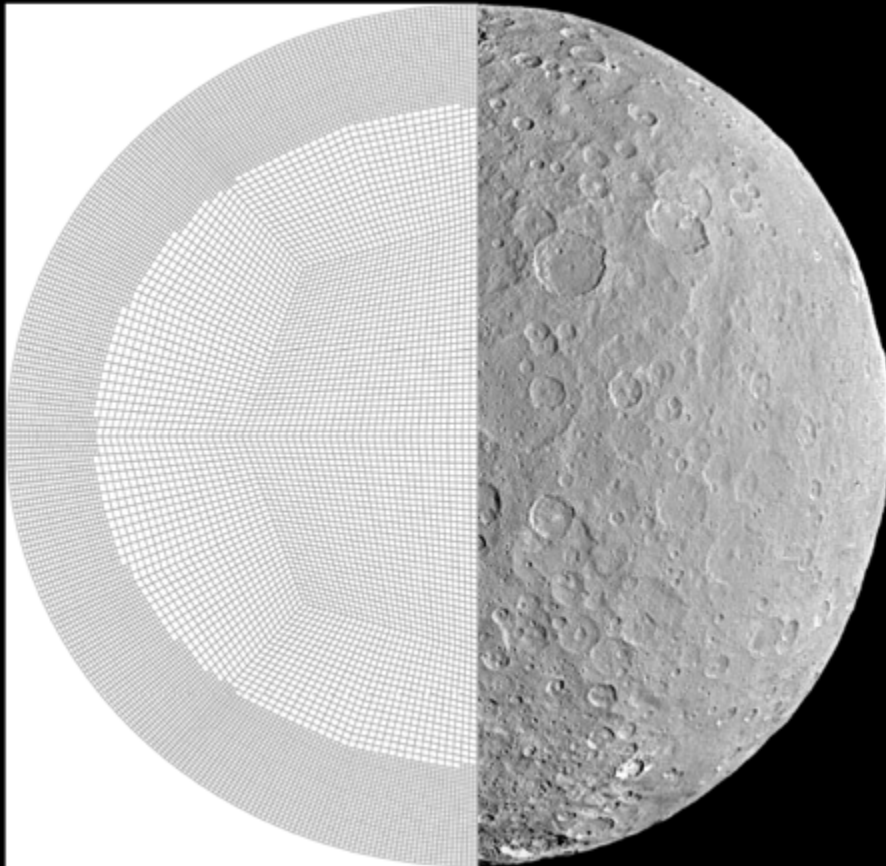
# Finite element model



- Assume a density and rheology structure
- Solve Stokes equation for an incompressible flow using deal.ii library
- Compute the evolution of the outer surface power spectrum

Fu et al., 2014; Fu et al., 2017

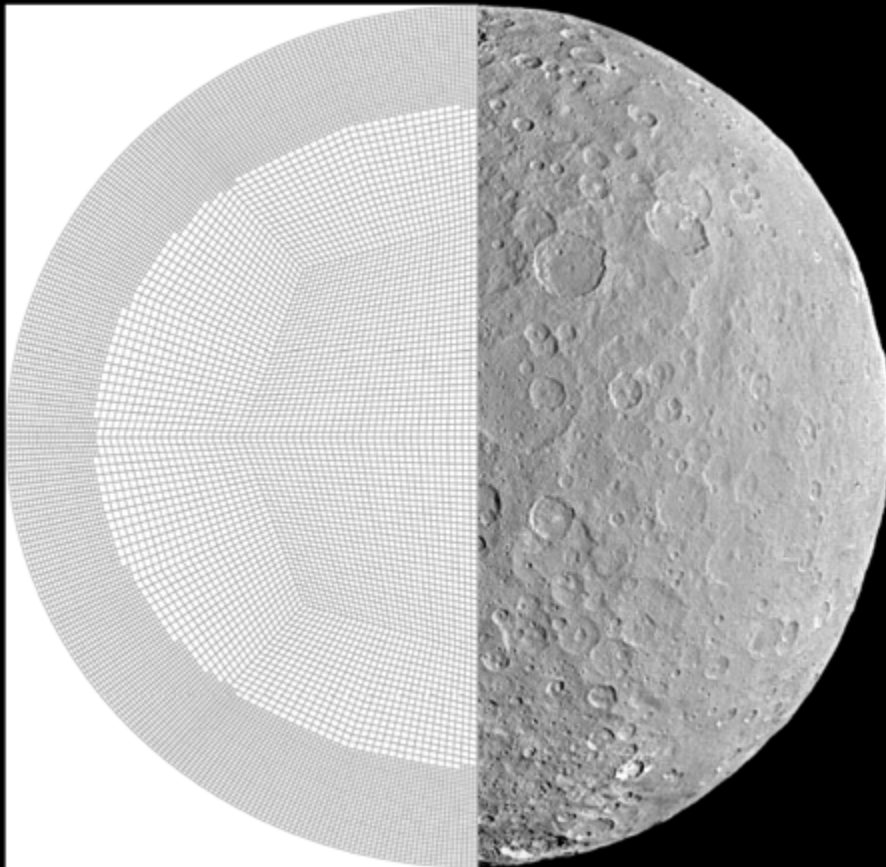
# Finite element model



- Assume a density and rheology structure
- Solve Stokes equation for an incompressible flow using deal.ii library
- Compute the evolution of the outer surface power spectrum

Fu et al., 2014; Fu et al., 2017

# Finite element model

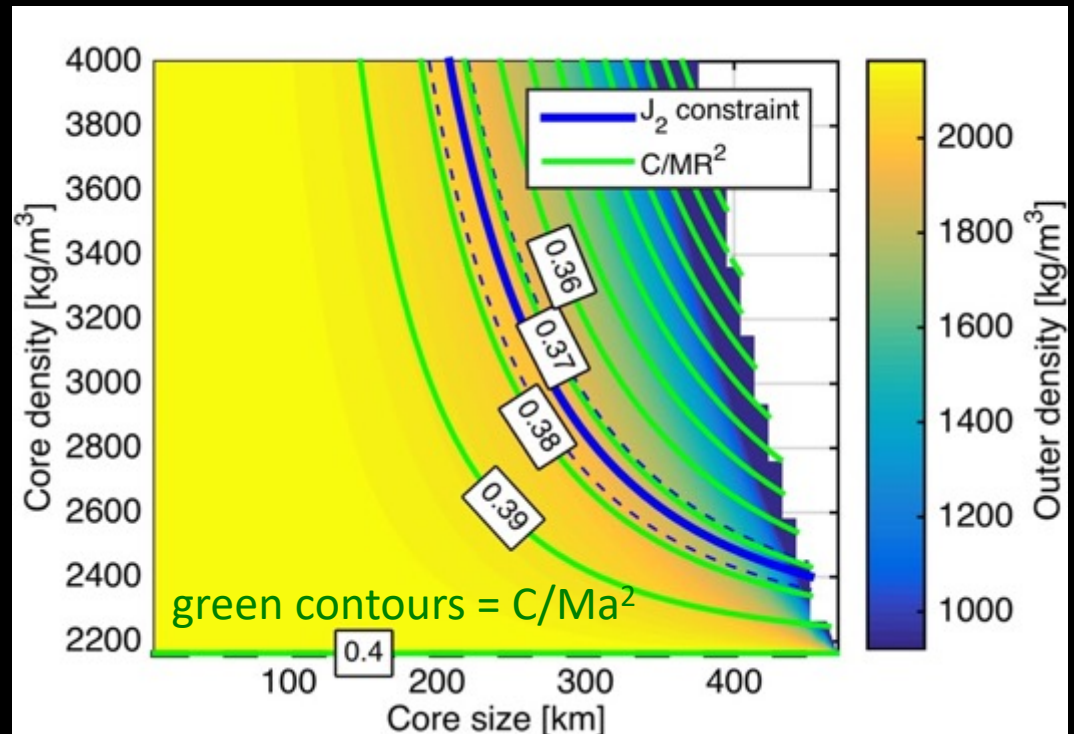


- Assume a density and rheology structure
- Solve Stokes equation for an incompressible flow using deal.ii library
- Compute the evolution of the outer surface power spectrum

Fu et al., 2014; Fu et al., 2017

# Ceres internal structure

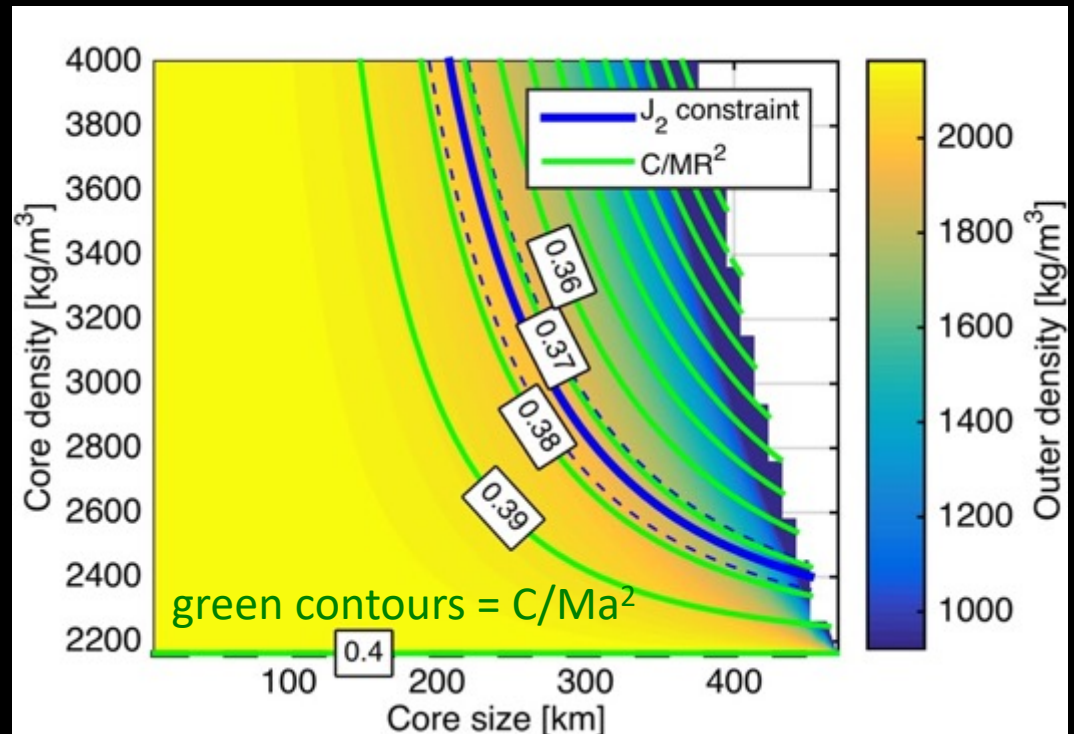
- Two-layer model - simplest model to interpret the gravity-topography data
- Only 5 parameters: two densities, two radii and rotation rate
- Yields  $C/Ma^2 = 0.373$   
 $C/M(R_{vol})^2 = 0.392$



Using Tricarico 2014 for computing hydrostatic equilibrium

# Ceres internal structure

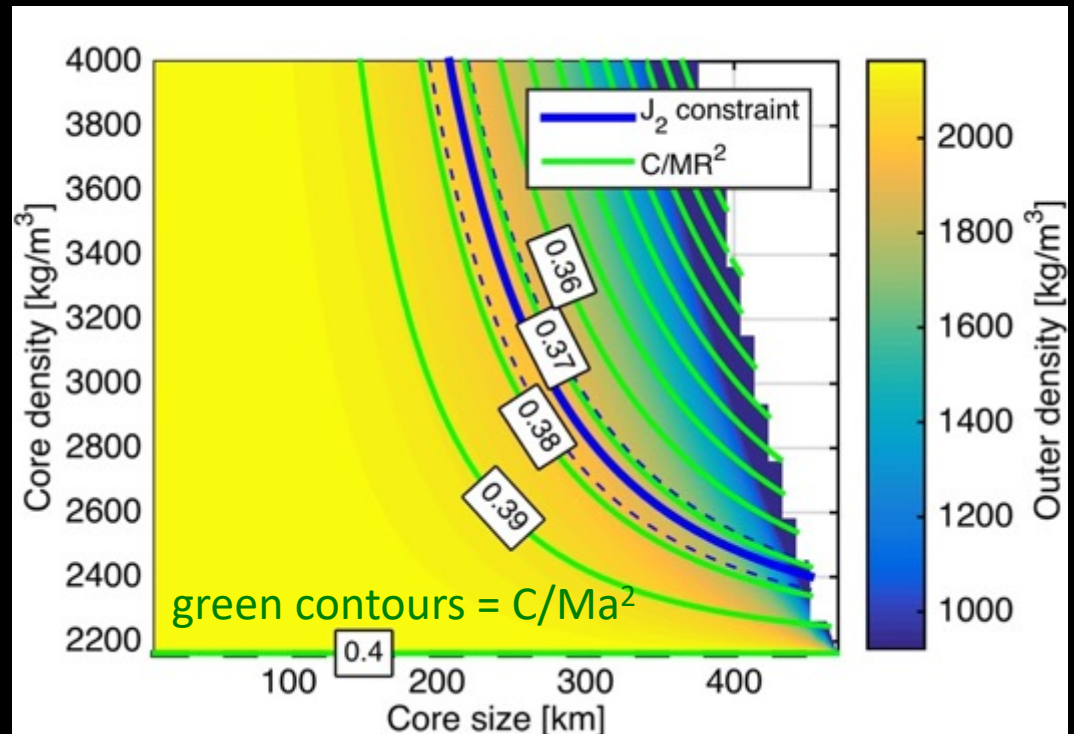
- Two-layer model - simplest model to interpret the gravity-topography data
- Only 5 parameters: two densities, two radii and rotation rate
- Yields  $C/Ma^2 = 0.373$   
 $C/M(R_{vol})^2 = 0.392$



Using Tricarico 2014 for computing hydrostatic equilibrium

# Ceres internal structure

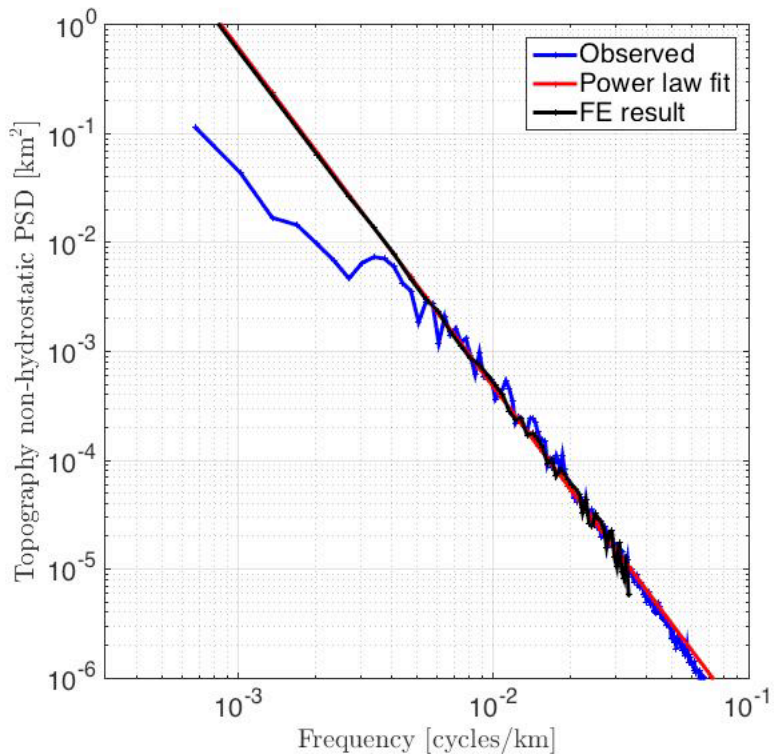
- Two-layer model - simplest model to interpret the gravity-topography data
- Only 5 parameters: two densities, two radii and rotation rate
- Yields  $C/Ma^2 = 0.373$   
 $C/M(R_{vol})^2 = 0.392$



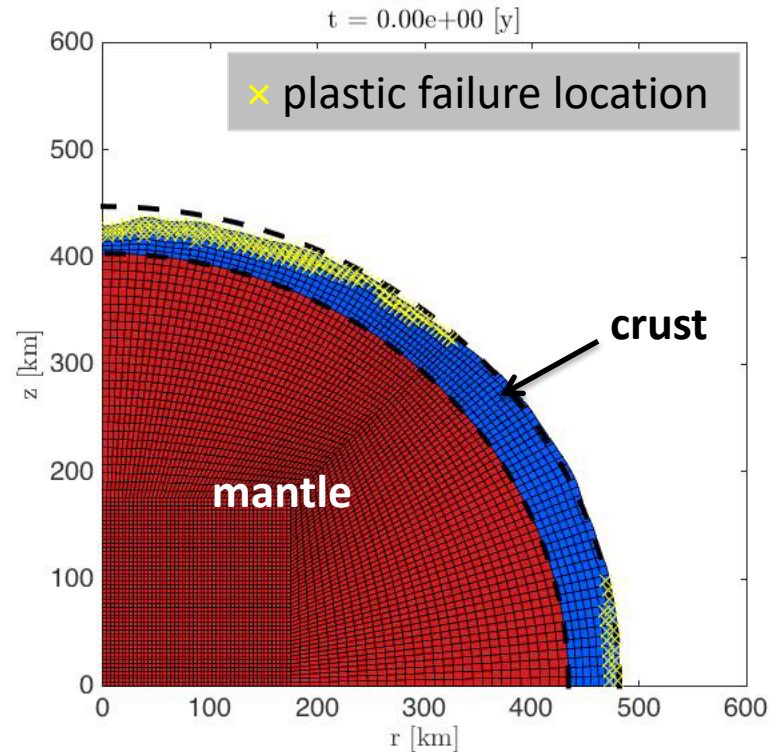
Using Tricarico 2014 for computing hydrostatic equilibrium

# Example of a FE modeling run

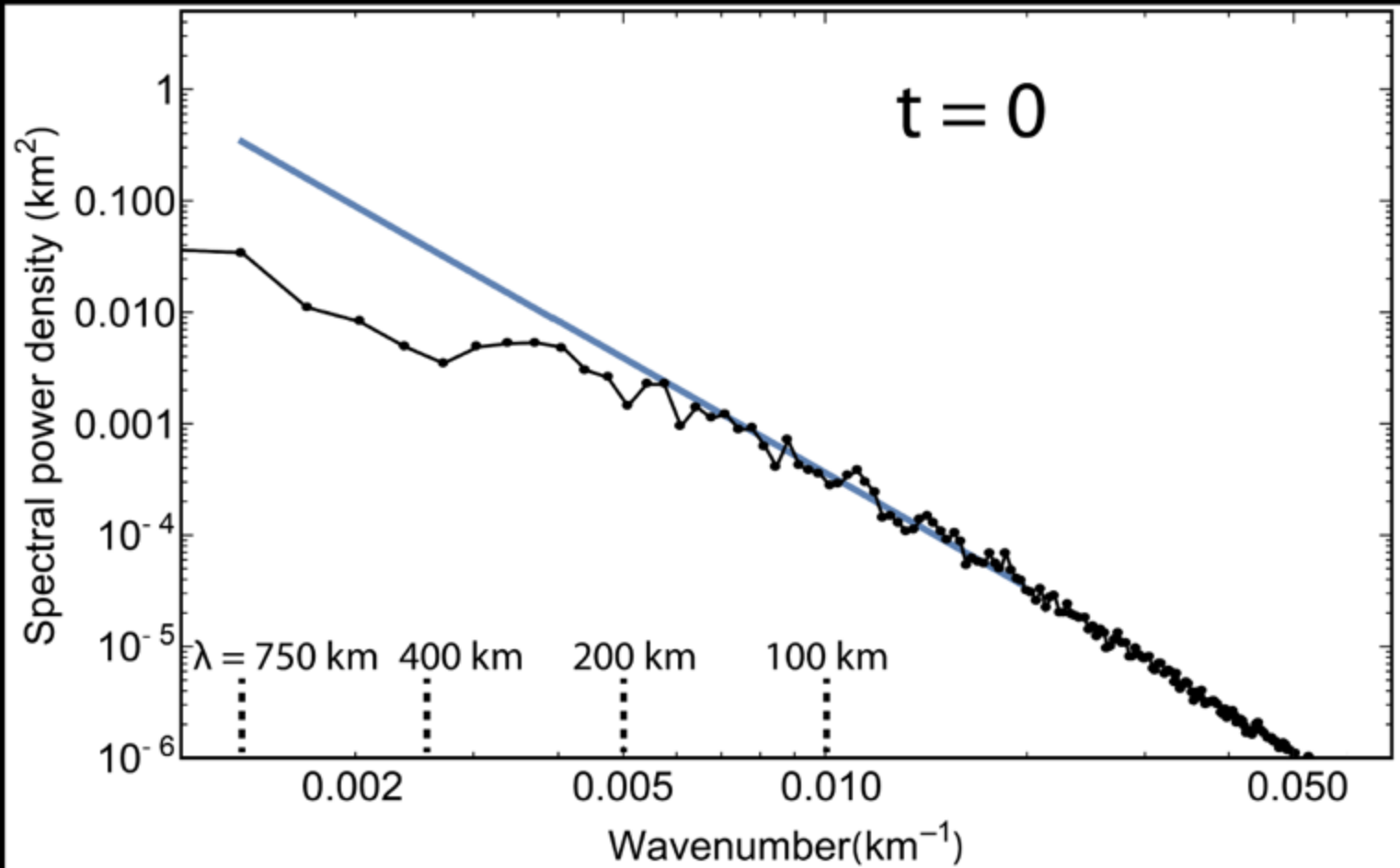
relaxation in the frequency domain



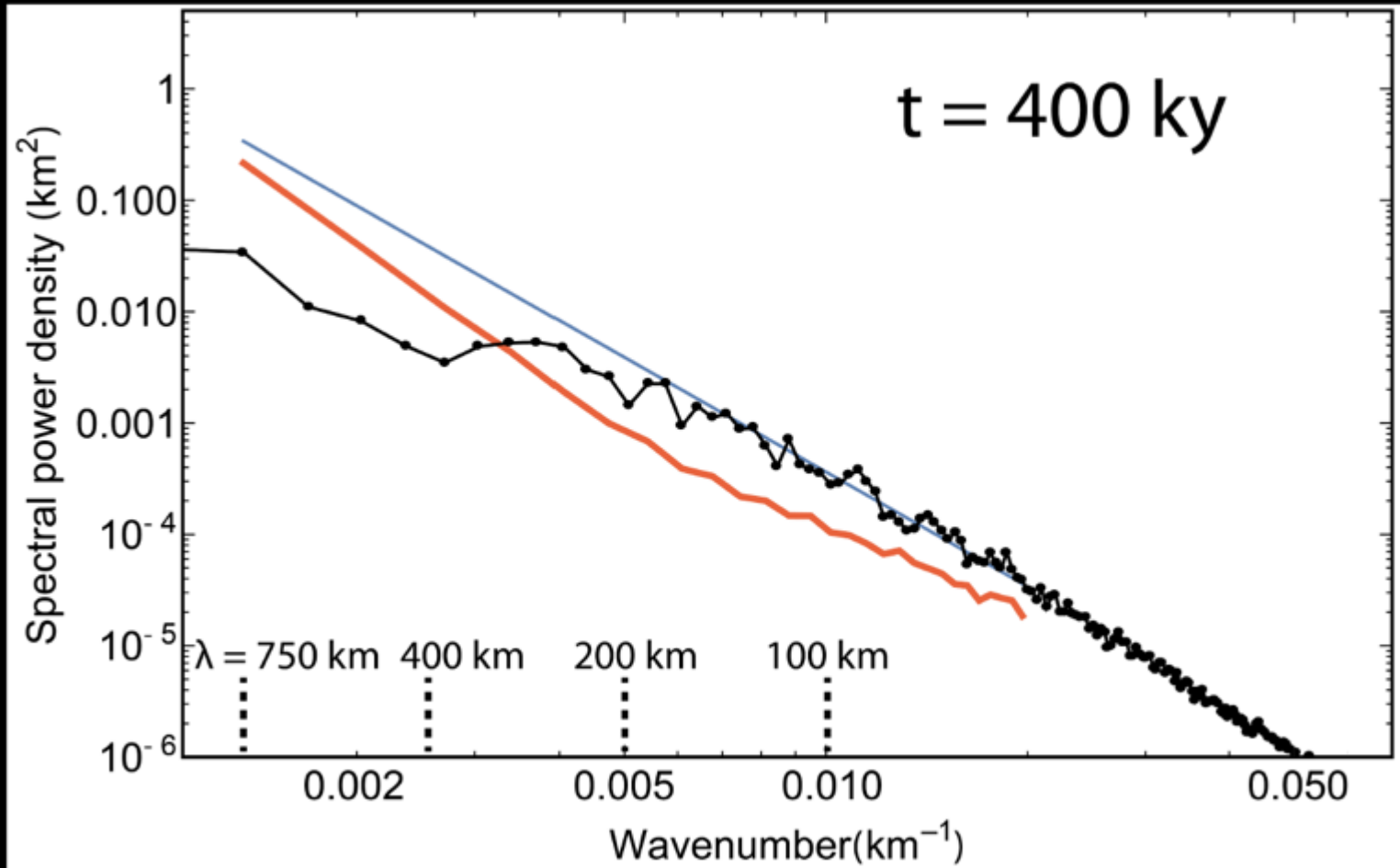
relaxation in the spatial domain



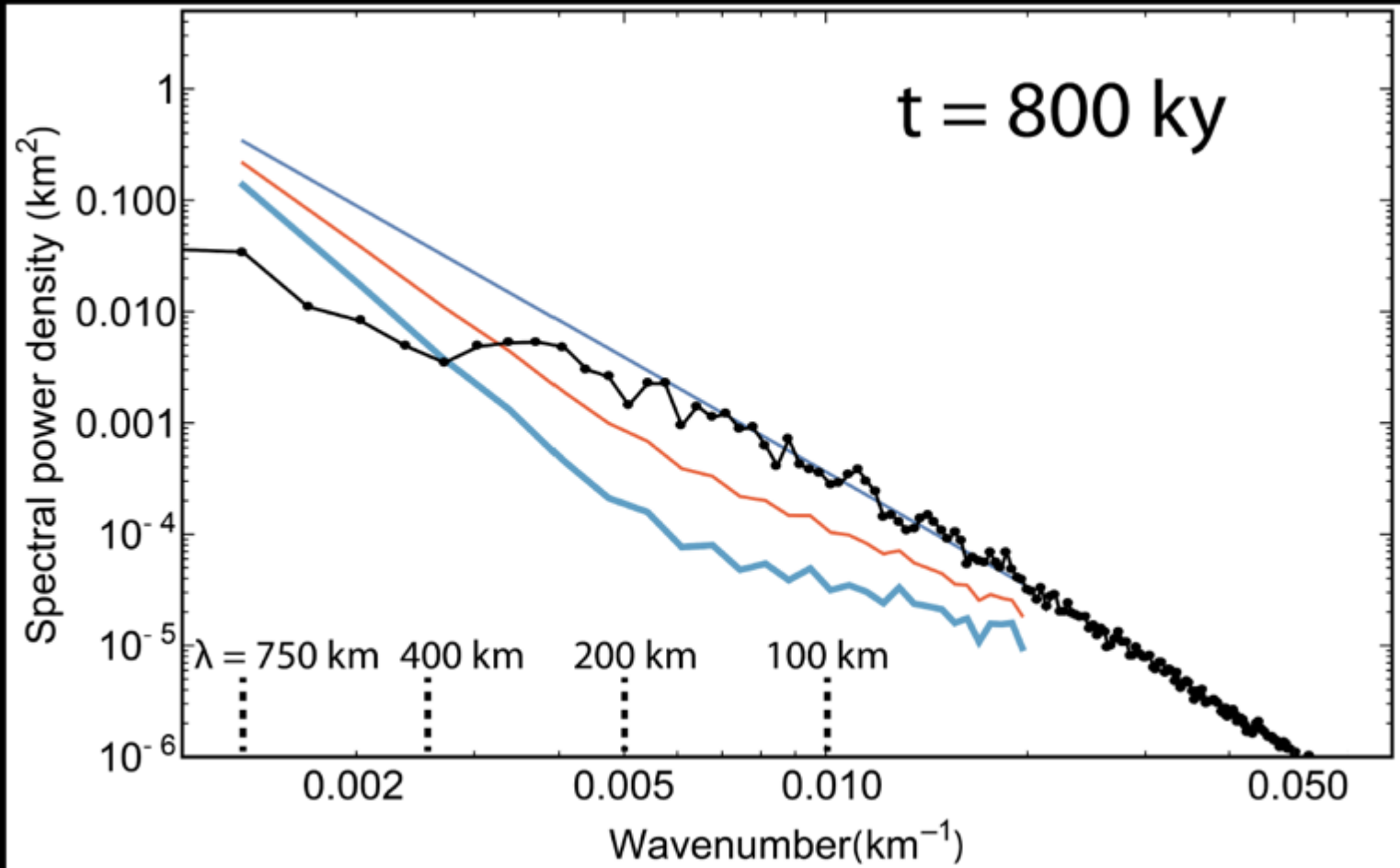
# Ice shell, rocky interior



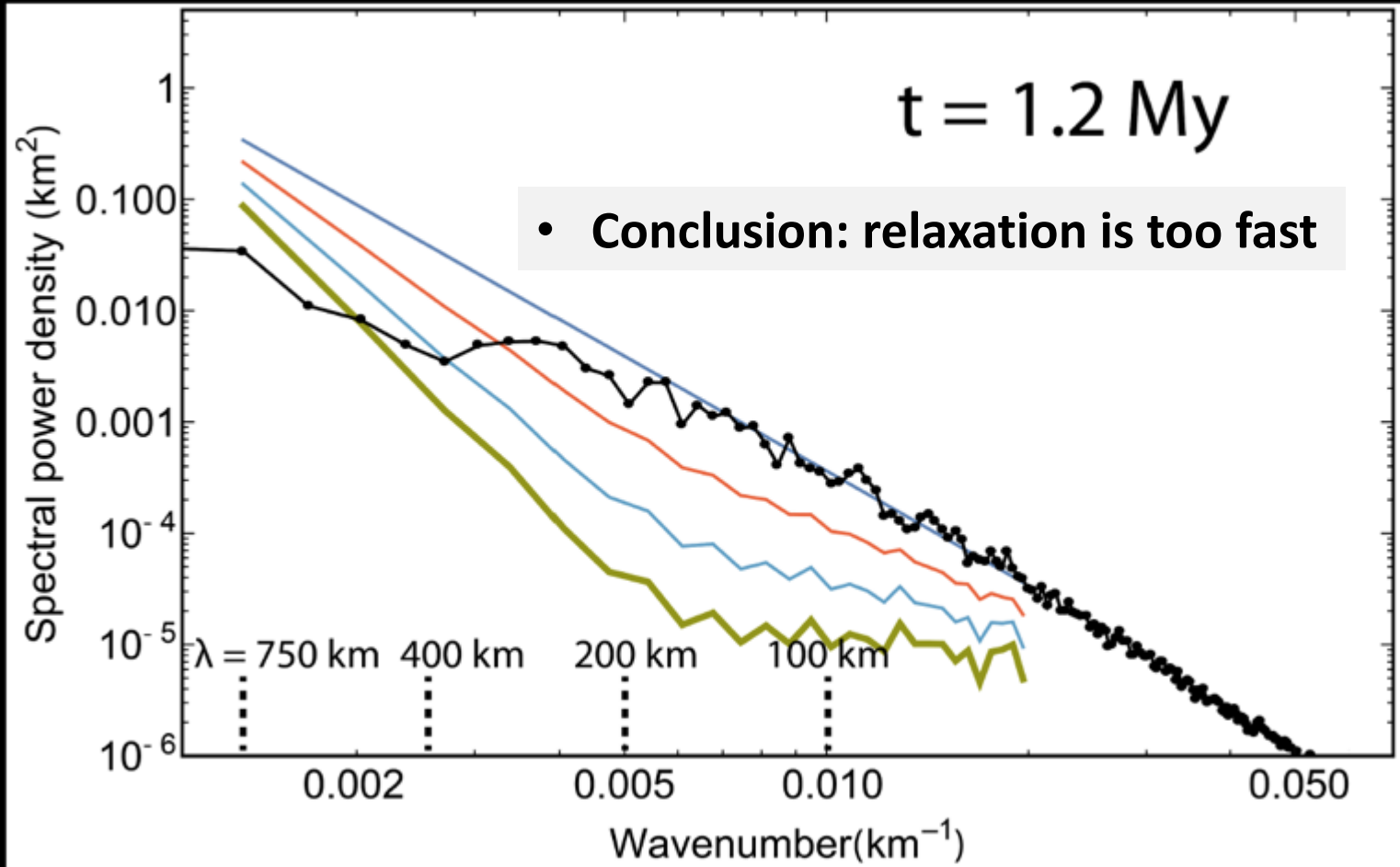
# Ice shell, rocky interior



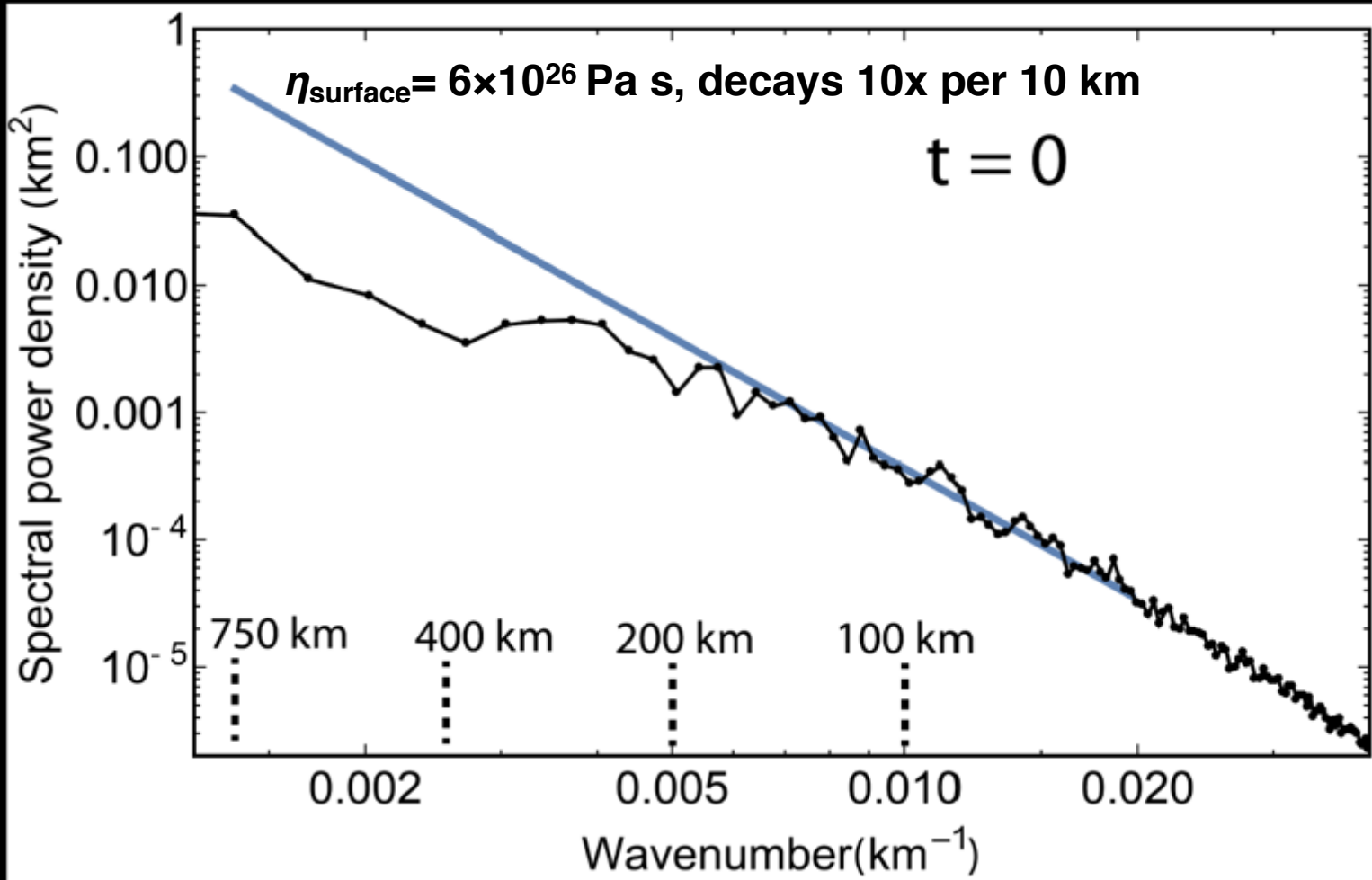
# Ice shell, rocky interior



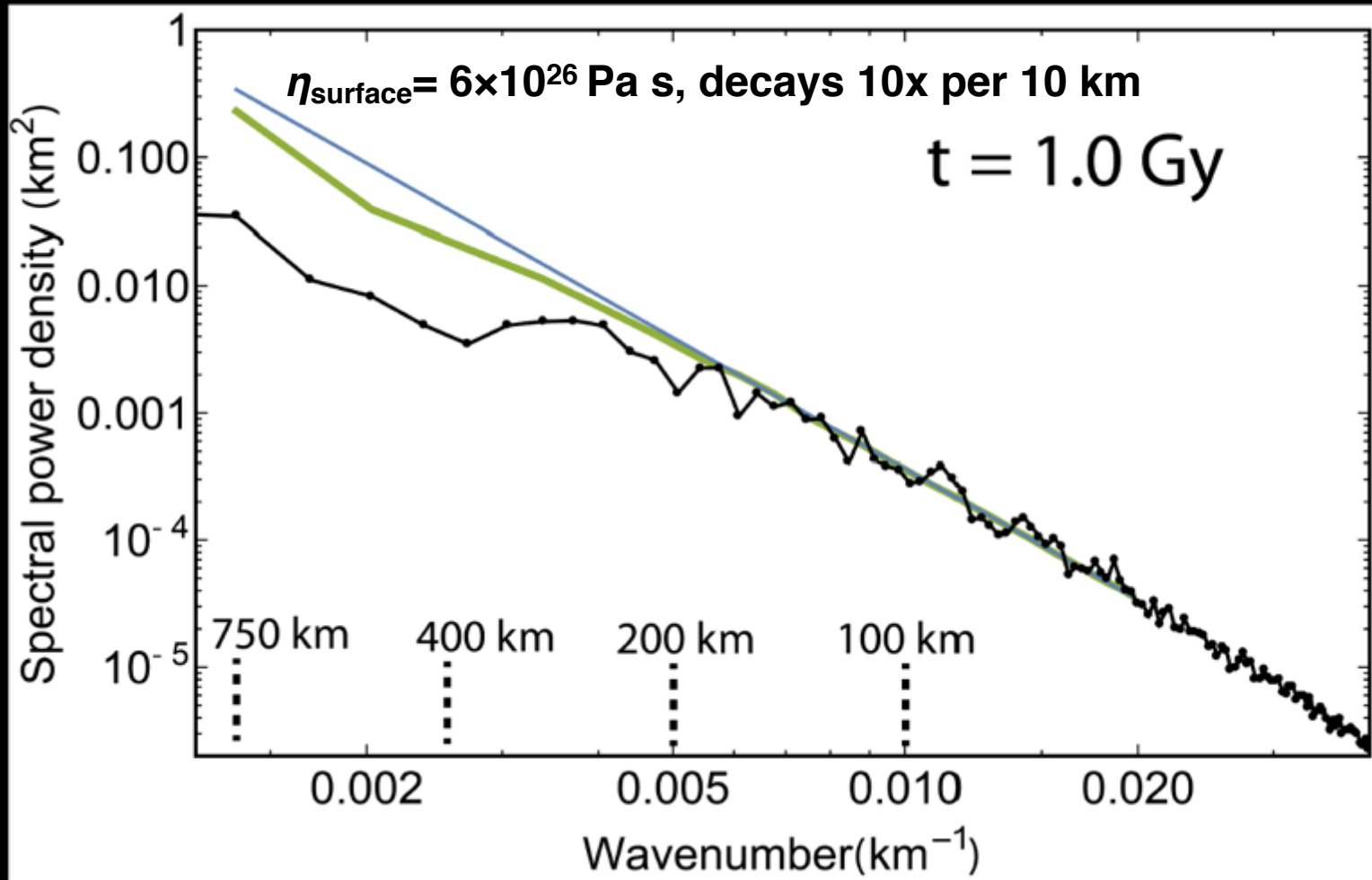
# Ice shell, rocky interior



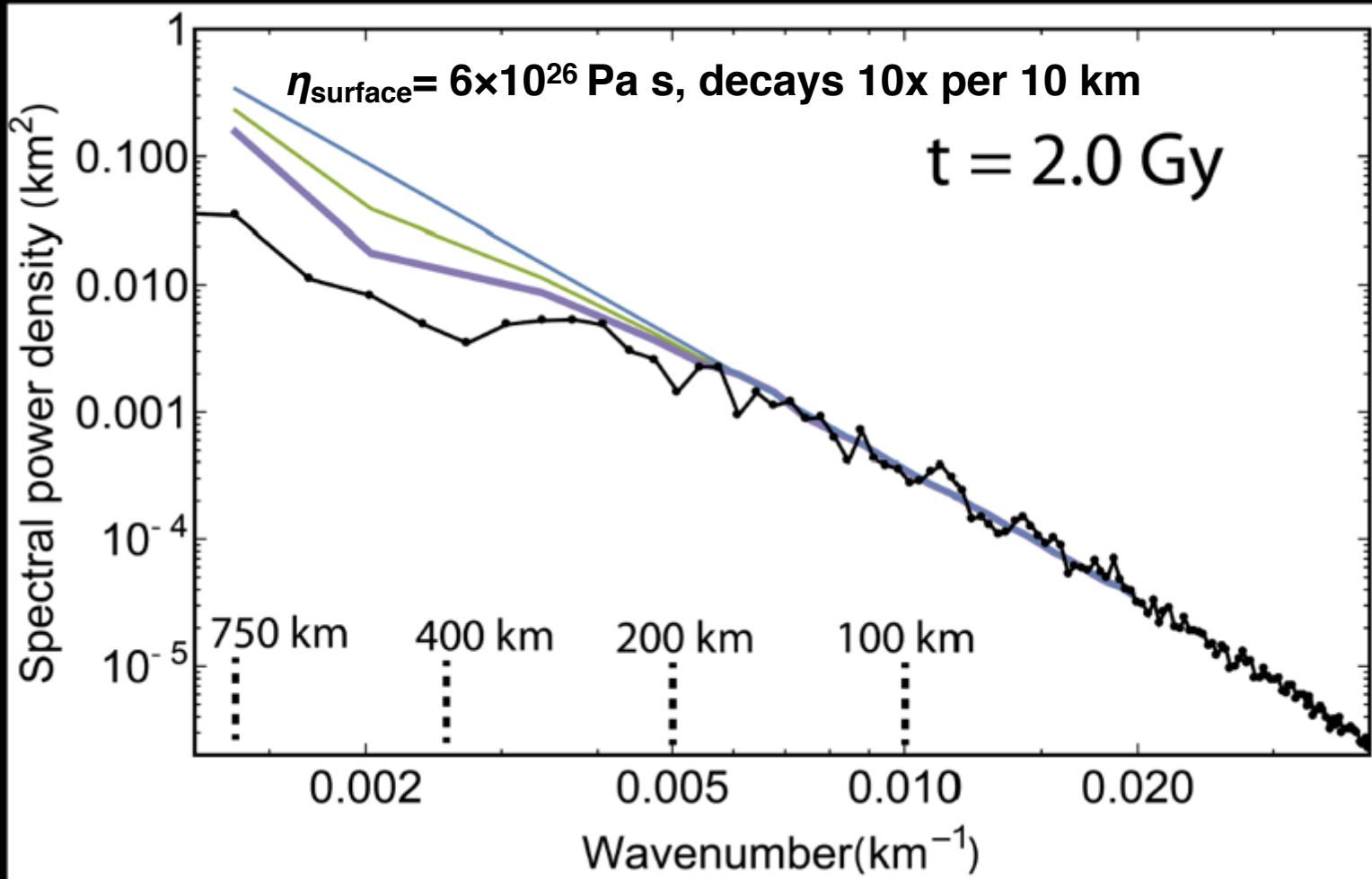
# Stiff surface, weak interior



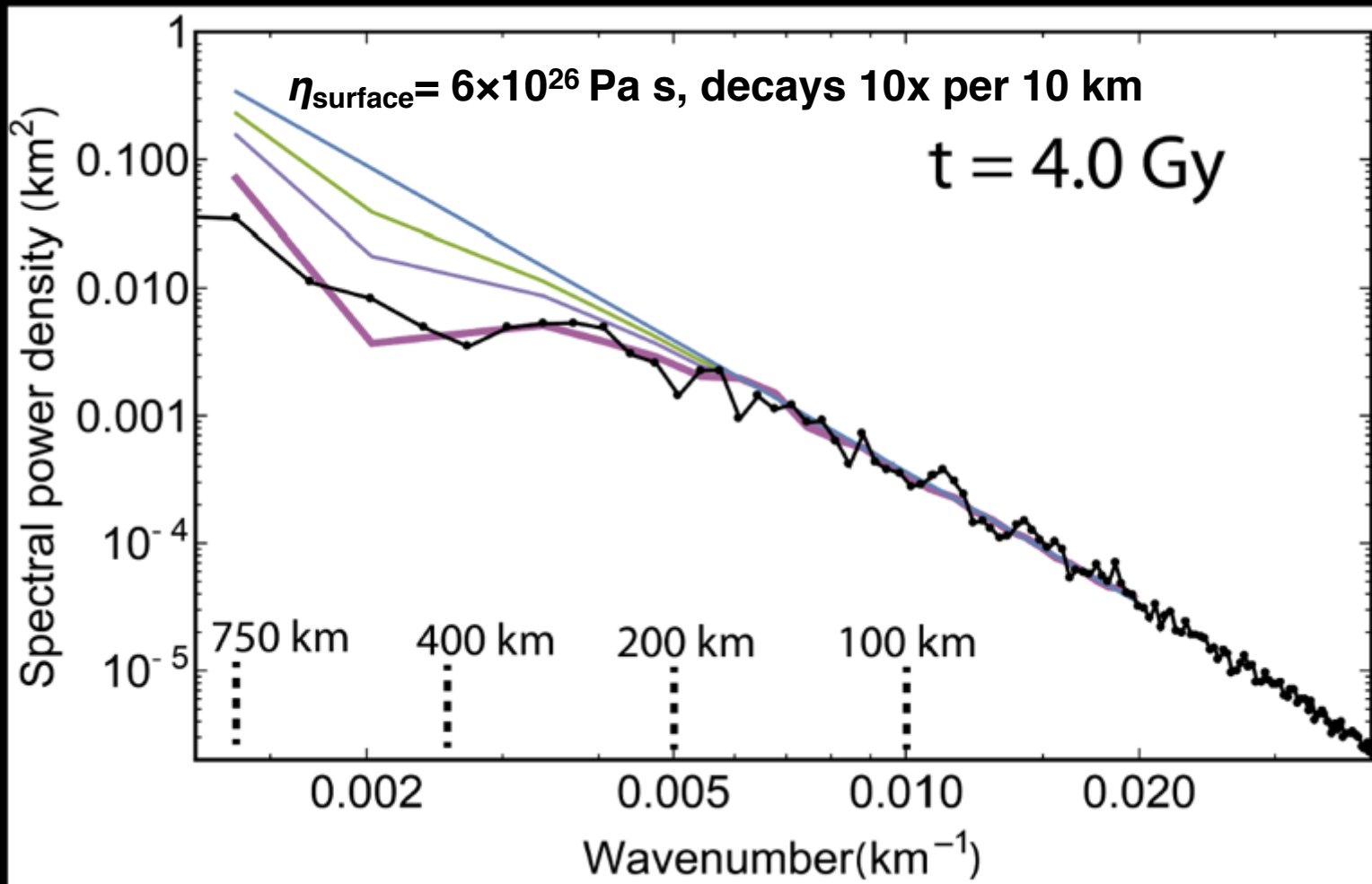
# Stiff surface, weak interior



# Stiff surface, weak interior

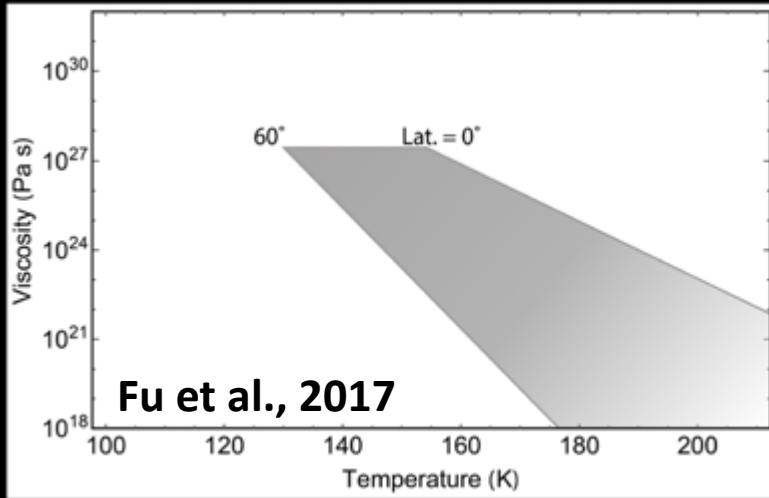


# Stiff surface, weak interior



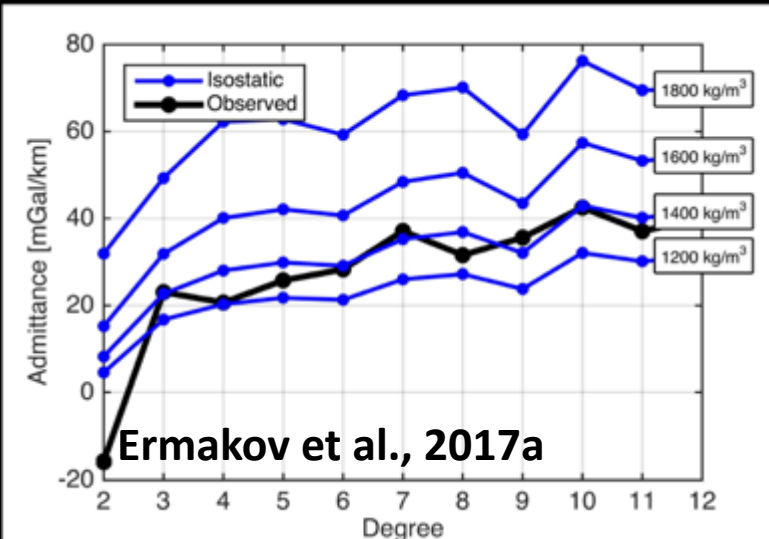
# Rheology and density constraints

Rheology constraint  
from FE modeling



- Ceres crust is  $\sim 1000$  times stronger than water ice
- Must be dominated by rock-like materials. Water ice in the Ceres' crust  $< 35$  vol%

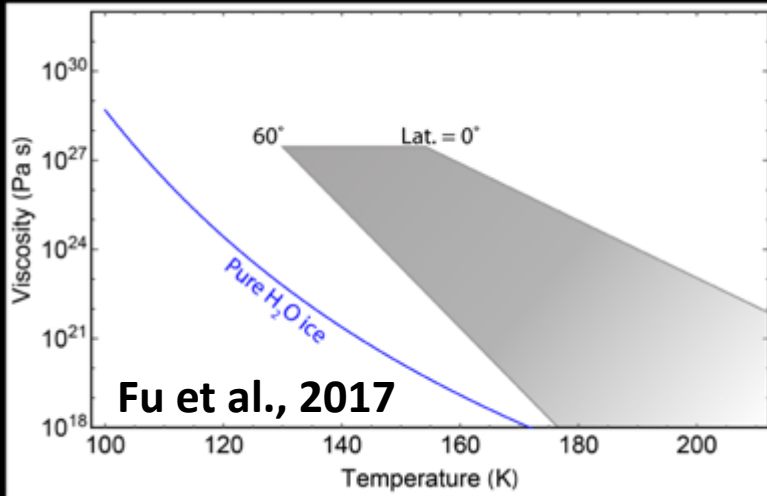
Density constraint from  
admittance modeling



- Light and strong crust
- Low core density (2.4 g/cc) implies its hydrated state

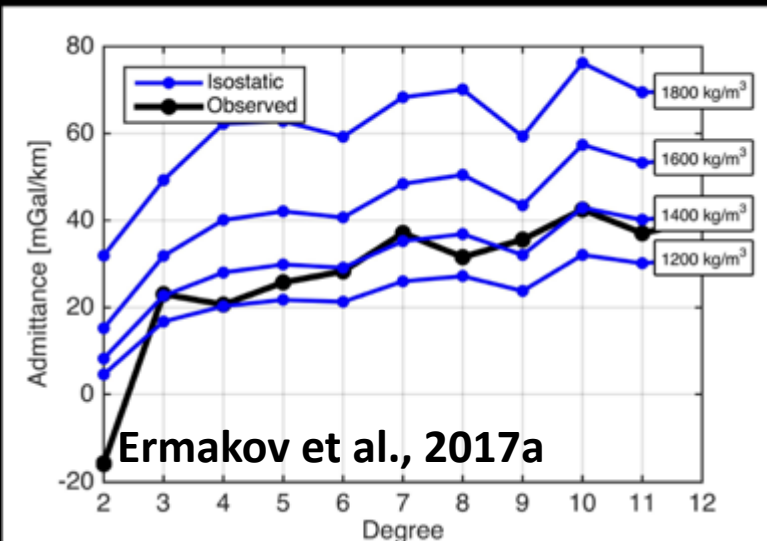
# Rheology and density constraints

Rheology constraint  
from FE modeling



- Ceres crust is ~ 1000 times stronger than water ice
- Must be dominated by rock-like materials. Water ice in the Ceres' crust <35 vol%

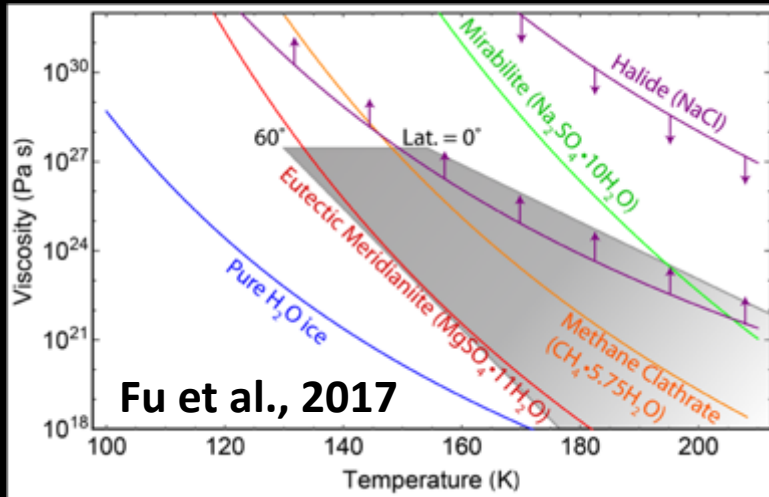
Density constraint from  
admittance modeling



- Light and strong crust
- Low core density (2.4 g/cc) implies its hydrated state

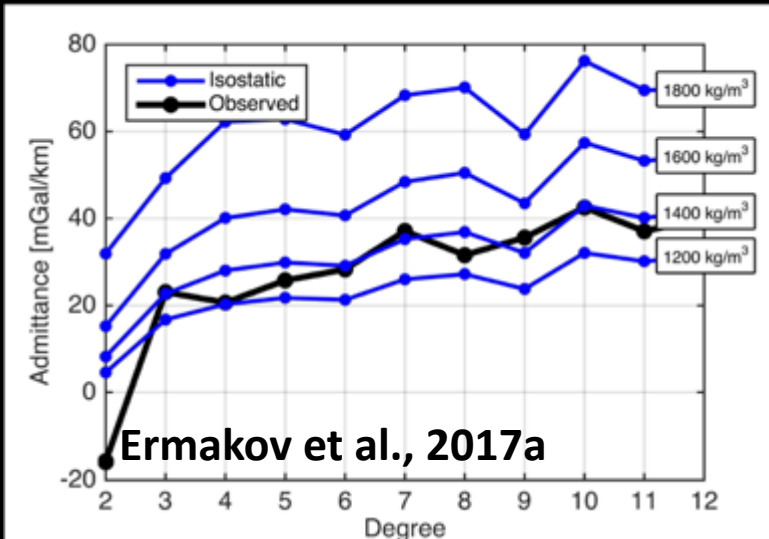
# Rheology and density constraints

Rheology constraint  
from FE modeling



- Ceres crust is ~ 1000 times stronger than water ice
- Must be dominated by rock-like materials. Water ice in the Ceres' crust <35 vol%

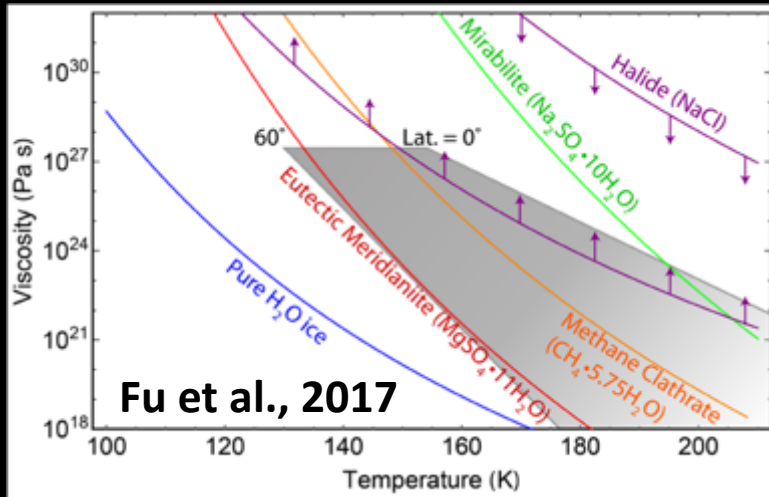
Density constraint from  
admittance modeling



- Light and strong crust
- Low core density (2.4 g/cc) implies its hydrated state

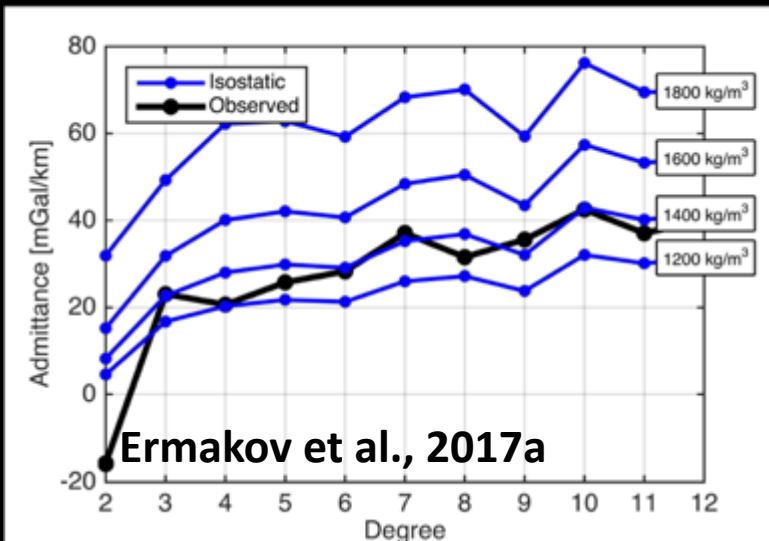
# Rheology and density constraints

Rheology constraint  
from FE modeling



- Ceres crust is  $\sim 1000$  times stronger than water ice
- Must be dominated by rock-like materials. Water ice in the Ceres' crust  $< 35$  vol%

Density constraint from  
admittance modeling



- Light and strong crust
- Low core density (2.4 g/cc) implies its hydrated state

# Compensation: Vesta vs Ceres

## ➤ Homogeneous admittance

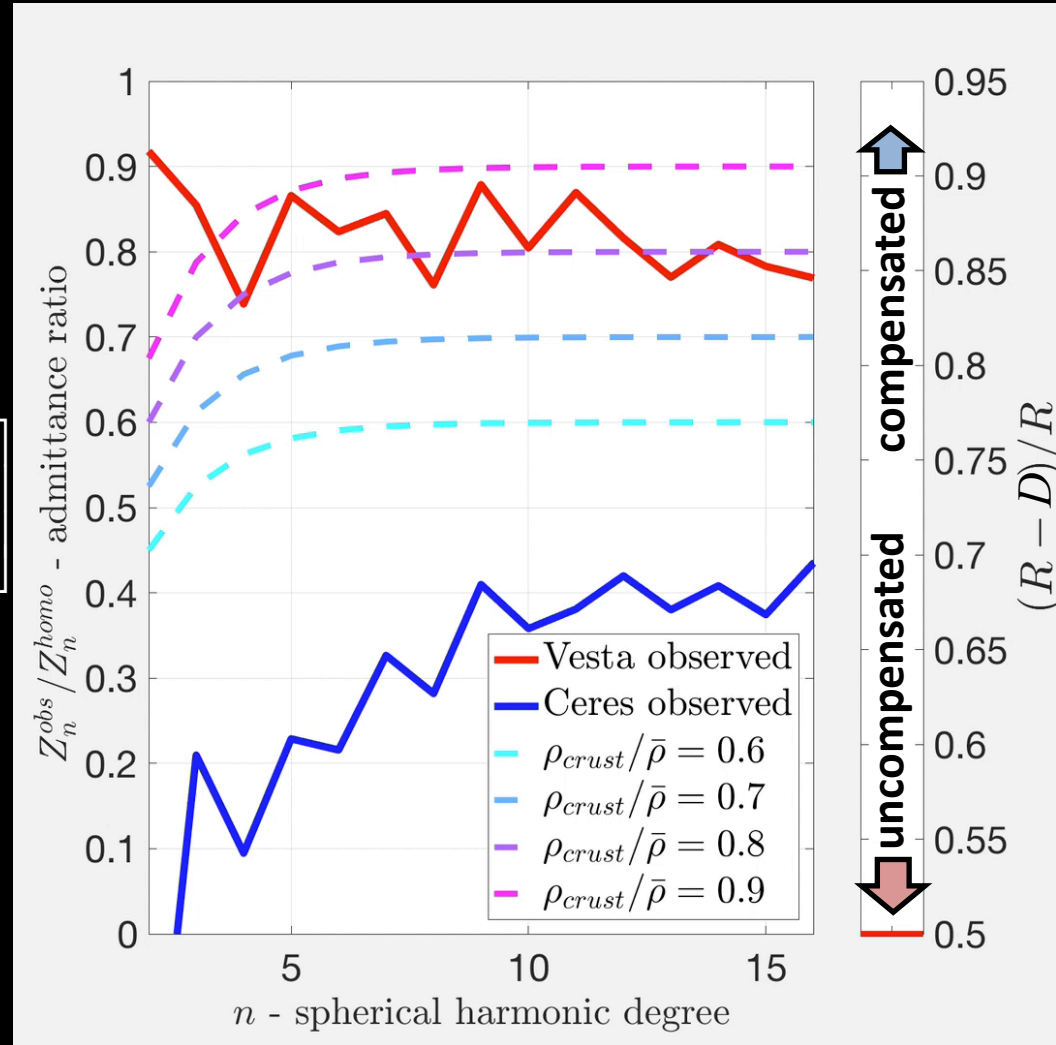
$$Z_n = \frac{GM}{R^3} \frac{3(n+1)}{2n+1}$$

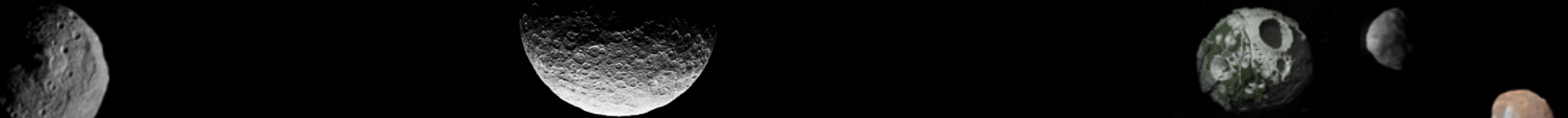
## ➤ Isostatic model admittance

$$Z_n = \frac{GM}{R^3} \frac{3(n+1)}{2n+1} \frac{\rho_{crust}}{\bar{\rho}} \left[ 1 - \left( \frac{R - D_{comp}}{R} \right)^{n+2} \right]$$

## ➤ Effective density spectrum

$$\tilde{\rho}_n = \frac{Z_n^{obs}}{Z_n^{homo}} \cdot \bar{\rho}$$



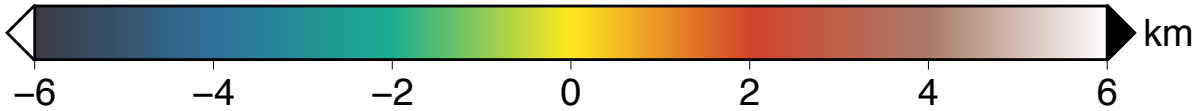


# Compensation for **Vesta** and **Ceres**

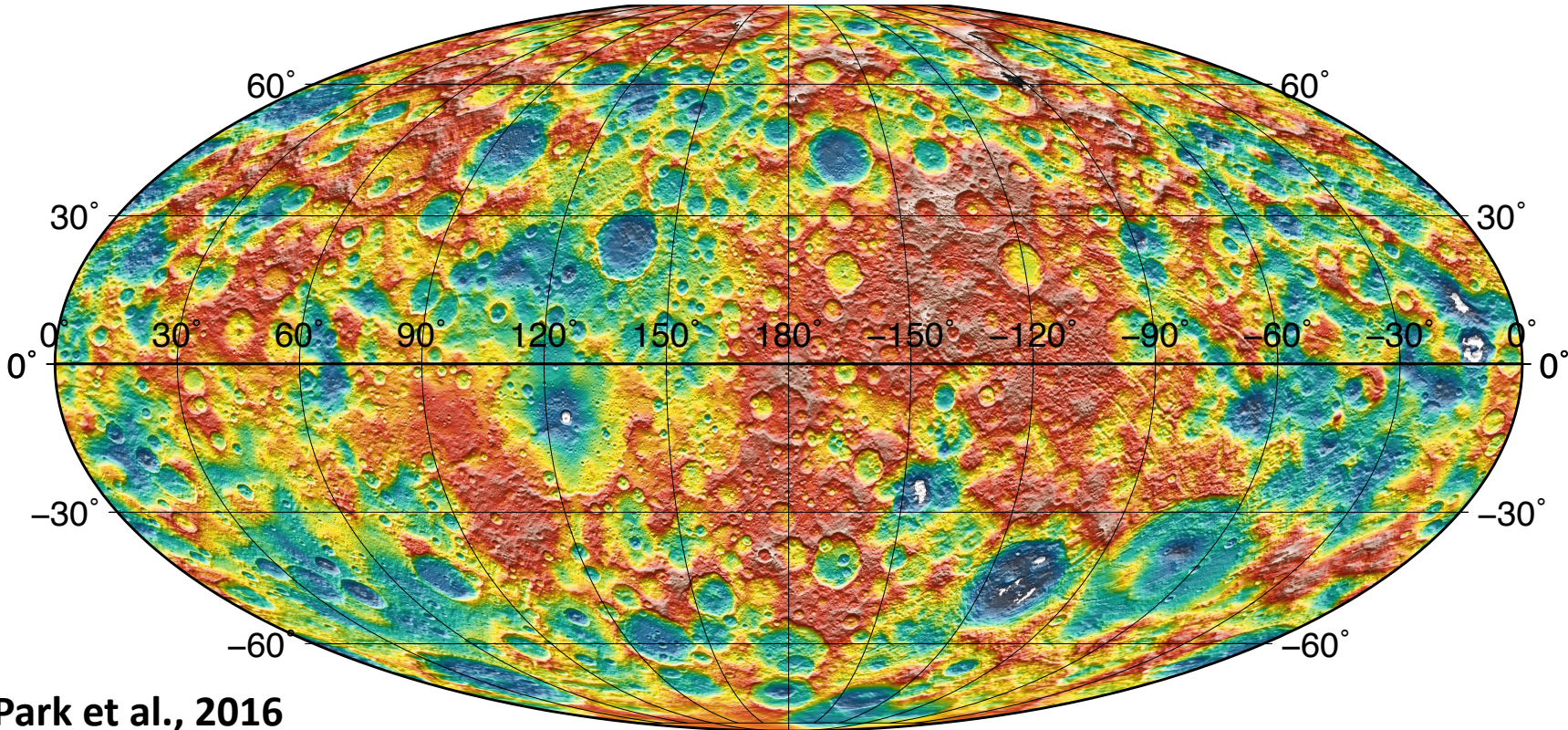
- **Vesta** topography is uncompensated
- **Vesta** acquired most of its topography when the crust was already cool and not-relaxing
- **Ceres** topography is compensated
- Lower viscosities (compared to Vesta) enabled relaxation of topography to the isostatic state



# Local structures on Ceres



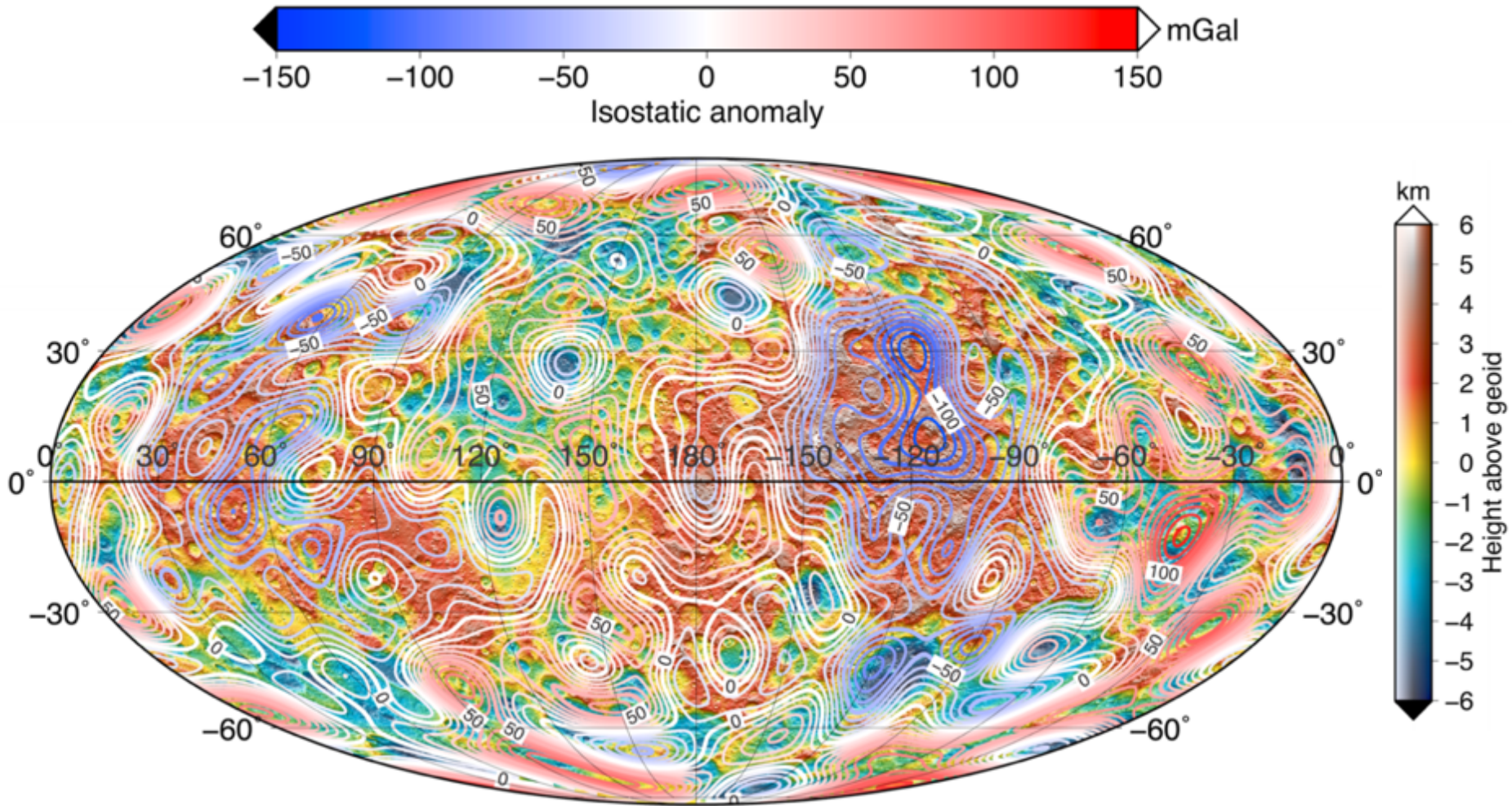
Height above geoid



Park et al., 2016



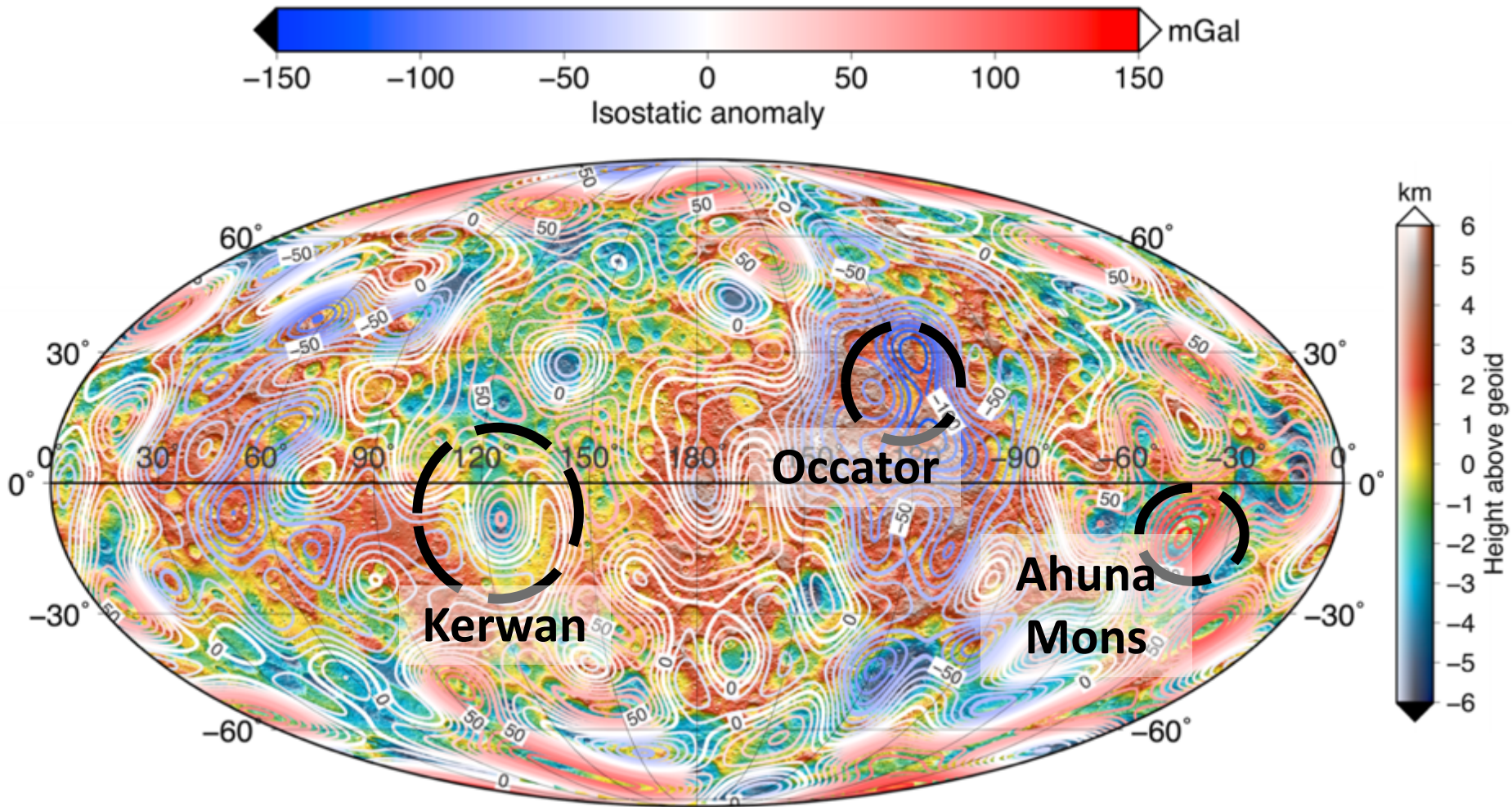
# Isostatic anomaly



Ermakov et al., 2017a

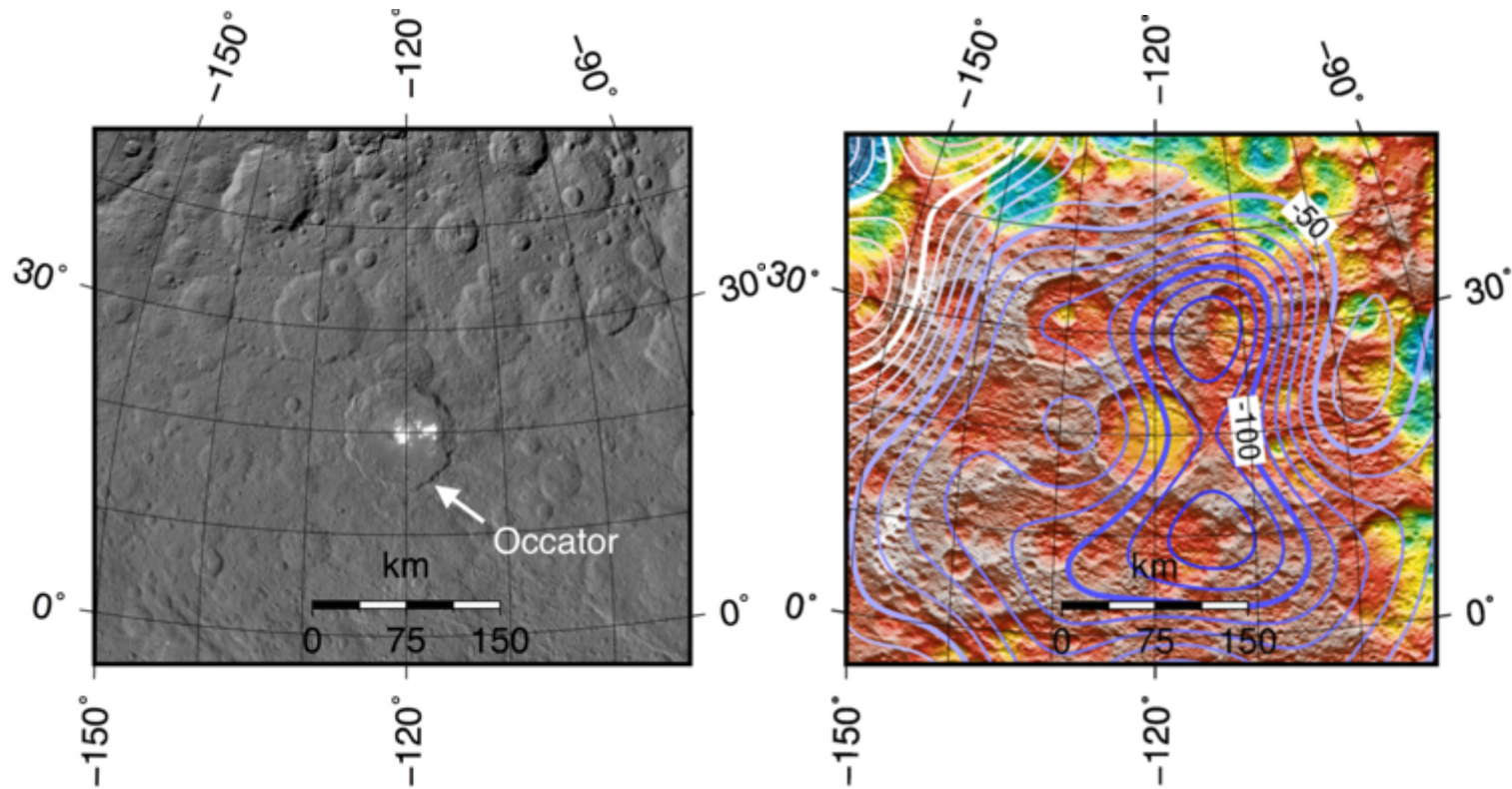


# Isostatic anomaly



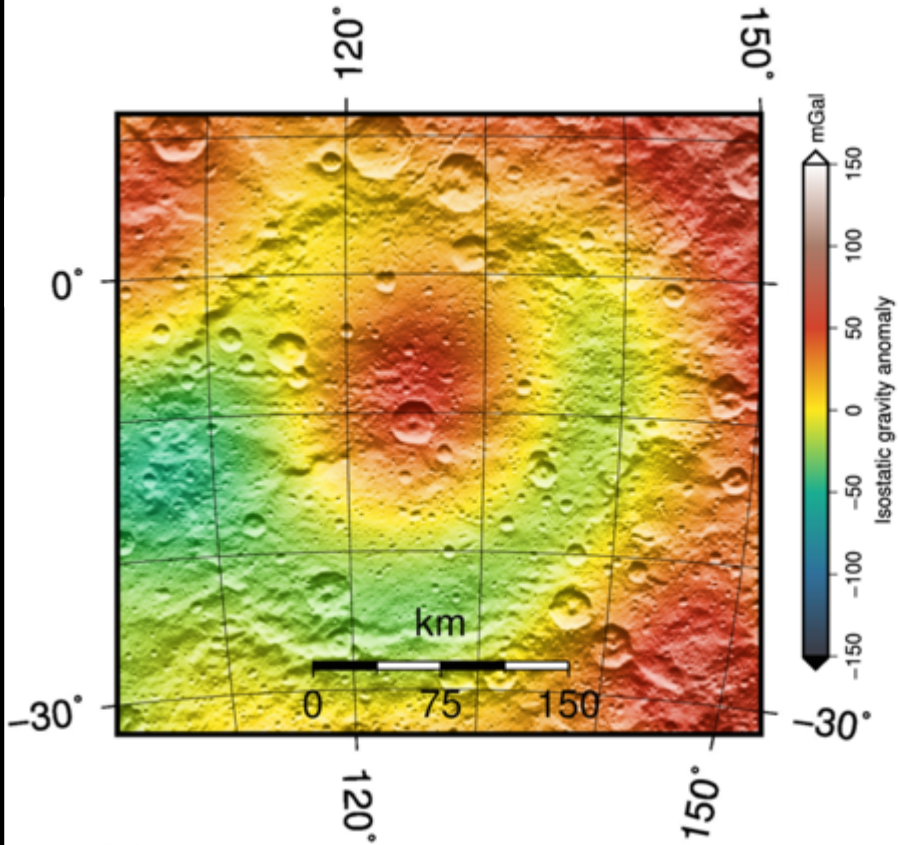
Ermakov et al., 2017a

# Occator isostatic anomaly



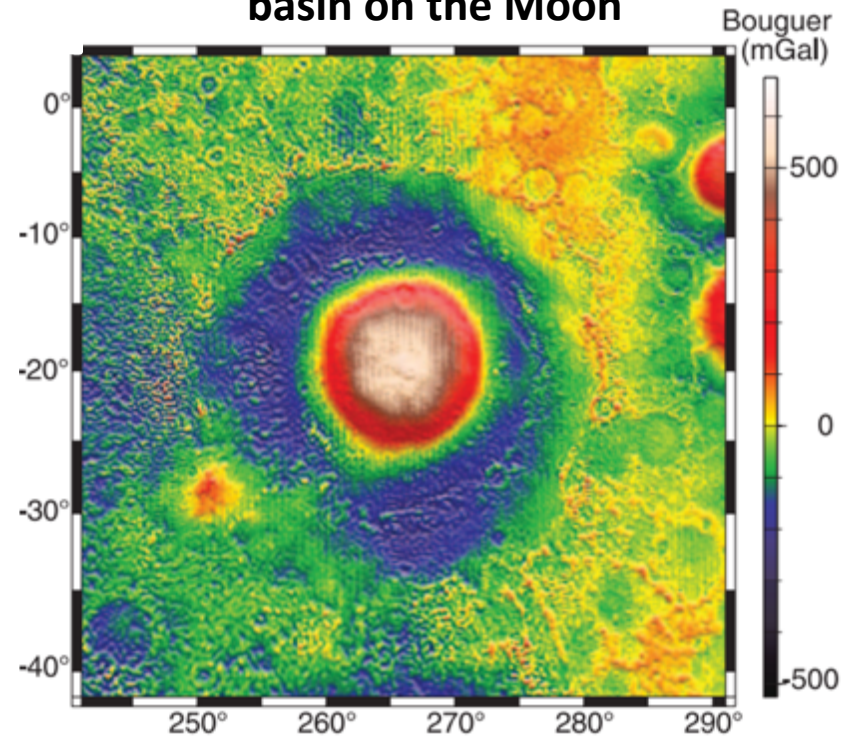
# Mascons

Kerwan isostatic anomaly



Ermakov et al., 2017a

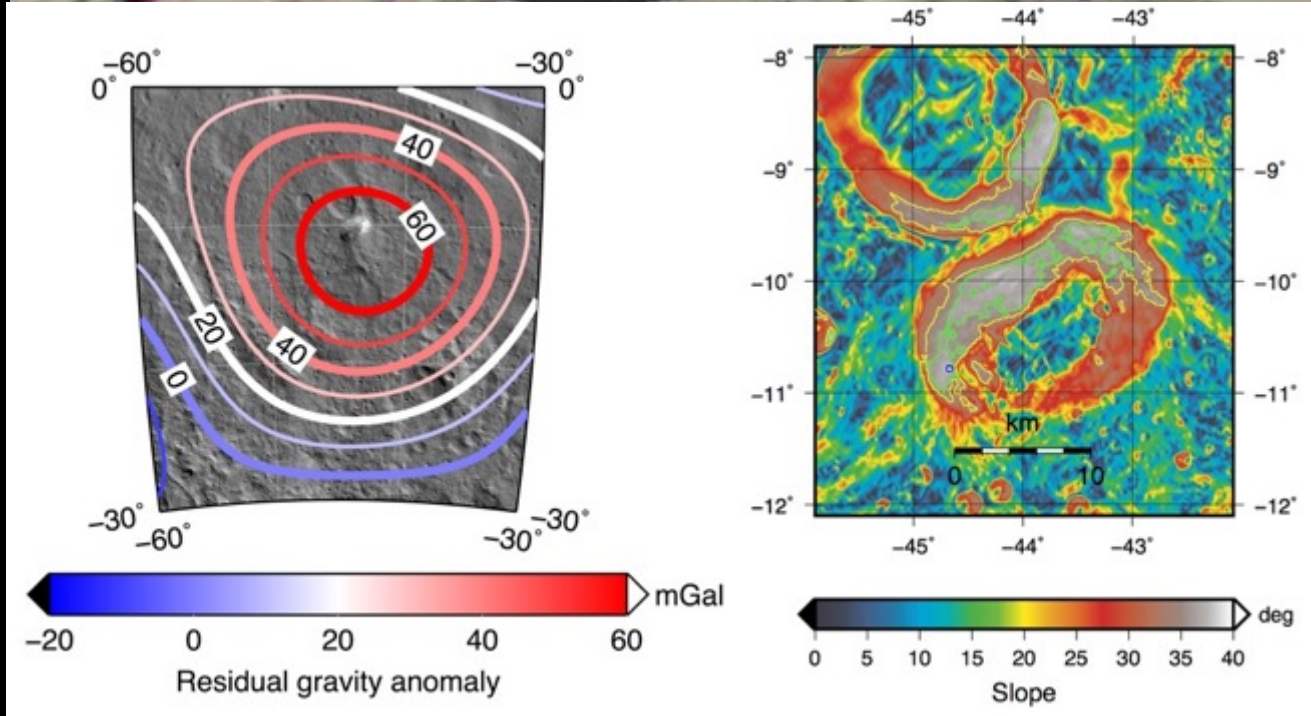
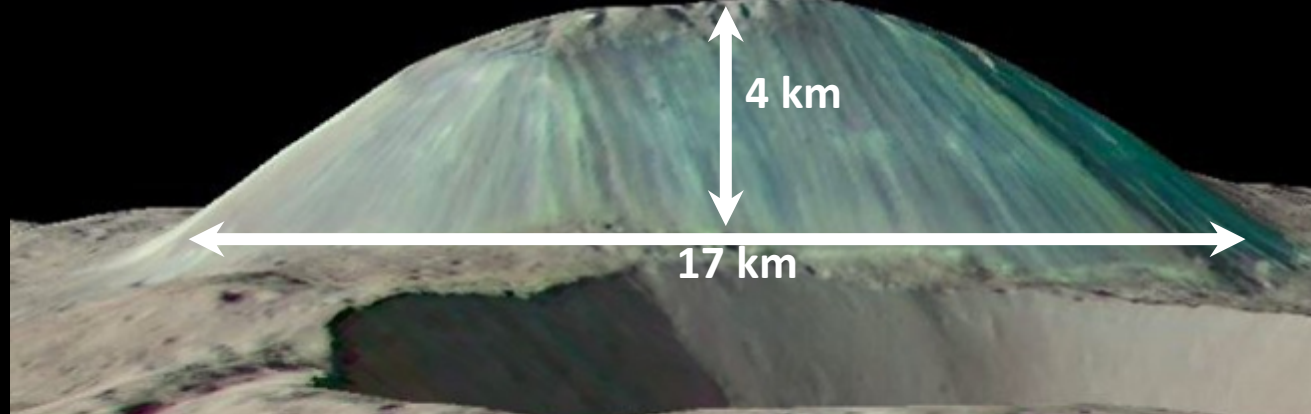
Bouguer anomaly in Orientale basin on the Moon



Zuber et al., 2016



# Ahuna Mons



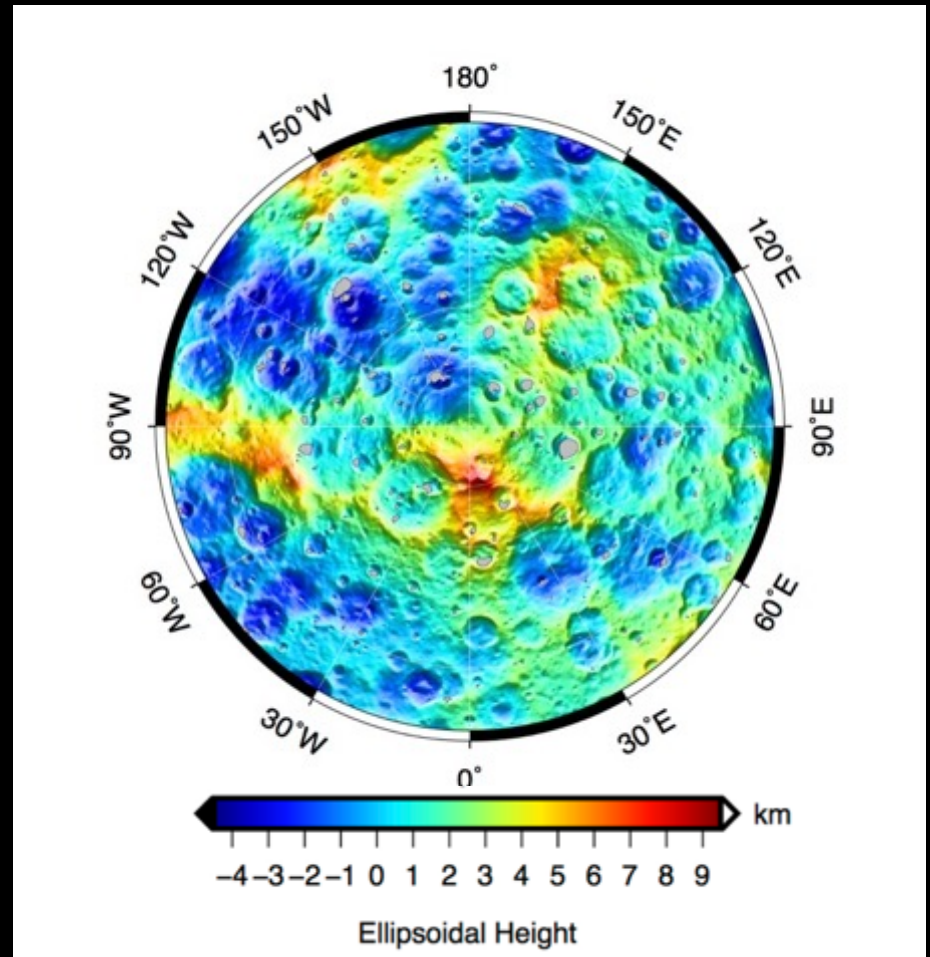
Ermakov et al., 2017a

JPL post-doc seminar

Park et al., 2019

# Permanently Shadowed Areas (PSRs)

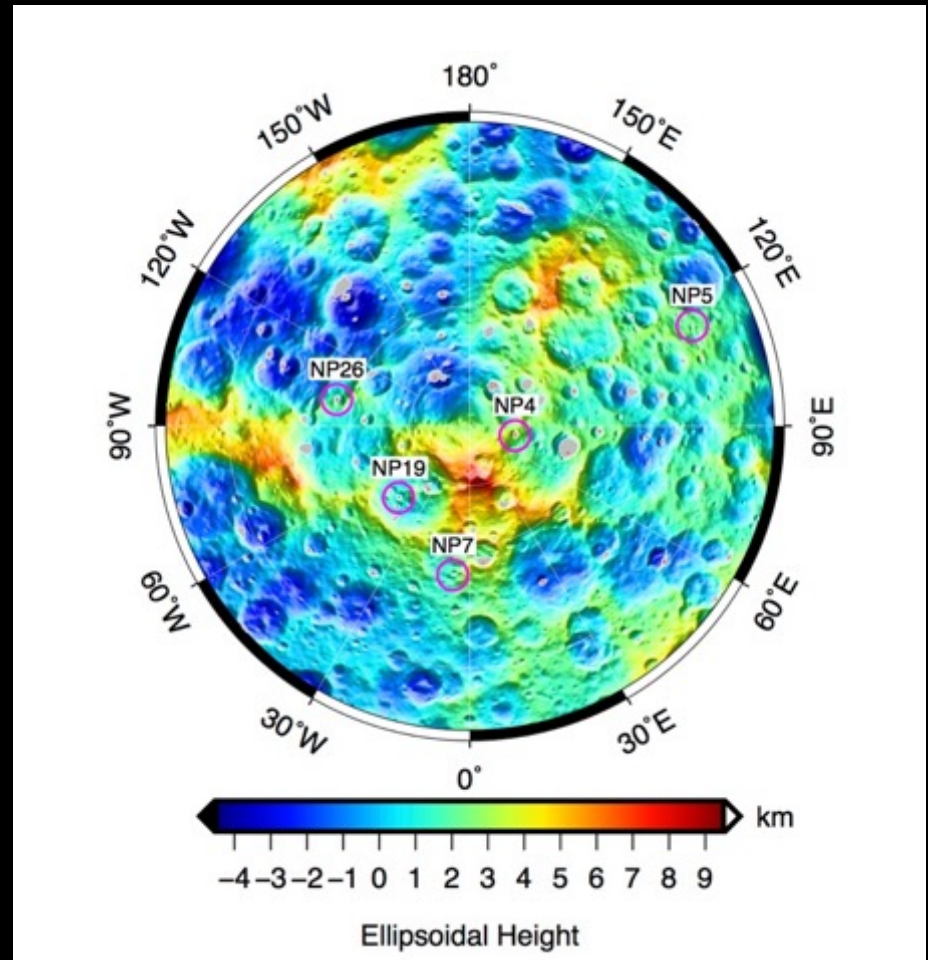
- Present-day obliquity  $\approx 4^\circ$
- $\approx 2000 \text{ km}^2$  are in permanent shadow
- Some polar craters have bright crater floor deposits



Ermakov et al., 2017b

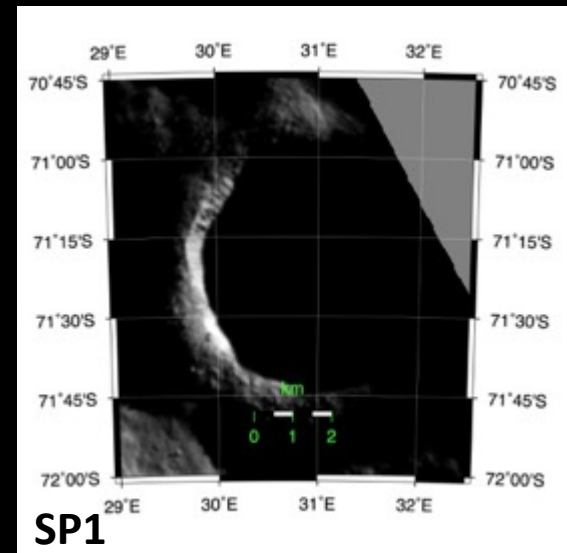
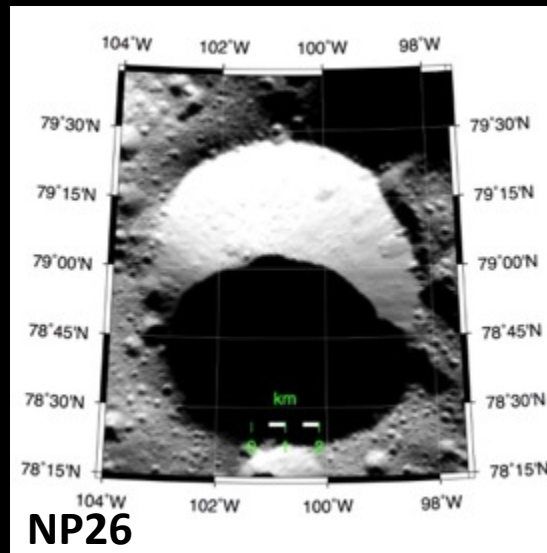
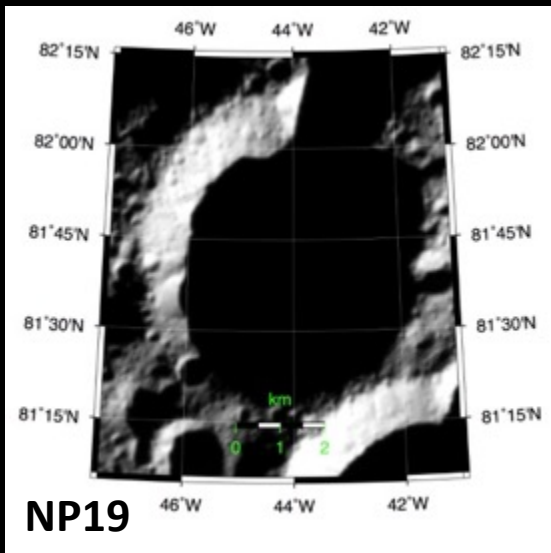
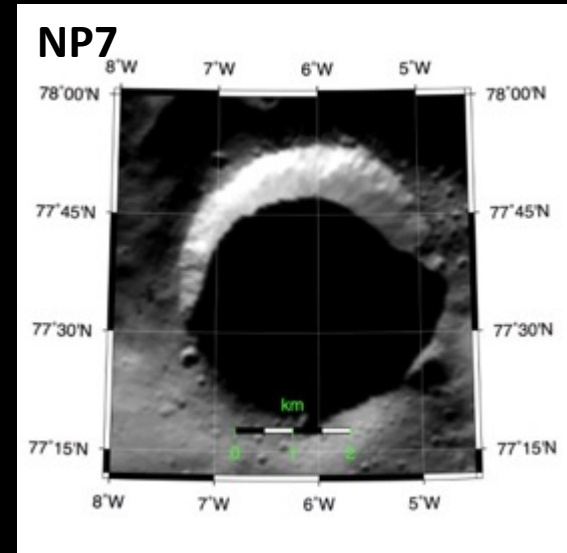
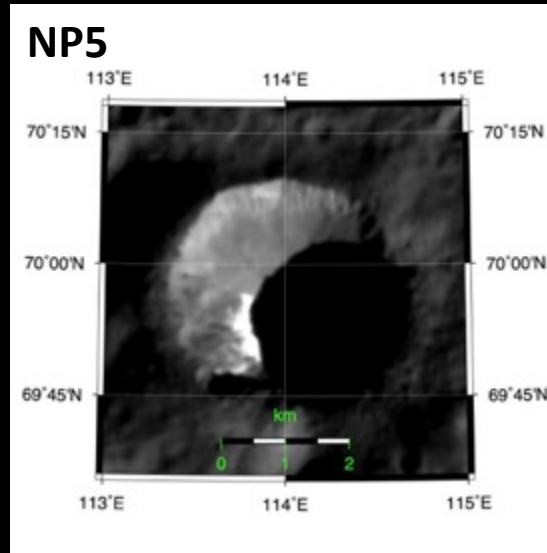
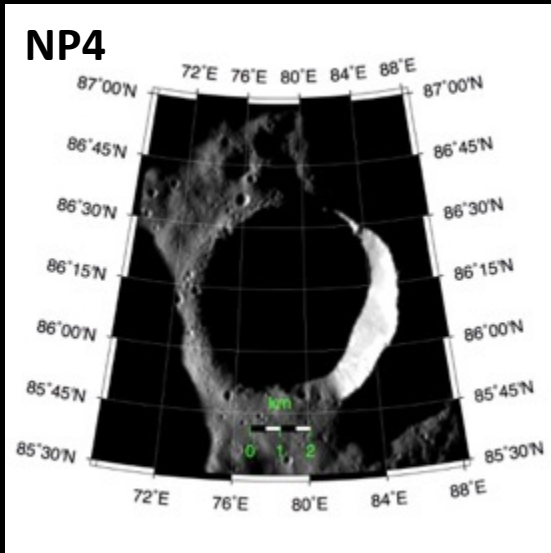
# PSRs and Bright Crater Floor Deposits (BCFDs)

- Present-day obliquity  $\approx 4^\circ$
- $\approx 2000 \text{ km}^2$  are in permanent shadow
- Some polar craters have bright crater floor deposits

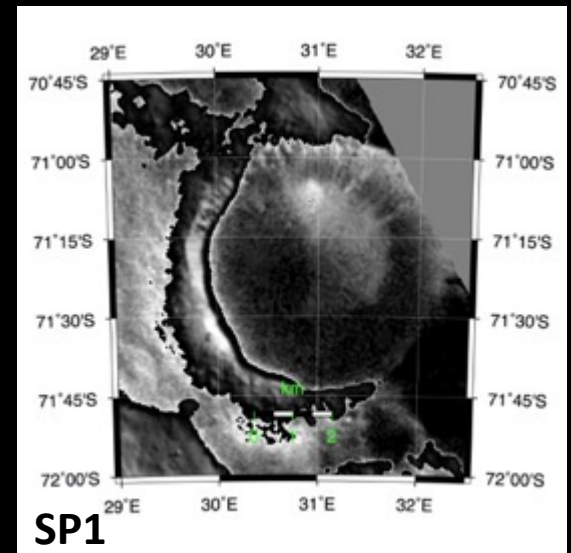
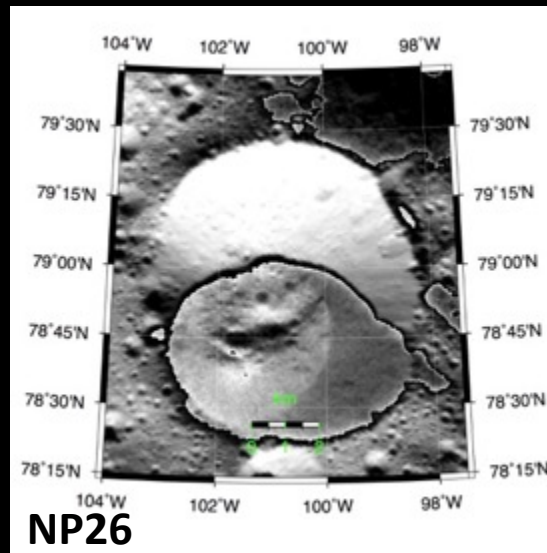
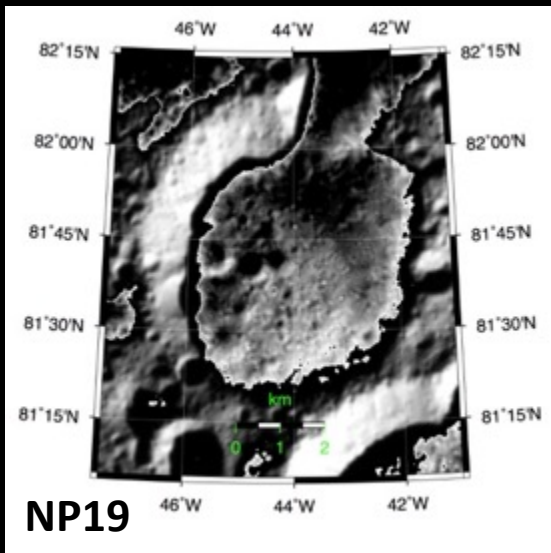
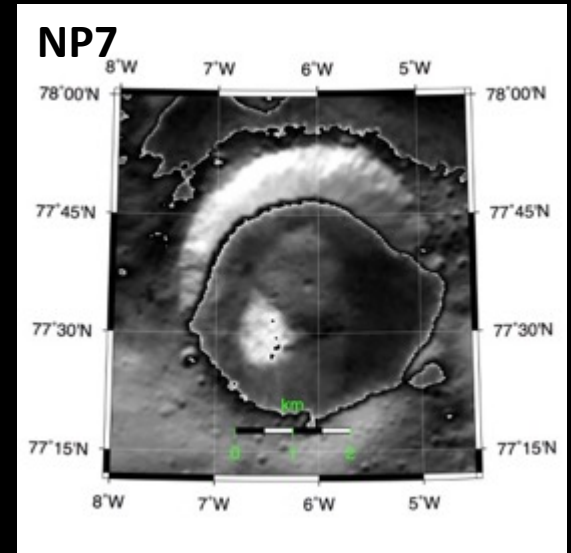
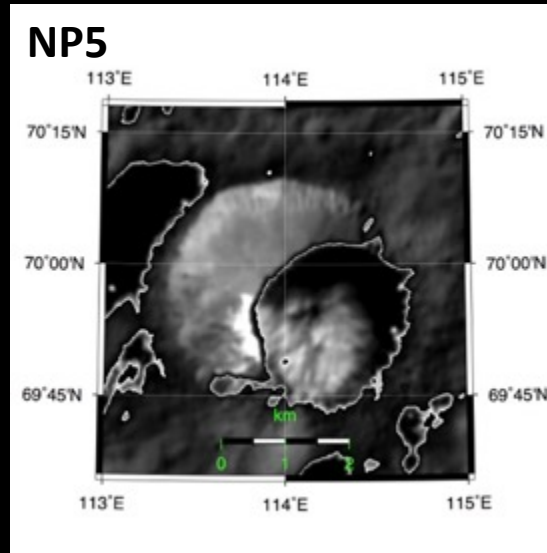
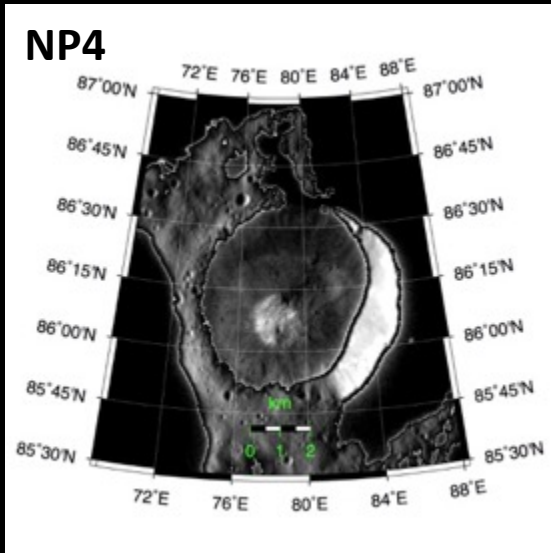


Ermakov et al., 2017b

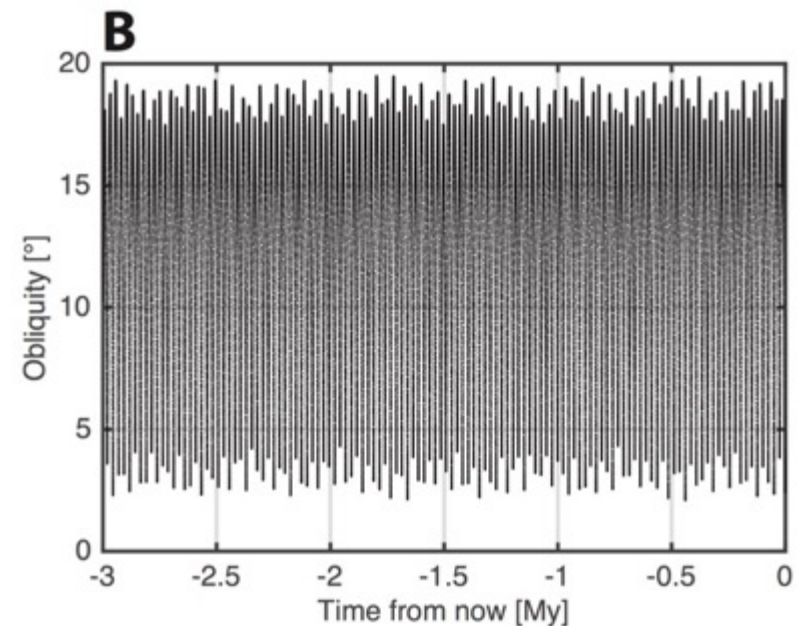
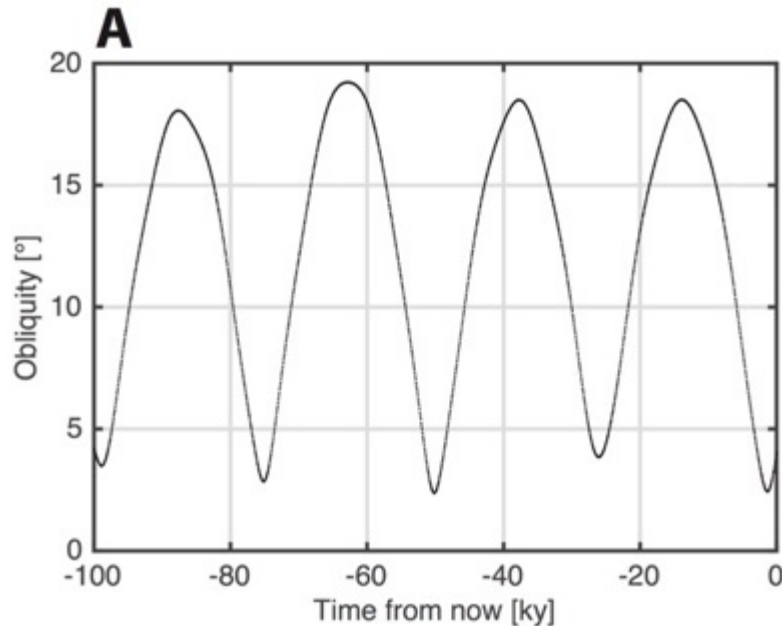
# Bright crater floor deposits (BCFDs)



# Bright crater floor deposits (BCFDs)

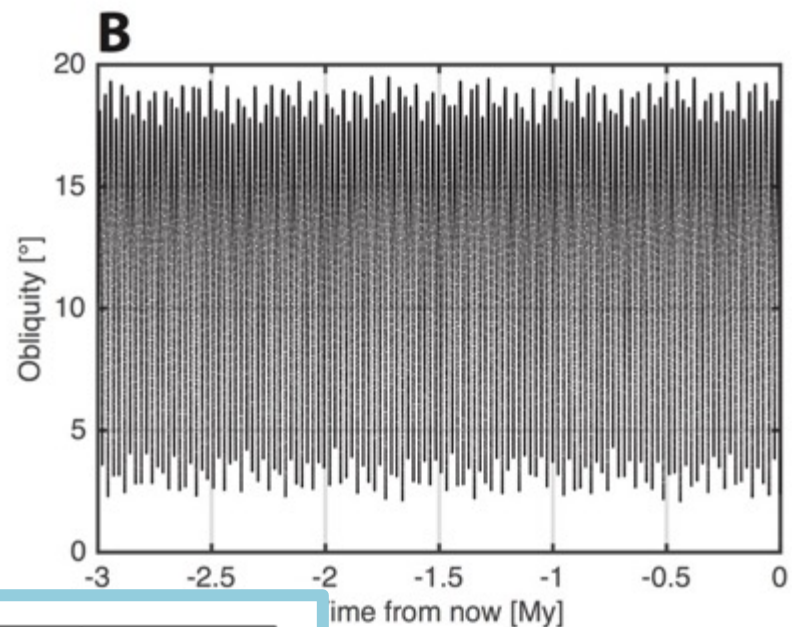
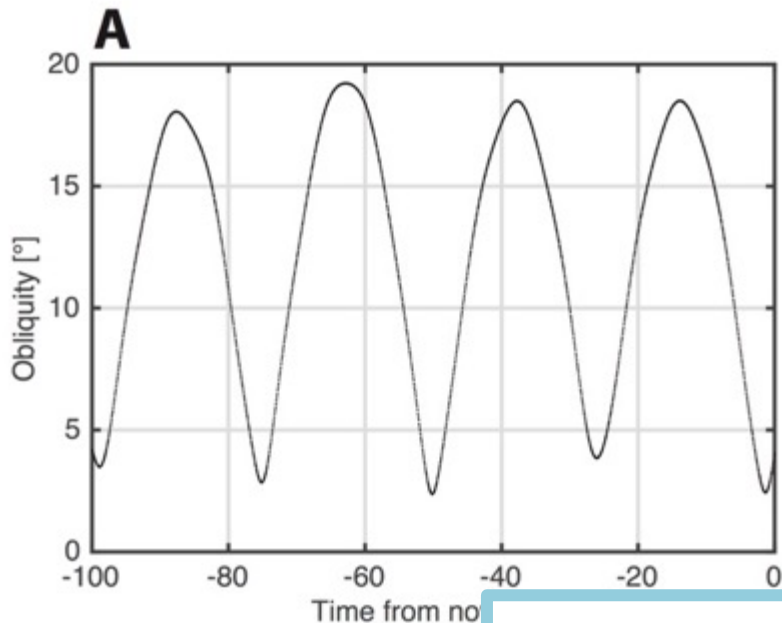


# Ceres Obliquity Evolution



- 8 planetary barycenters + Vesta and Ceres.
- Relativity is implemented as a velocity kick.
- Ceres full degree-2 field.
- Ceres moments of inertia constrained by degree-2 field
- Symplectic leap-frog integrator

# Ceres Obliquity Evolution

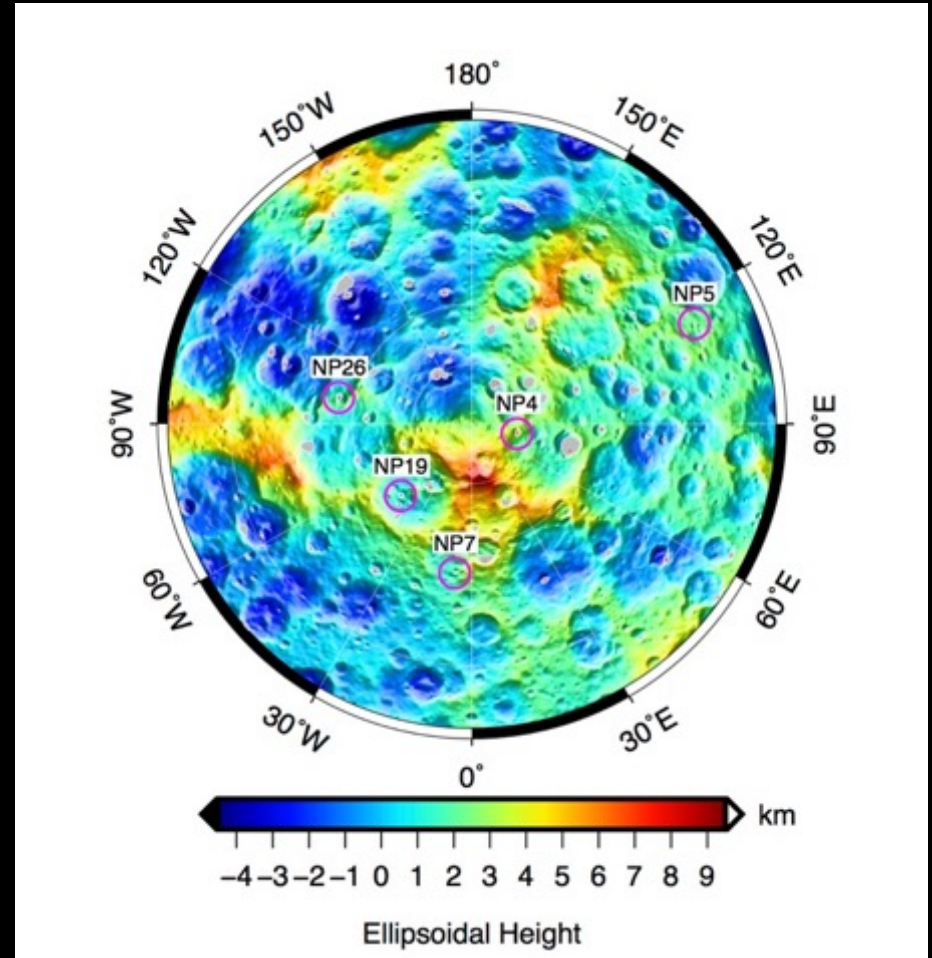
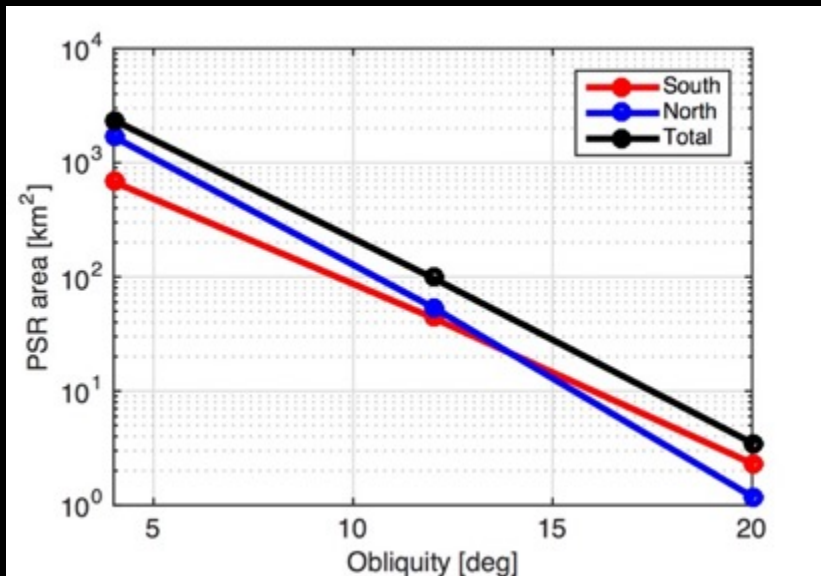


- 8 planetary bary
- Relativity is impl
- Ceres full degree
- Ceres moments
- Symplectic leap-

$C/MR_{vol}^2$	min ( $\epsilon$ )	max ( $\epsilon$ )
0.387	2.06°	19.76°
0.392	1.97°	19.71°
0.397	1.95°	19.64°

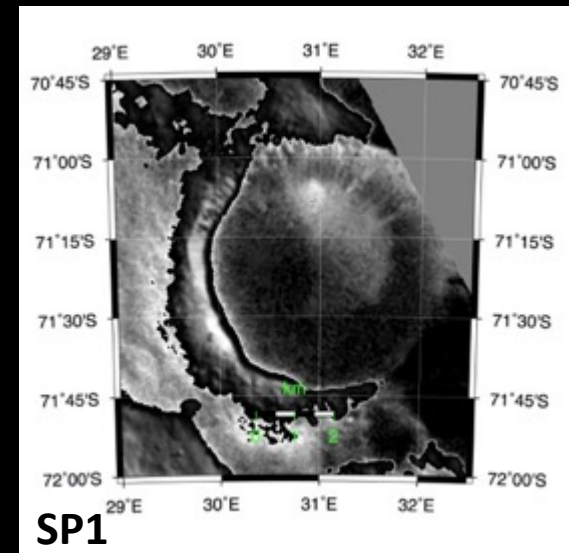
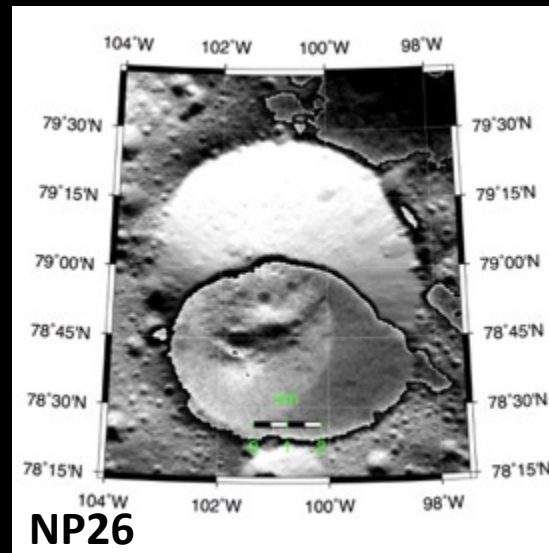
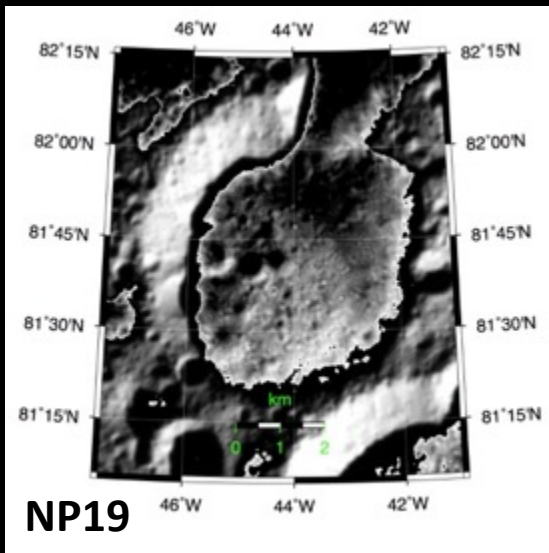
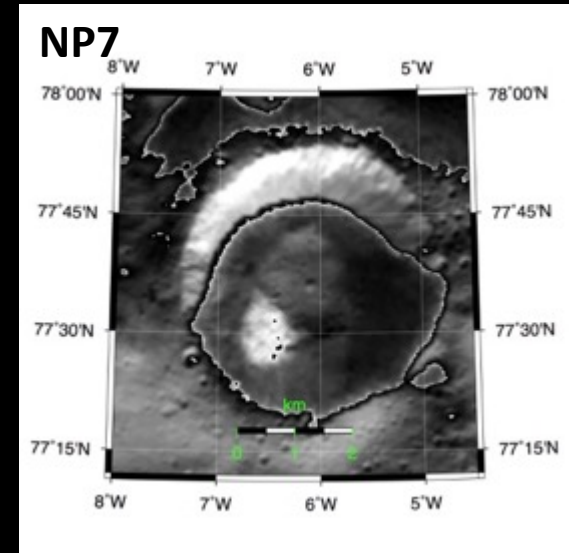
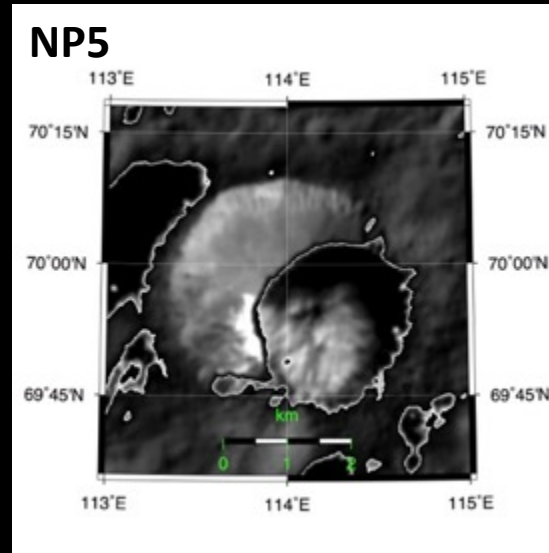
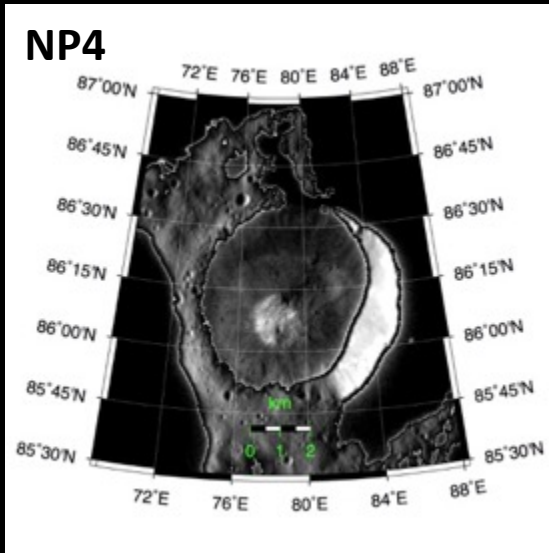
ee-2 field

# PSR area shrinks at high obliquity

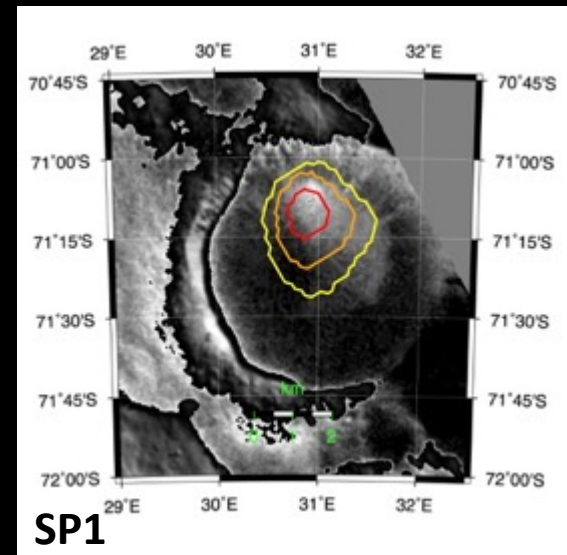
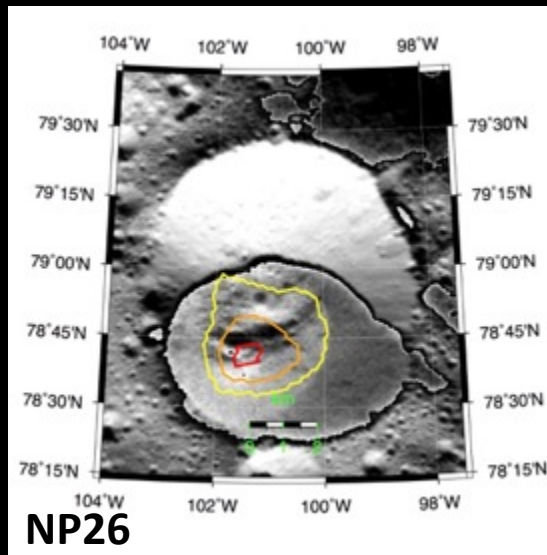
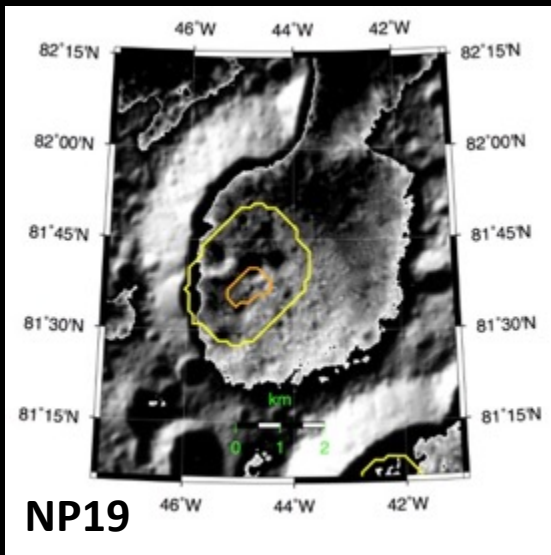
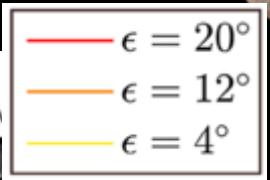
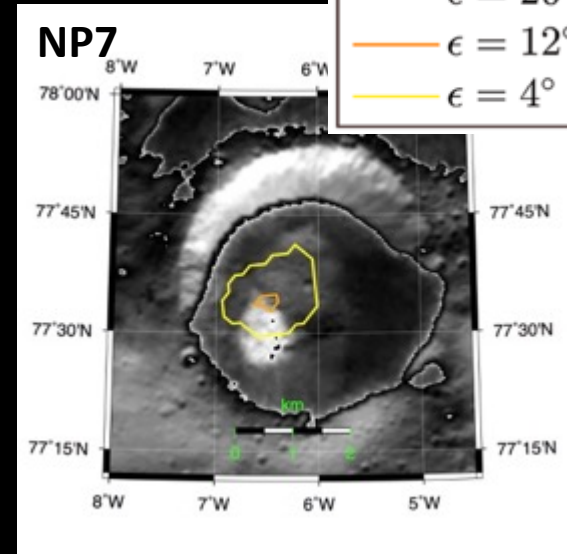
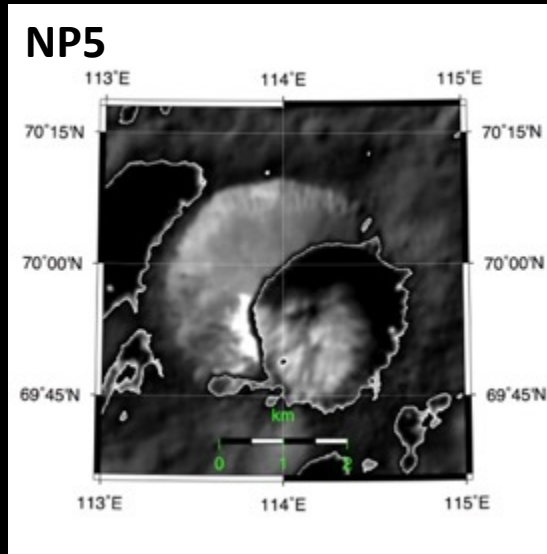
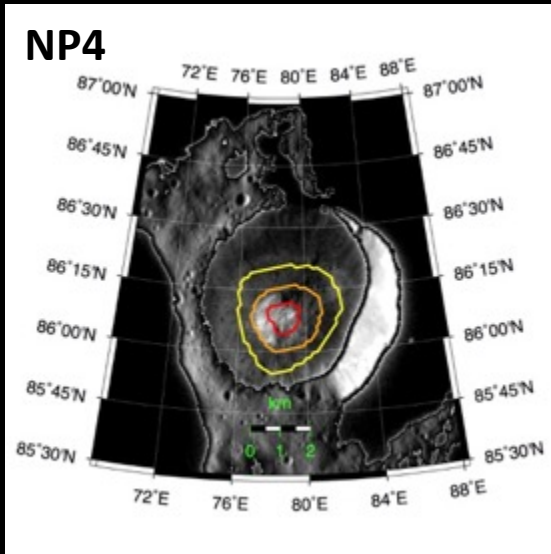


Ermakov et al., 2017b

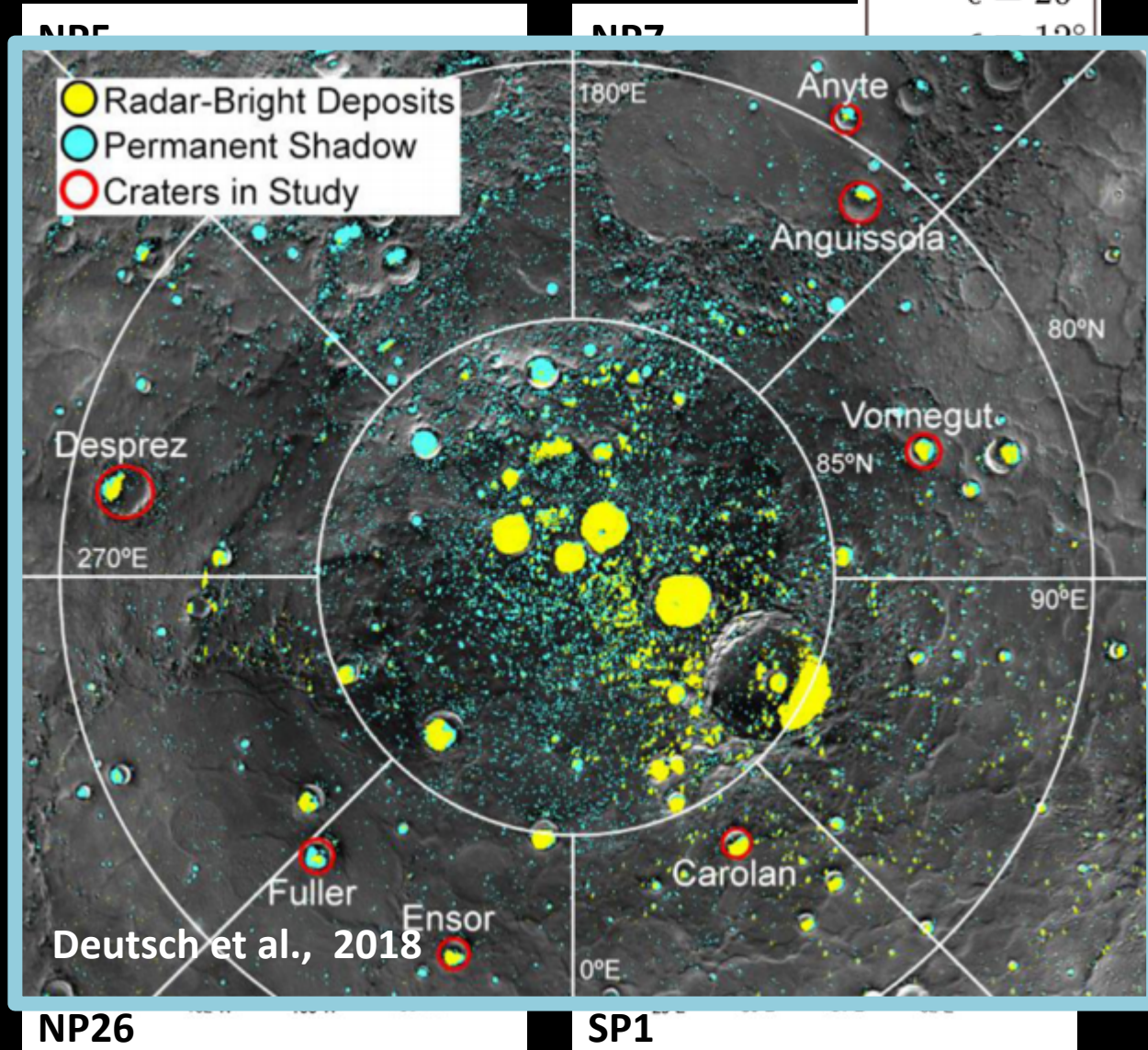
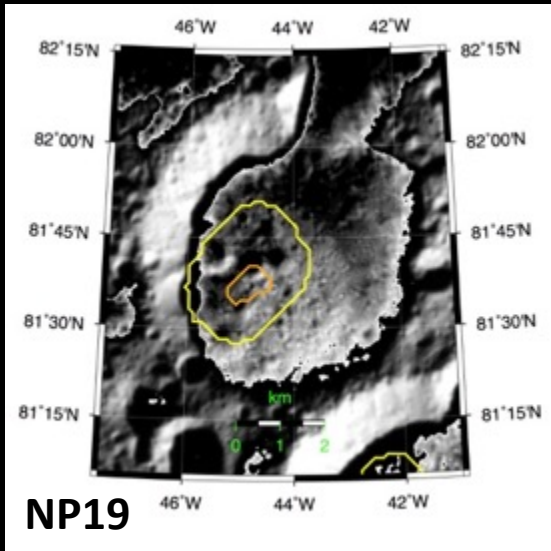
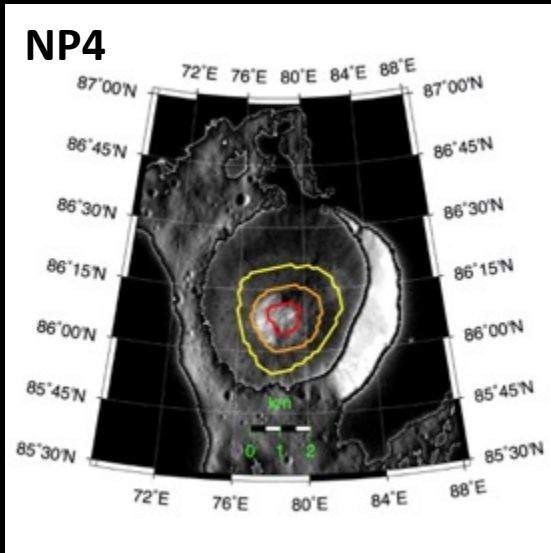
# PSRs and bright crater floor deposits



# PSRs and bright crater floor deposits



# PSRs and bright crater floor deposits



# PSRs and bright crater floor deposits

- The obliquity of Ceres undergoes large oscillations with the main period of 25 ky, a maximum of  $19.7^\circ$  and a minimum of  $2.0^\circ$
- At  $\epsilon_{\max}=20^\circ$ , most of the present-day PSRs receive direct sunlight.
- Correlation between bright deposits and the most persistent PSRs
- Bright deposits likely consist of volatiles, either water molecules from the exosphere or exposed ground ice.

# Vesta and Ceres comparative evolution

Vesta

Early accretion

Presumably  
chondritic

Ceres

chondritic +  
volatiles

Late accretion

Time

# Vesta and Ceres comparative evolution

Vesta

Early accretion

Presumably  
chondritic

magma ocean and  
differentiation

Ceres

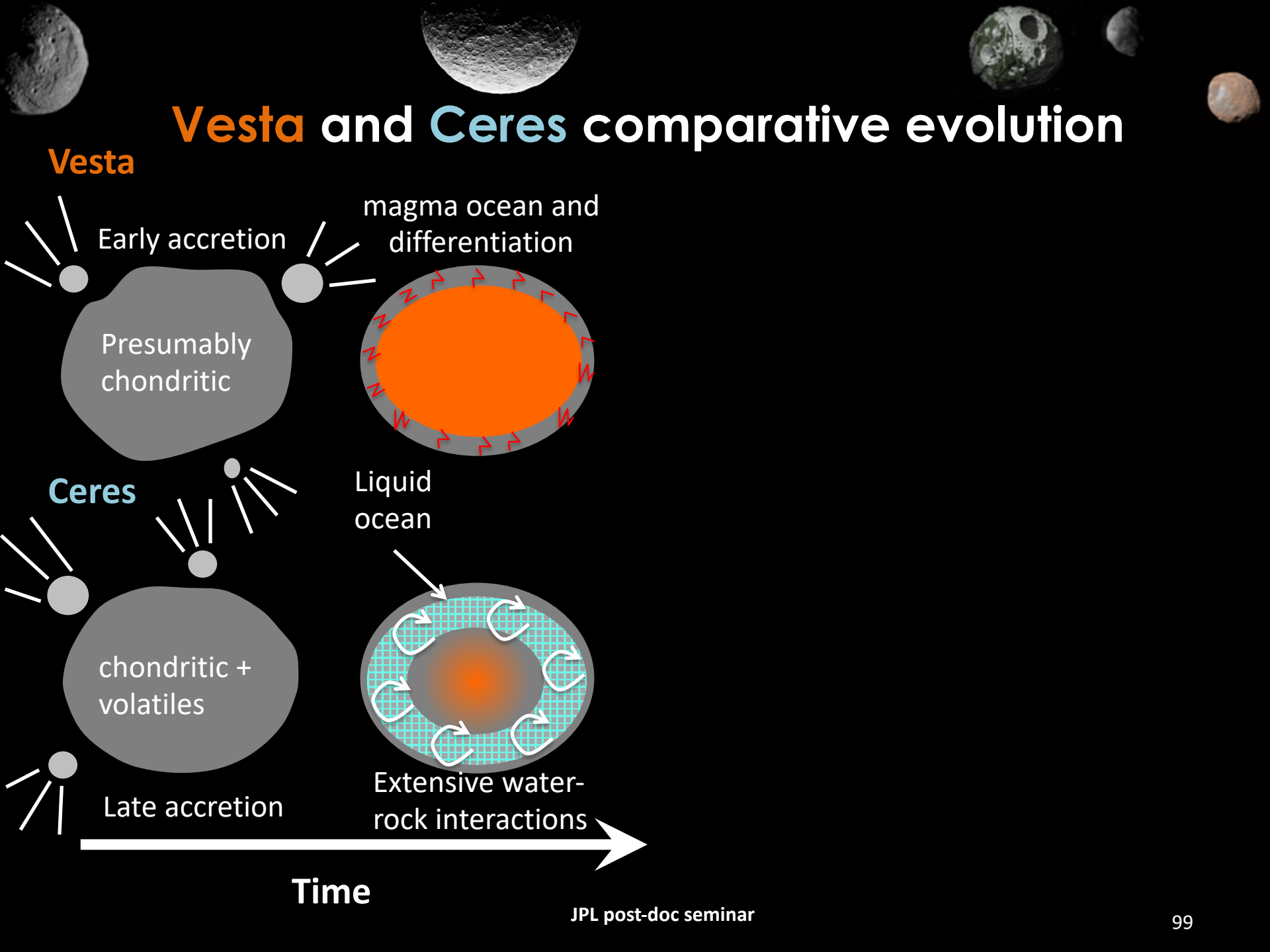
chondritic +  
volatiles

Liquid  
ocean

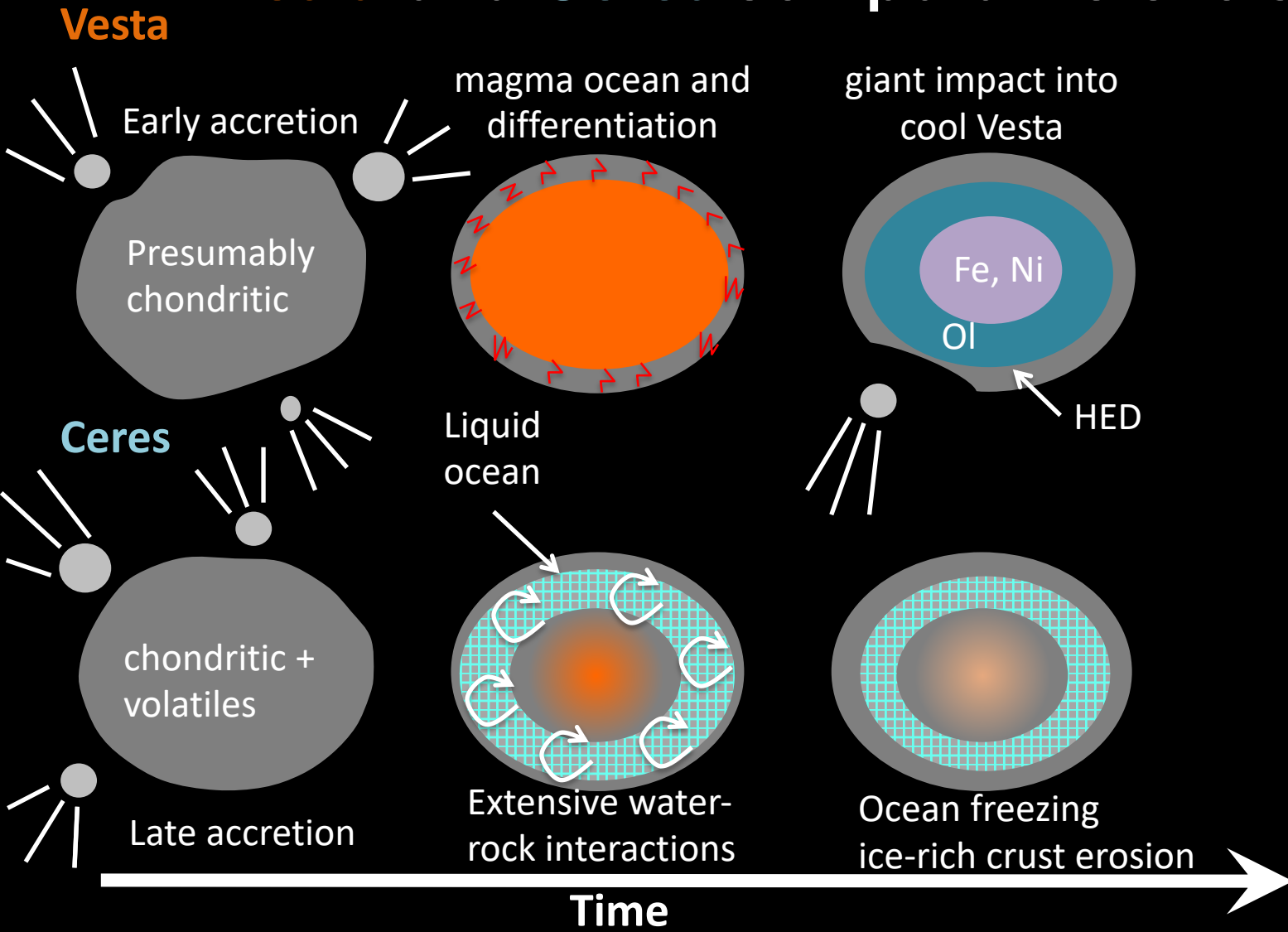
Late accretion

Extensive water-  
rock interactions

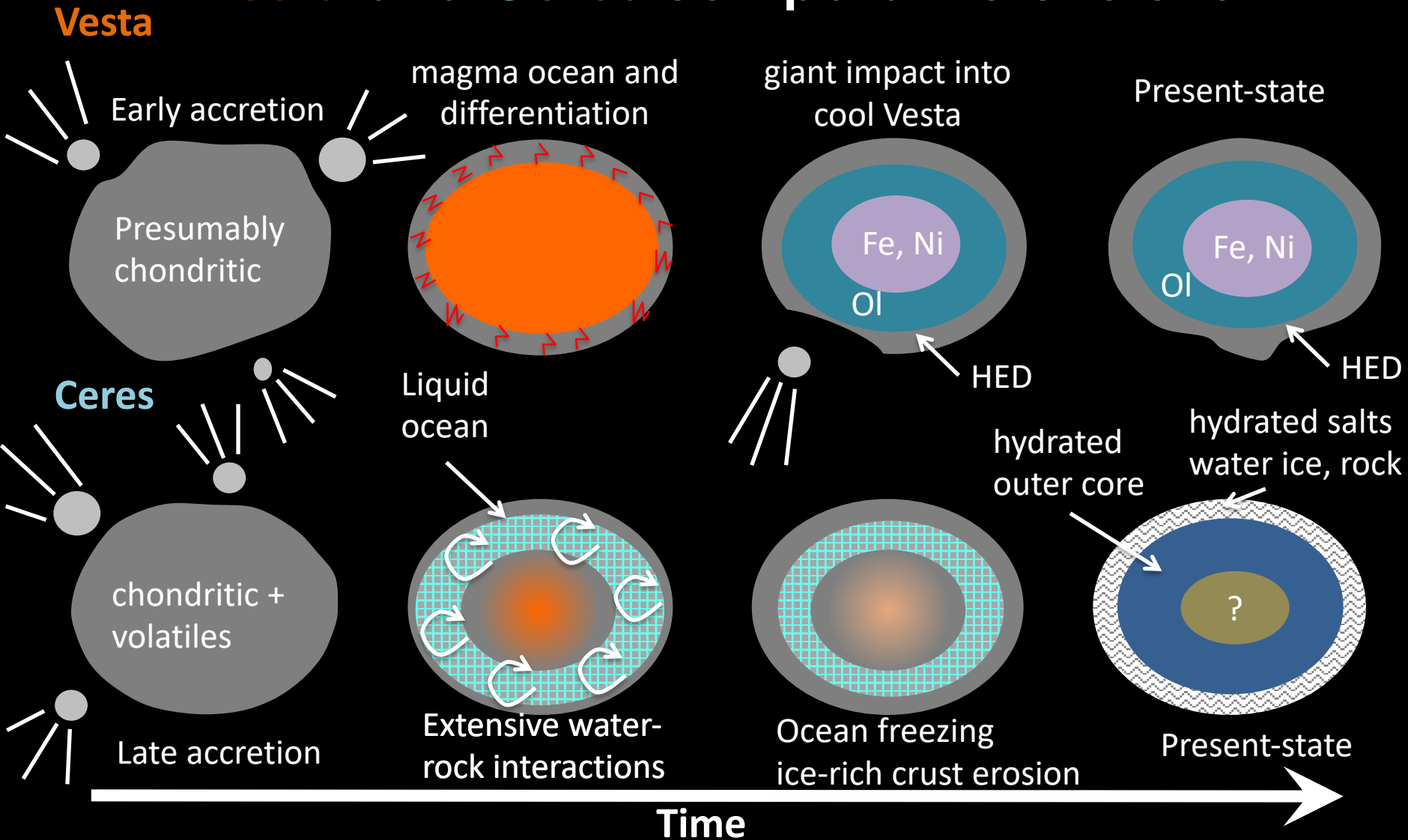
Time



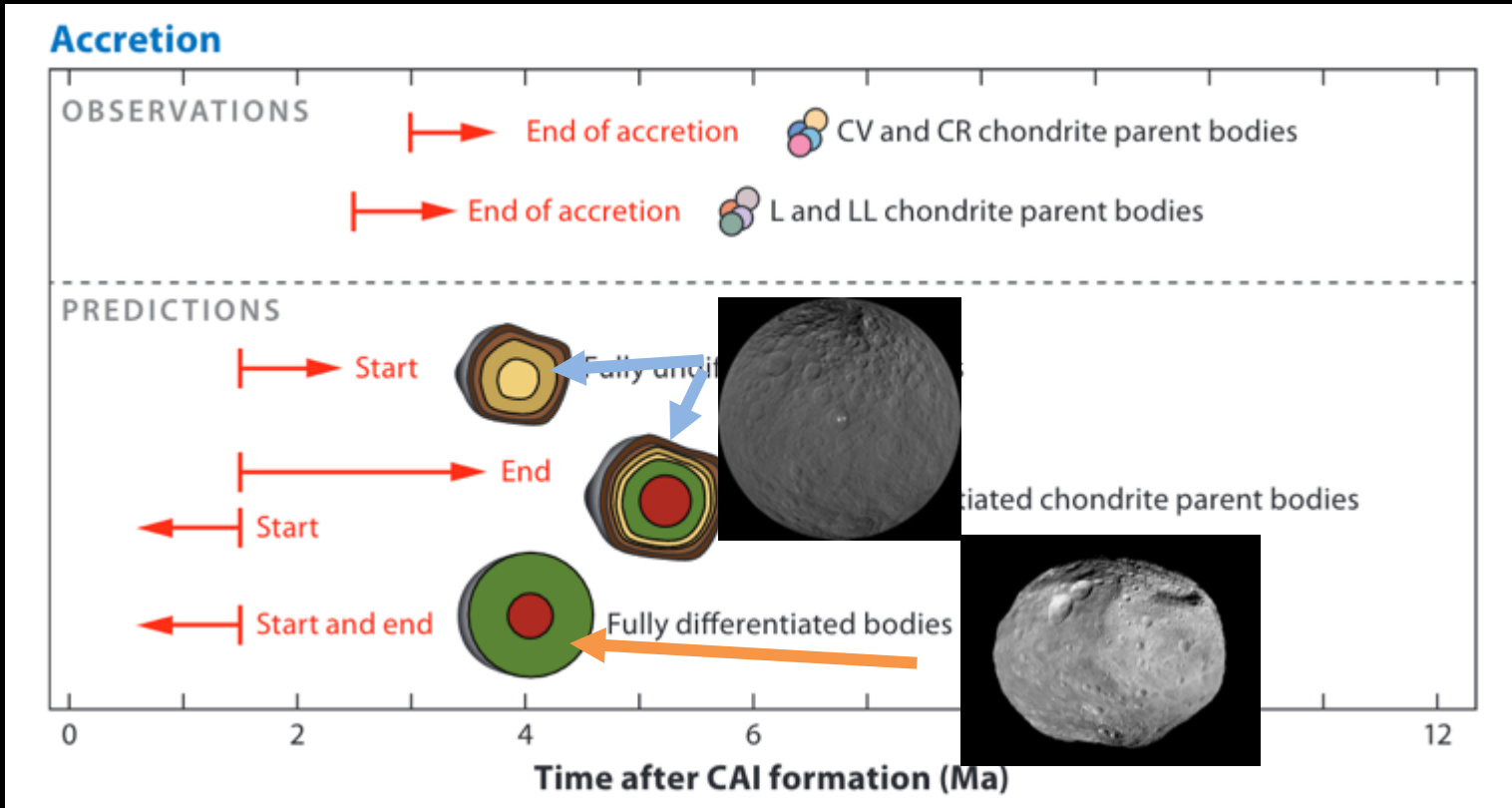
# Vesta and Ceres comparative evolution



# Vesta and Ceres comparative evolution



# A spectrum of planetesimal differentiation



Weiss & Elkins-Tanton, 2013

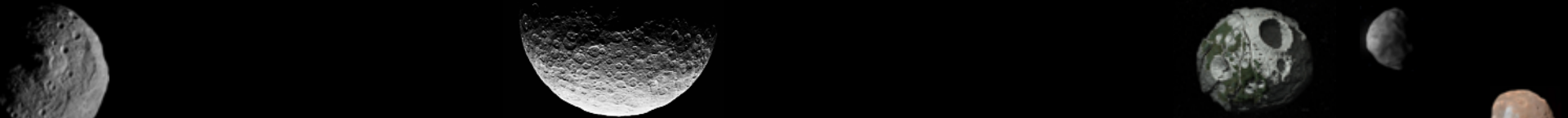
# Summary



- Formed early (< 5 My after CAI)
- Once hot and hydrostatic, **Vesta** is no longer either
- Differentiated interior
- Most of topography acquired when **Vesta** was already cool
  - uncompensated topography
- Combination of gravity/topography data with meteoritic geochemistry data provides constraints on the internal structure



- Cooler history
  - late formation
  - and/or heat transfer due to hydrothermal circulation
- Partially differentiated interior
- Experienced viscous relaxation
- Much lower surface viscosities (compared to Vesta) allowed compensated topography
- **Ceres'** crust is light (based on admittance analysis) and strong (based on FE relaxation modeling)
- Not much water ice in **Ceres** crust (<35 vol%) now
- Cold trapping of volatiles at polar craters



# Bennu & Ryugu

- Surface slopes
- Constraints on the internal density distribution
- The rotational state
- YORP estimate
- Model of the Yarkovsky effect

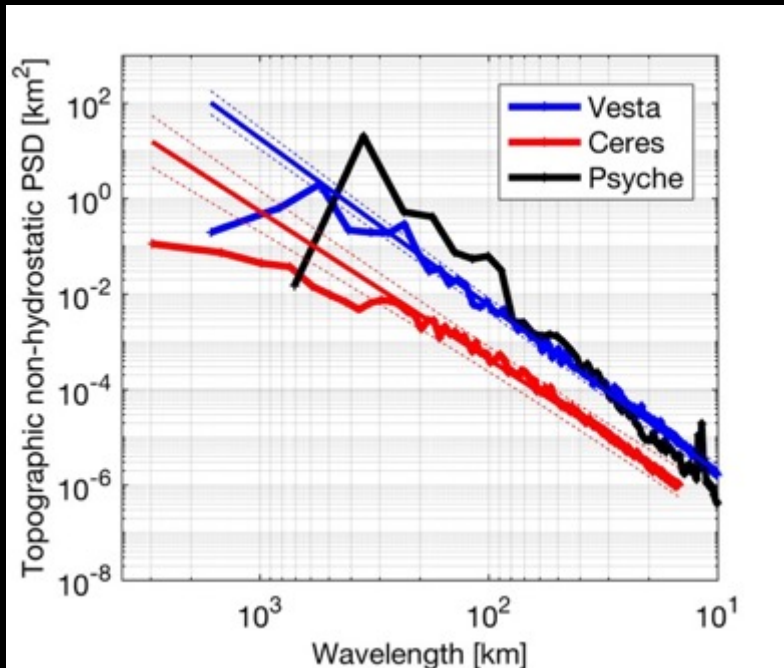
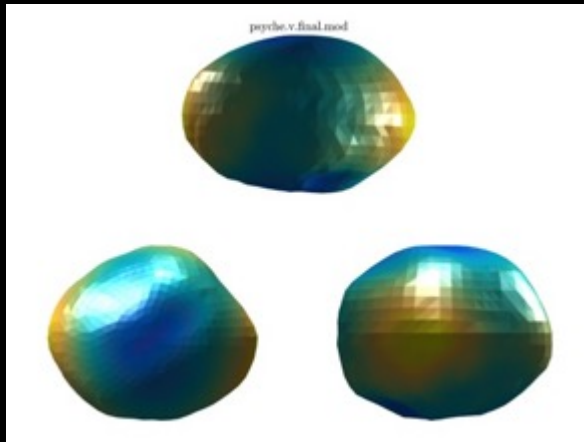


**Ryugu**  
Credit: JAXA



**Bennu**  
Credit: NASA-GSFC/University of Arizona

# Psyche



- Psyche has a metal surface based on radar albedo data (Ostro et al., 1985)
- Psyche density is 4500 +/- 1500 kg/m<sup>3</sup> (Shepard et al., 2017)
- Leading hypothesis: Psyche is a planetesimal core
- Key questions of the gravity investigation of Psyche:
  - density
  - differentiation

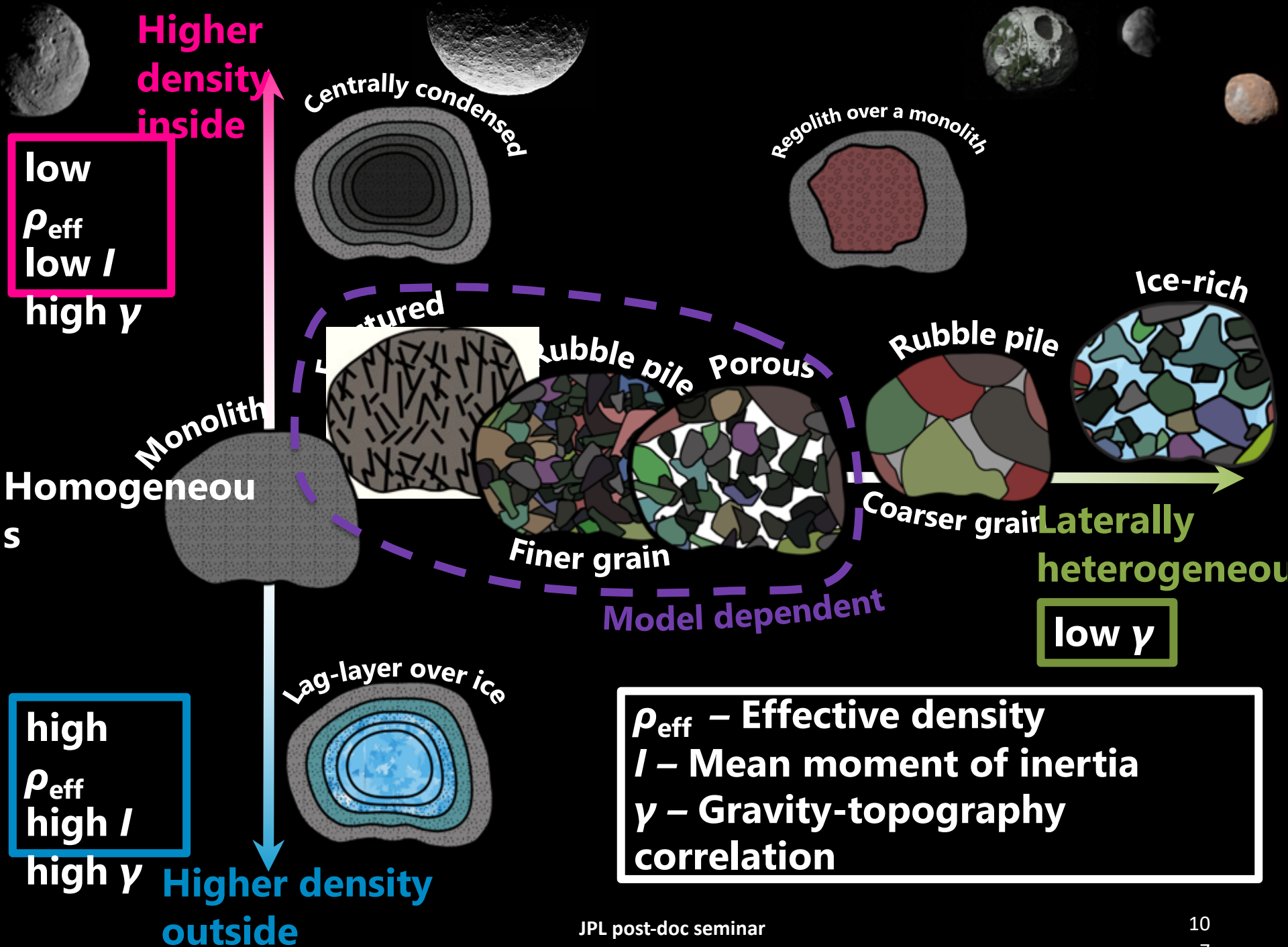
$$M^{tt} \propto \Delta\sigma_{\max} \bar{\rho}^{-2} R^{-2}$$

# Phobos & Deimos

- Phobos' and Deimos' origins are unknown despite > century of research
- Martian moons are targets of JAXA's MMX mission
- Three leading hypotheses
  - In-situ formation (e.g. Burnes, 1972)
  - Capture (e.g. Murchie et al., 1999)
  - Re-accretion after giant impact (e.g. Citron et al., 2015)
- Key gravity science questions:
  - Internal structure
  - Central density concentration
  - Lateral density variations



No unique interpretation



# Mascons on Ceres

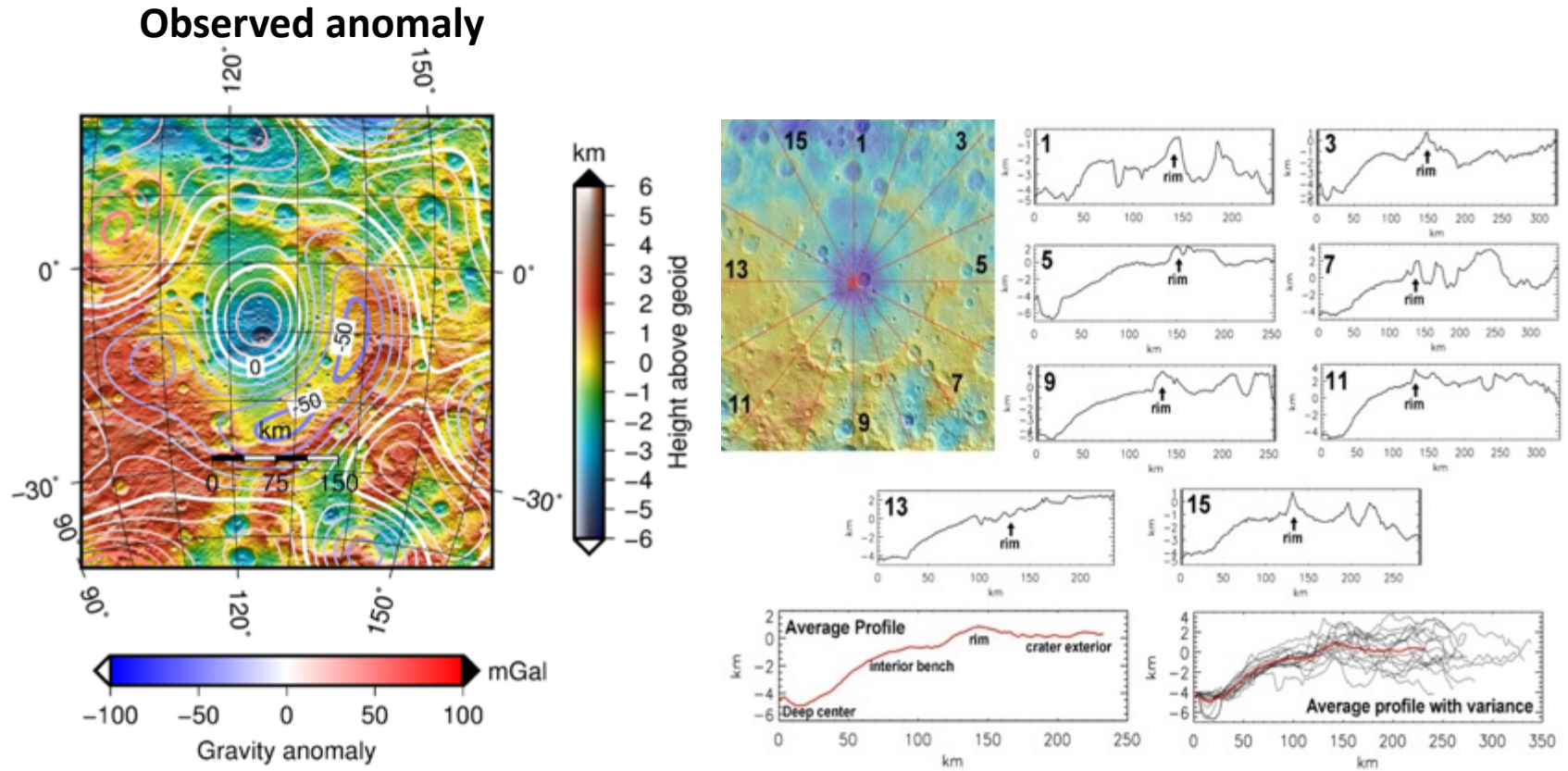
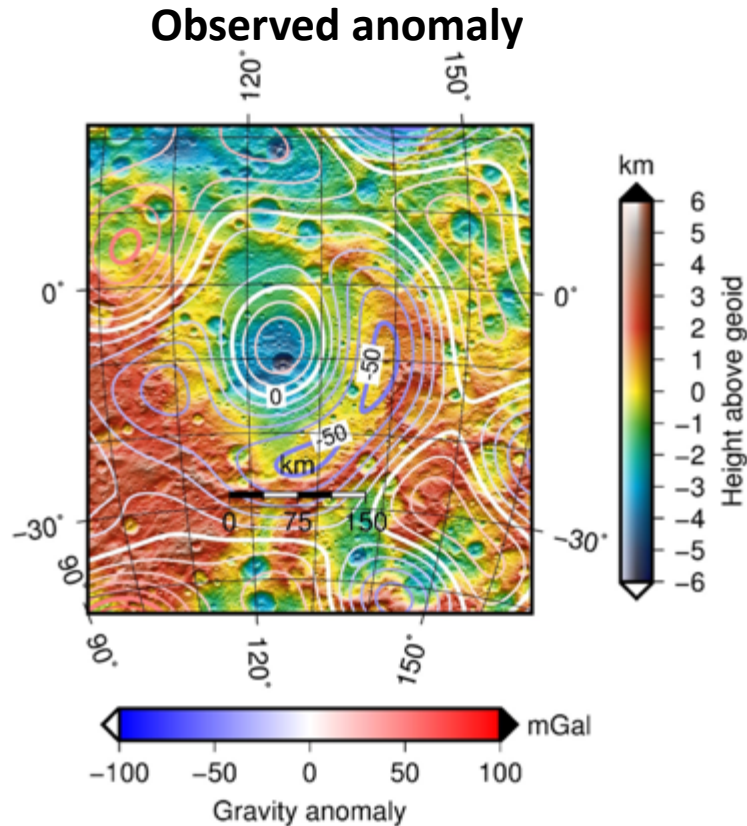
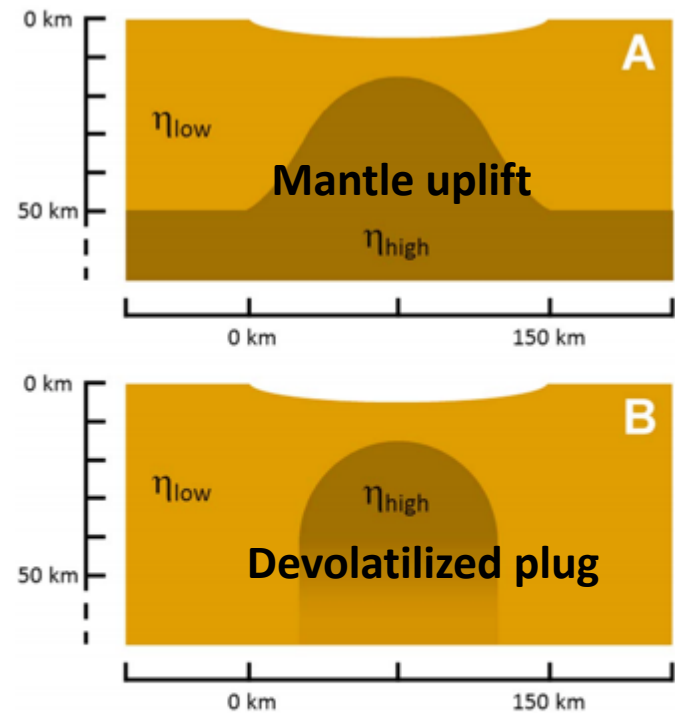


Figure S6. Isostatic gravity anomaly at Kerwan including gravity degree 3 to 16. Contours are for gravity anomaly and the contour interval is 10 mGal. Colors show relative topography in the Kerwan region. After Ermakov et al. 2017.

# Mascons on Ceres



**Figure S6.** Isostatic gravity anomaly at Kerwan including gravity degree 3 to 16. Contours are for gravity anomaly and the contour interval is 10 mGal. Colors show relative topography in the Kerwan region. After Ermakov et al. 2017.



**Figure 3.** Two possible inferred subsurface structures beneath Kerwan. (a) Upward deflection of a high-viscosity ( $\eta$ ) mantle beneath the crater. (b) Devolatilization of a plug of material beneath Kerwan, which increased the density and viscosity of the material. The details of the subsurface structure shown here have been selected to reproduce Kerwan's specific morphology. The latter case (b) is more consistent with other Dawn observations.

# Mascons on Ceres

## Modeled anomaly

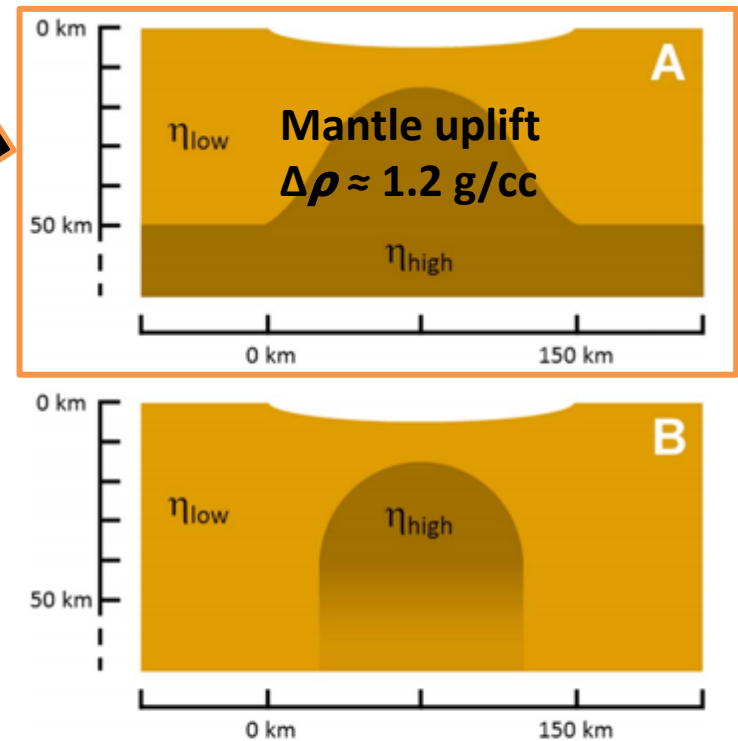
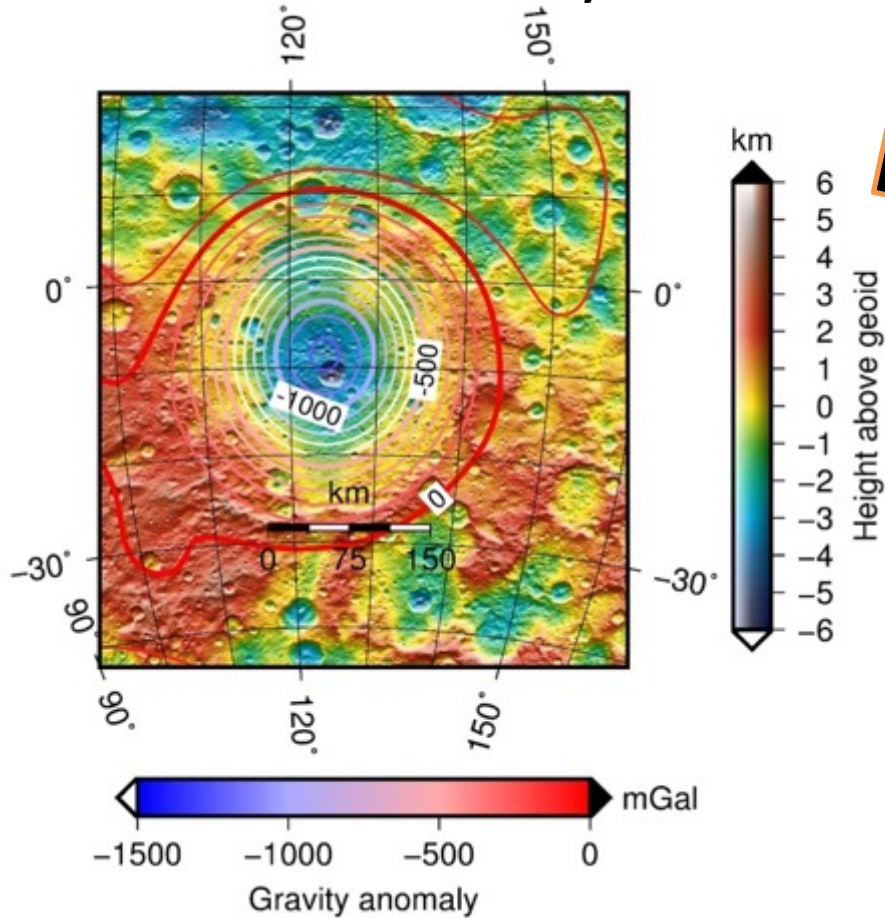


**Figure 3.** Two possible inferred subsurface structures beneath Kerwan. (a) Upward deflection of a high-viscosity ( $\eta$ ) mantle beneath the crater. (b) Devolatilization of a plug of material beneath Kerwan, which increased the density and viscosity of the material. The details of the subsurface structure shown here have been selected to reproduce Kerwan's specific morphology. The latter case (b) is more consistent with other Dawn observations.

# Mascons on Ceres

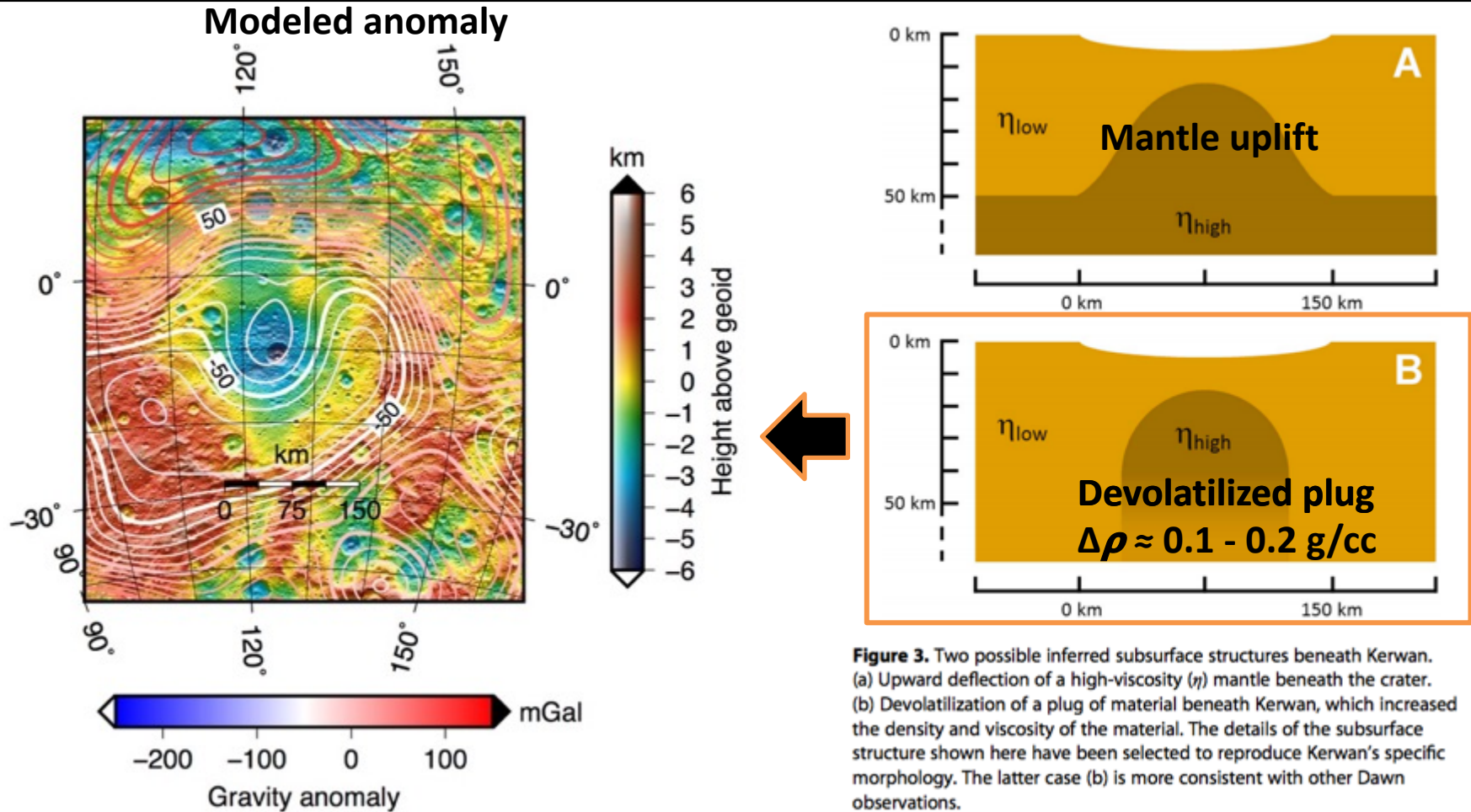
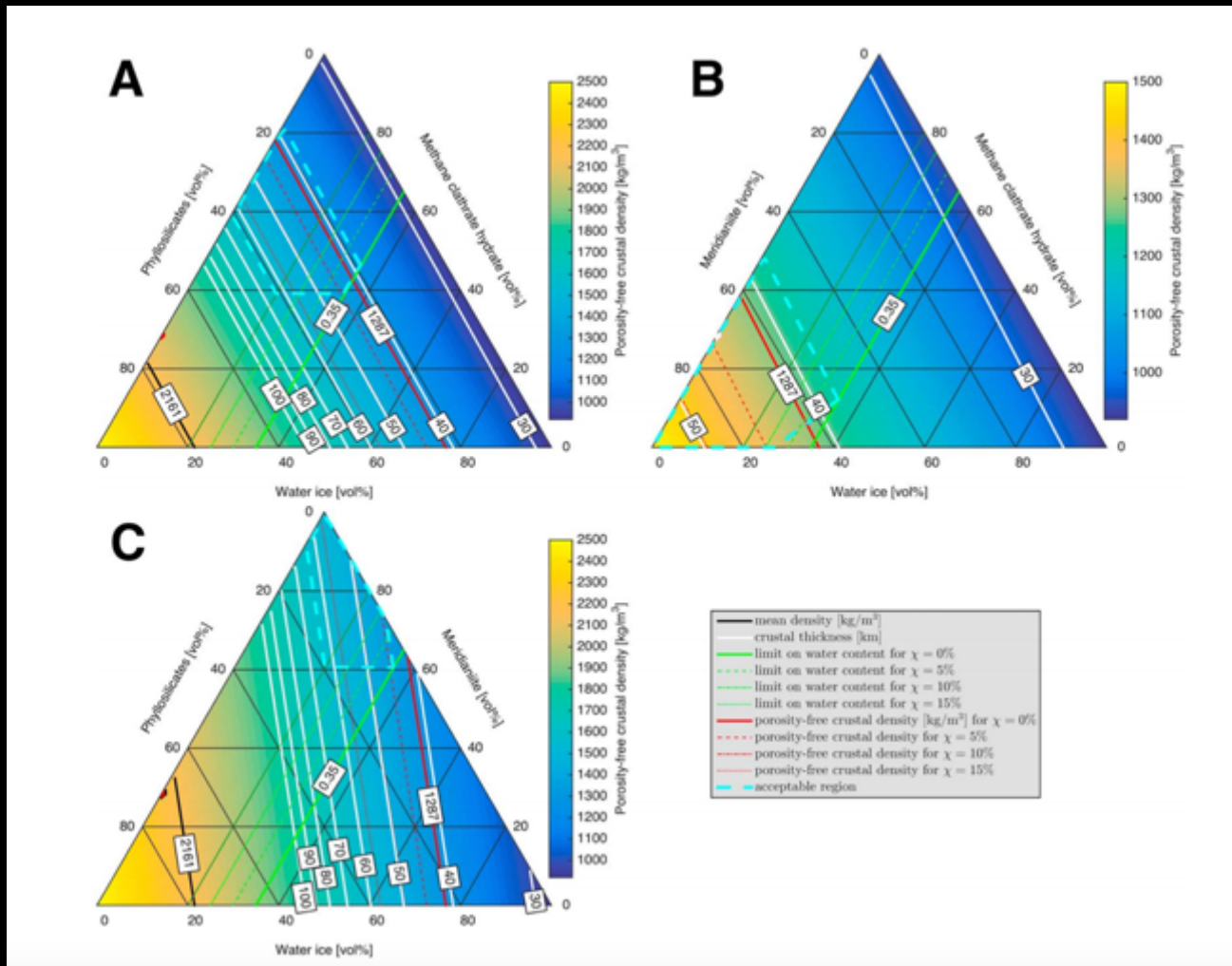


**Figure 3.** Two possible inferred subsurface structures beneath Kerwan. (a) Upward deflection of a high-viscosity ( $\eta$ ) mantle beneath the crater. (b) Devolatilization of a plug of material beneath Kerwan, which increased the density and viscosity of the material. The details of the subsurface structure shown here have been selected to reproduce Kerwan's specific morphology. The latter case (b) is more consistent with other Dawn observations.

# Crustal composition constraints

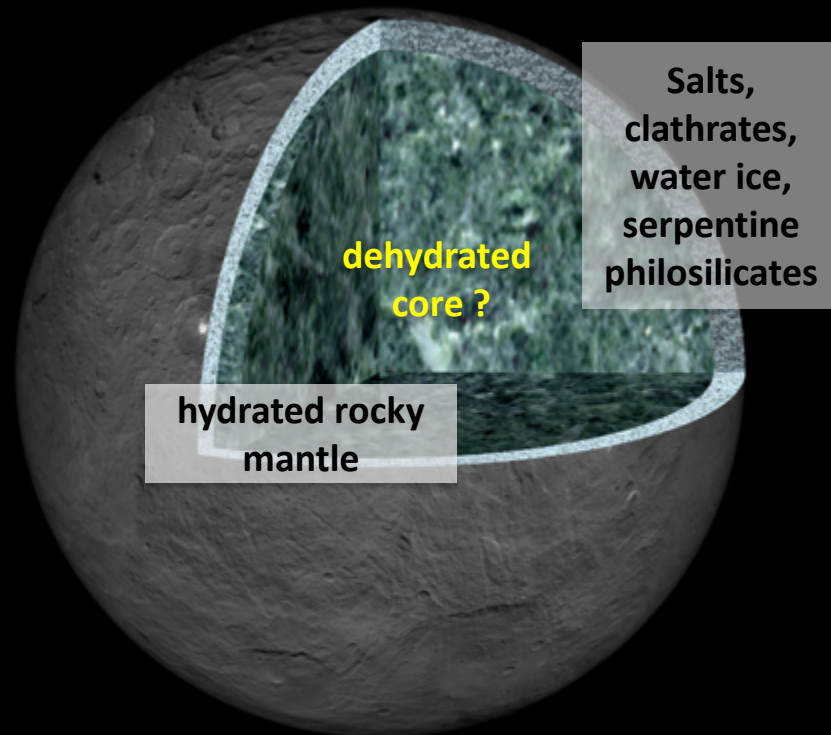


Ermakov et al., 2017

# Internal structures of Vesta and Ceres

## Ceres →

- Crust is light (1.1-1.4 g/cc) and mechanically rock-like w
- Mantle density ~2.4 g/cc and unlithified at least to a depth of 100 km
- Possible dehydrated rocky core remains unconstrained

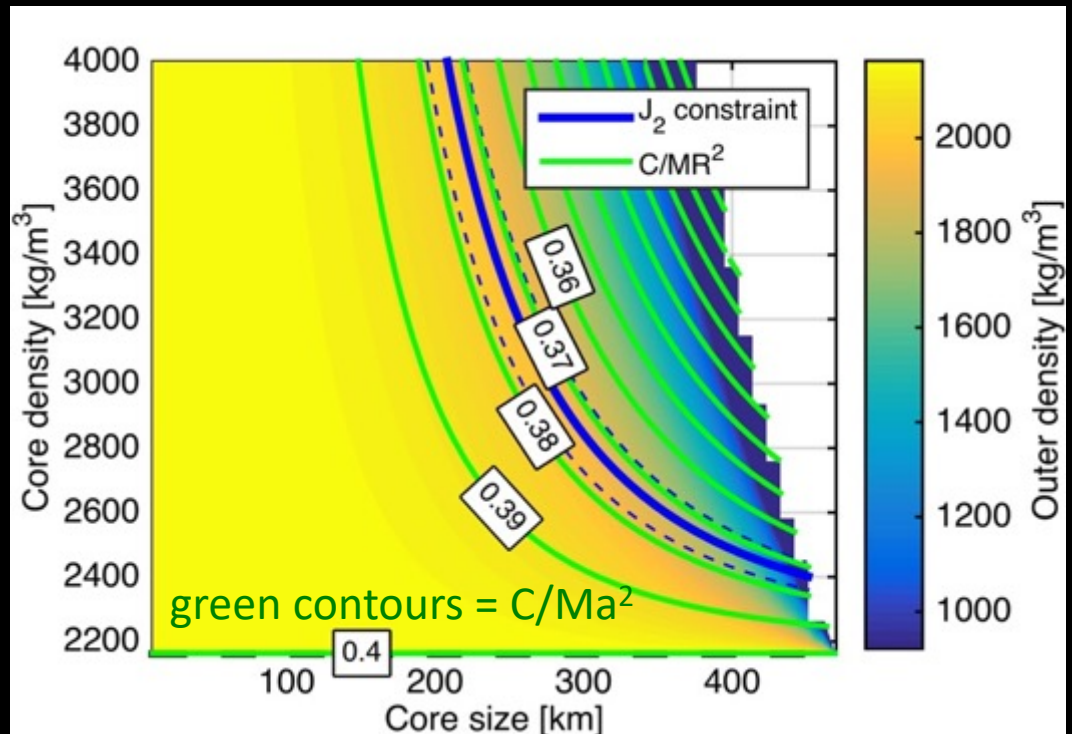


## ← Vesta

- Crustal density constrained by HEDs and admittance (2.8 g/cc)
- Assuming density of iron meteorites (5-8 g/cc), the core radius is 110 – 155 km

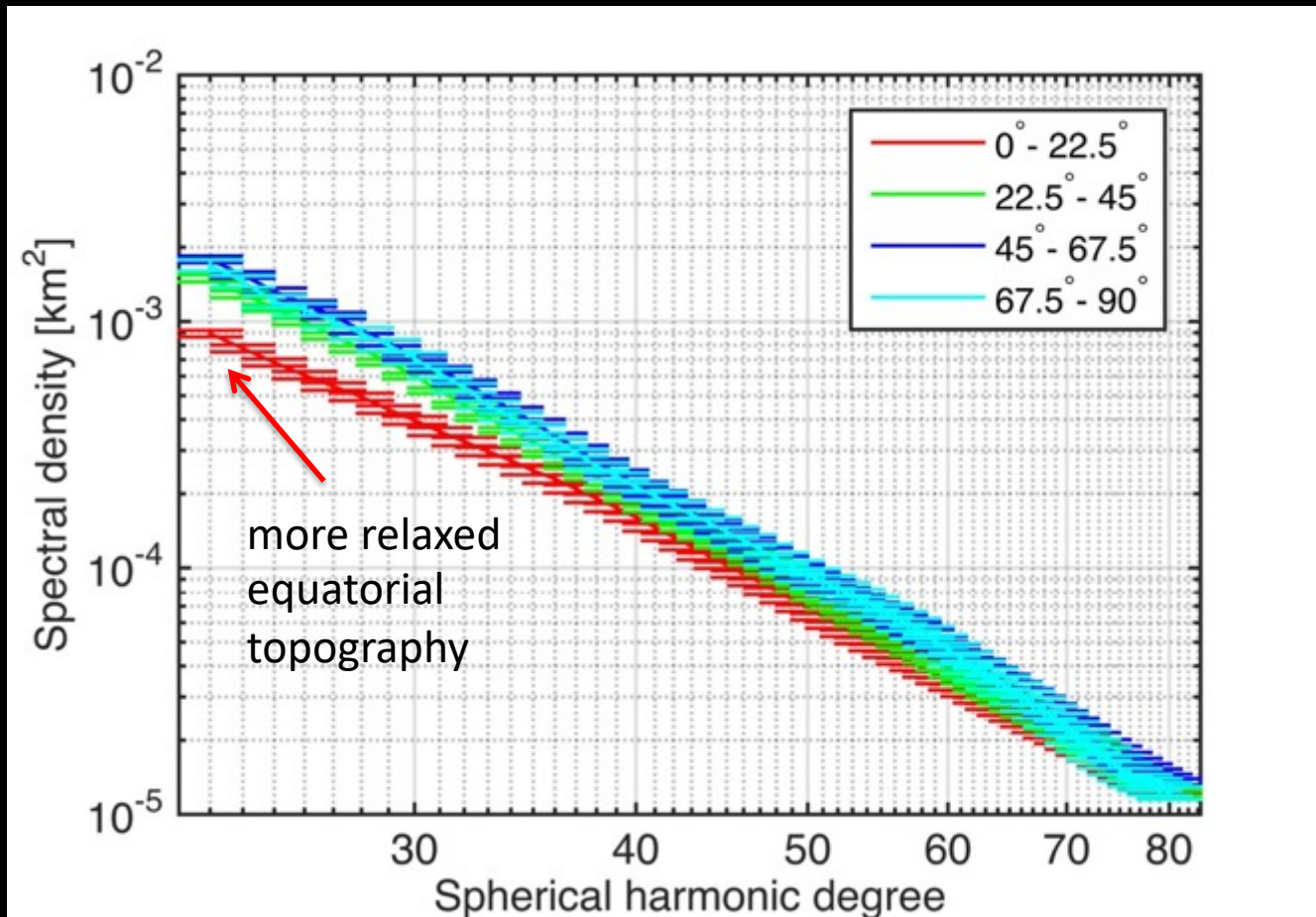
# Two-layer model

- Simplest model to interpret the gravity-topography data
- Only 5 parameters: two densities, two radii and rotation rate
- Yields  $C/Ma^2 = 0.373$   
 $C/M(R_{vol})^2 = 0.392$



Using Tricarico 2014 for computing hydrostatic equilibrium

# Latitude dependence of relaxation



Ermakov et al., in prep

# Gravity and topography in spherical harmonics

- **Shape radius vector**

$$r(\phi, \lambda) = R_0 \left[ \sum_{n=1}^{\infty} \sum_{m=0}^n (A_{nm} \cos(m\lambda) + B_{nm} \sin(m\lambda)) P_{nm}(\sin \phi) \right]$$

- **Gravitational potential**

$$U(r, \phi, \lambda) = \frac{GM}{R} \left[ 1 + \sum_{n=2}^{\infty} \sum_{m=0}^n \left( \frac{R_0}{r} \right)^n (C_{nm} \cos(m\lambda) + S_{nm} \sin(m\lambda)) P_{nm}(\sin \phi) \right]$$

- **Power Spectral Density**

$$S_n^{gg} = \sum_{m=0}^n \frac{C_{nm}^2 + S_{nm}^2}{2n+1}$$

gravity

$$S_n^{tt} = \sum_{m=0}^n \frac{A_{nm}^2 + B_{nm}^2}{2n+1}$$

topography

$$S_n^{gt} = \sum_{m=0}^n \frac{A_{nm} C_{nm} + B_{nm} S_{nm}}{2n+1}$$

gravity-topography  
cross power

# Isostatic model

$Z_n$  - gravity-topography admittance

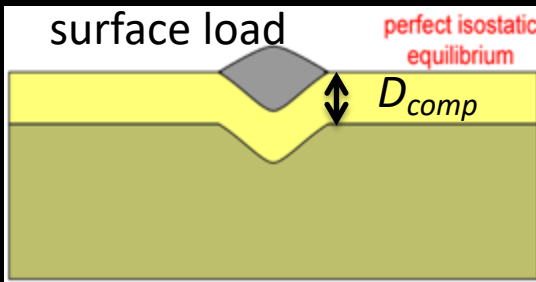
$$Z_n = \frac{S_{gt}}{S_{tt}}$$

➤ Linear two-layer hydrostatic model

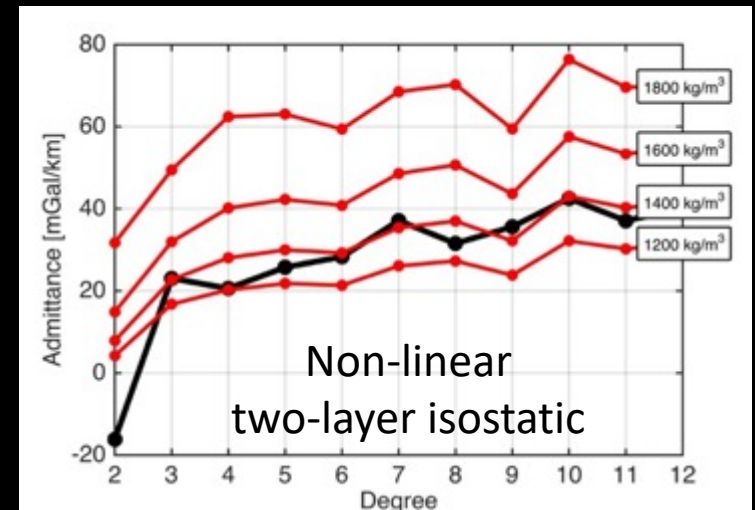
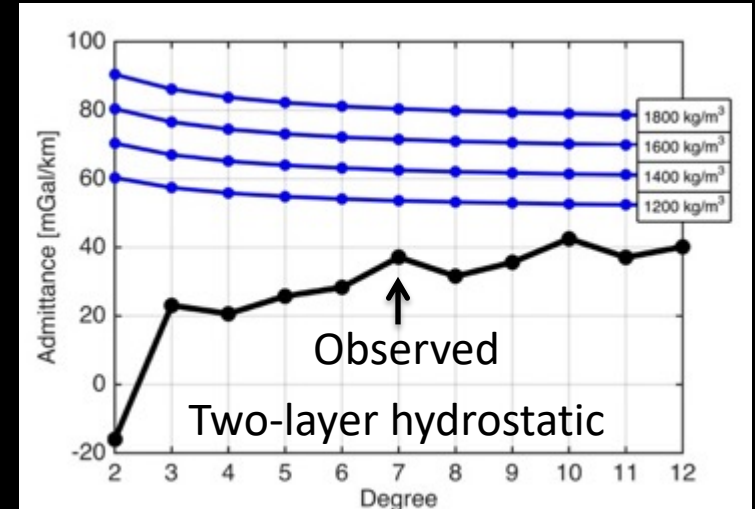
$$Z_n = \frac{GM}{R^3} \frac{3(n+1)}{2n+1} \frac{\rho_{crust}}{\rho_{mean}}$$

➤ Linear isostatic model

$$Z_n = \frac{GM}{R^3} \frac{3(n+1)}{2n+1} \frac{\rho_{crust}}{\rho_{mean}} \left[ 1 - \left( 1 - \frac{D_{comp}}{R} \right)^n \right]$$

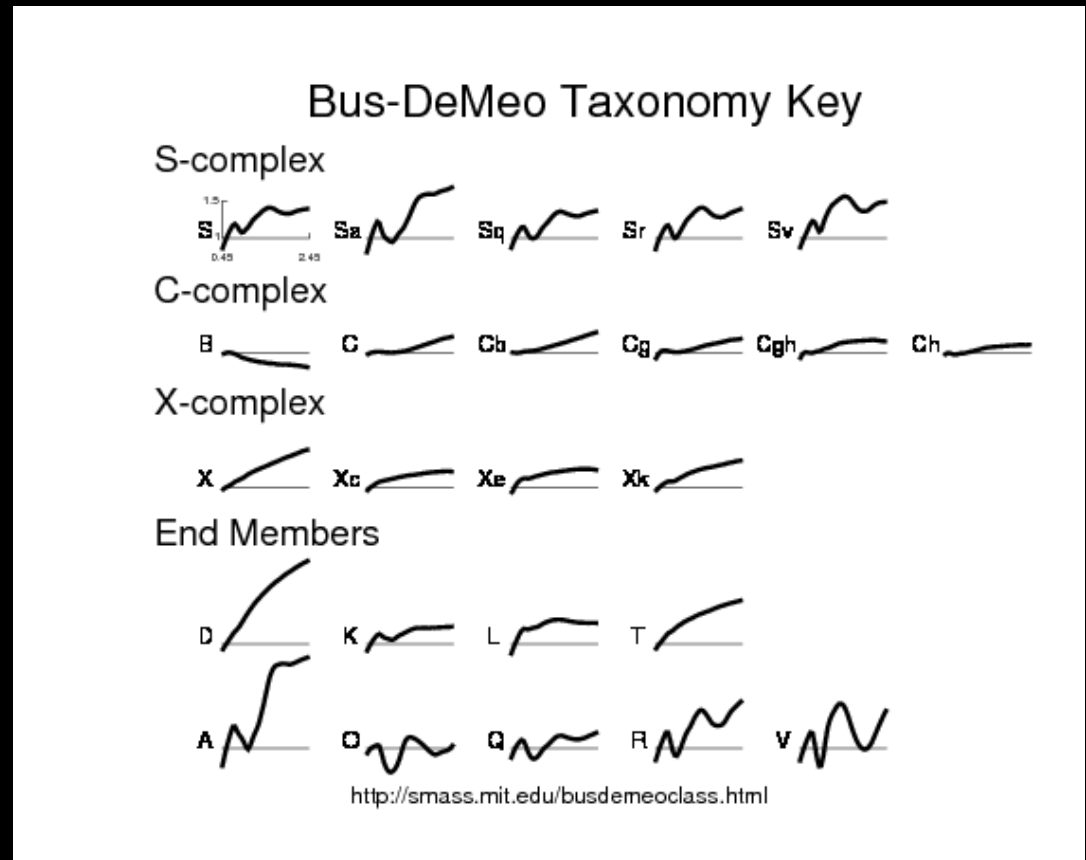


$D_{comp}$  - depth of compensation



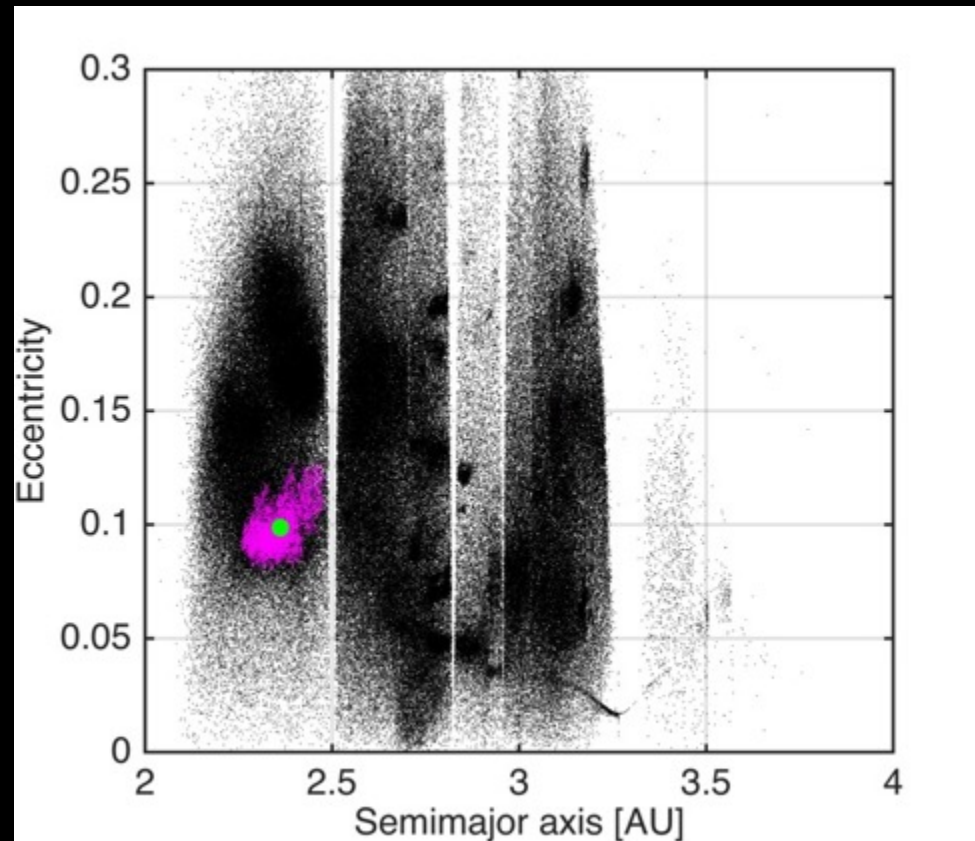
# Why Vesta?

- Unique basaltic spectrum



# Why Vesta?

- **Unique basaltic spectrum**
- **A group of asteroids in the dynamical vicinity of Vesta with similar spectra**



# Why Vesta?

- Unique basaltic spectrum
- A group of asteroids in the dynamical vicinity of Vesta with similar spectra
- Large depression in the southern hemisphere of Vesta

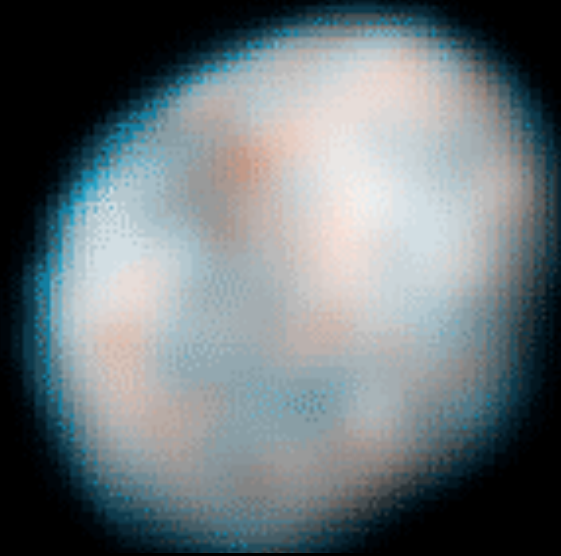
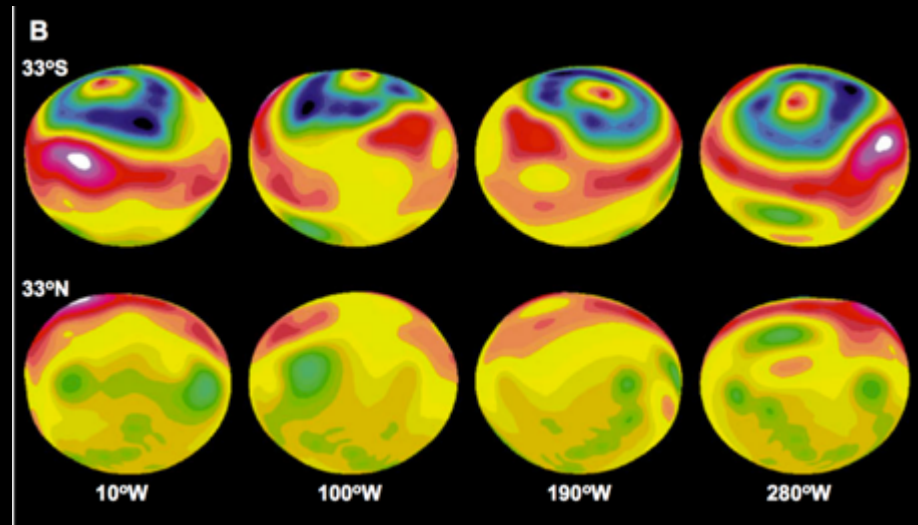


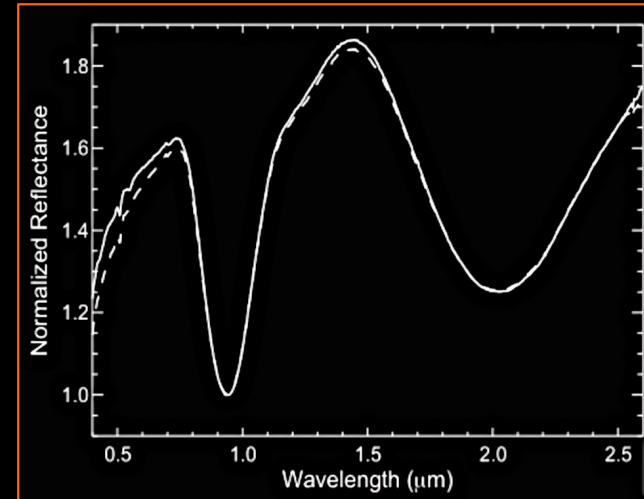
Image credit: NASA/HST



JPL postdoc Thomas et al., 1997

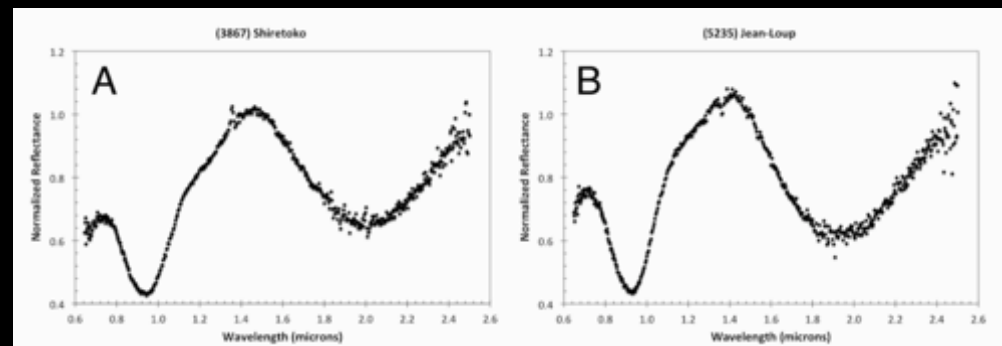
# Why Vesta?

- **Unique basaltic spectrum**
- **A group of asteroids in the dynamical vicinity of Vesta with similar spectra**
- **Large depression in the southern hemisphere of Vesta**
- **A group of Howardite-Eucrite-Diogenite (HED) meteorites, with similar reflectance spectra**



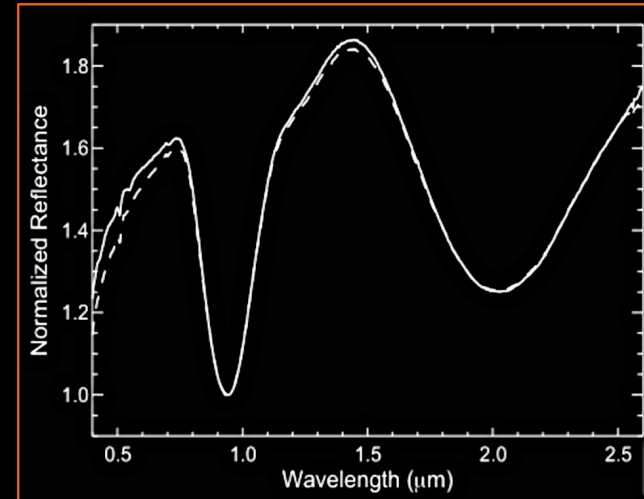
↑ Reflectance spectra of eucrite Millbillillie from Wasson et al. (1998)

↓ V-type asteroids spectra from Hardensen et al., (2014)



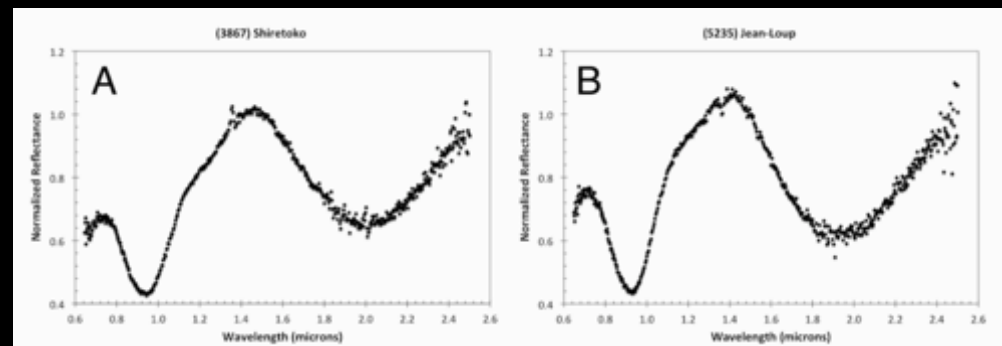
# Why Vesta?

- **Unique basaltic spectrum**
- **A group of asteroids in the dynamical vicinity of Vesta with similar spectra**
- **Large depression in the southern hemisphere of Vesta**
- **A group of Howardite-Eucrite-Diogenite (HED) meteorites, with similar reflectance spectra**
- **Strongest connection between a class of meteorites and an asteroidal family**



↑ Reflectance spectra of eucrite Millbillillie from Wasson et al. (1998)

↓ V-type asteroids spectra from Hardensen et al., (2014)



# Note on Vening-Meinesz and Kaula rules

- Vening-Meinesz rule for variance of topography (Vening-Meinesz, 1951)

$$V_t \sim 1/n^2$$

- Kaula law for RMS of gravity (Kaula, 1963)

$$M_g \sim 1/n^2$$

- Are these two rules consistent assuming uncompensated topography?

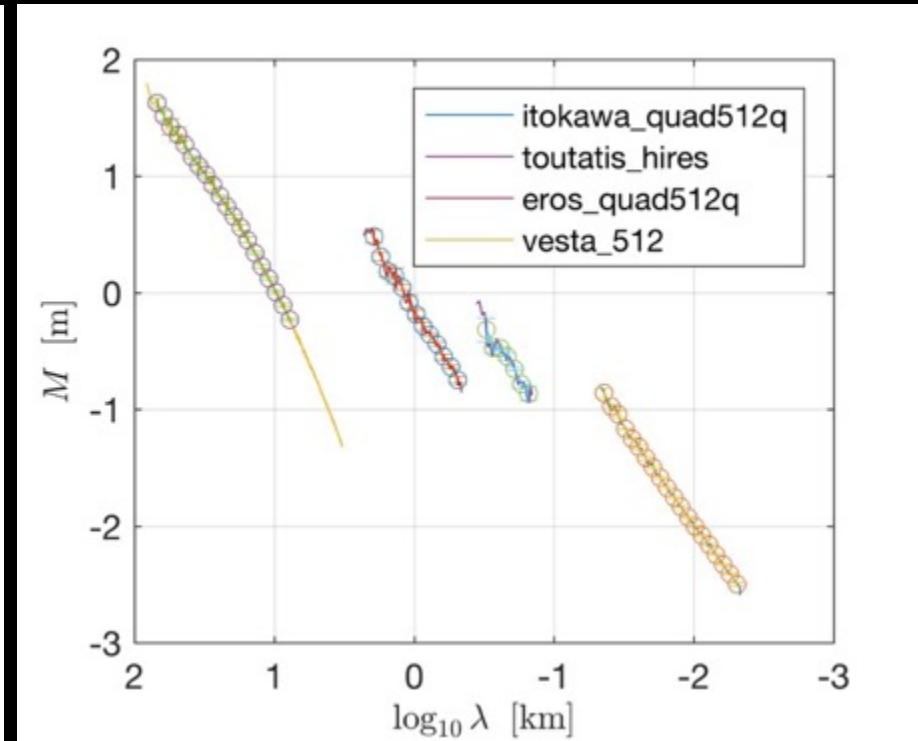
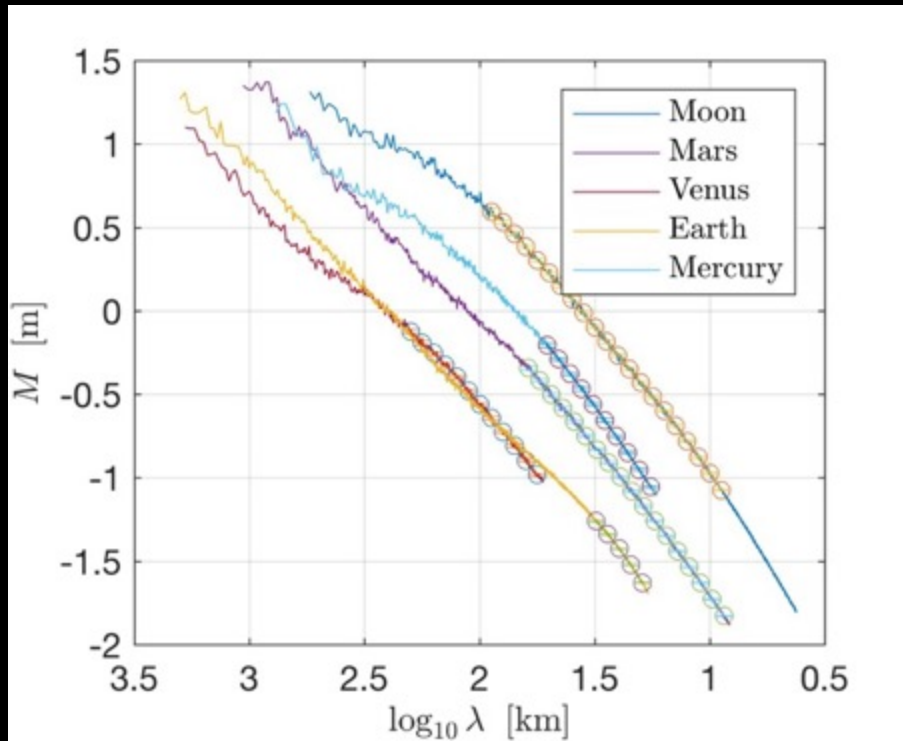
$$V_t \sim 1/n^2 \Rightarrow M_t \sim 1/n^{1.5} \Rightarrow M_g \sim 1/n^{2.5}$$

- But Kaula rule says  $M_g \sim 1/n^2$  NOT  $M_g \sim 1/n^{2.5}$



- Typically assumed in the literature Kaula and Vening-Meinesz rules are not mutually consistent assuming uncompensated topography

# RMS spectra



# Power laws

- General form of a power law

$$M = AR^{\alpha_1} Q^{\alpha_2} \lambda^{\alpha_3}$$

- Power law assuming (inverse) surface gravity scaling ( $g \sim R^* \rho$ )

$$M = AR^{-1} Q^{-1} \lambda^{\alpha_3}$$

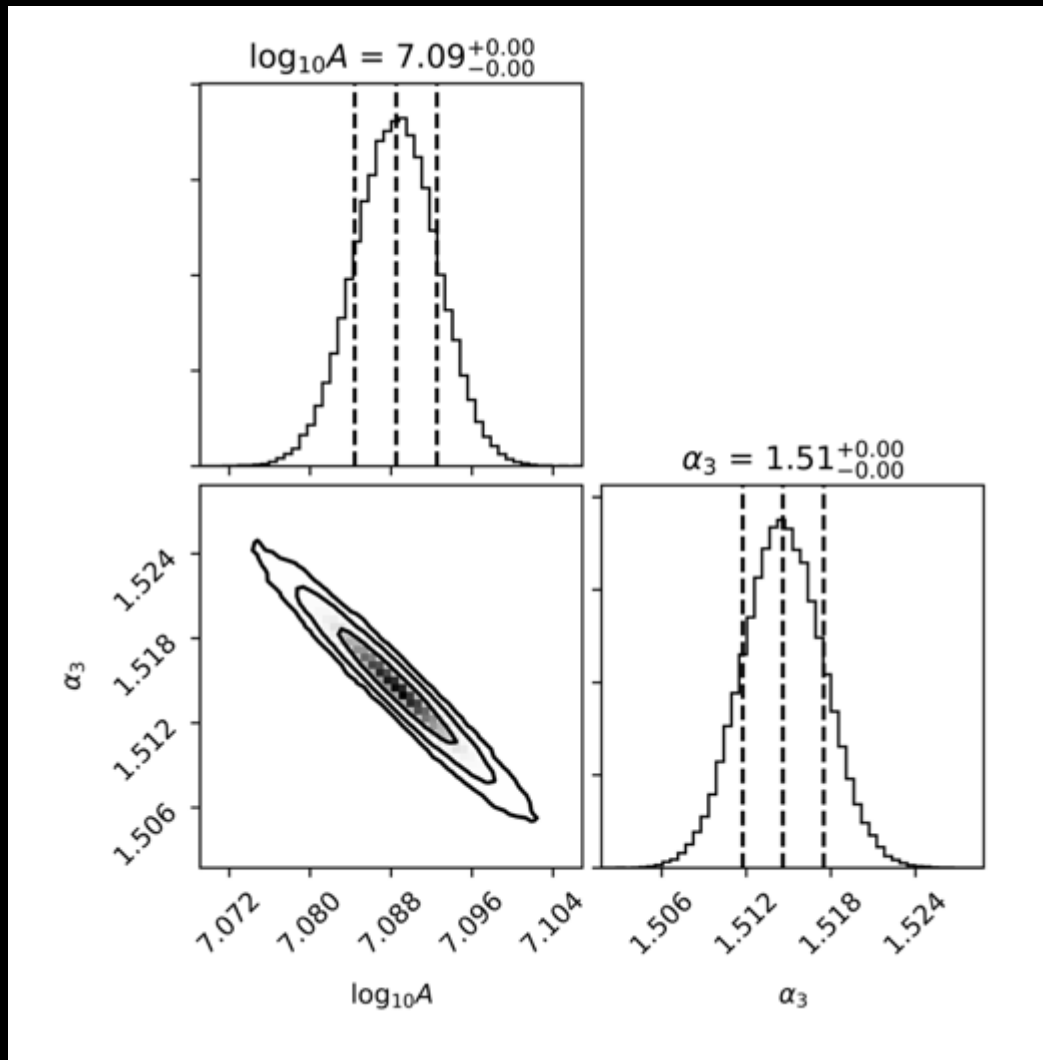
- If we take a  $\log_{10}$  of  $M$ , we get an equation of a hyperplane

$$\log_{10} M = \log_{10} A + \alpha_1 \log_{10} R + \alpha_2 \log_{10} Q + \alpha_3 \log_{10} \lambda$$

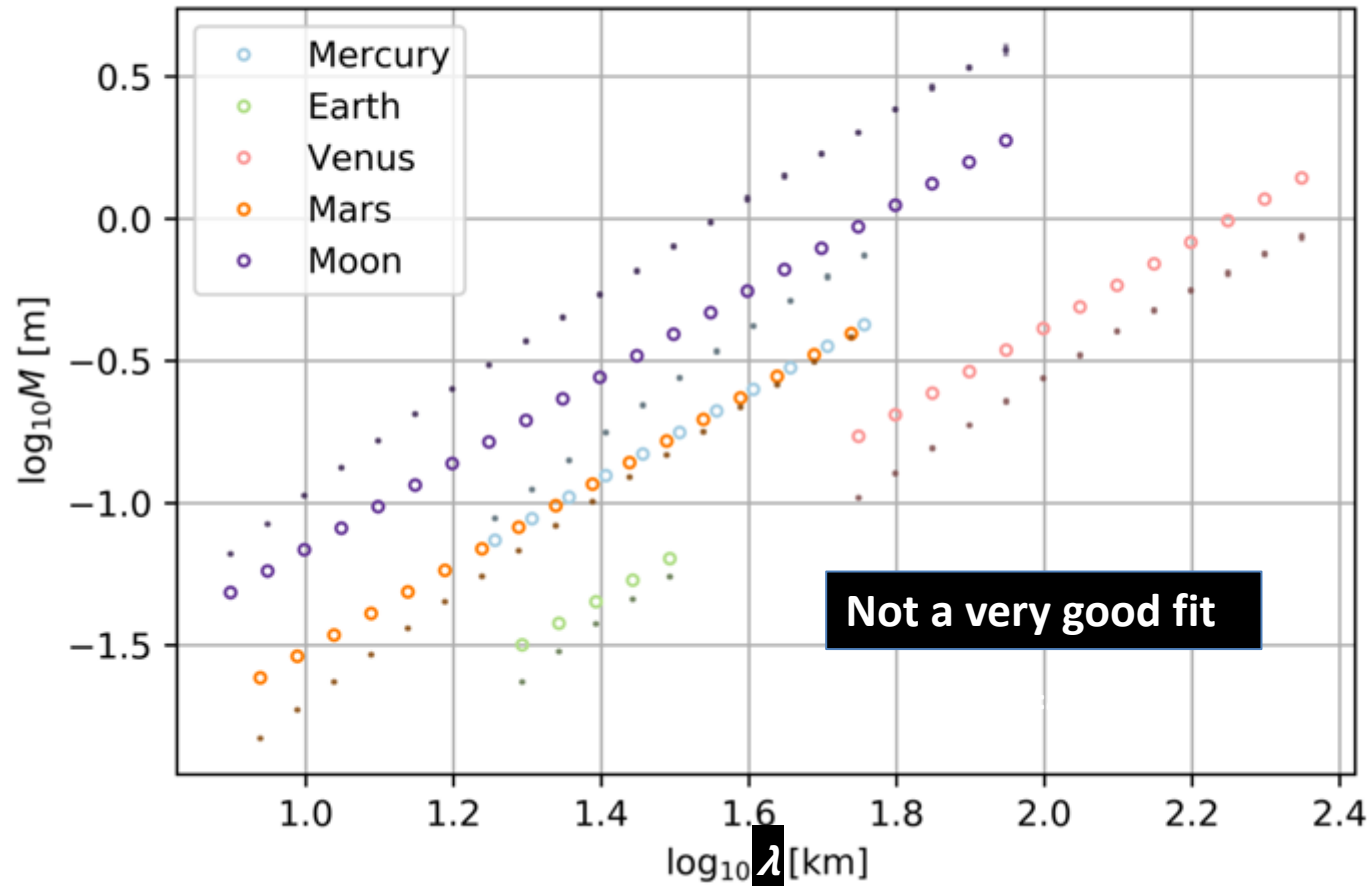
- In our data set, we have a lot of points along the  $\lambda$  direction and not as many points on the other two ( $R$  and  $\rho$ ) directions.
  - In the  $R$  and  $\rho$  directions, we have as many data points as we have bodies
  - In the  $\lambda$  direction, we have as many data points as many we have  $\lambda$  bins.

# Results of the MCMC runs

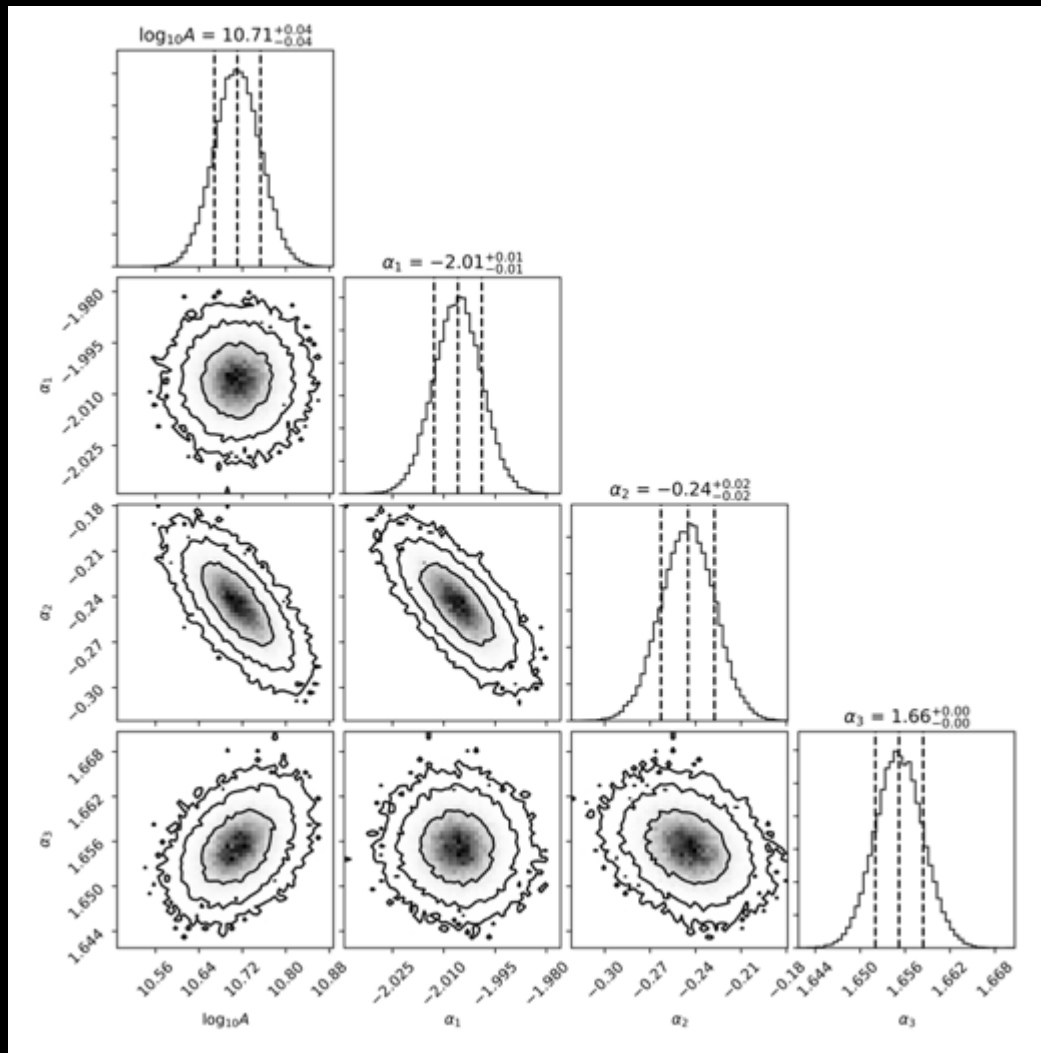
# Planets, gravity scaling



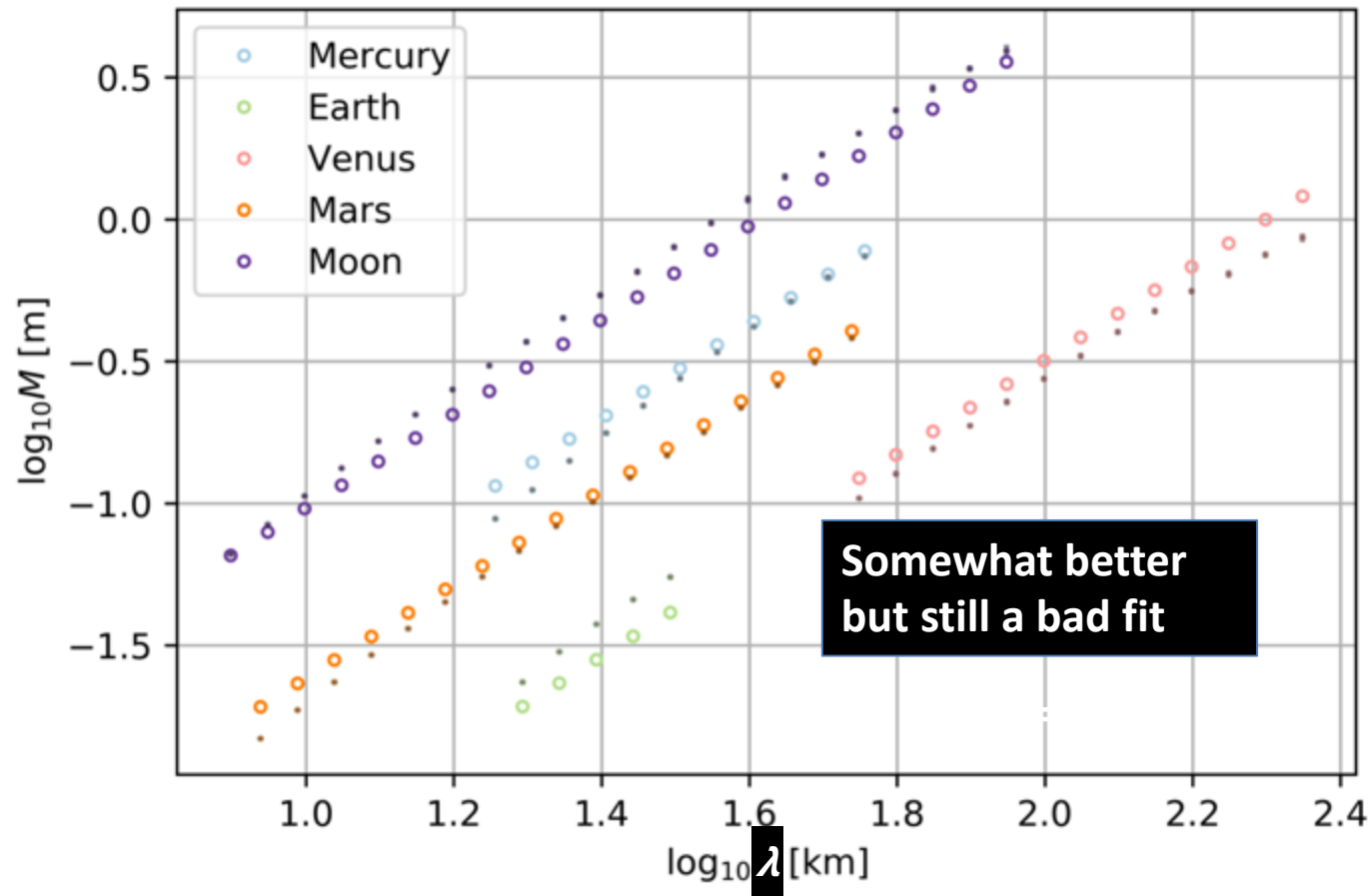
# Planets, gravity scaling



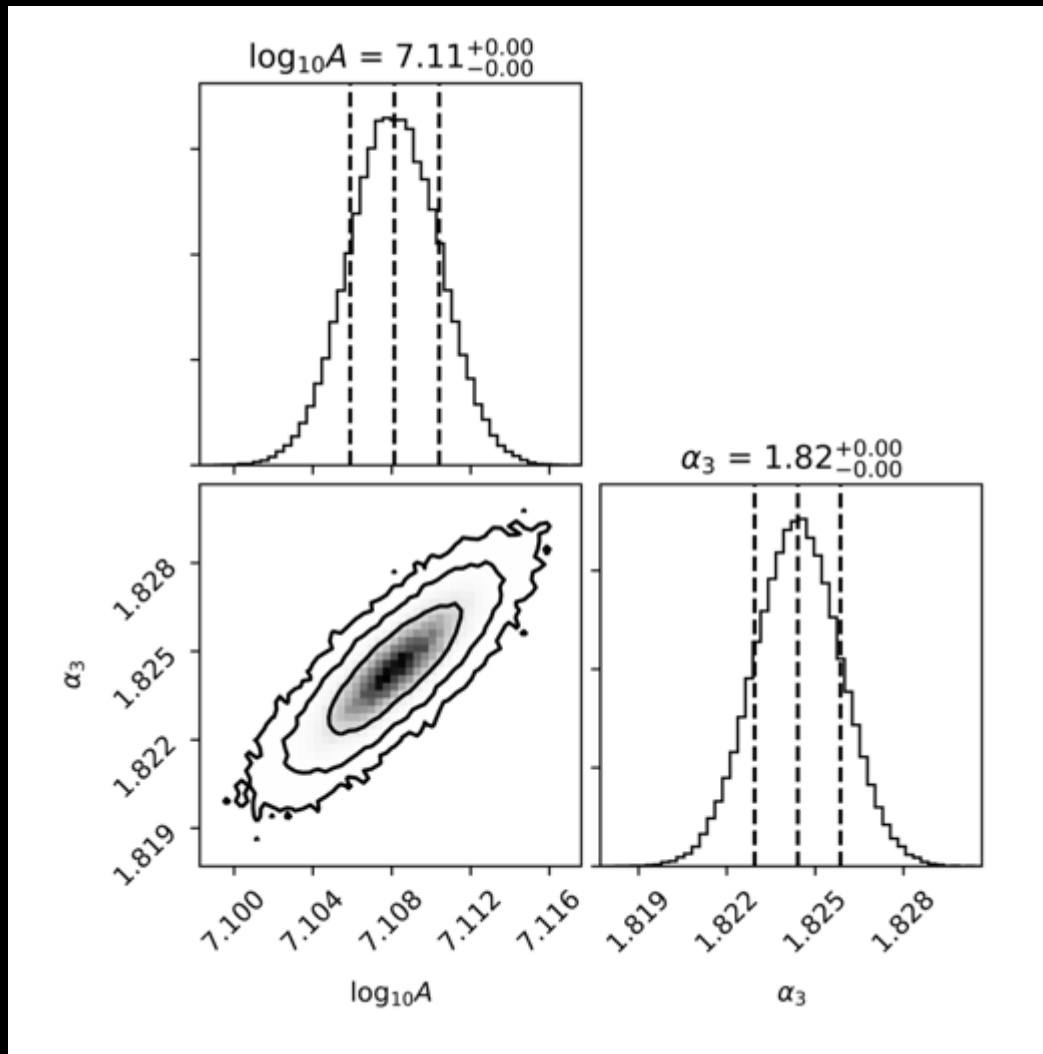
# Planets, general scaling



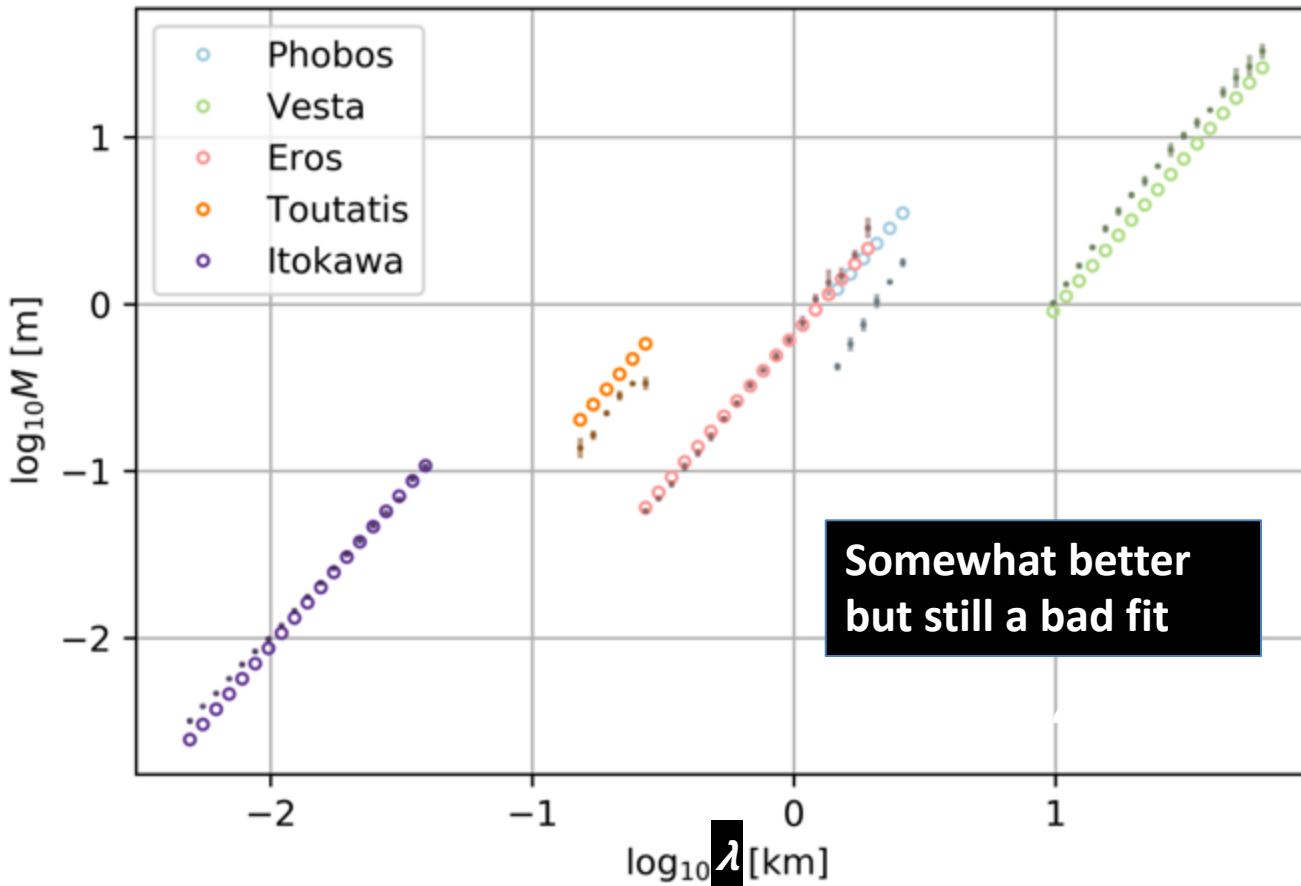
# Planets, general scaling



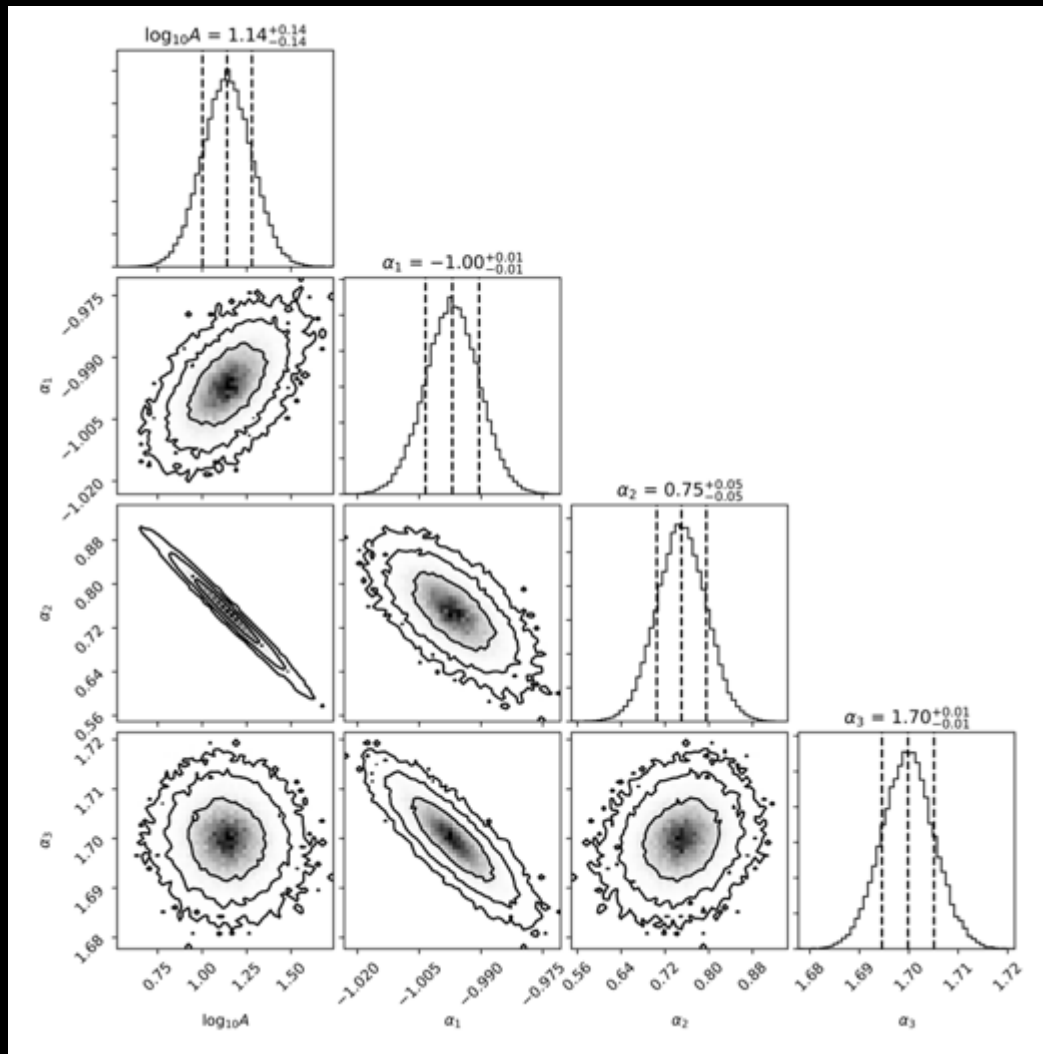
# Asteroids, gravity scaling



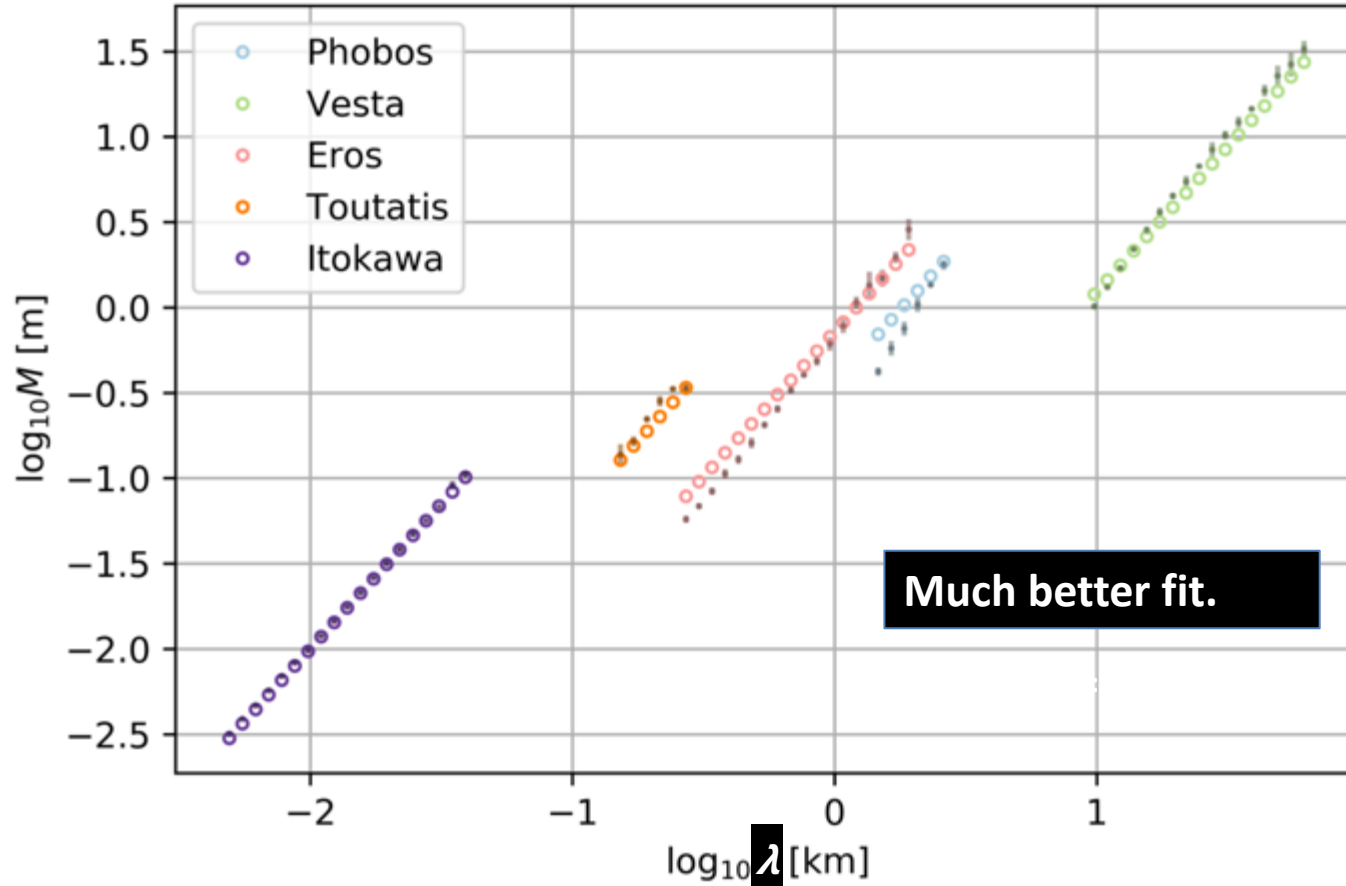
# Asteroids, gravity scaling



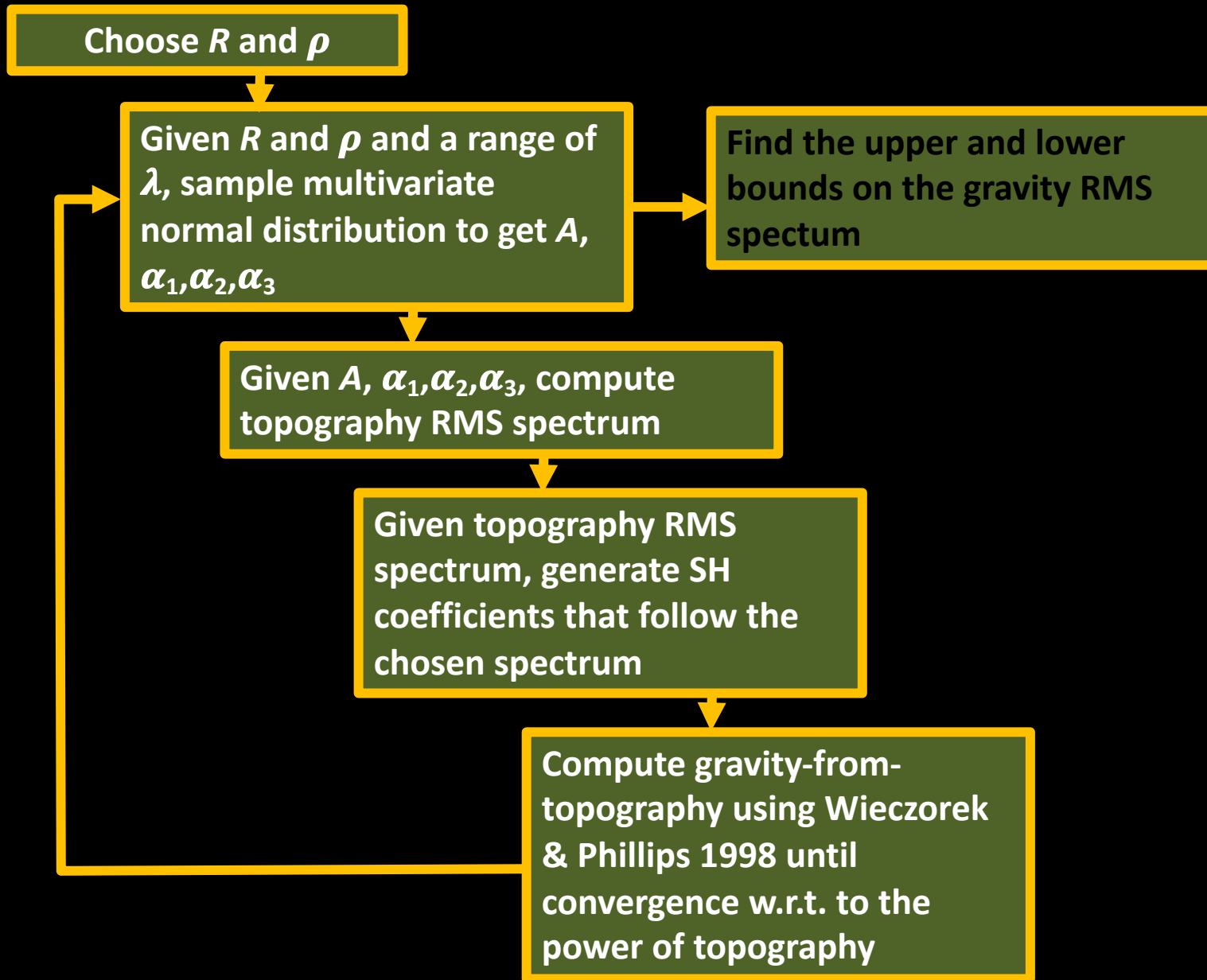
# Asteroids, general scaling



# Asteroids, general scaling



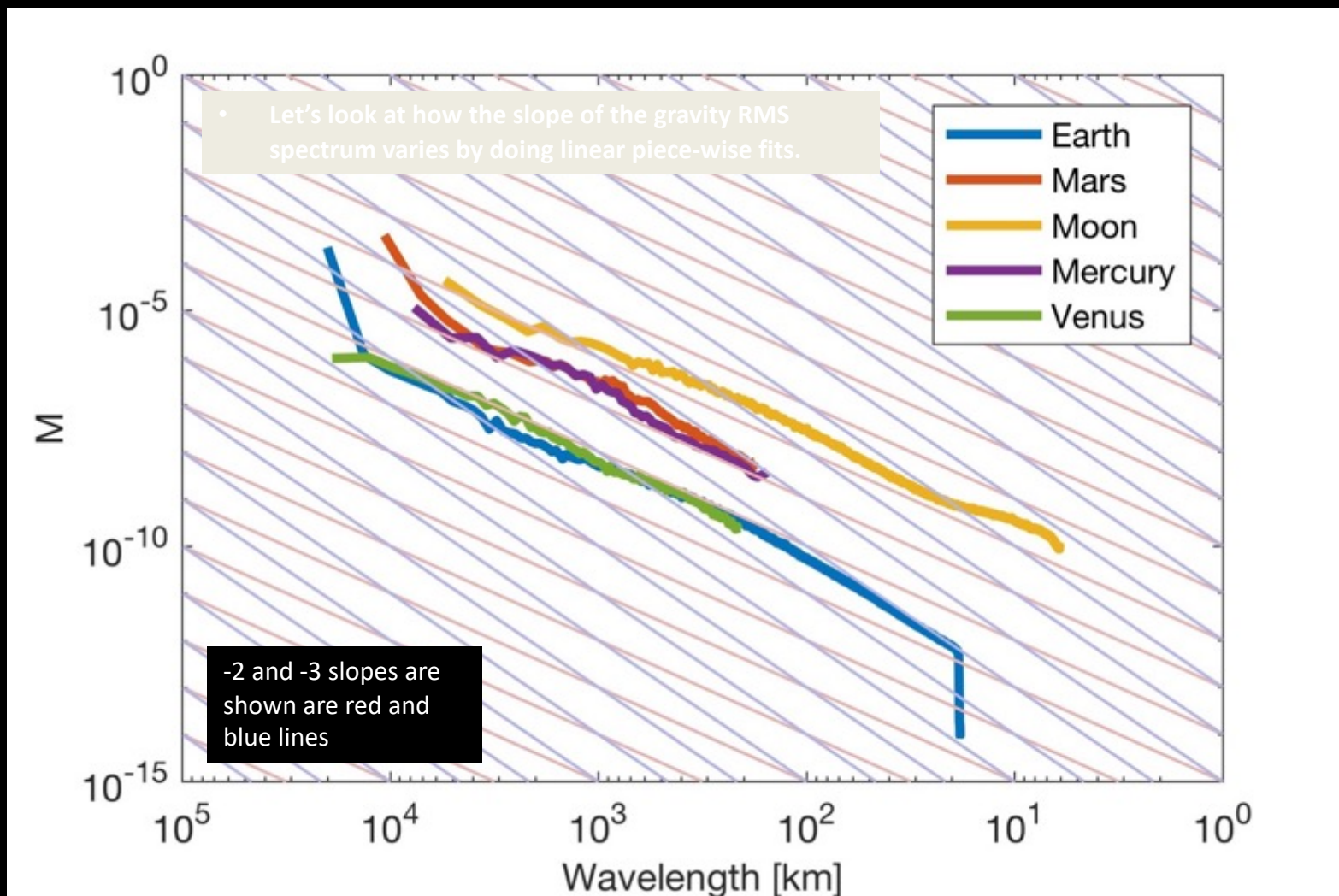
# A priori constraint on gravity RMS



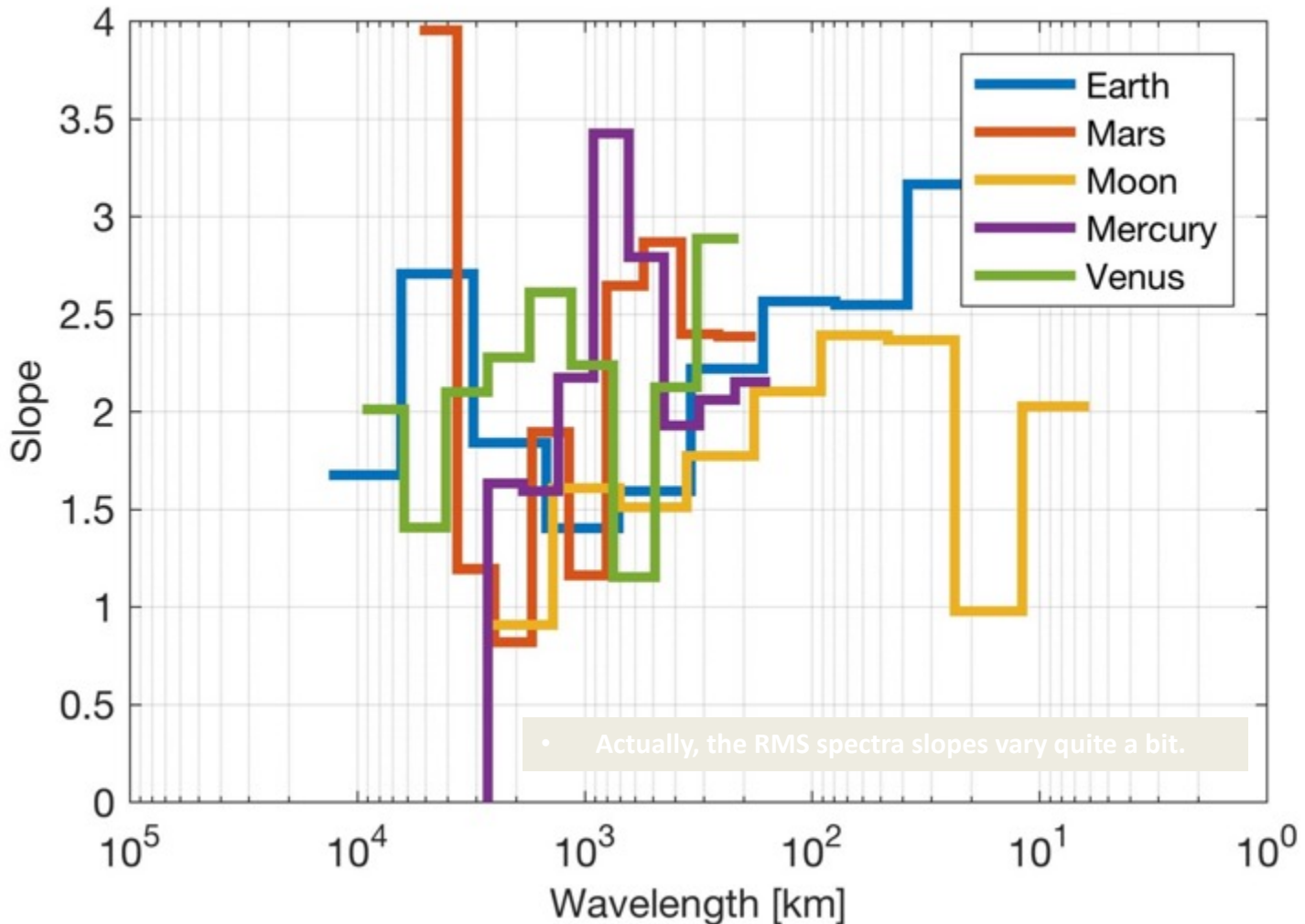
# Summary

- **Topography RMS spectra of 4 terrestrial planets and the Moon cannot be simultaneously fit with a single power law of the gravity-scaling or general form.**
- **Topography RMS spectra of asteroids CANNOT be *satisfactorily* fit with a power law the gravity-scaling form.**
- **Topography RMS spectra of asteroids CAN be *satisfactorily* fit with a power law of the general form.**
- **Despite having different internal structure, composition and mechanical properties of the surface layer, the asteroid topography spectra can be effectively modeled as a general power law**

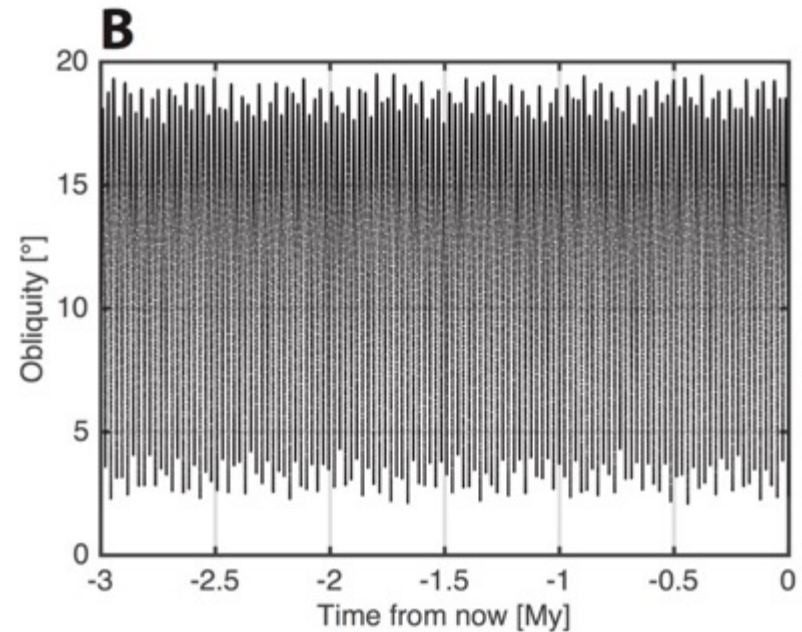
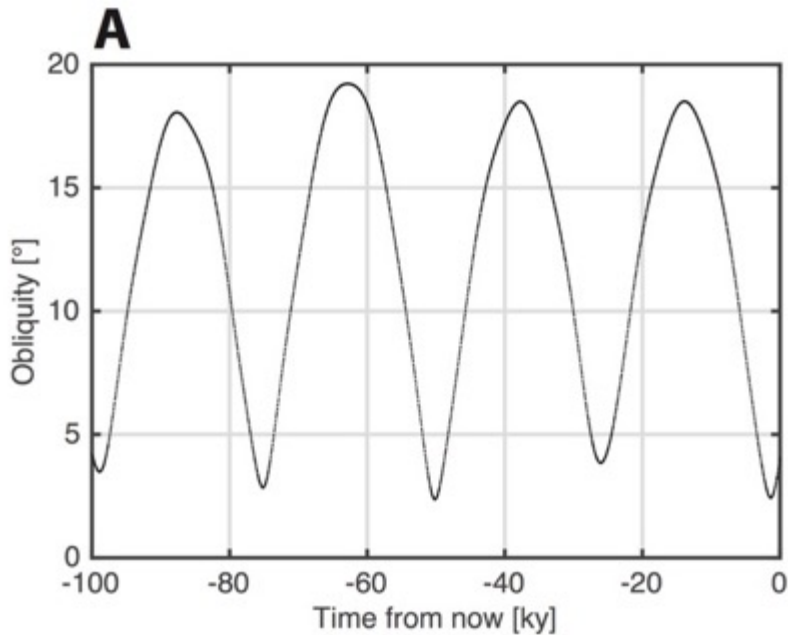
# Gravity RMS spectra



# Slopes of piecewise fitted gravity RMS spectra

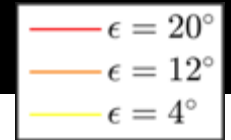
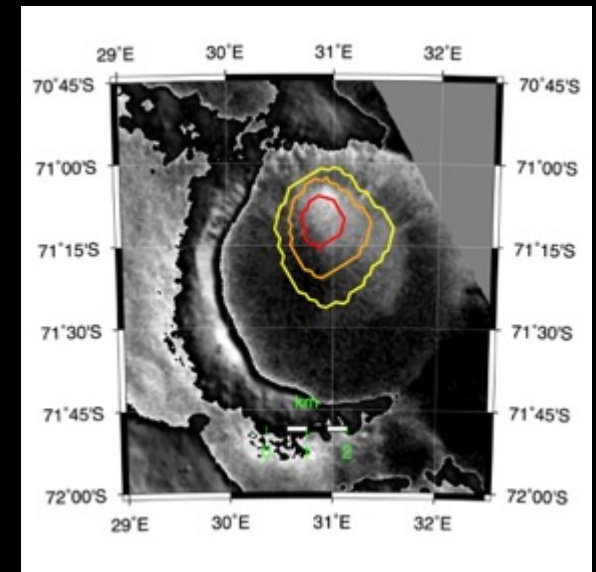
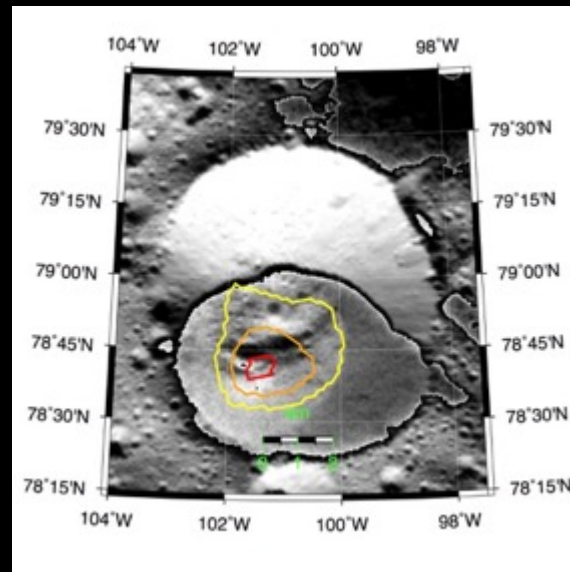
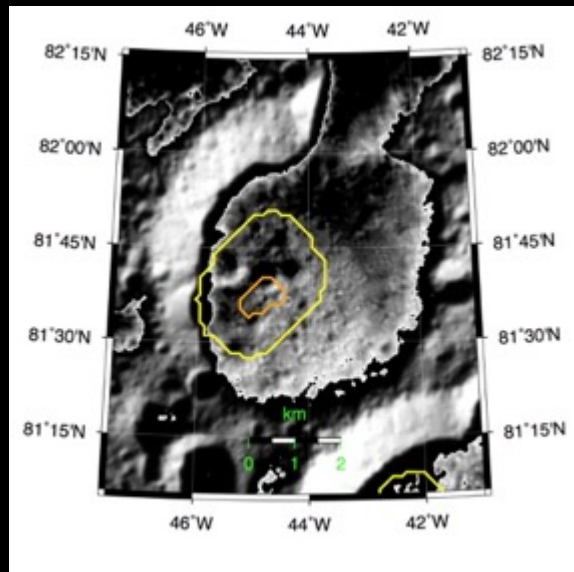
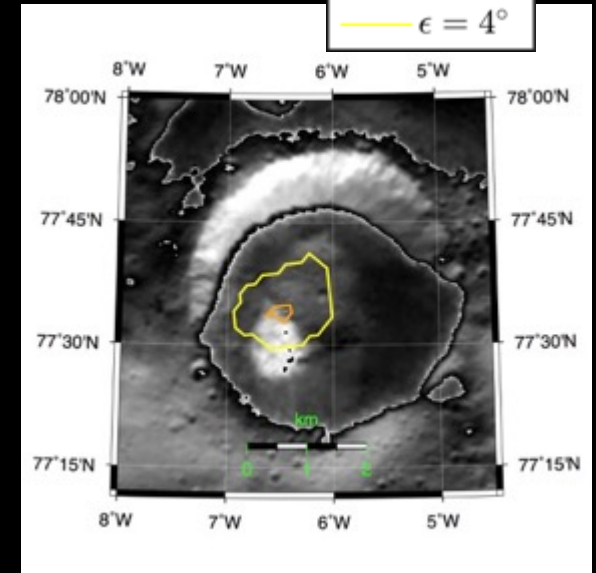
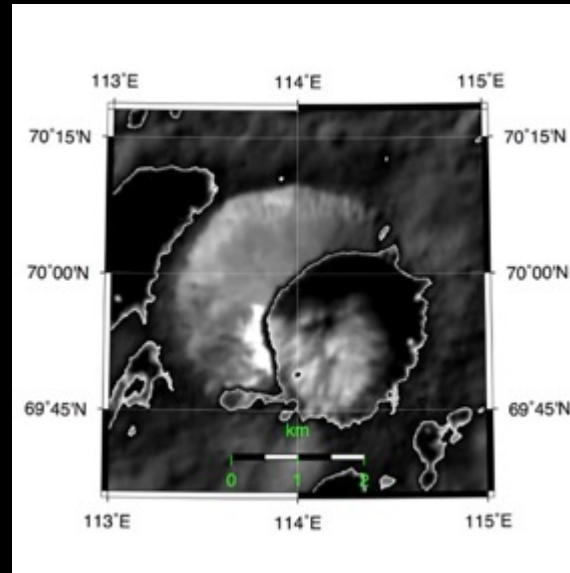
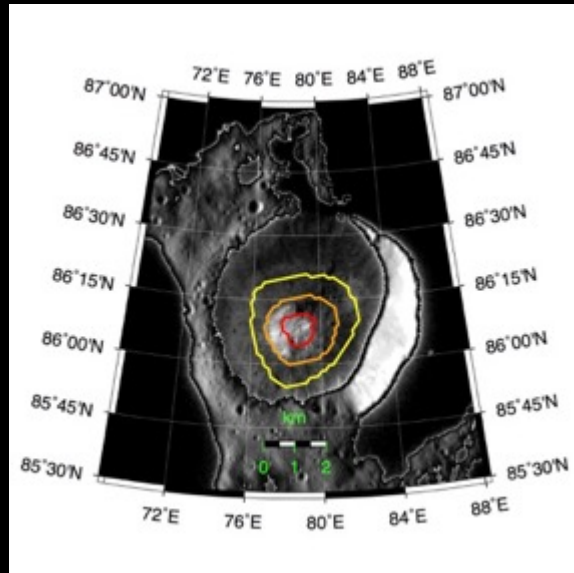


# Ceres' obliquity history



- **Obliquity varies between 2.4° and 19.7°**
- **The main period is 24.5 ky**
- **We happen to visit Ceres when its obliquity is minimal**

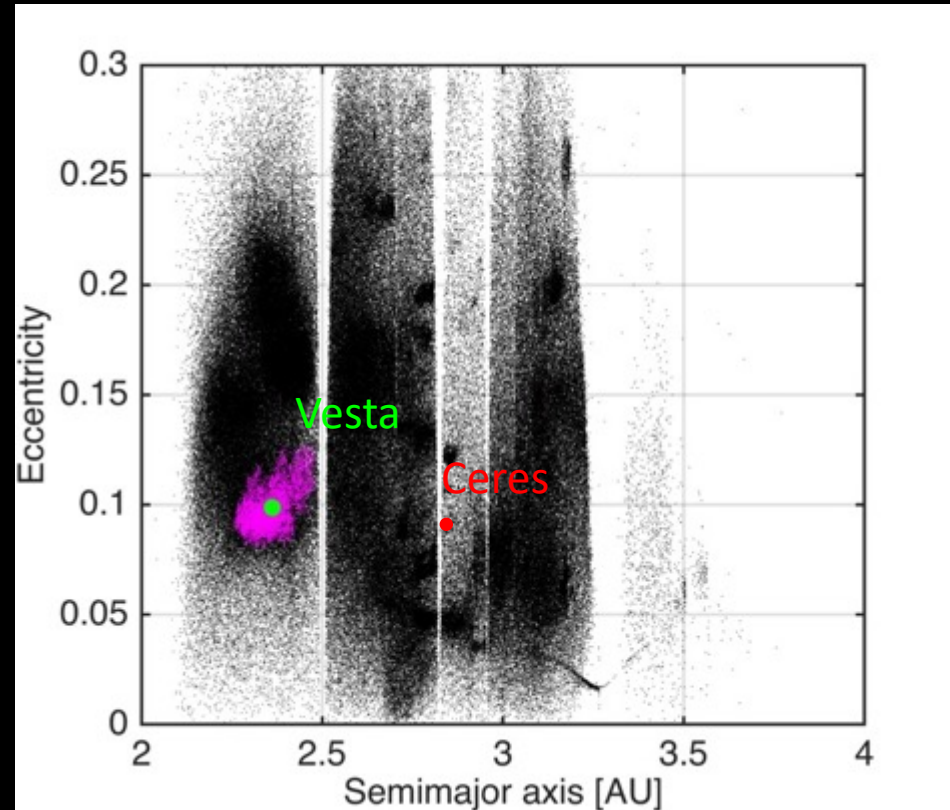
# Bright Crater Floor Deposits (BCFDs)



# Why Ceres?

- **Largest body in the asteroid belt**
- **Low density implies high volatile content**
- **Conditions for subsurface ocean**
- **Much easier to reach than other ocean worlds**

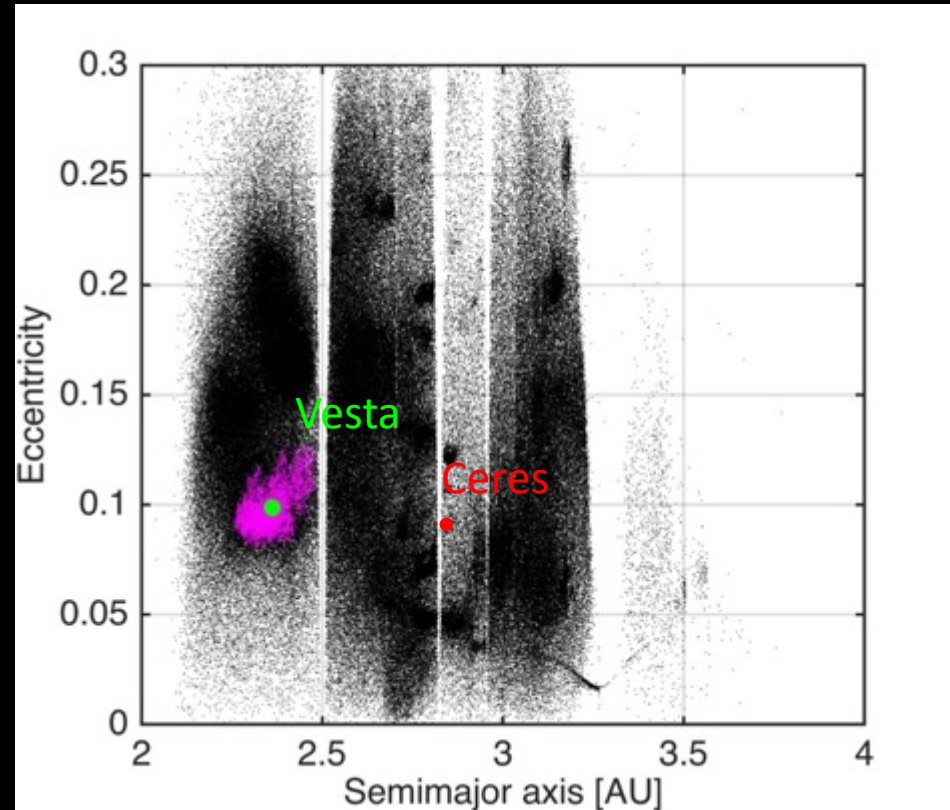
Ceres location in the asteroid belt



# Why Ceres?

- **Largest body in the asteroid belt**
- **Low density implies high volatile content**
- **Conditions for subsurface ocean**
- **Much easier to reach than other ocean worlds**
- **Major unexplored object in the asteroid belt**

Ceres location in the asteroid belt



# What did we know before Dawn

- **Castillo-Rogez and McCord 2010**

**Ceres accreted as a mixture of ice and rock just a few My after the condensation of Calcium Aluminum-rich Inclusions (CAIs), and later differentiated into a water mantle and a mostly anhydrous silicate core.**

# What did we know before Dawn

- **Castillo-Rogez and McCord 2010**

Ceres accreted as a mixture of ice and rock just a few My after the condensation of Calcium Aluminum-rich Inclusions (CAIs), and later differentiated into a water mantle and a mostly anhydrous silicate core.

- **Zolotov 2009**

Ceres formed relatively late from planetesimals consisting of hydrated silicates.

# What did we know before Dawn

- **Castillo-Rogez and McCord 2010**

Ceres accreted as a mixture of ice and rock just a few My after the condensation of Calcium Aluminum-rich Inclusions (CAIs), and later differentiated into a water mantle and a mostly anhydrous silicate core.

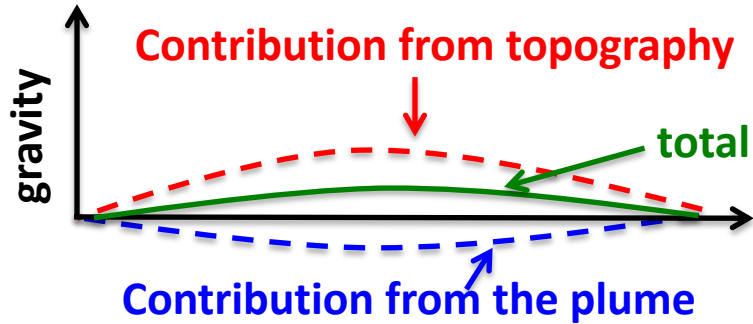
- **Zolotov 2009**

Ceres formed relatively late from planetesimals consisting of hydrated silicates.

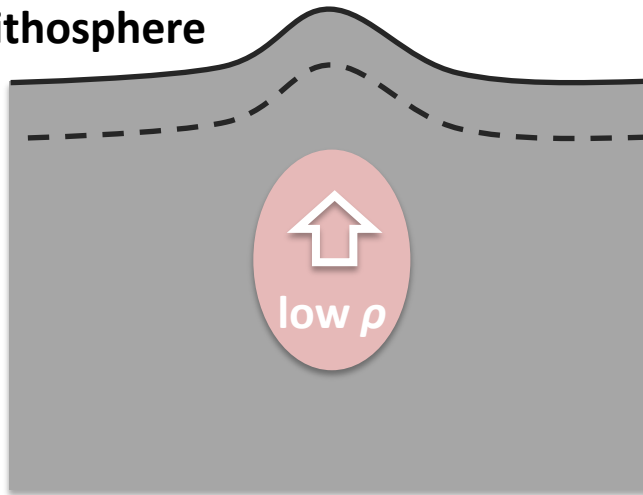
- **Bland 2013**

If Ceres *does* contain a water ice layer, its warm diurnally-averaged surface temperature ensures extensive viscous relaxation of even small impact craters especially near equator

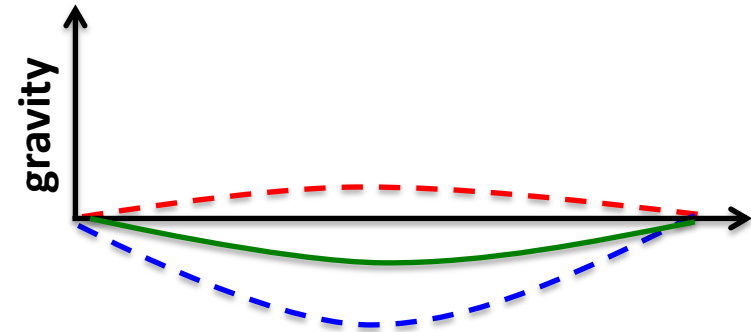
# Buoyancy-driven anomaly



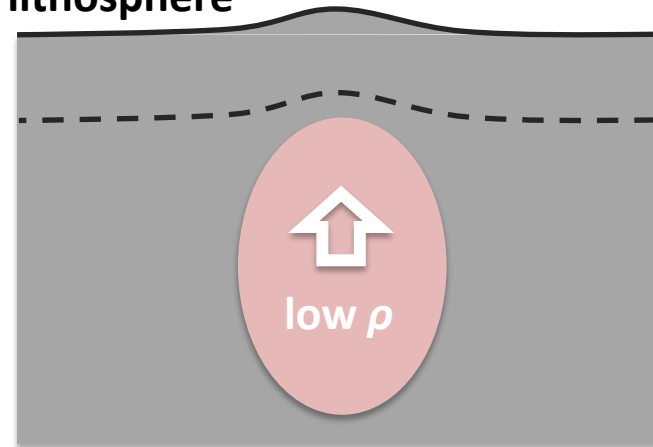
Weak lithosphere



Positive gravity-topography correlation

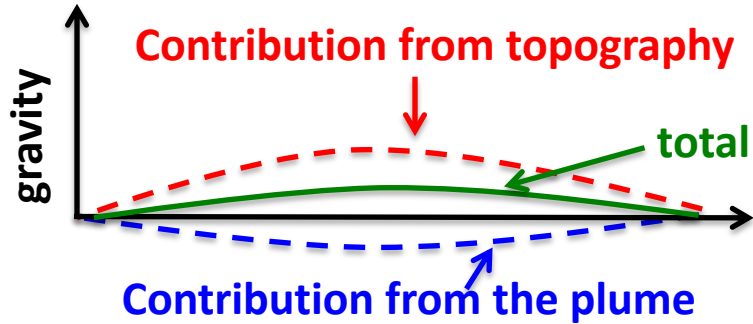


Strong lithosphere

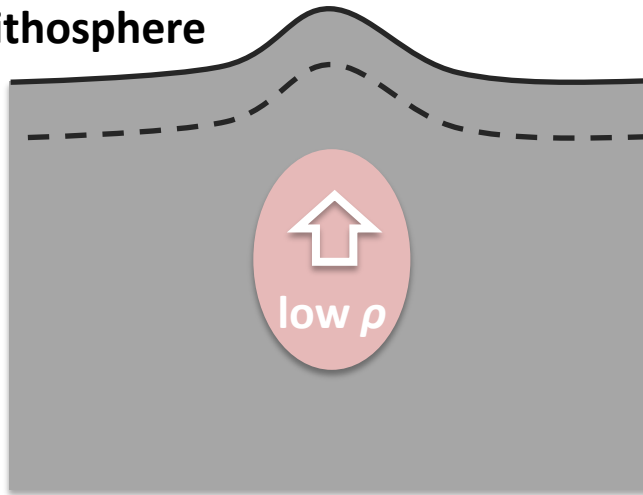


Negative gravity-topography correlation

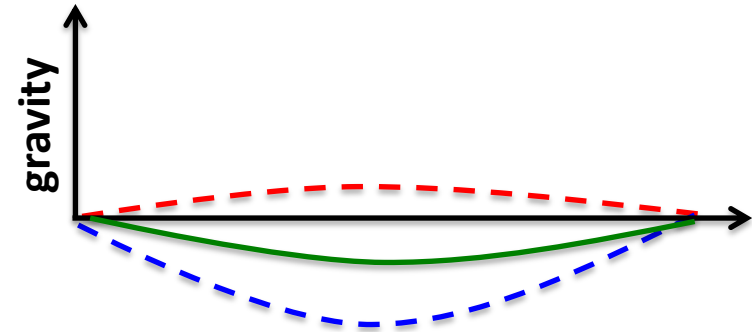
# Buoyancy-driven anomaly



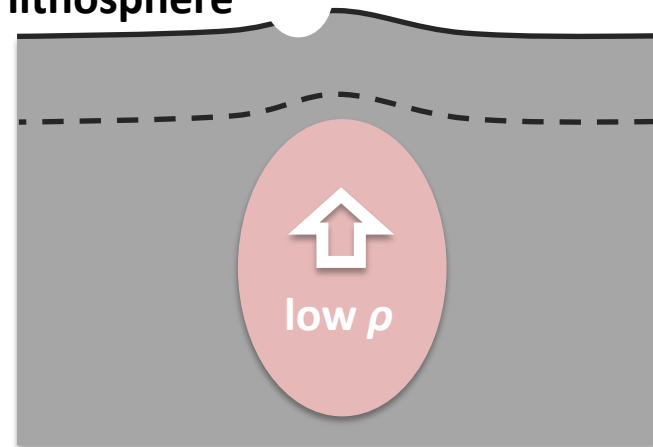
Weak lithosphere



Positive gravity-topography correlation

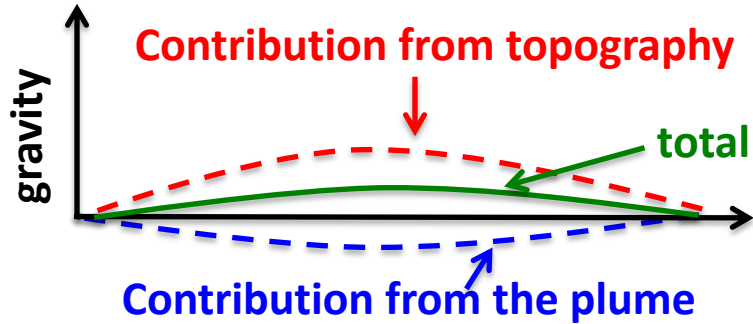


Strong lithosphere

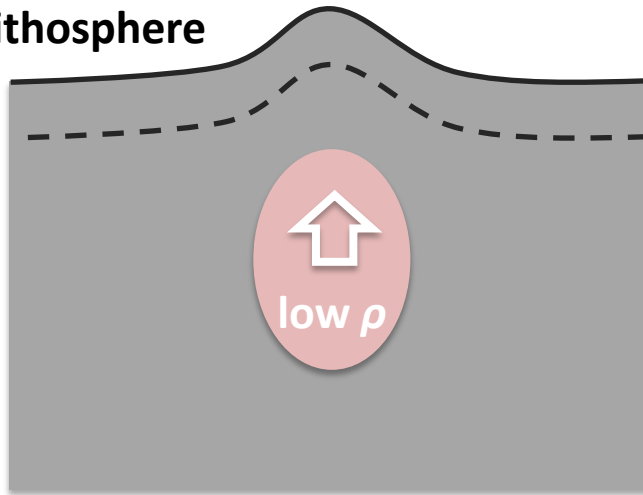


Negative gravity-topography correlation

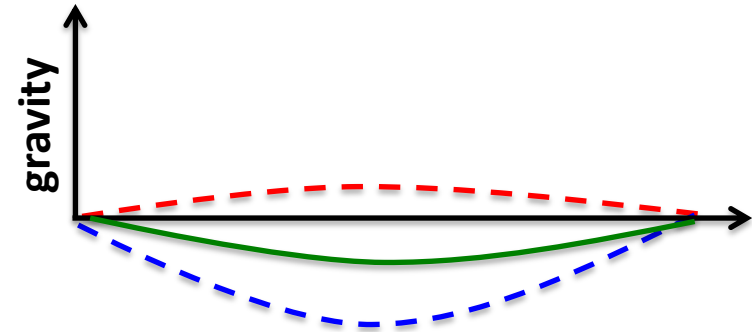
# Buoyancy-driven anomaly



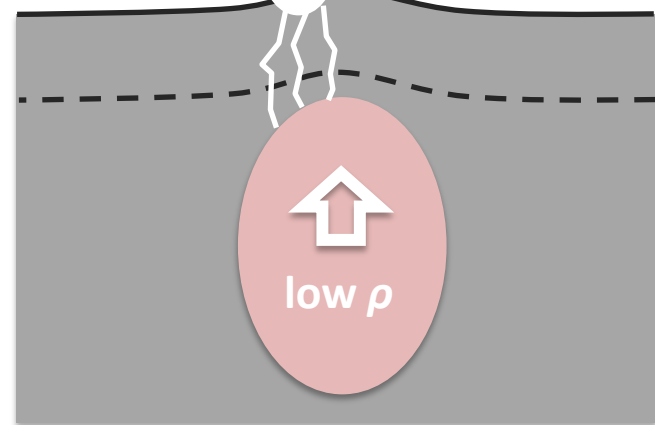
Weak lithosphere



Positive gravity-topography correlation



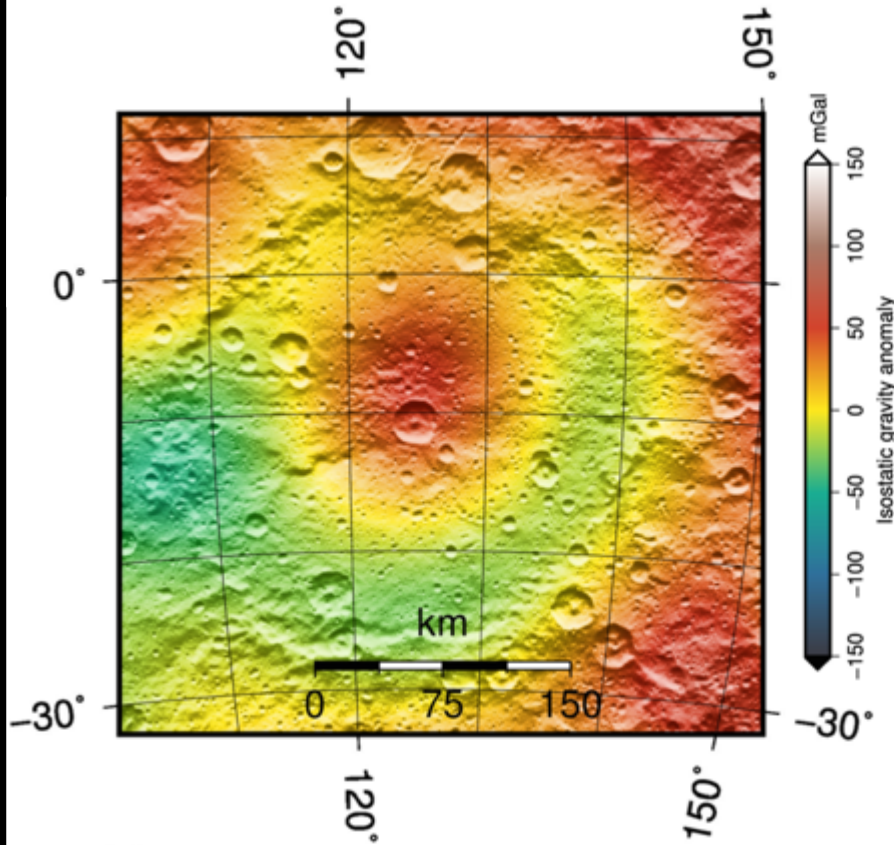
Strong lithosphere



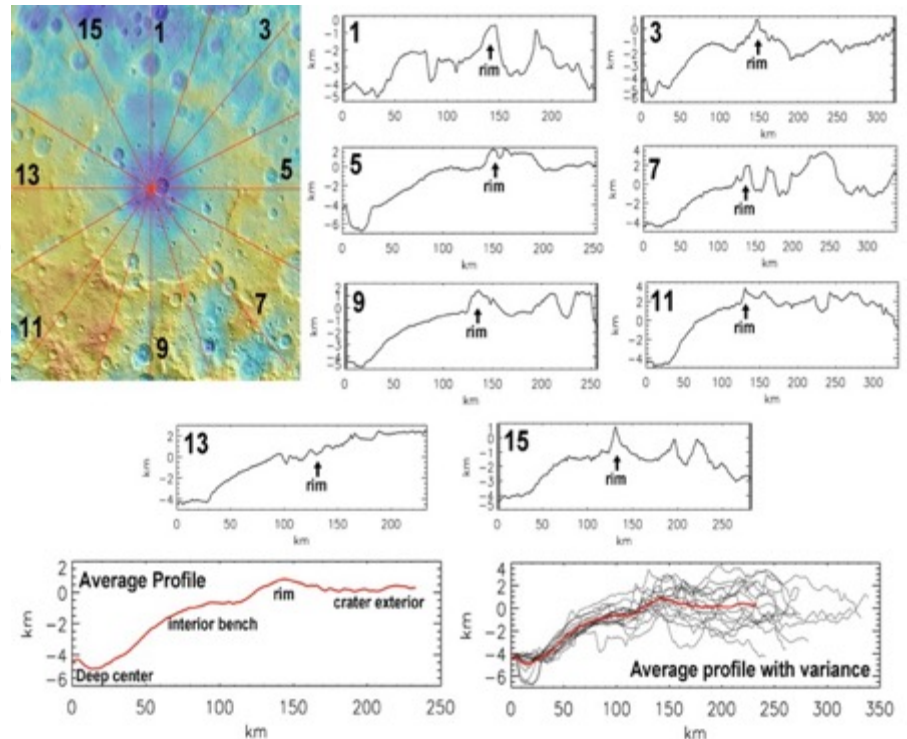
Negative gravity-topography correlation

# Mascons

Kerwan isostatic anomaly



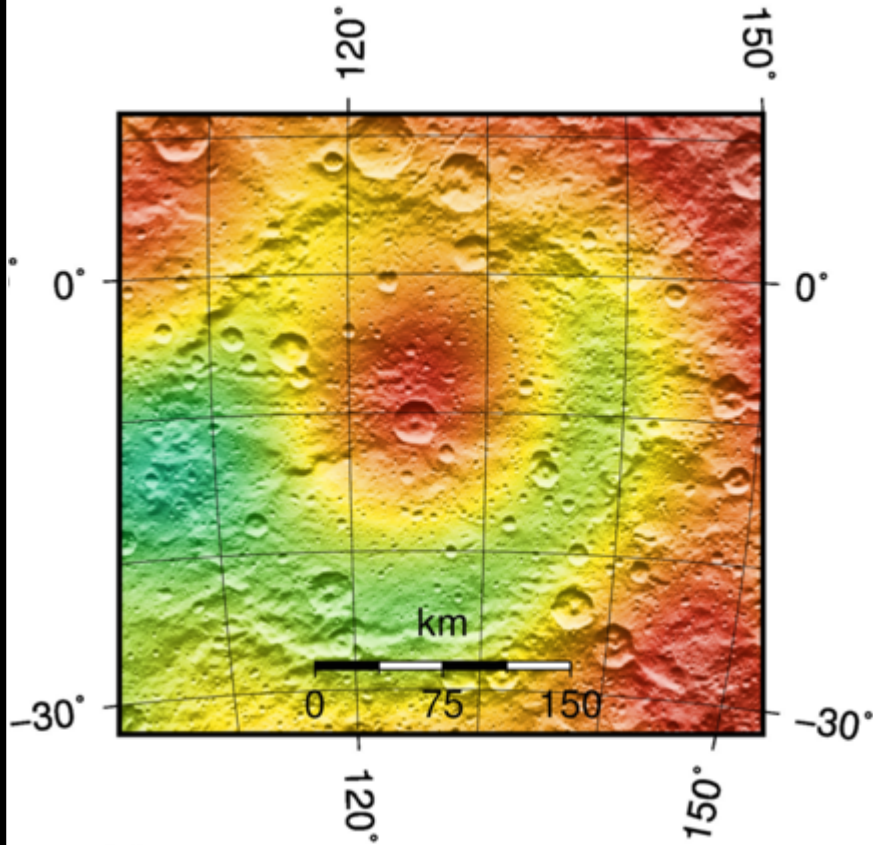
Ermakov et al., 2017



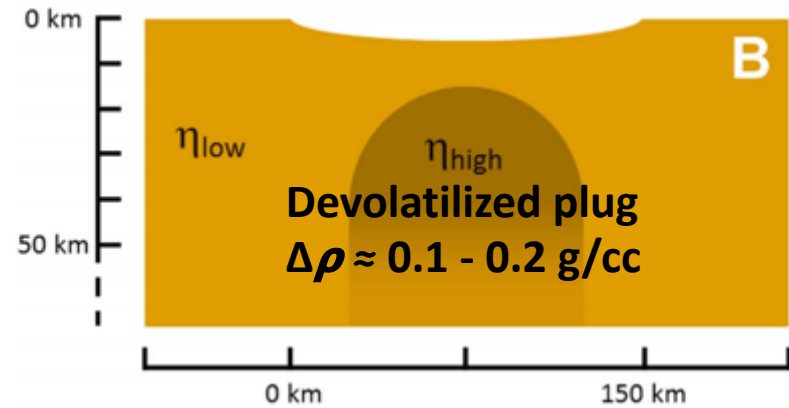
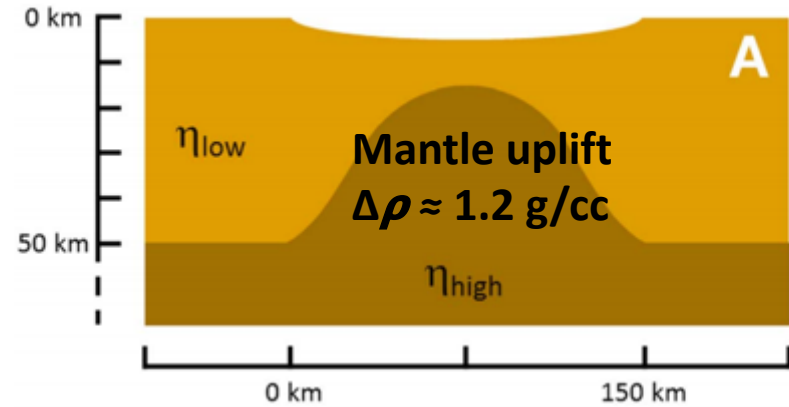
Bland et al., 2018

# Mascons

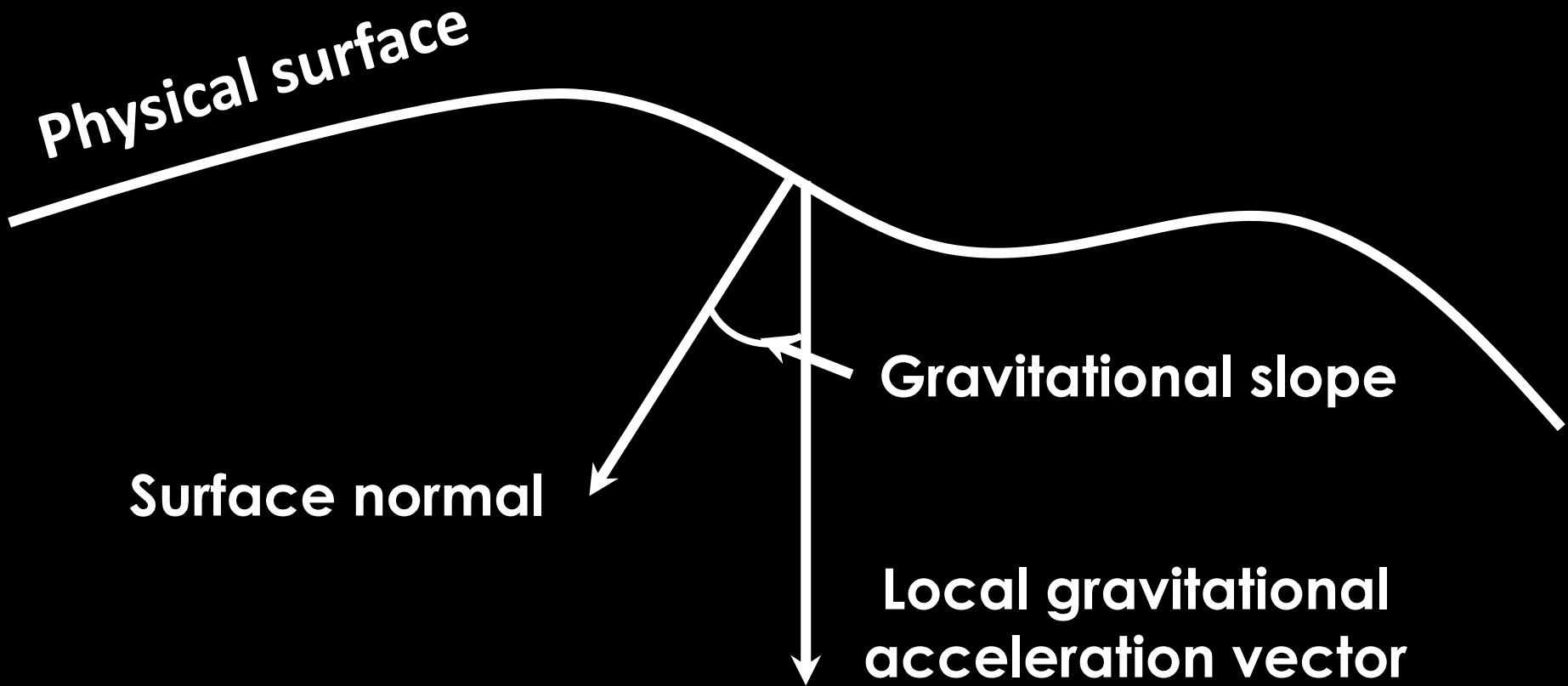
Kerwan isostatic anomaly



Ermakov et al., 2017

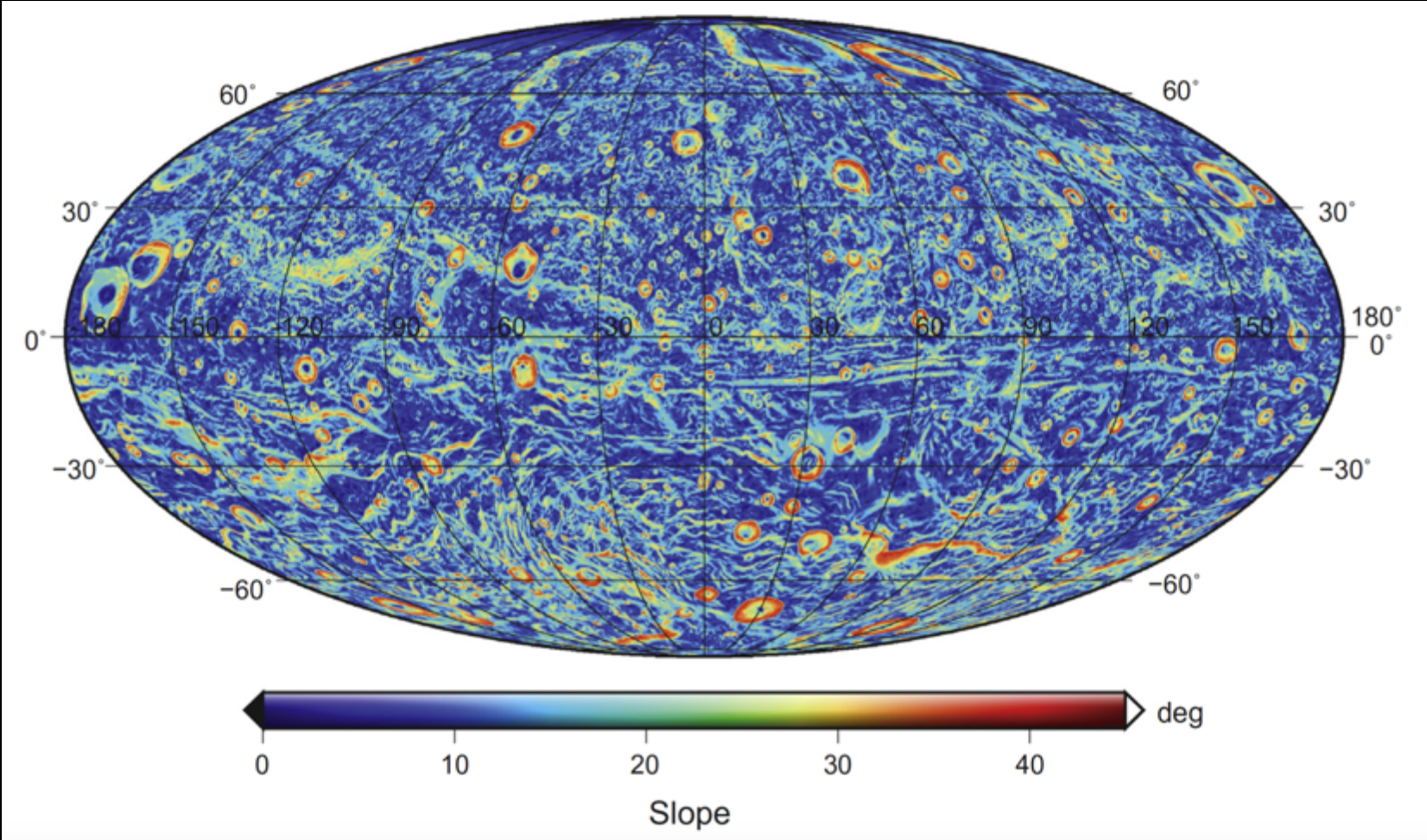


Bland et al., 2018

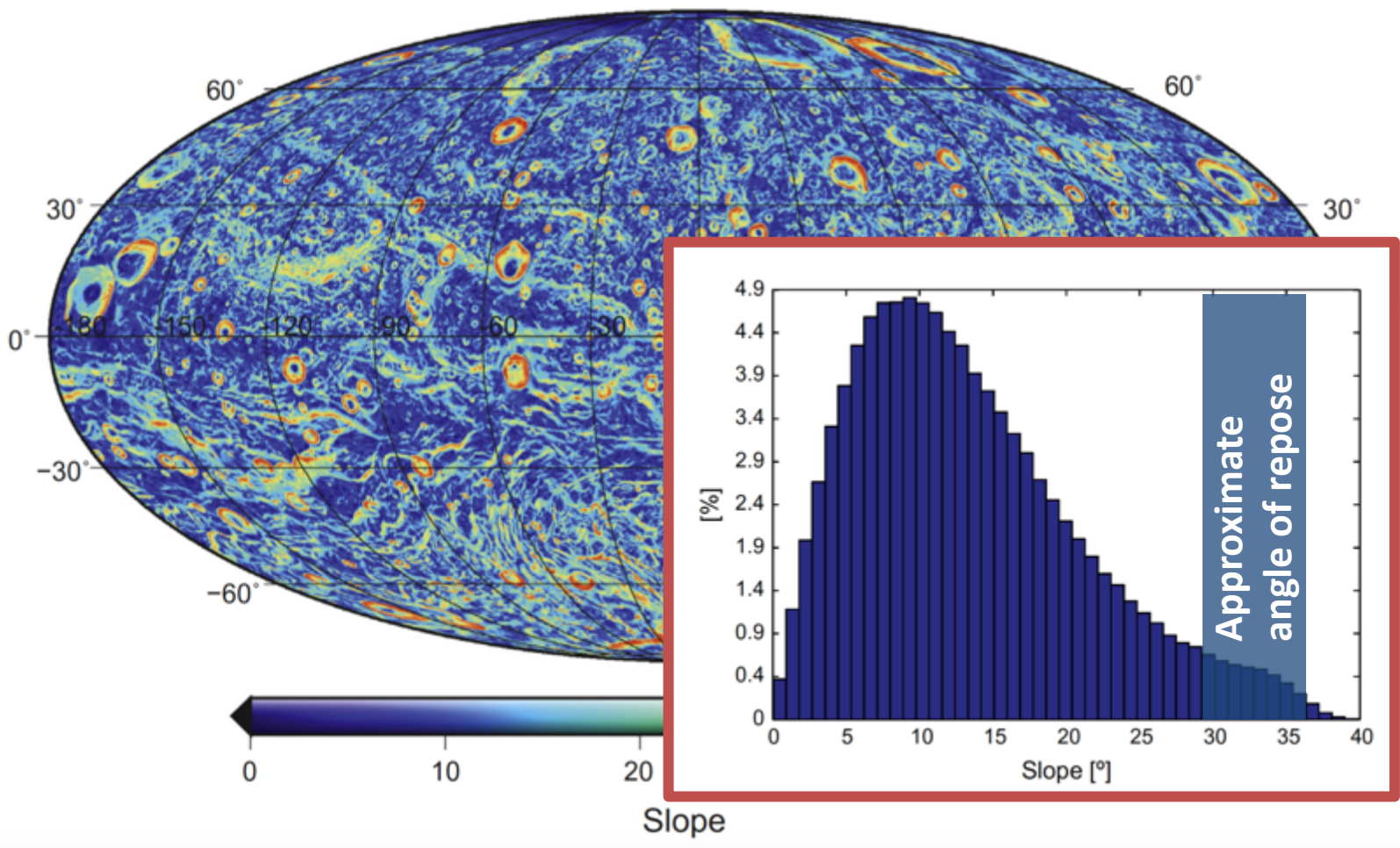


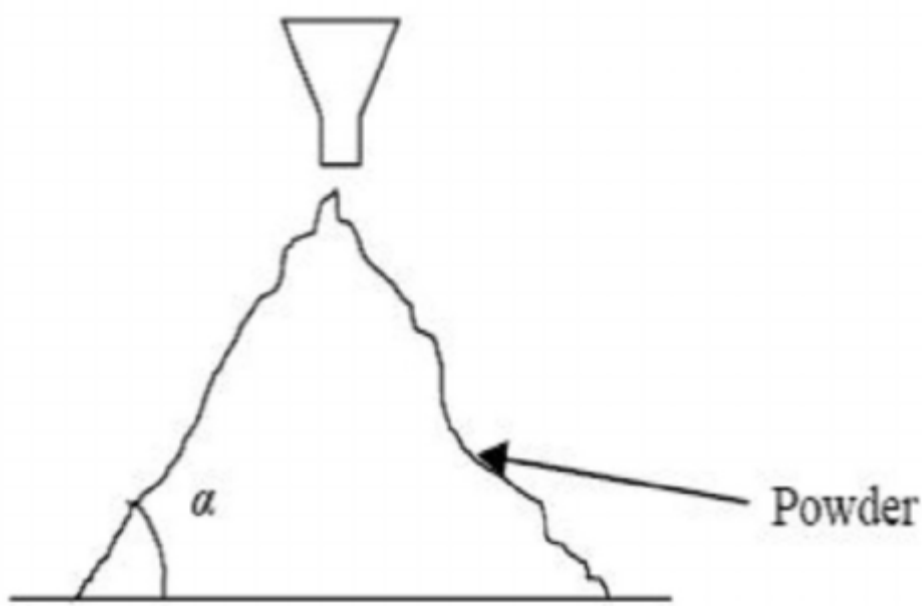


tional

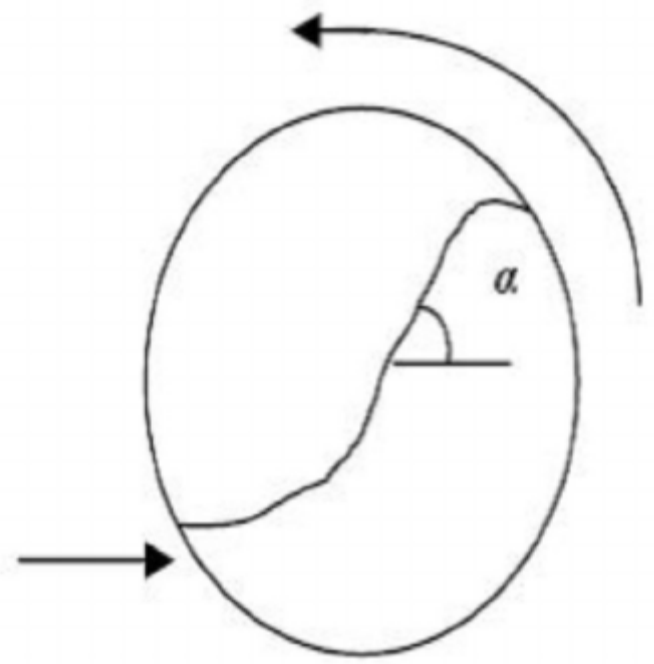


tiona

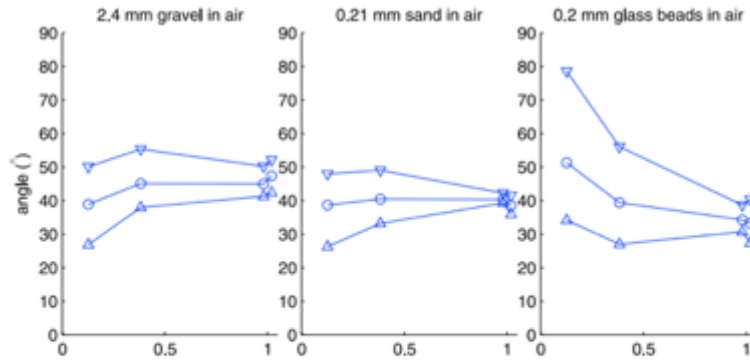




a) Static angle of repose ( $\alpha$ )



b) Dynamic angle of repose ( $\alpha$ )



**Result of the experiment:**

- Static angle of repose increased at lower gravity
- Dynamic angle of repose decreased at lower gravity

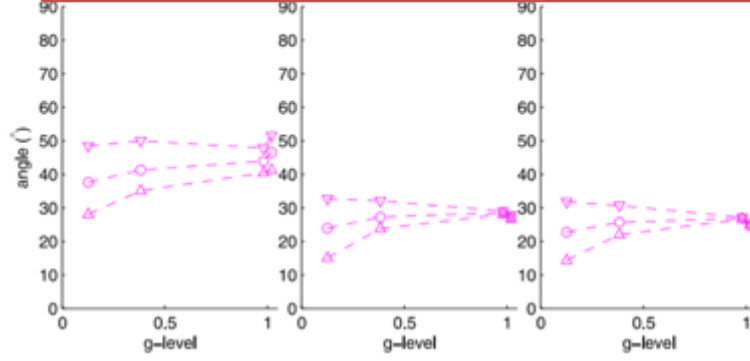
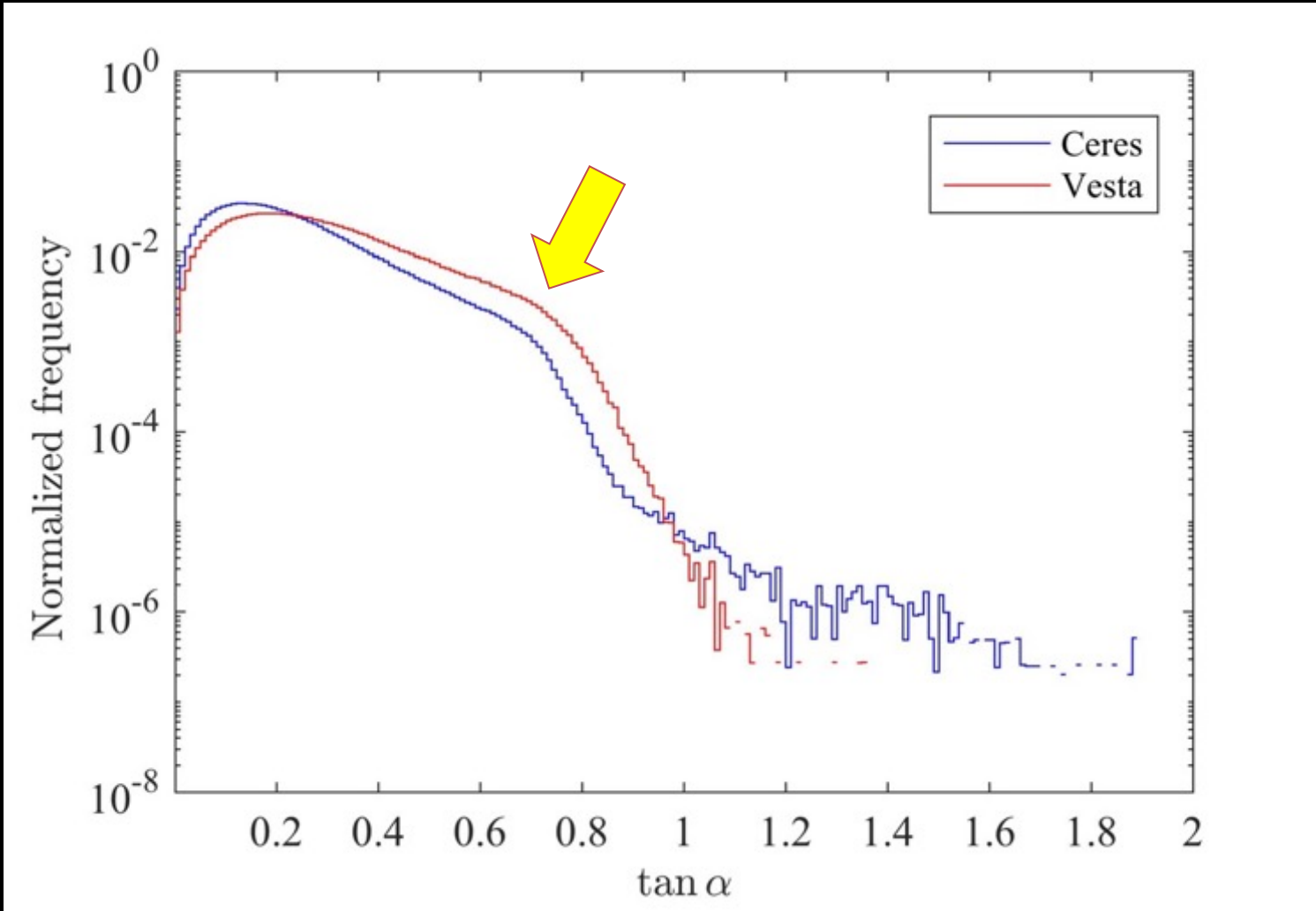


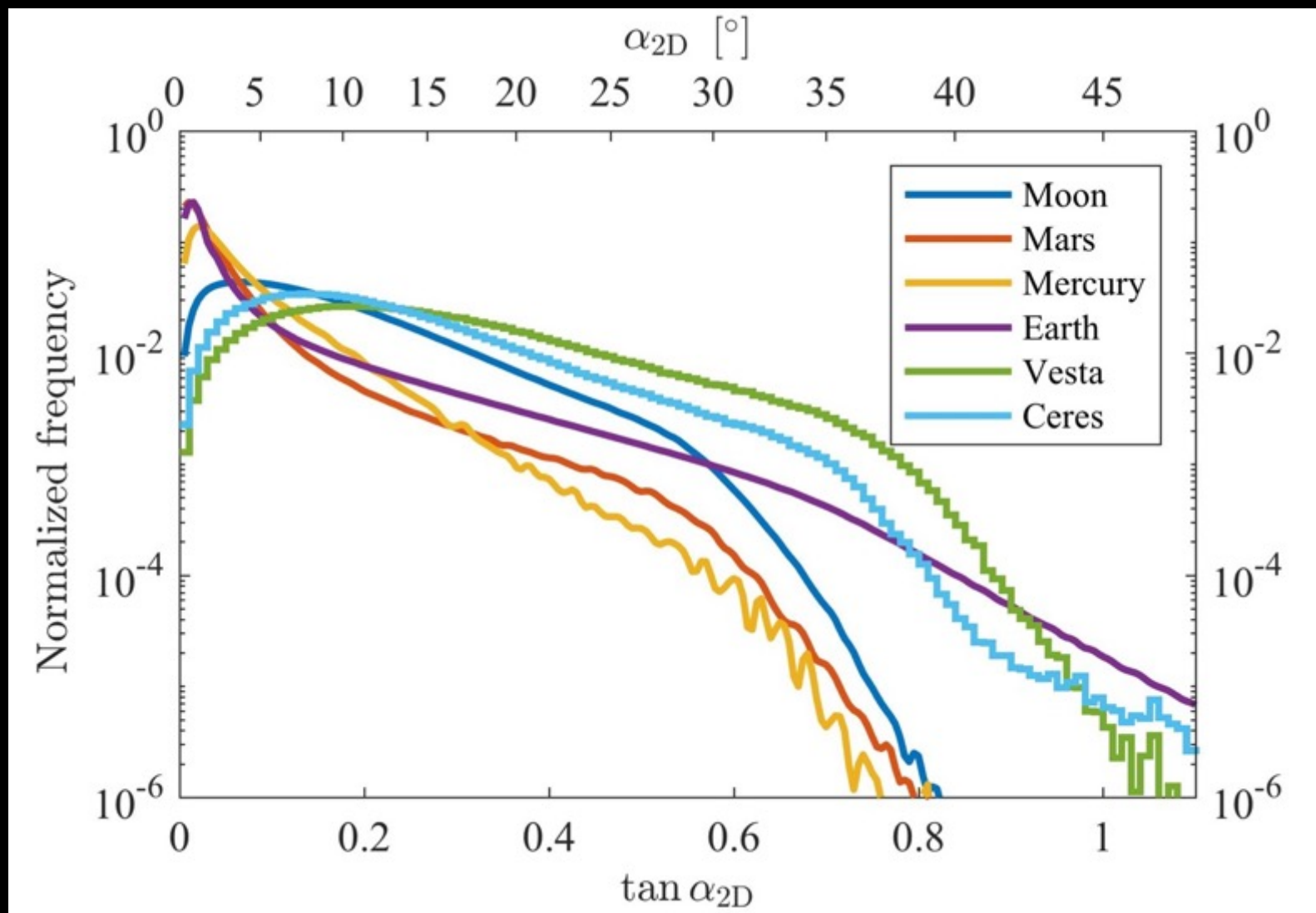
**Figure 5.** The experimental setup. Cylinders are 0.21 m in diameter. Cameras are located to the left.

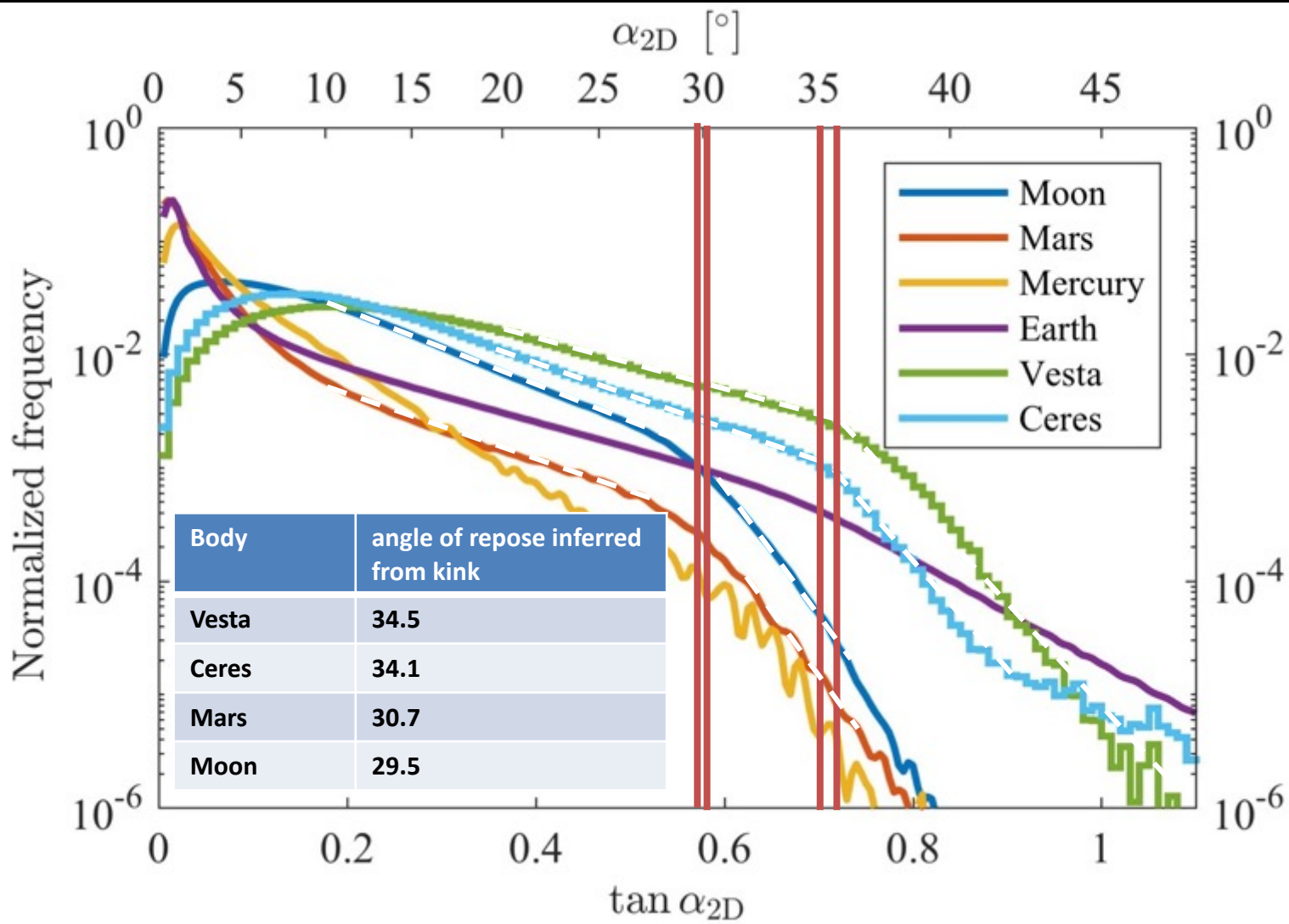


**Figure 2.** The Cessna Citation aircraft of Delft University of Technology and the Dutch National Aerospace Laboratory used for the parabolic flights.

**Figure 9.** Time-averaged angle, static angle of repose and dynamic angle of repose for each sediment. Same as Figure 8 without data. Maximum is calculated as 90% percentile from static angles (see Figure 6) and minimum is calculated as 10% percentile from dynamic angles.









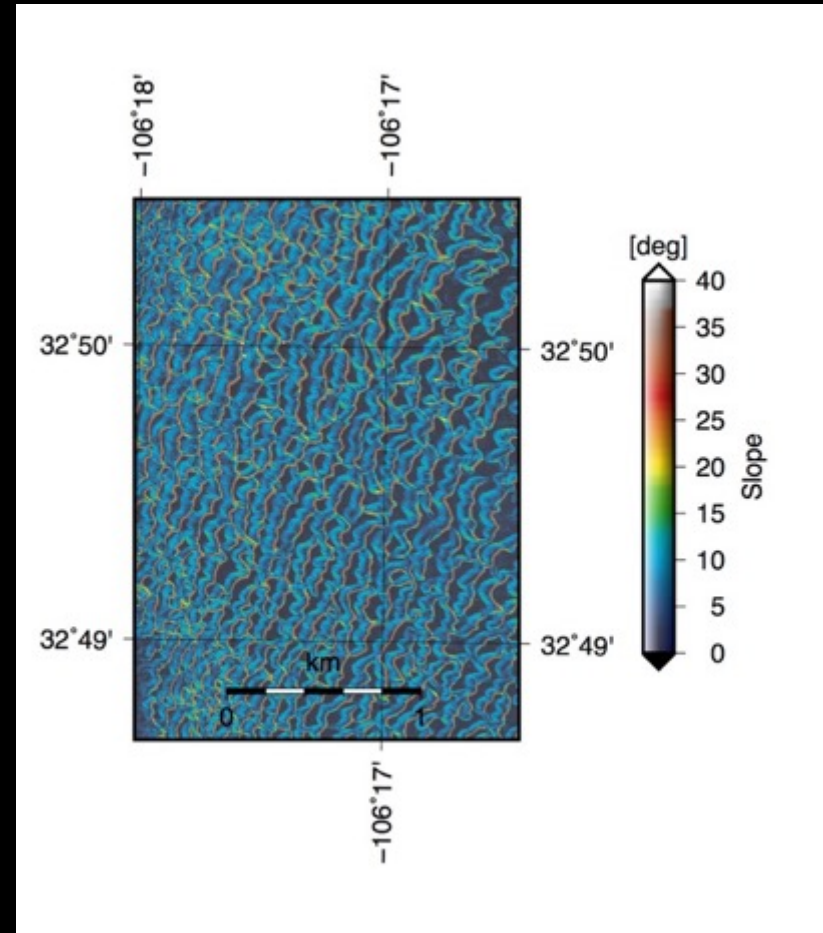
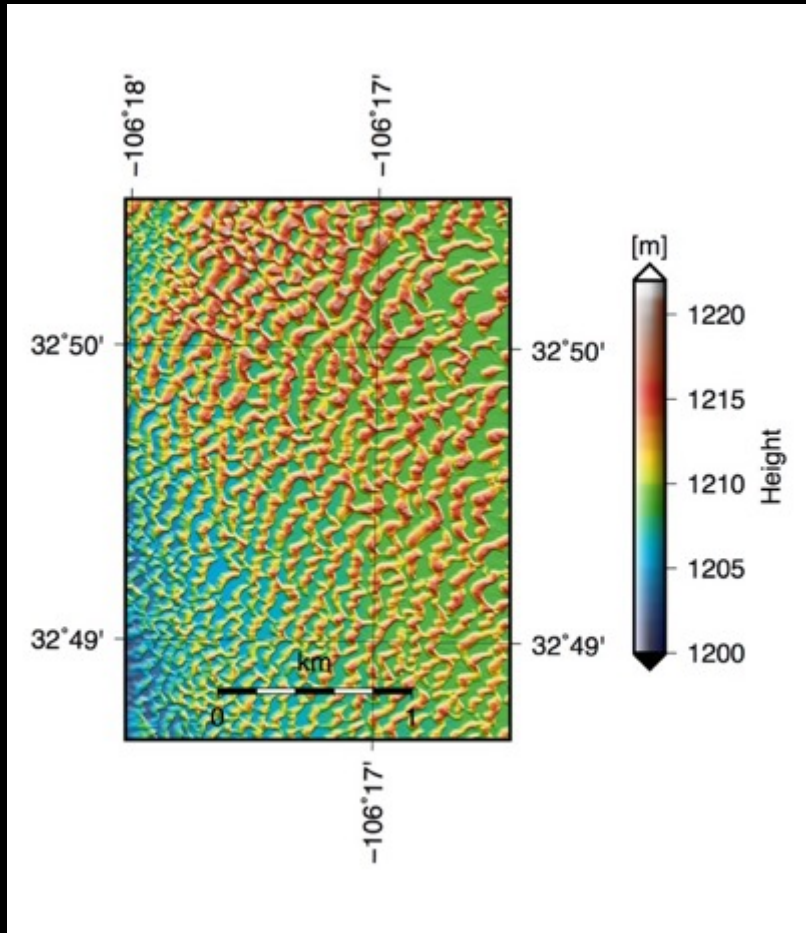
d

# White Sand National Monument, New Mexico



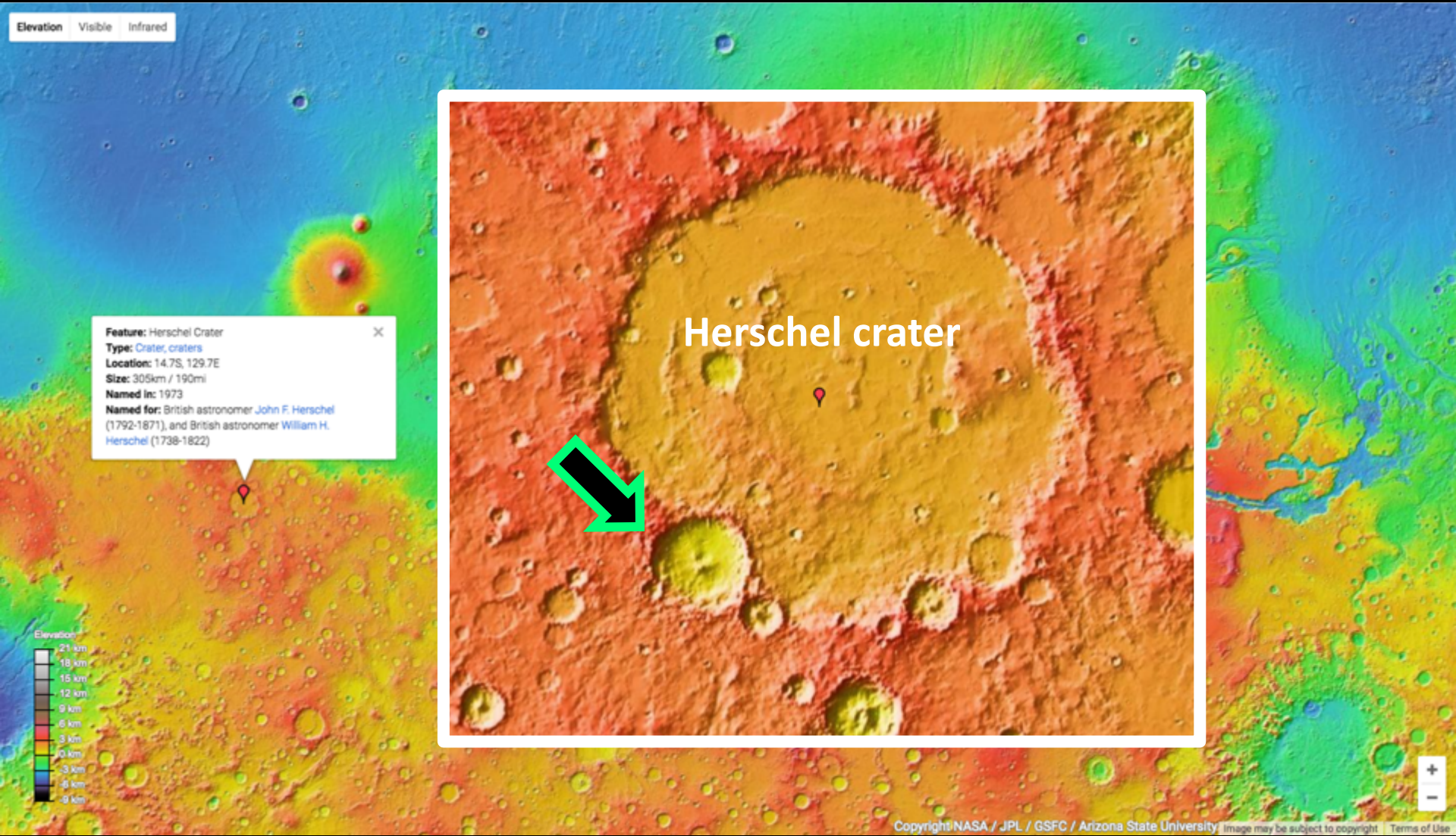
d

# White Sand National Monument, New Mexico





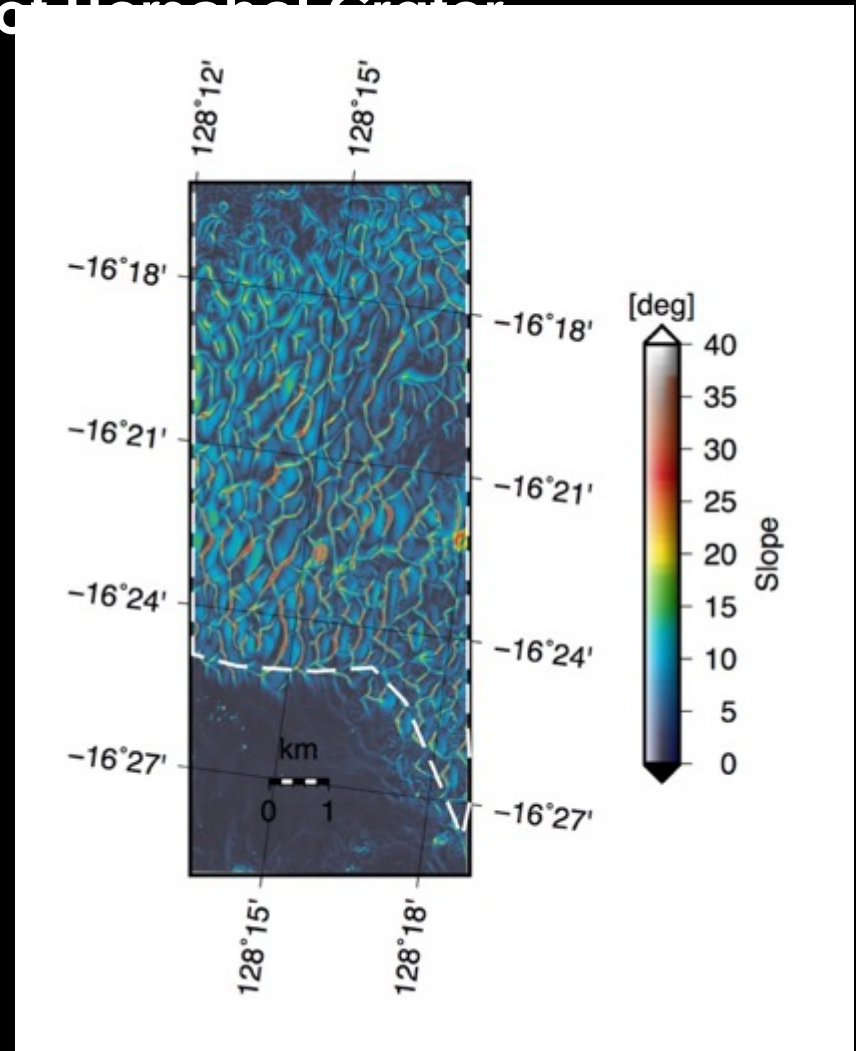
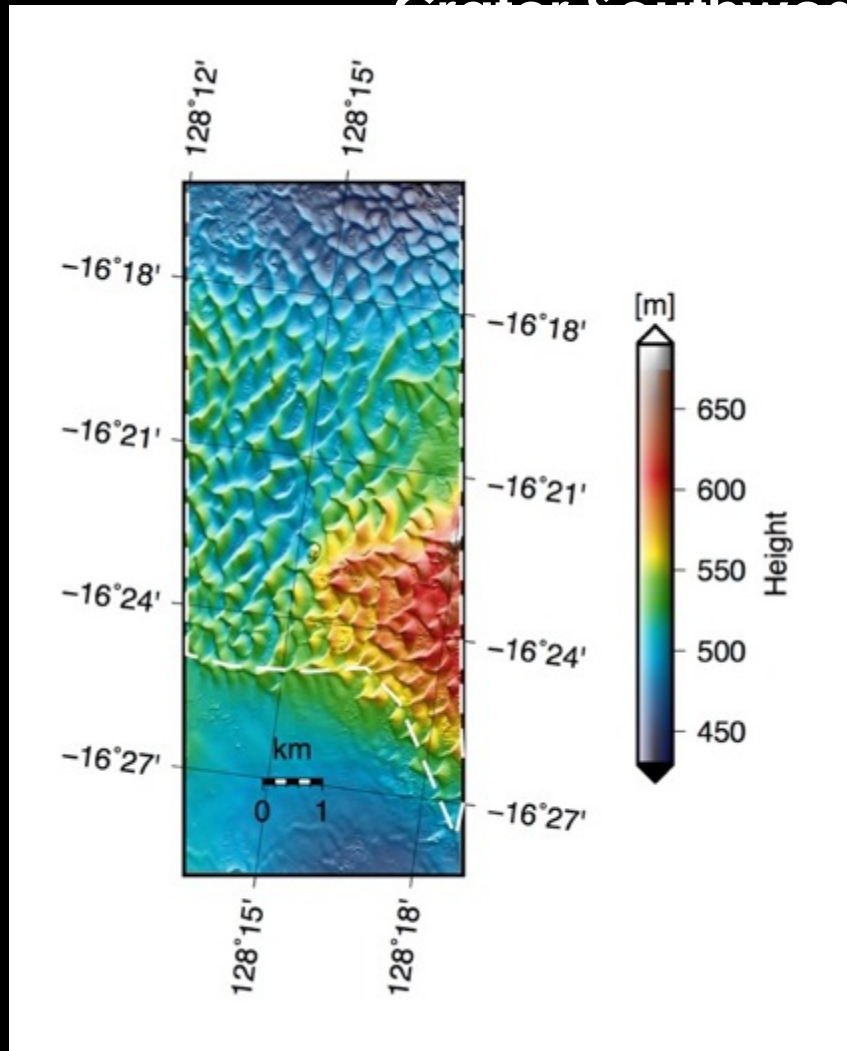
d



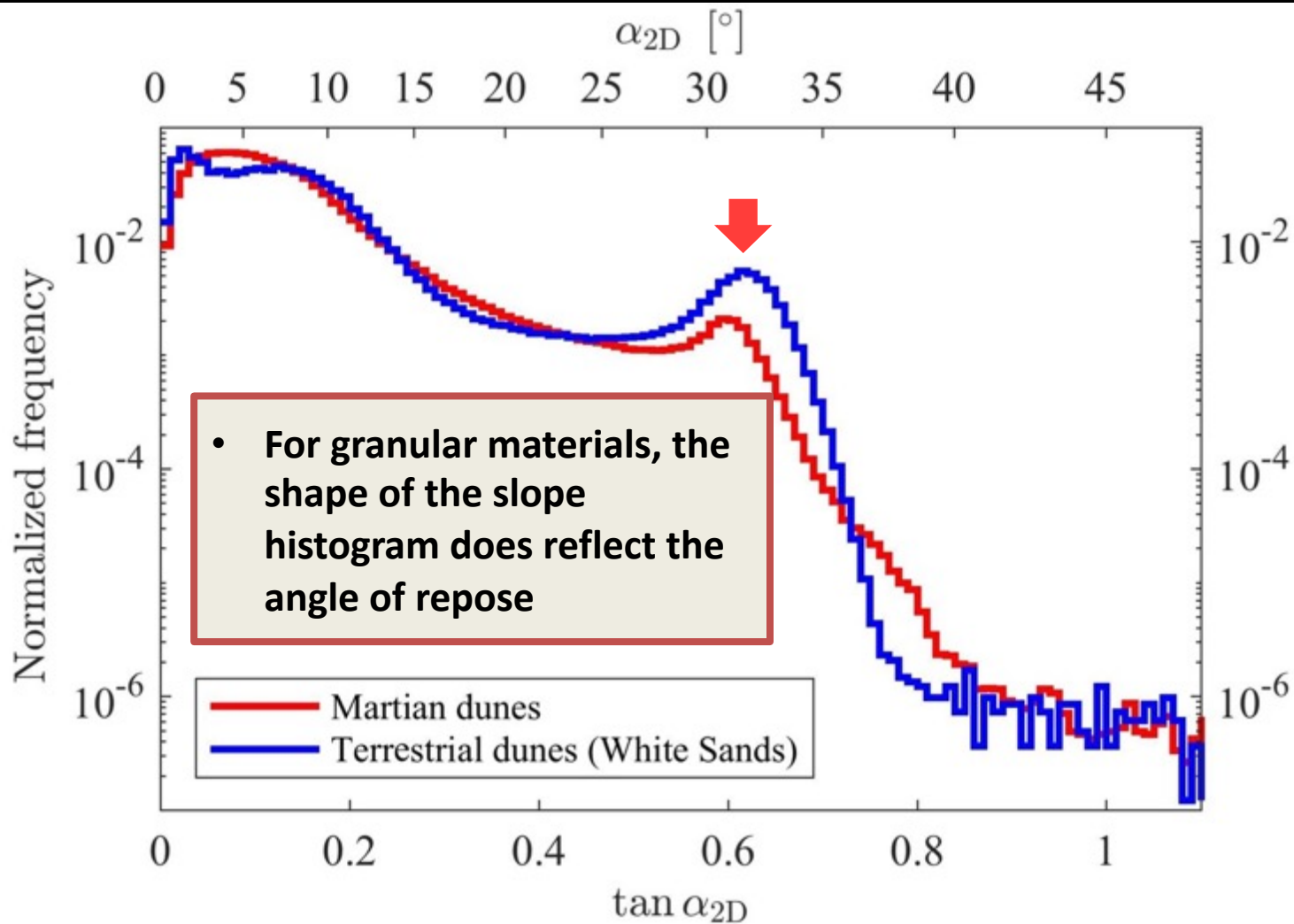


d

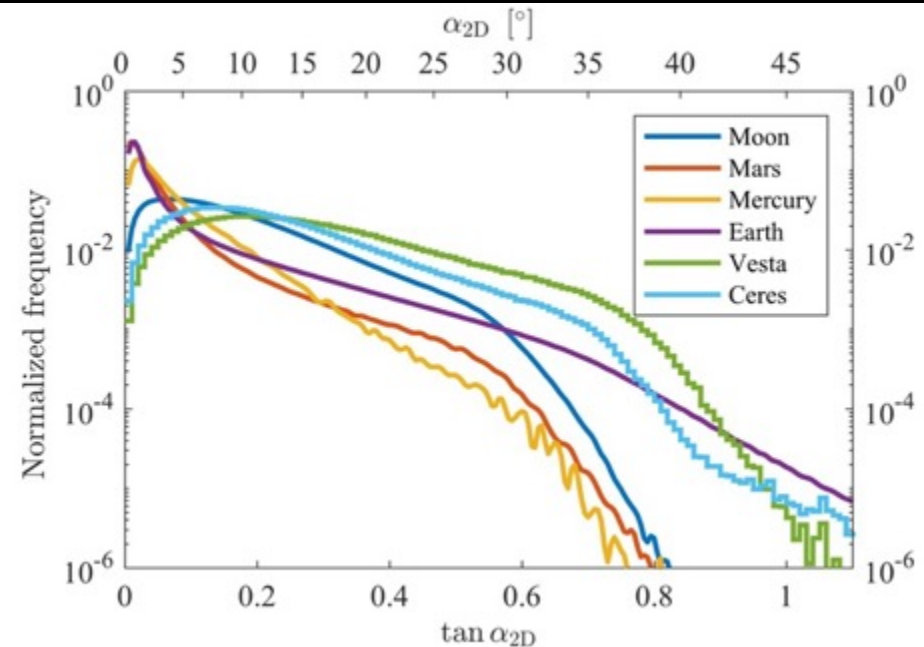
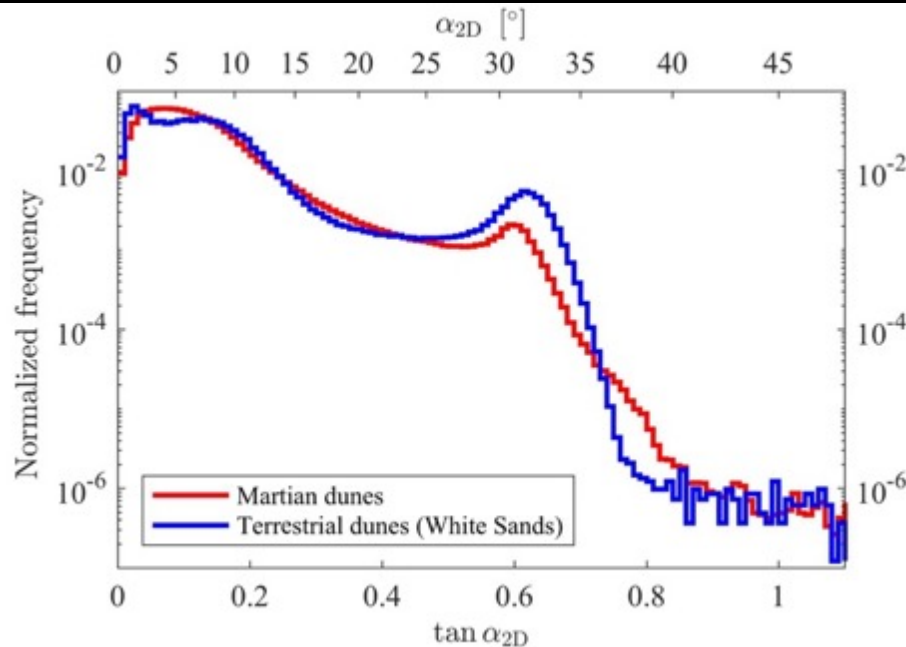
# Order Southwest of Herschel Crater

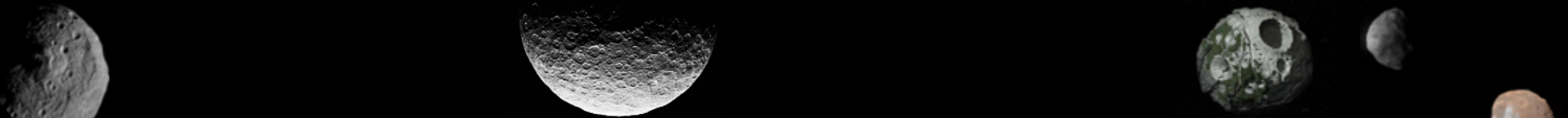


# Distribution of slopes on dunes

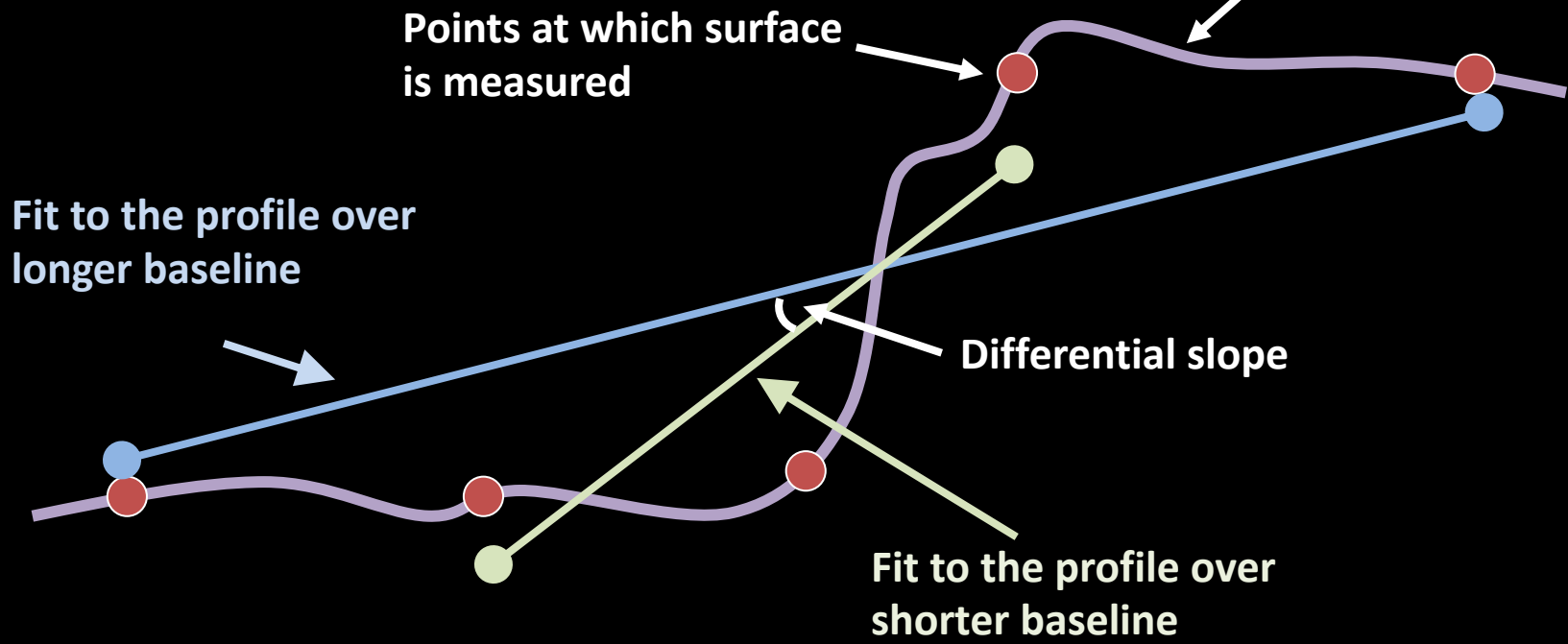


- Vesta and Ceres have a higher angle of repose ( $\phi$ ) than Mars and the Moon
  - $\phi_{\text{Vesta}}=35^\circ$ ;  $\phi_{\text{Ceres}}=34^\circ$ ;  $\phi_{\text{Mars}}=31^\circ$ ;  $\phi_{\text{Moon}}=30^\circ$
  - If interpreted as the dynamic angle of repose, contradicts experiments by Kleinhans et al., 2011
  - Surface gravity? Composition? Particle shape?

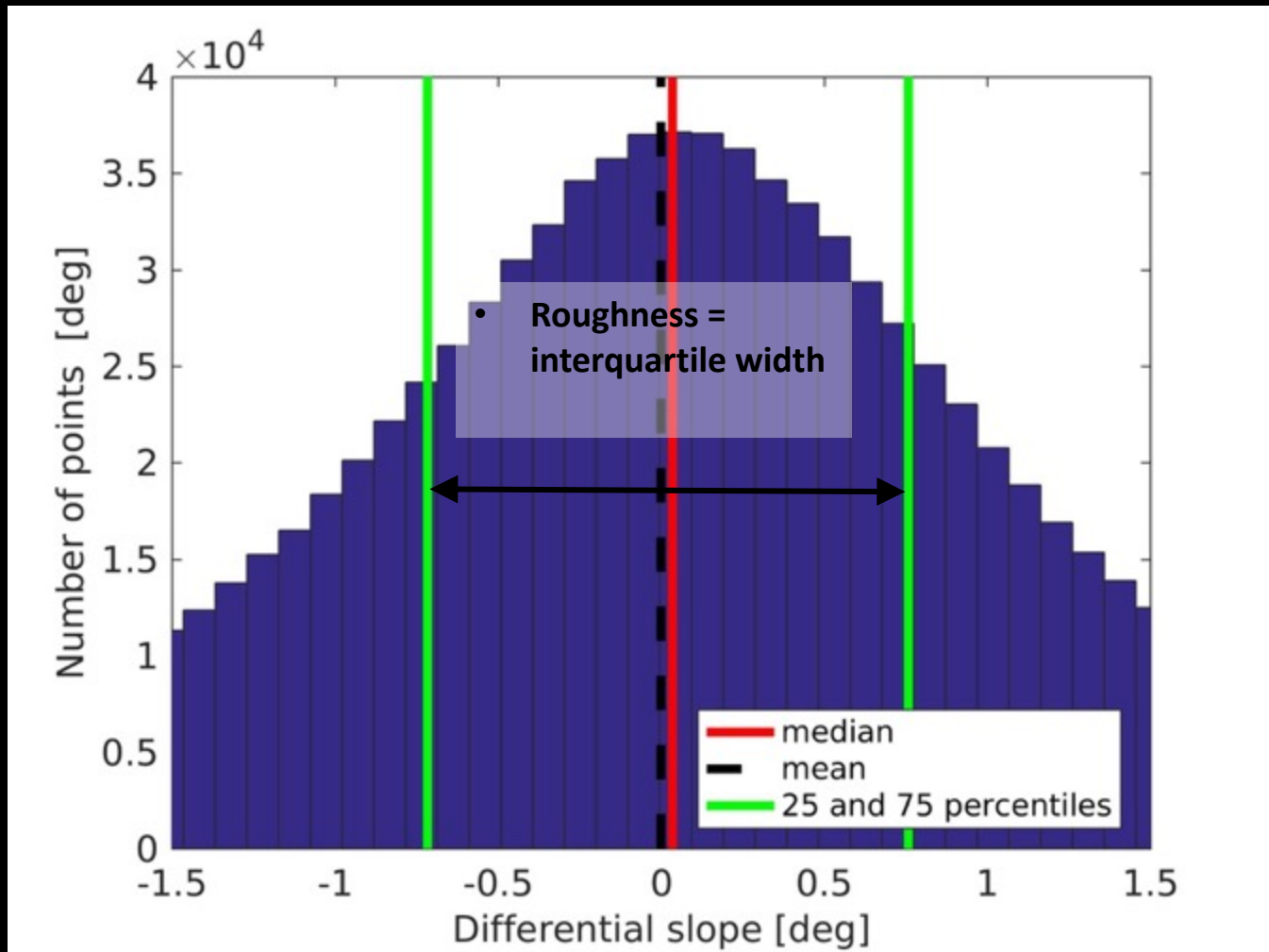




# Differential slope



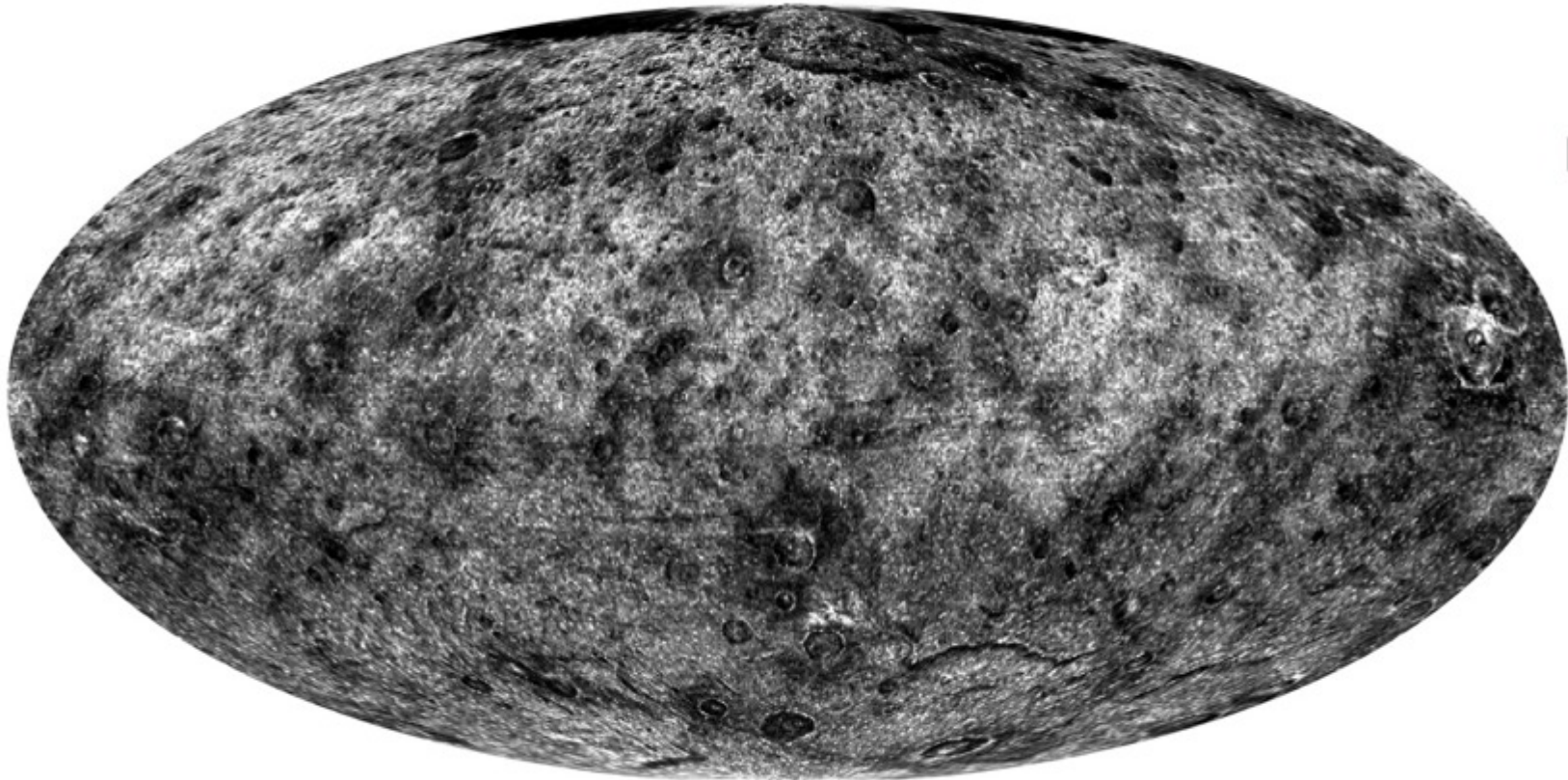
- By computing differential slopes, we subtract longer wavelength topography variations
- In other words, differential slope within a flat but highly inclined cliff is zero





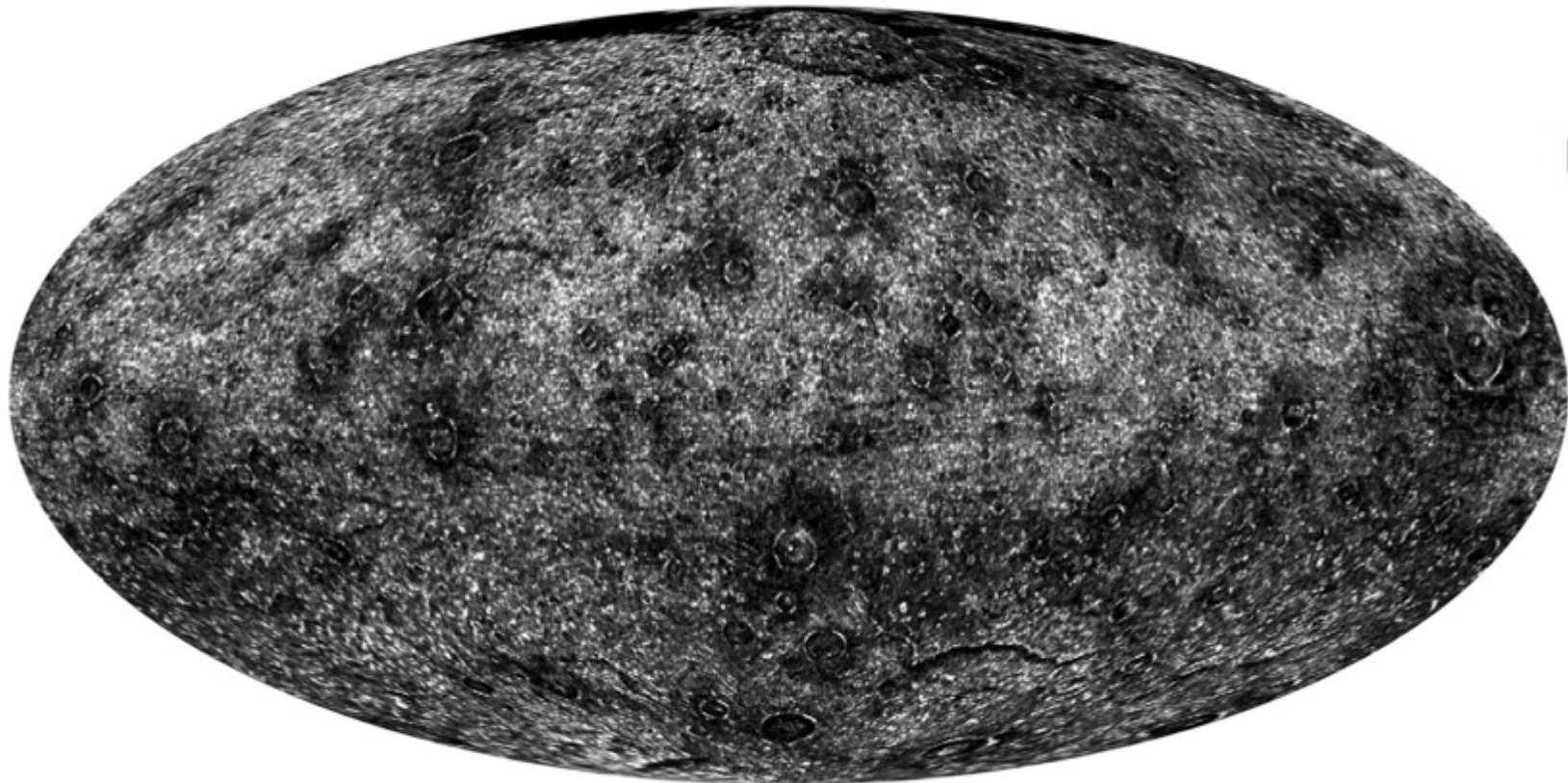
# Vesta SPC roughness composite

B=1065m/497m



# Vesta SPC roughness composite

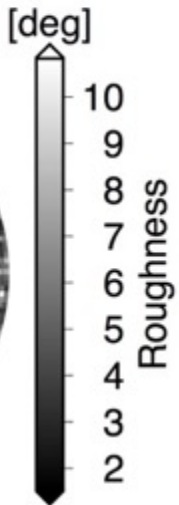
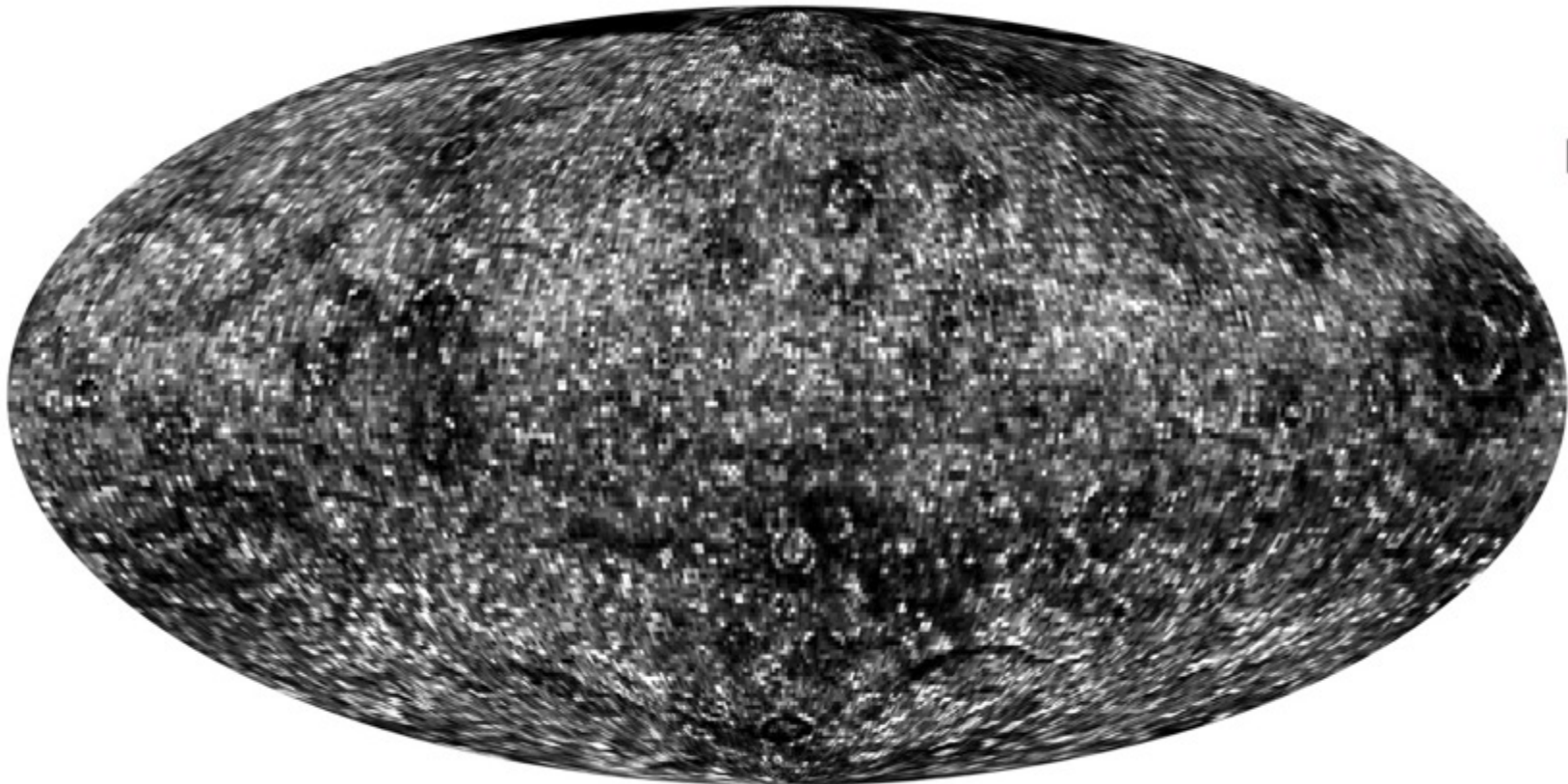
G=2769m/1349m





# Vesta SPC roughness composite

R=7313/3621 m



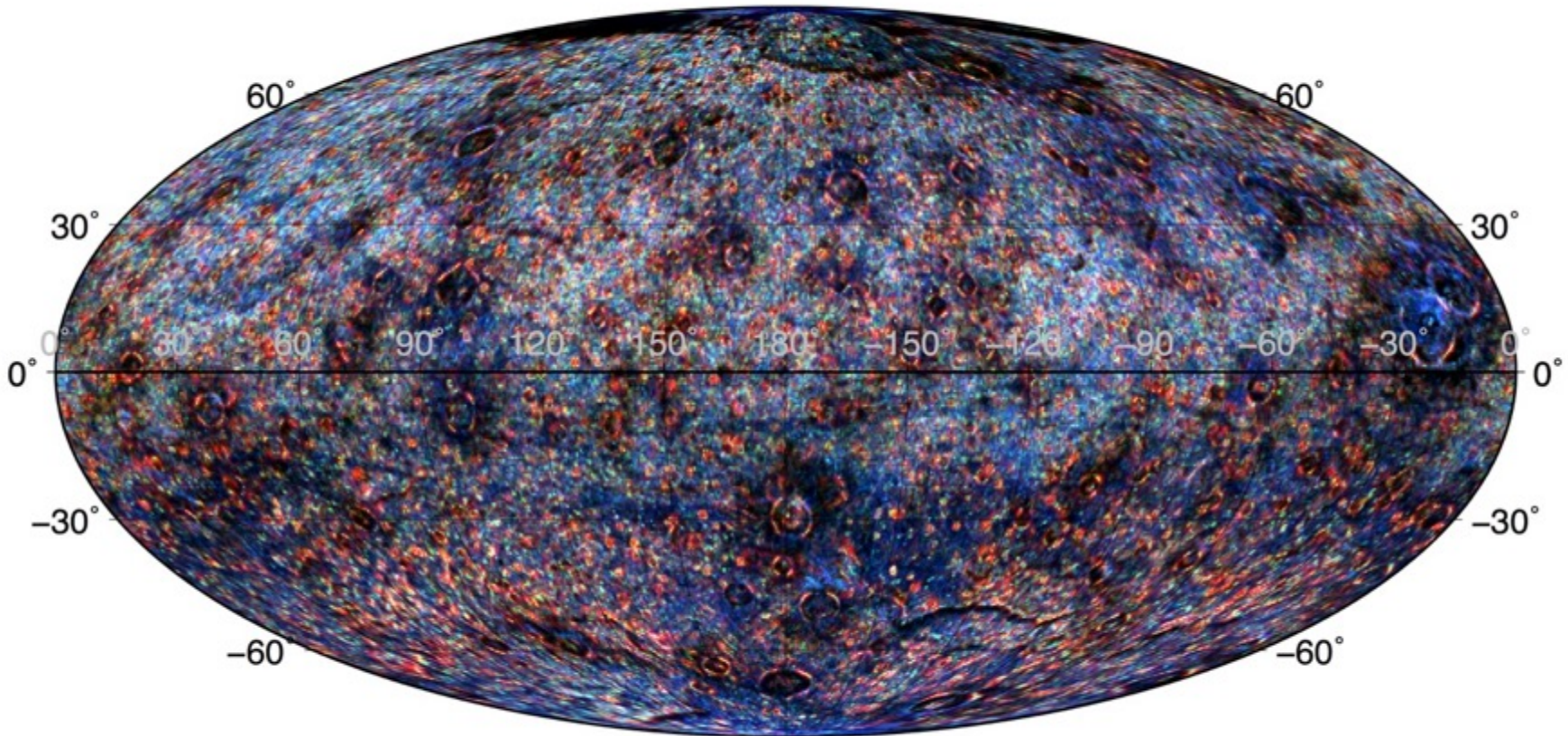


# Vesta SPC roughness composite

B=1065m/497m

G=2769m/1349m

R=7313/3621 m



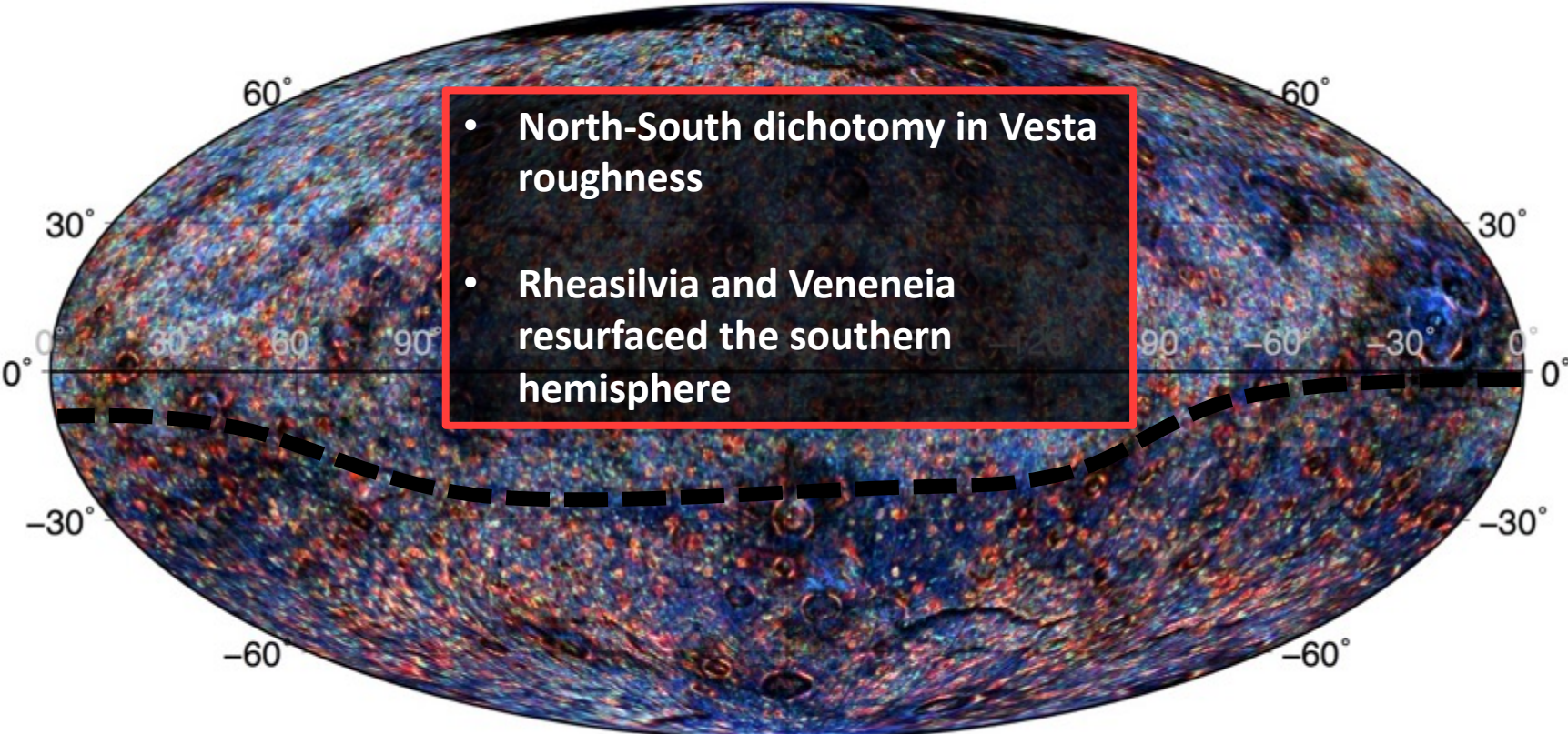


# North-South dichotomy

B=1065m/497m

G=2769m/1349m

R=7313/3621 m



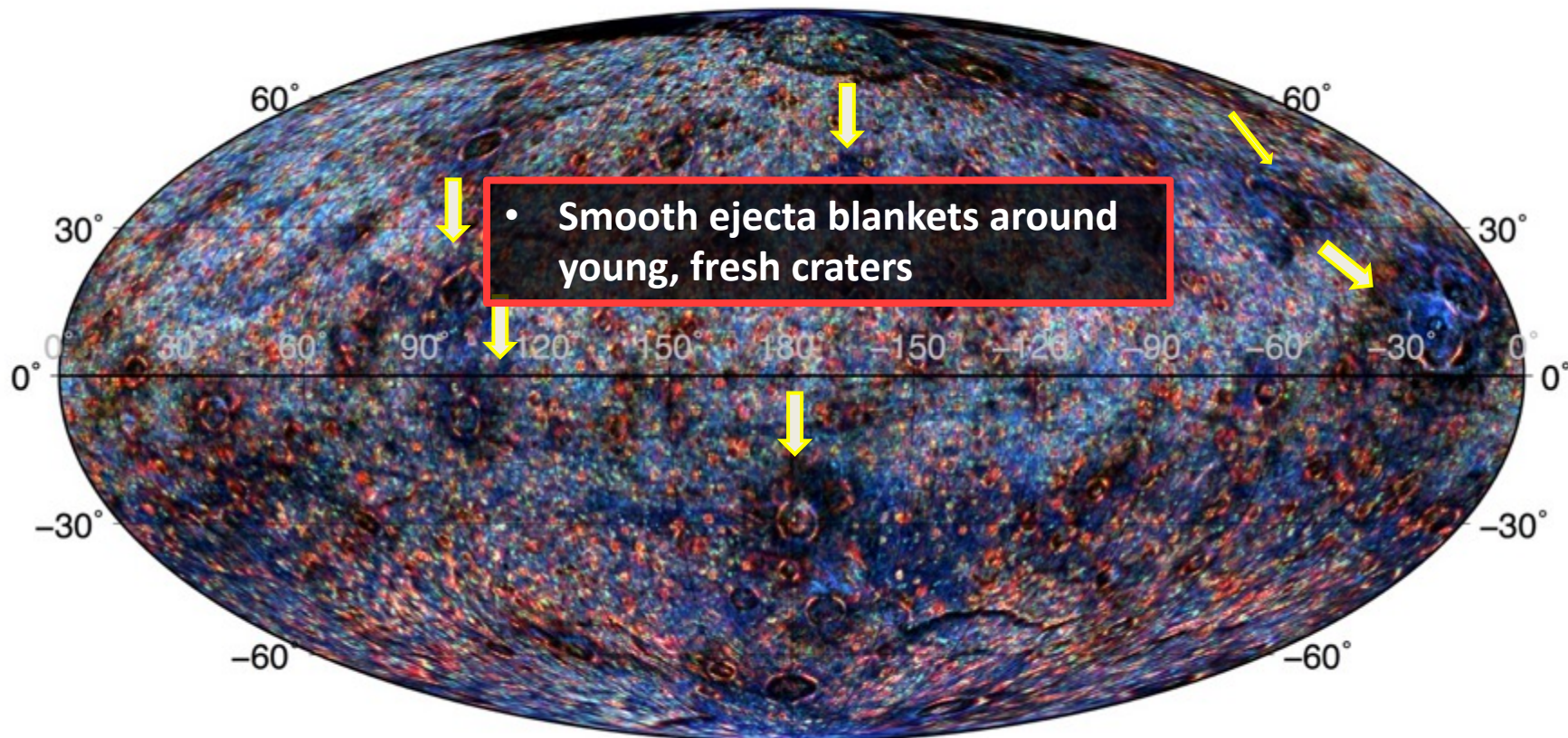


# Smooth ejecta blankets

B=1065m/497m

G=2769m/1349m

R=7313/3621 m



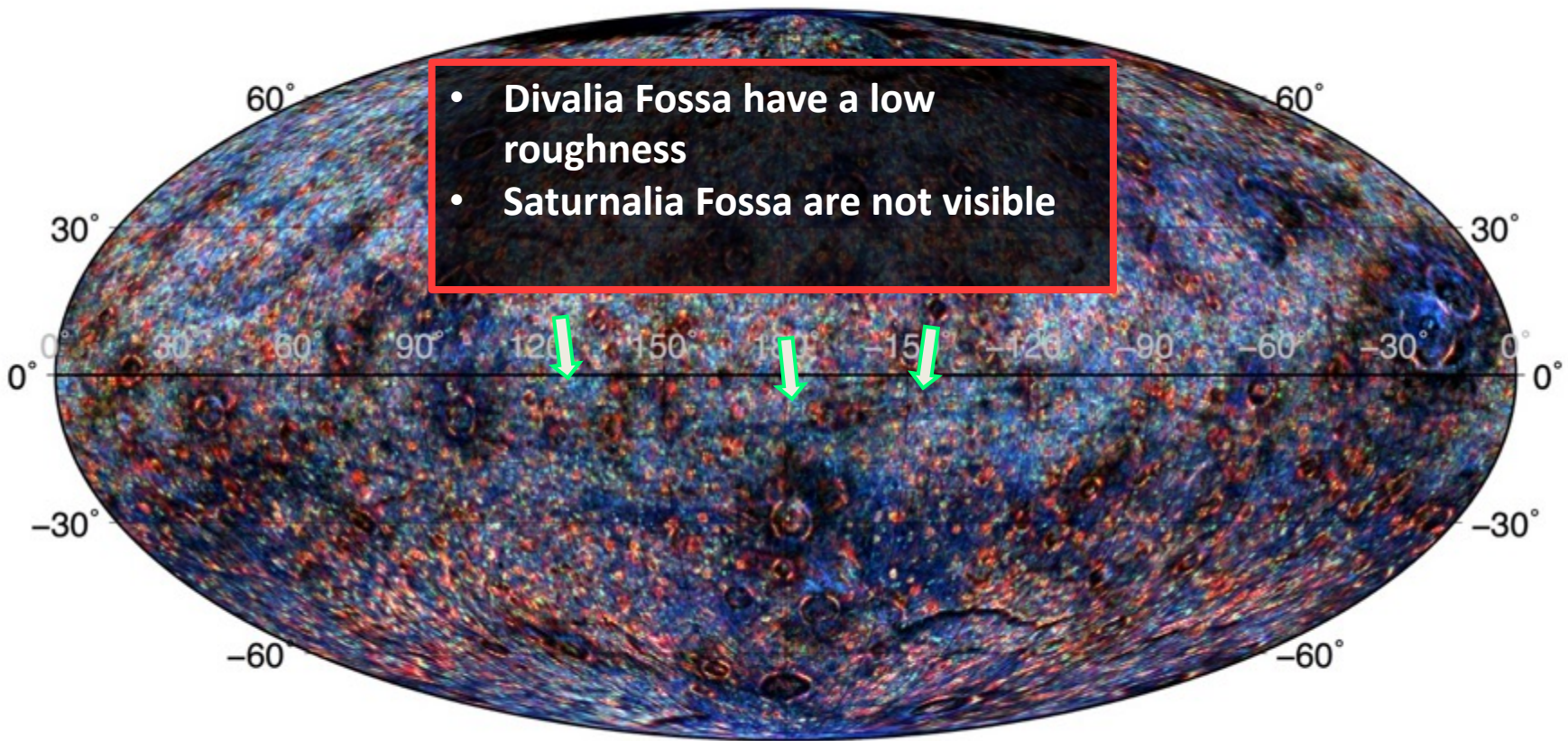


# Divalia Fossa

B=1065m/497m

G=2769m/1349m

R=7313/3621 m



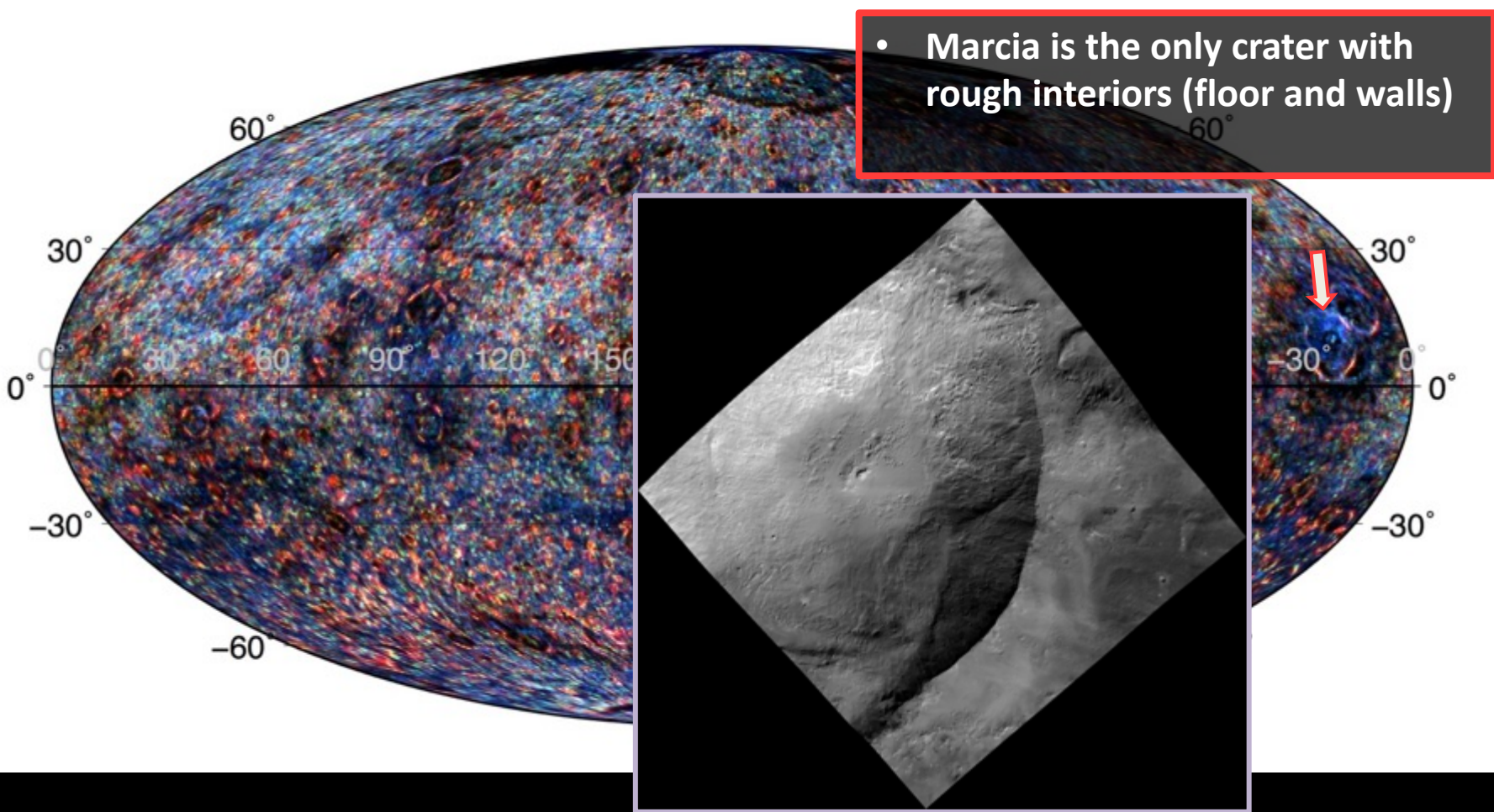


# Marcia

B=1065m/497m

G=2769m/1349m

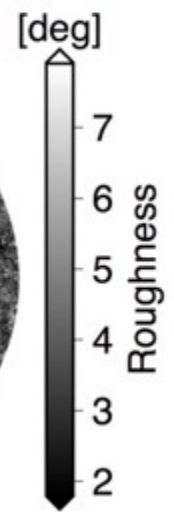
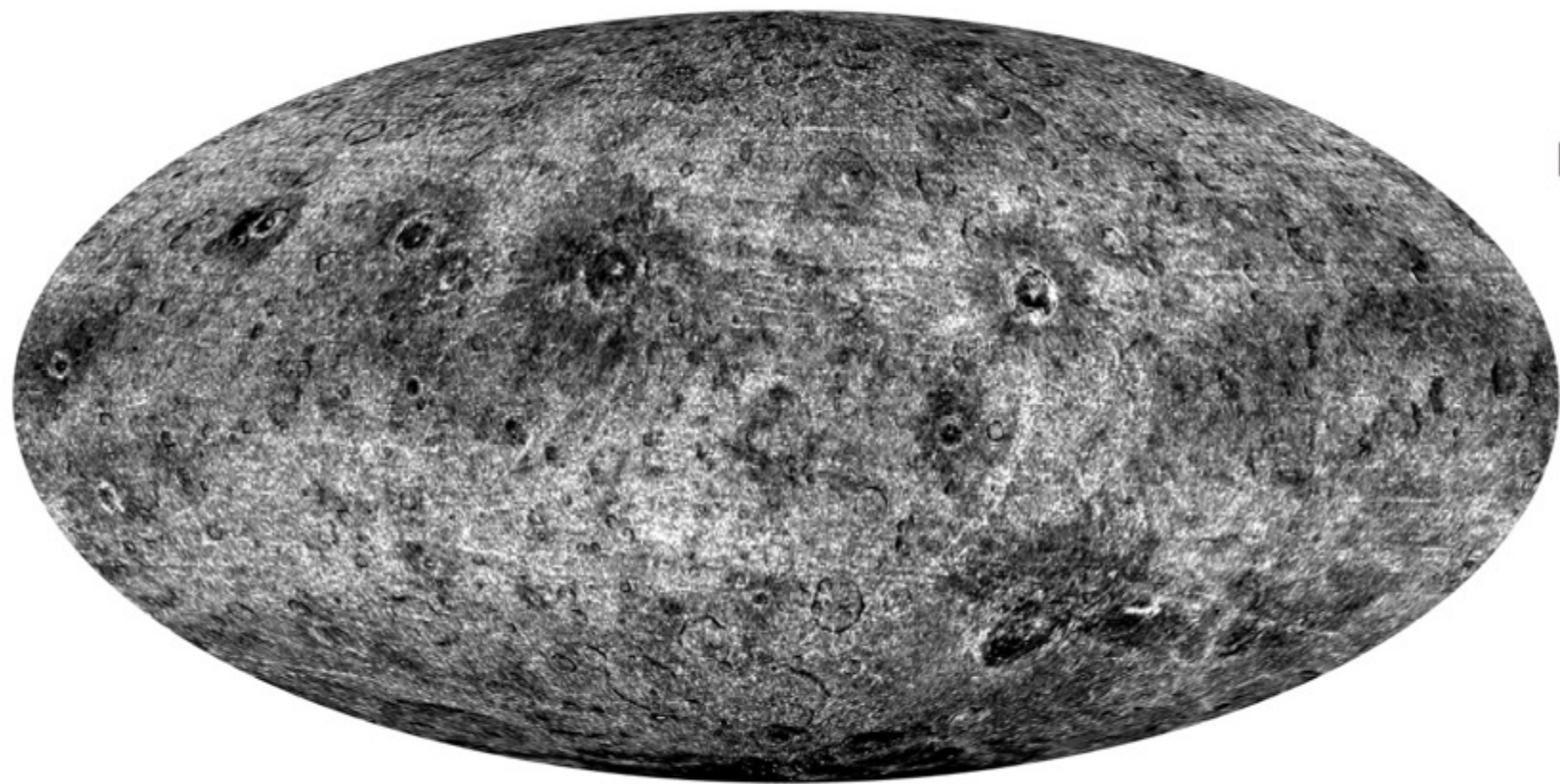
R=7313/3621 m





# Ceres SPC roughness composite

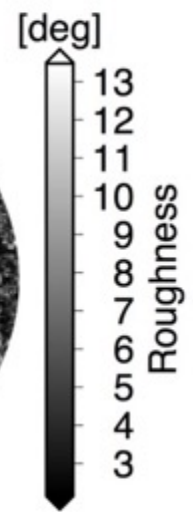
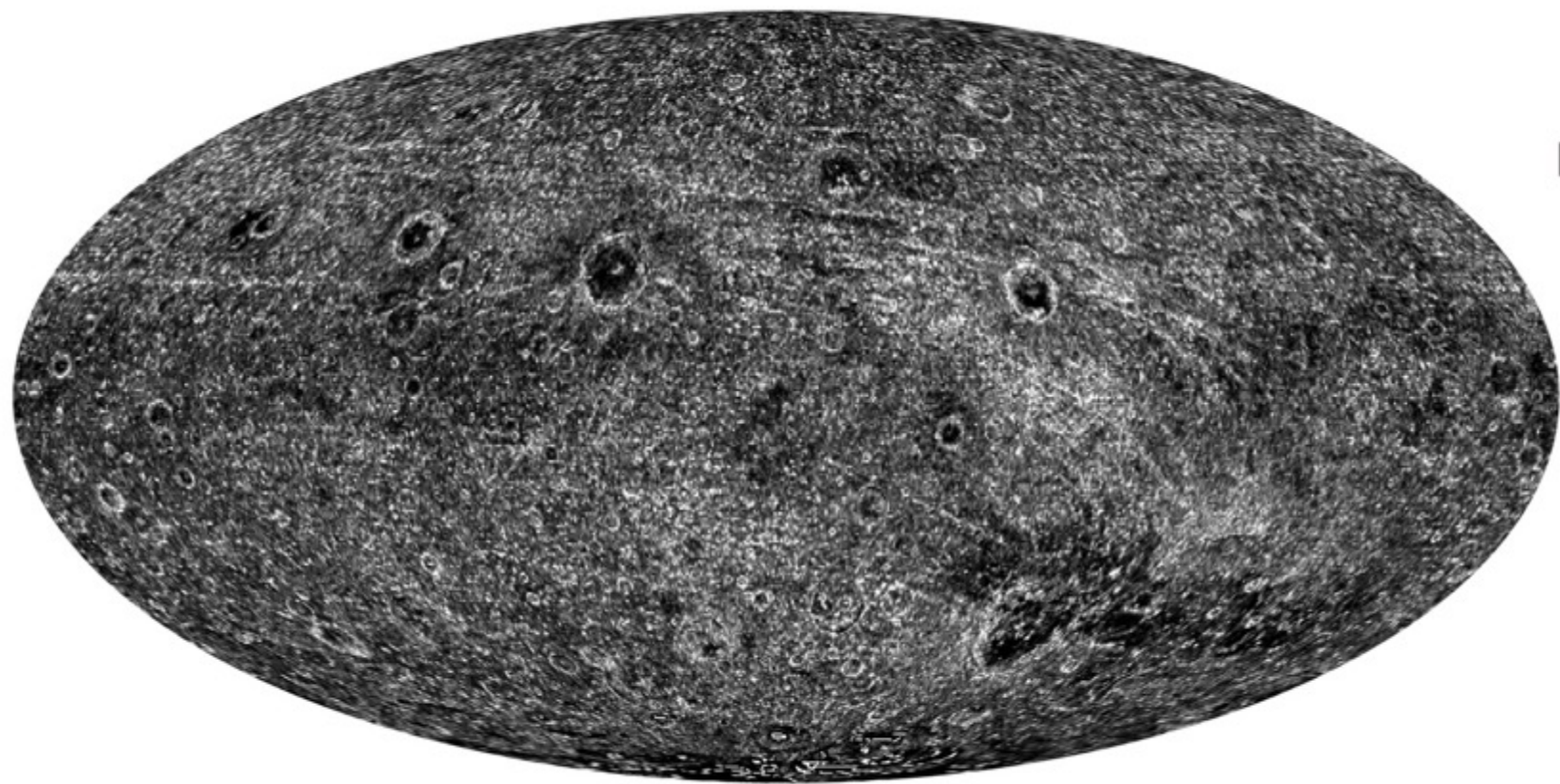
B=1230/574 m





# Ceres SPC roughness composite

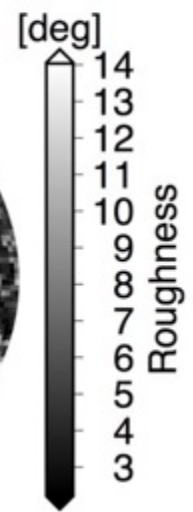
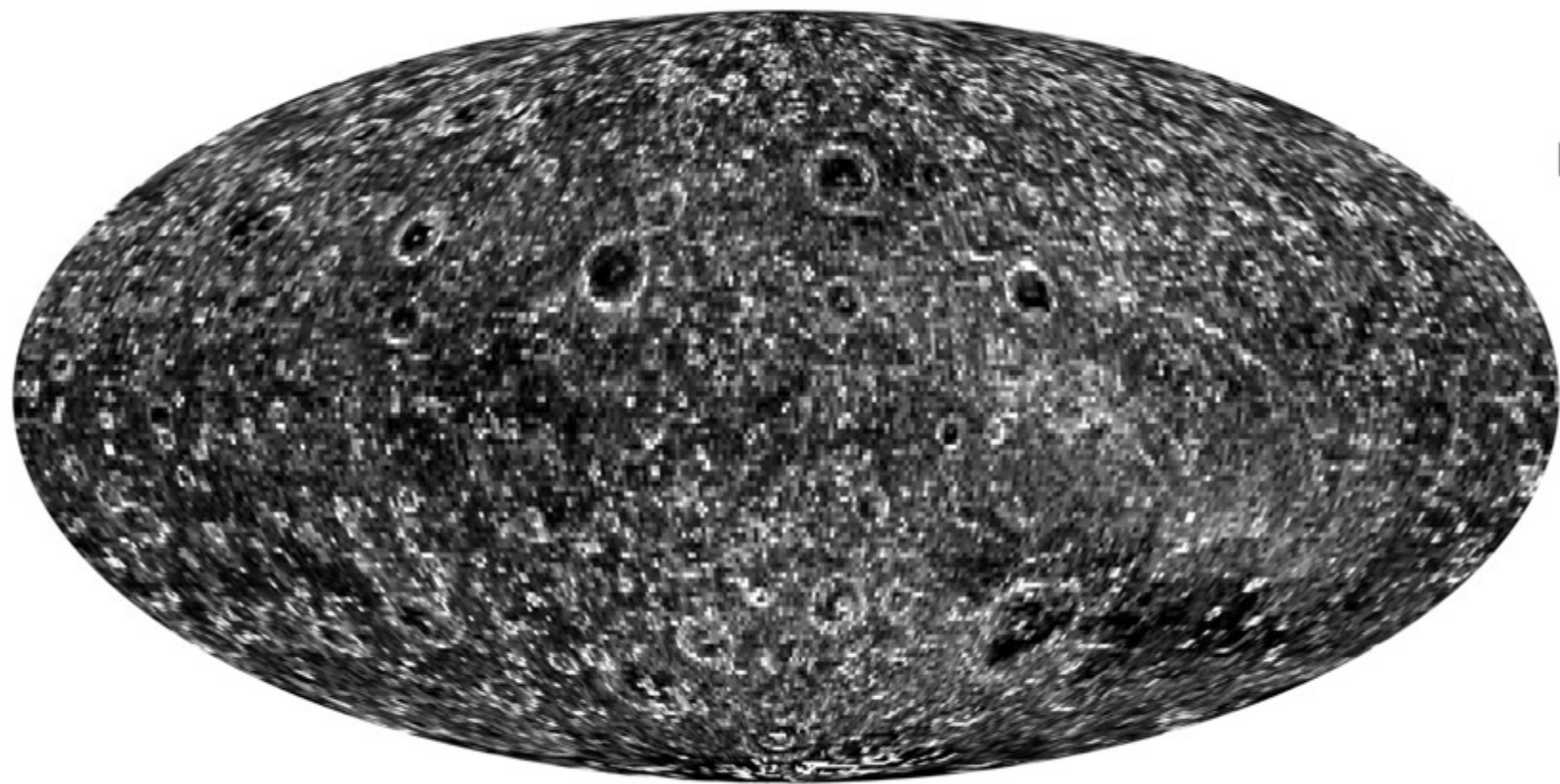
G=3198/1558 m





# Ceres SPC roughness composite

R=7134/3526 m



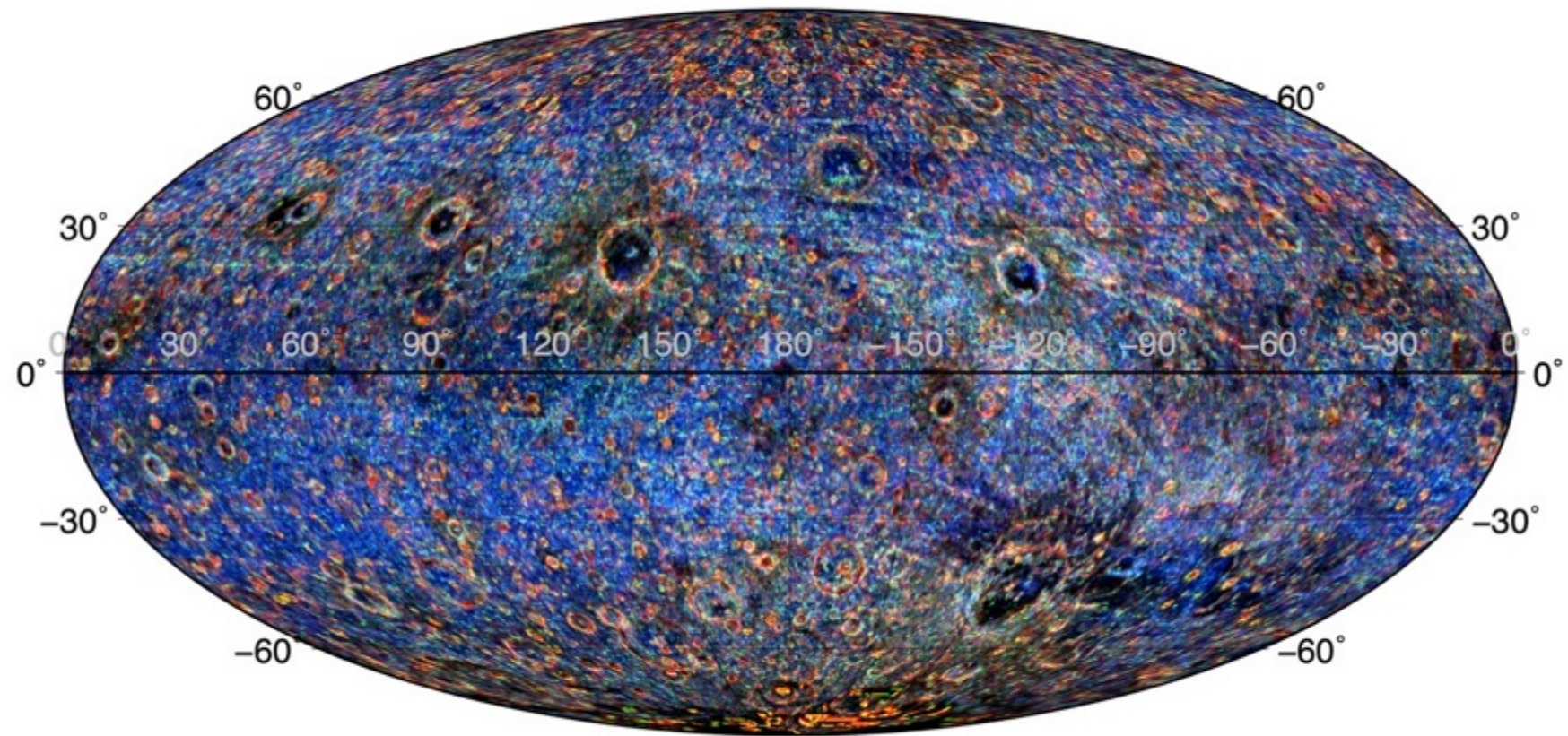


# Ceres SPC roughness composite

B=1230/574 m

G=3198/1558 m

R=7134/3526 m



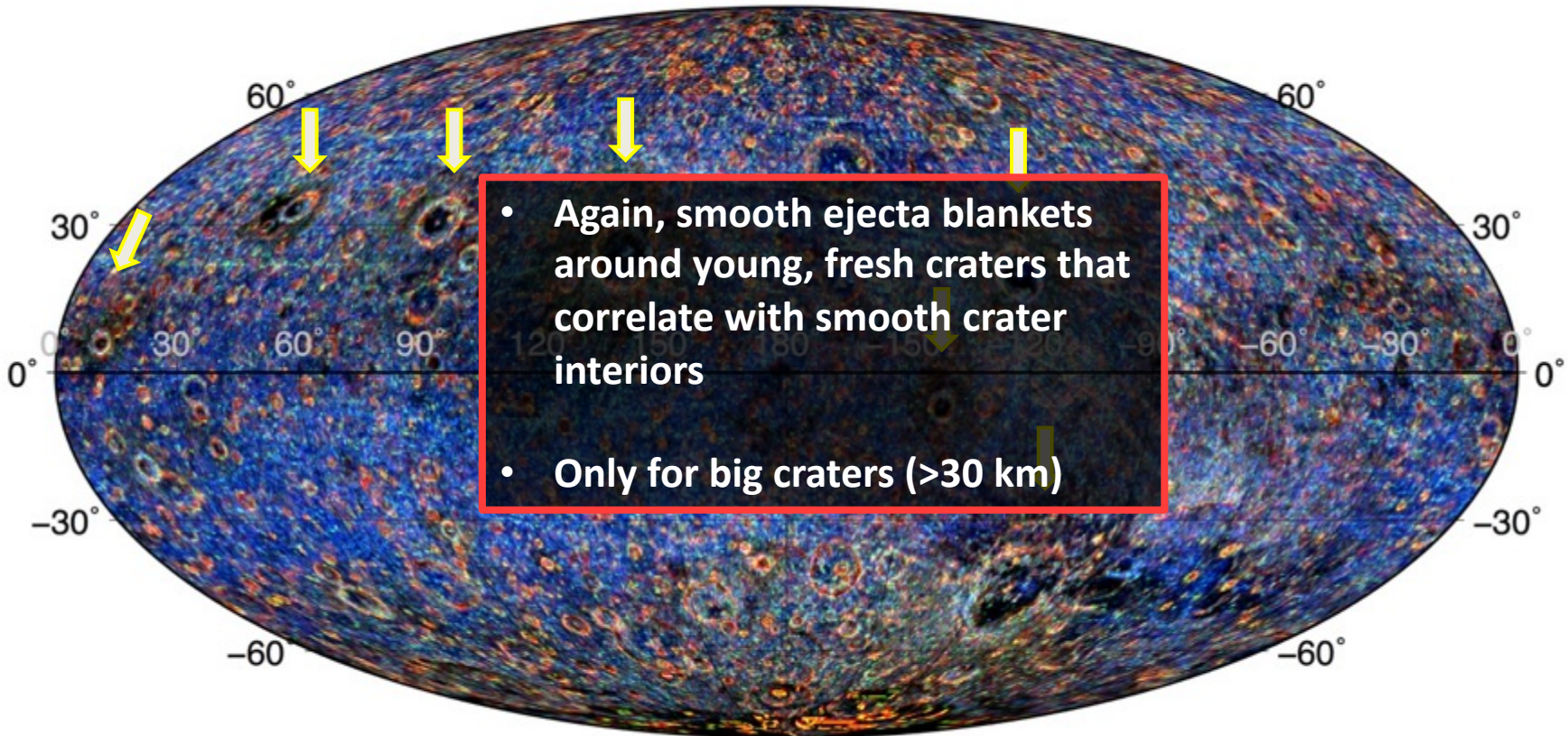


# Smooth ejecta blankets

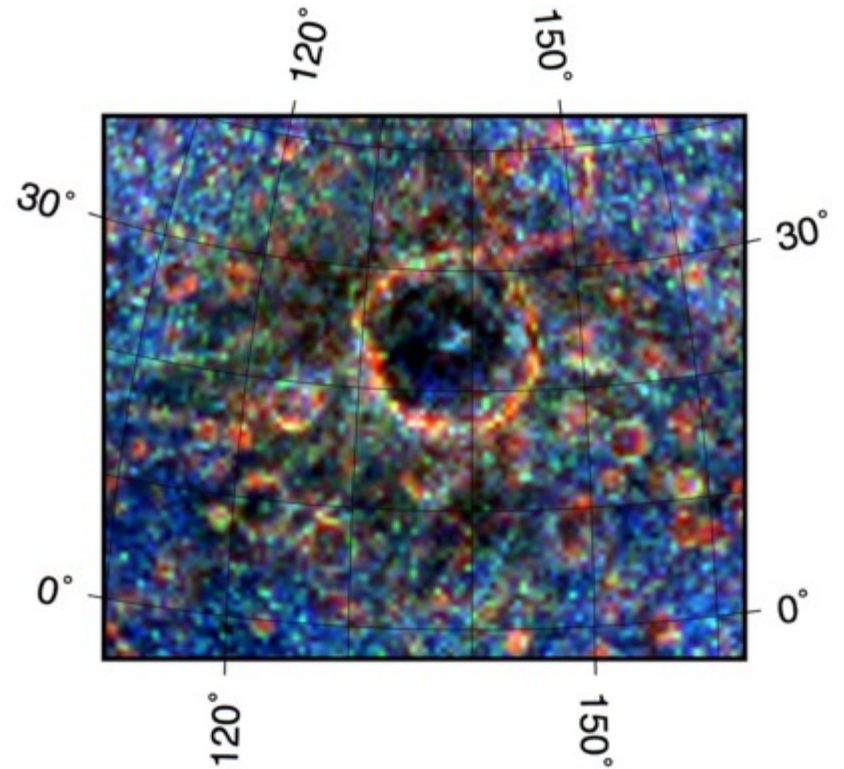
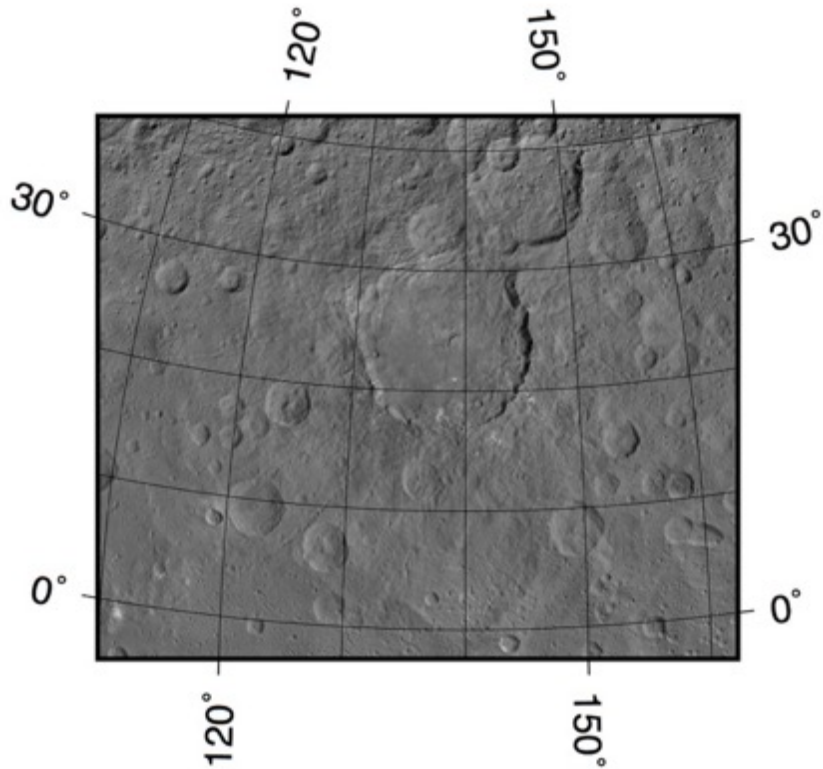
B=1230/574 m

G=3198/1558 m

R=7134/3526 m

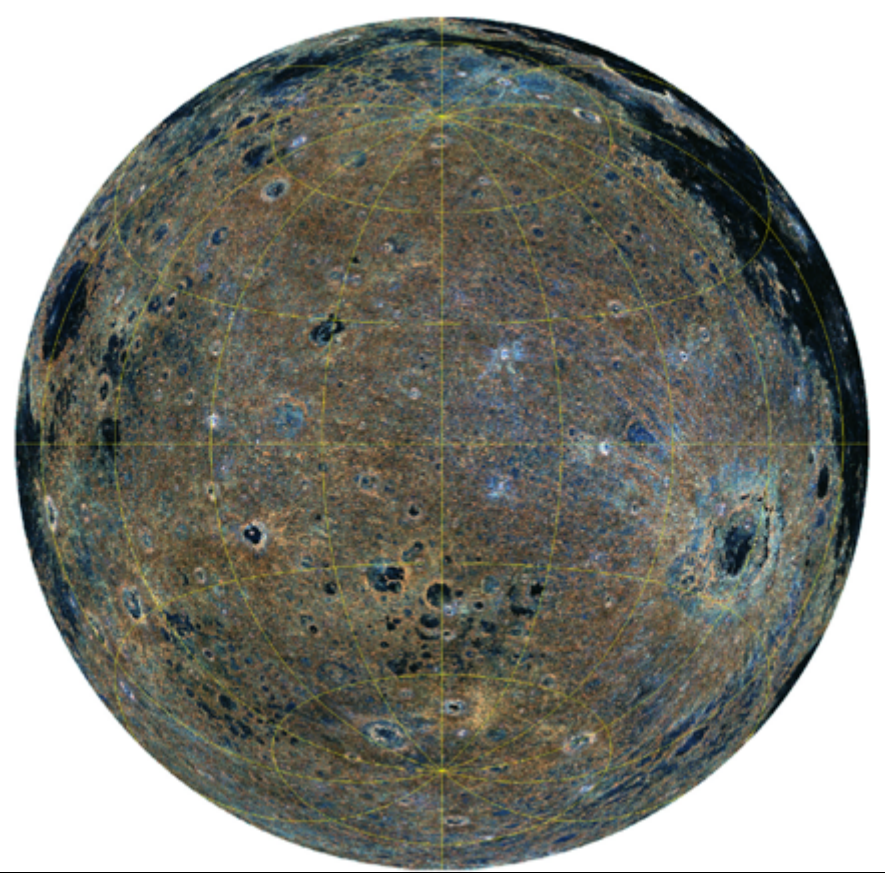
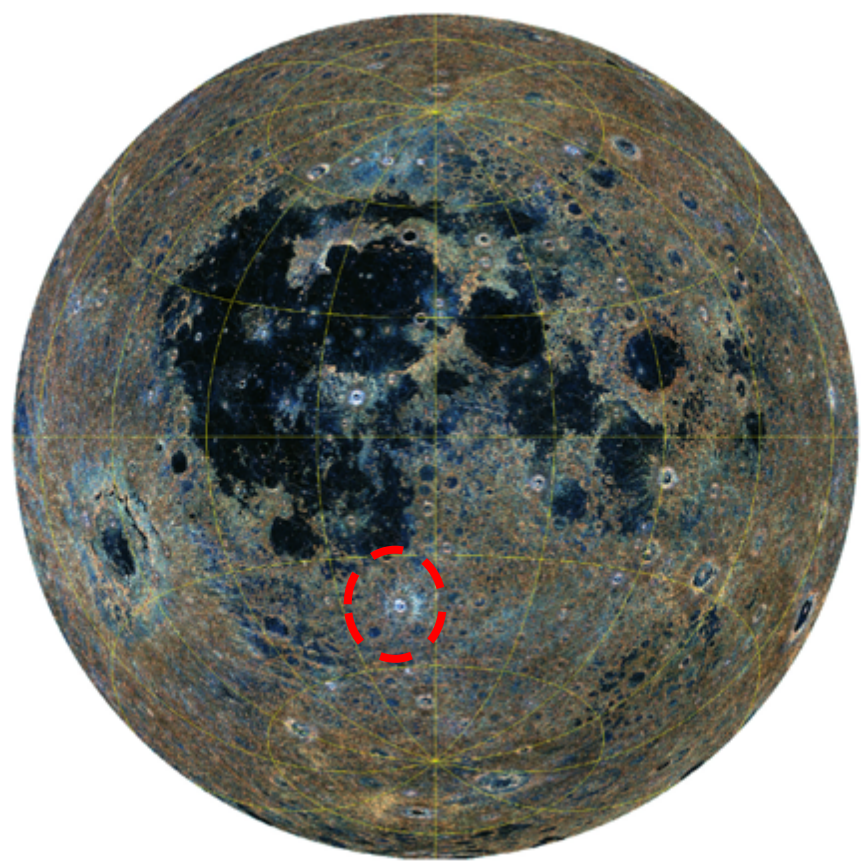


# Smooth ejecta blankets (Dantu)





# Lunar roughness



# Mercury roughness

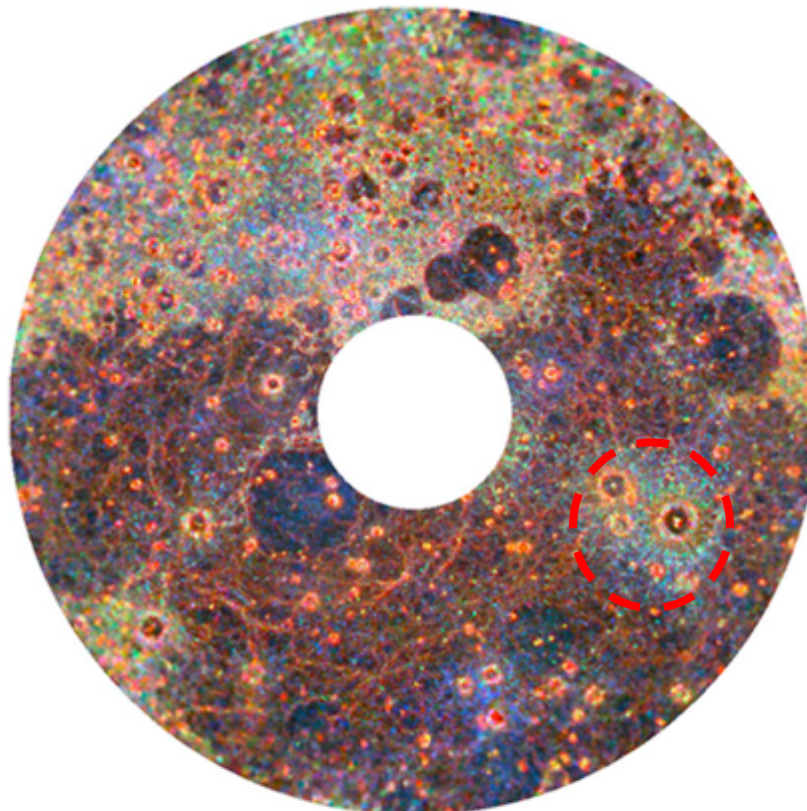


**Figure 3.** Topographic roughness map of the northern circumpolar region of Mercury (Figure 1). Blue, green, and red channels of this color composite represent roughness maps at the three baselines of 0.7 km, 2.8 km, and 11 km, respectively, with a different nonlinear stretch that optimizes visual perception of the map. Brighter shades denote rougher surface.

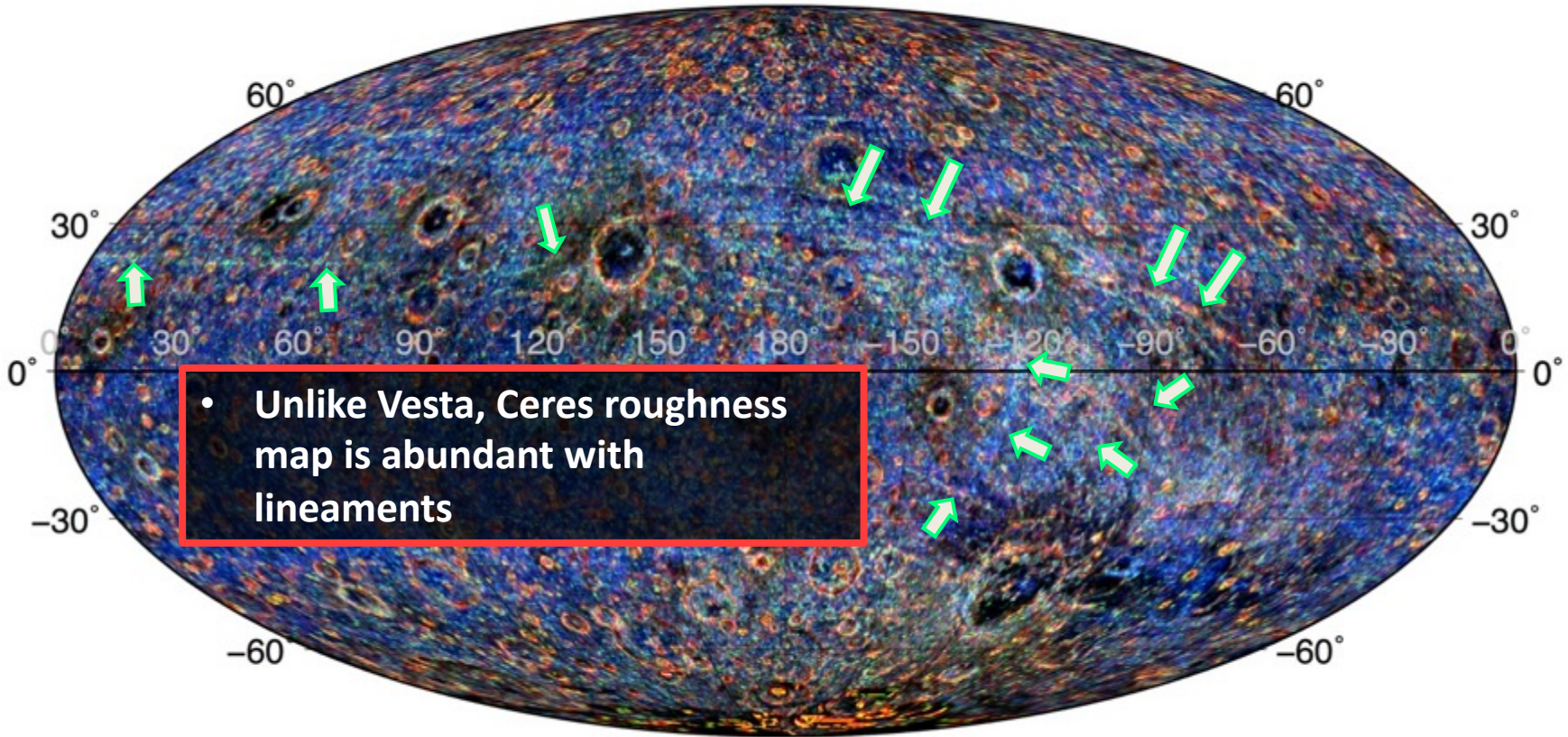


# Lineaments

B=1230/574 m

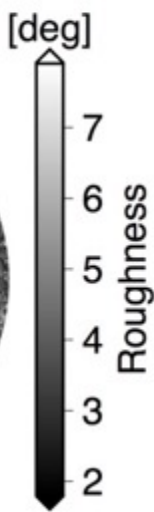
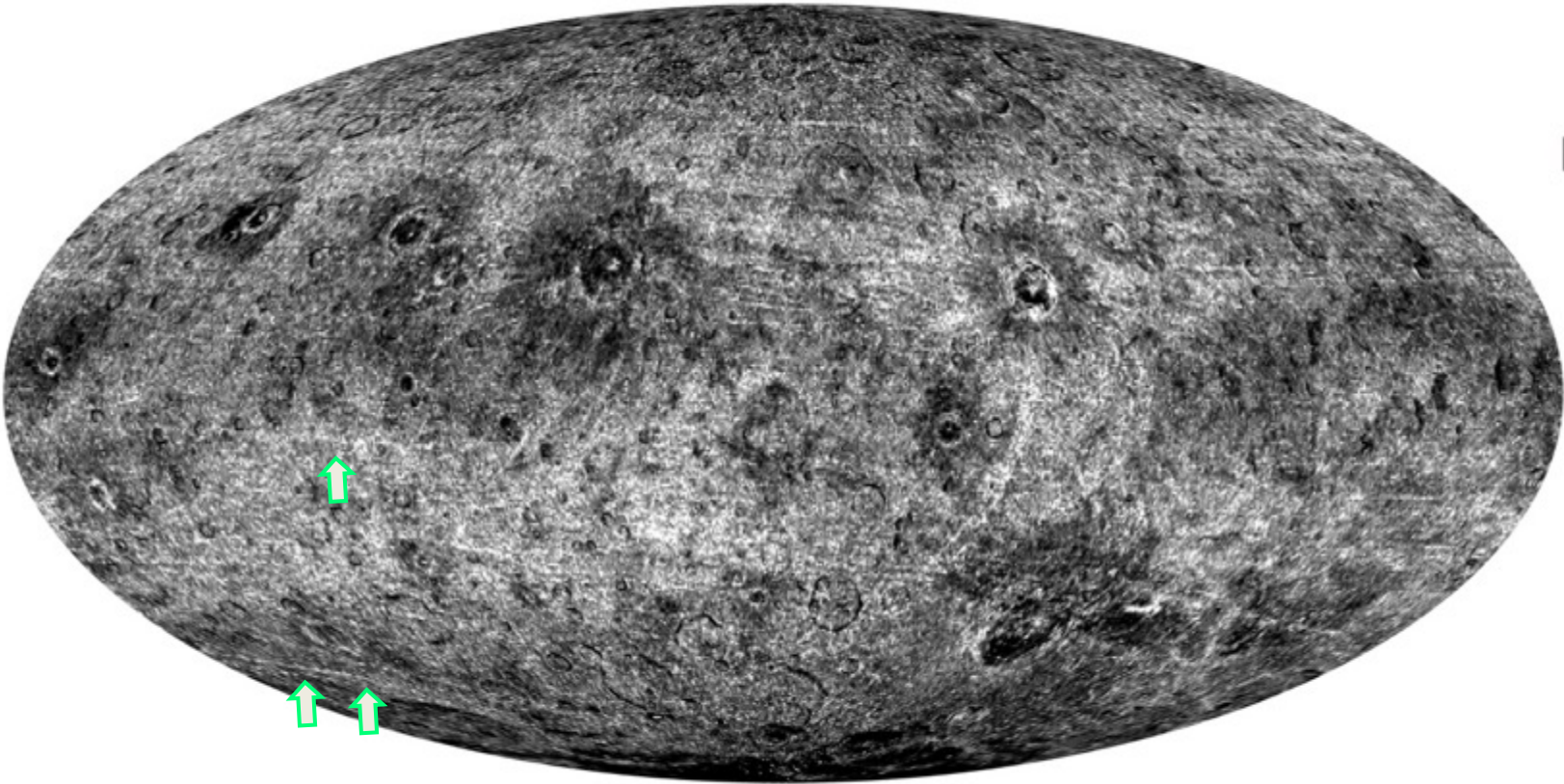
G=3198/1558 m

R=7134/3526 m

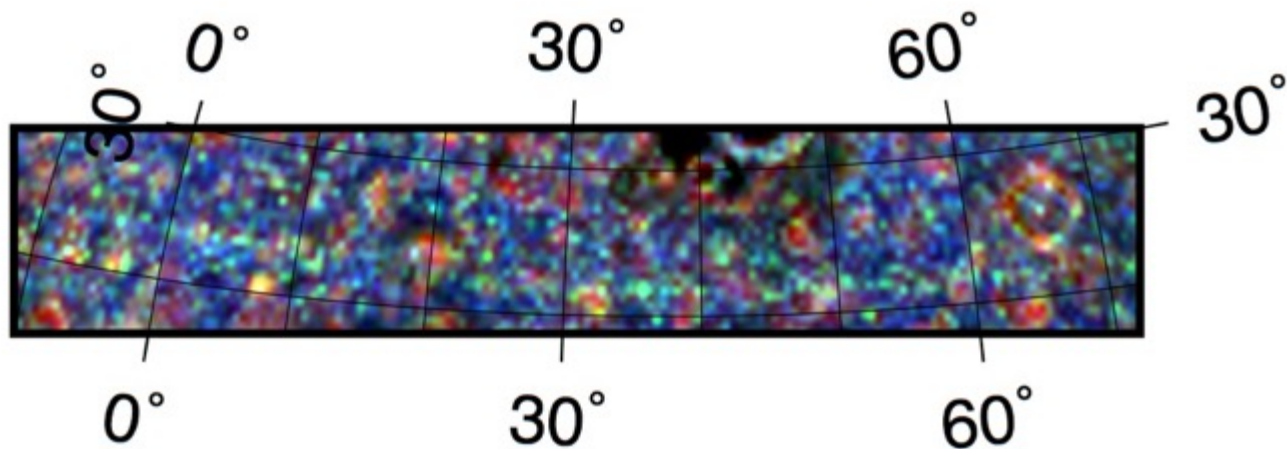
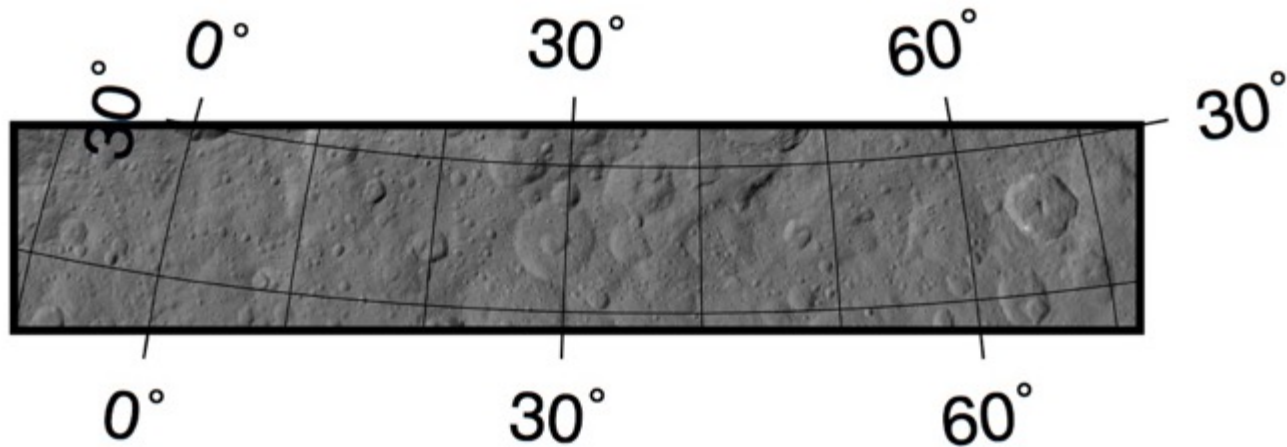




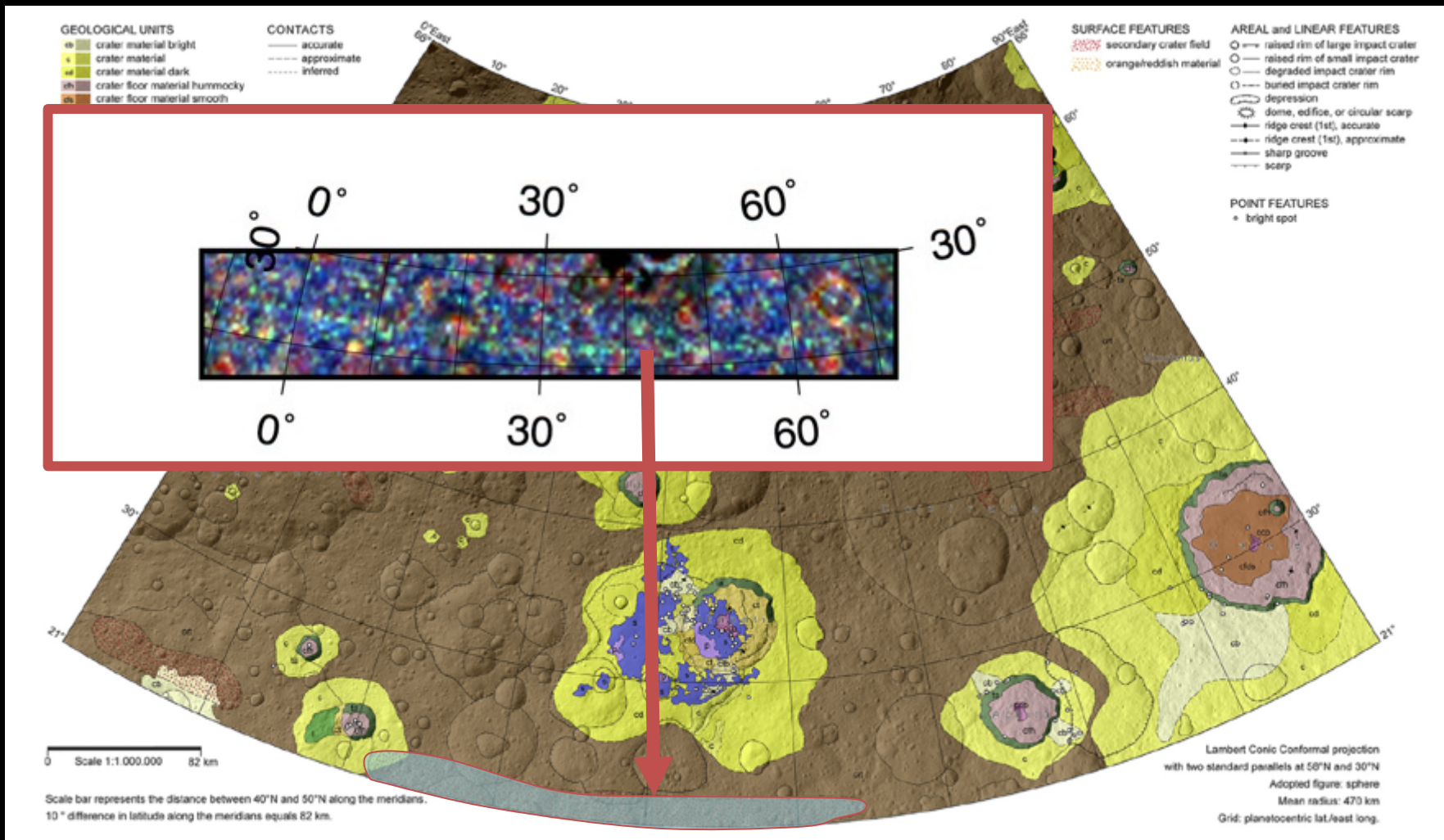
# Lineaments



# Example of a roughness lineament on Ceres



# Example of a roughness lineament on Ceres



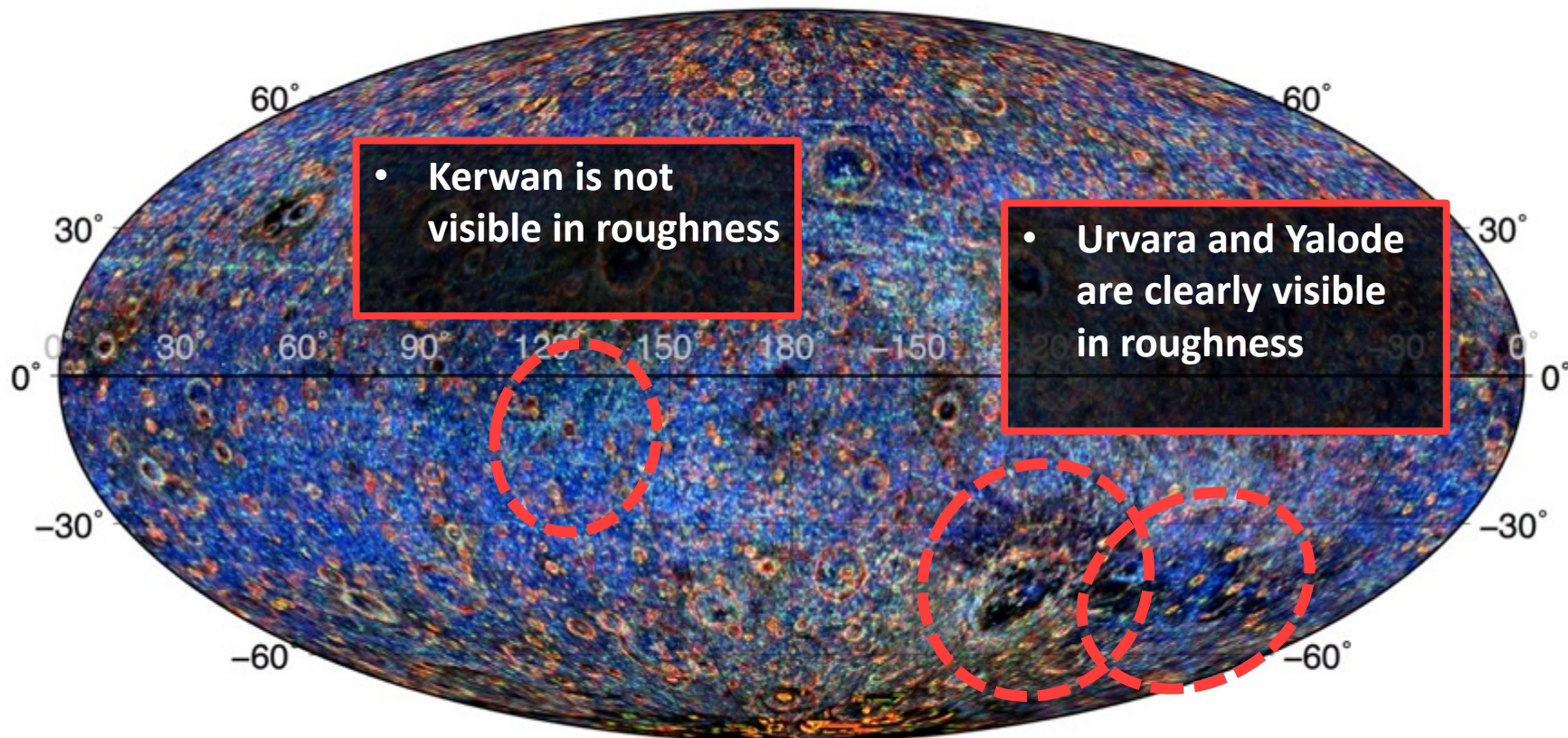


# Large basins

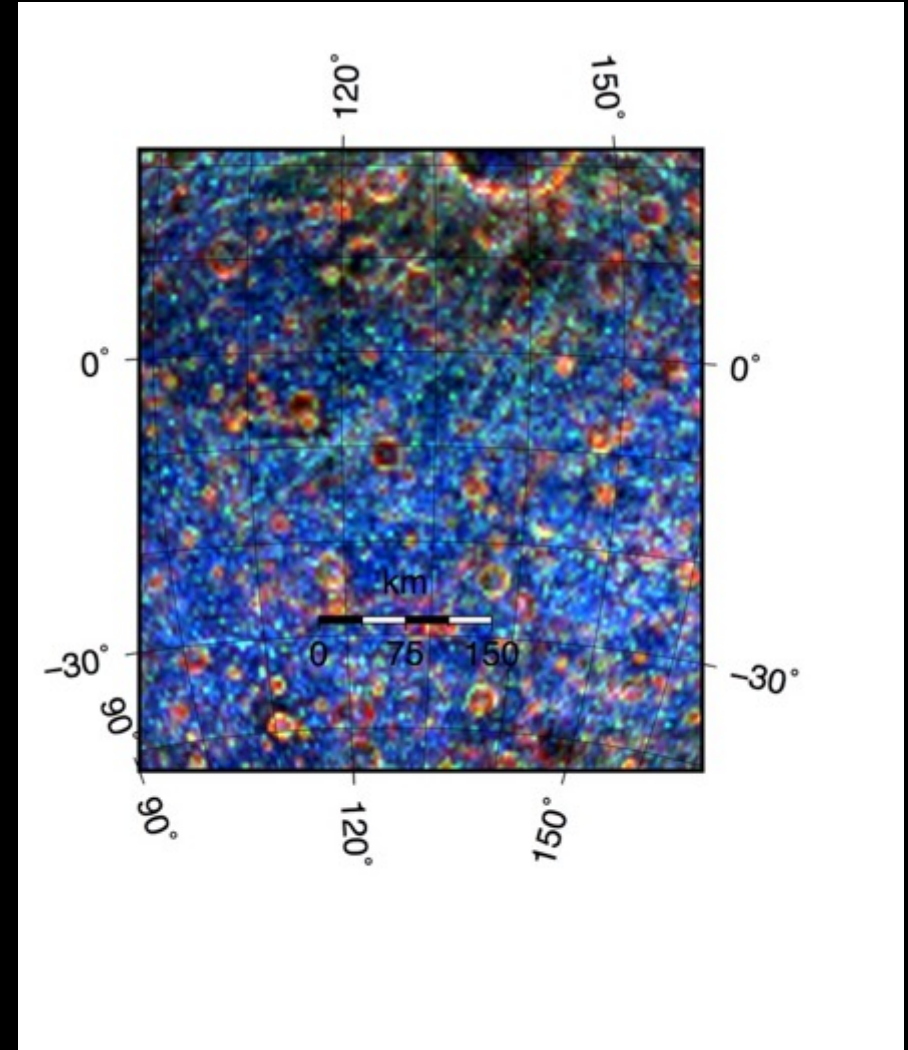
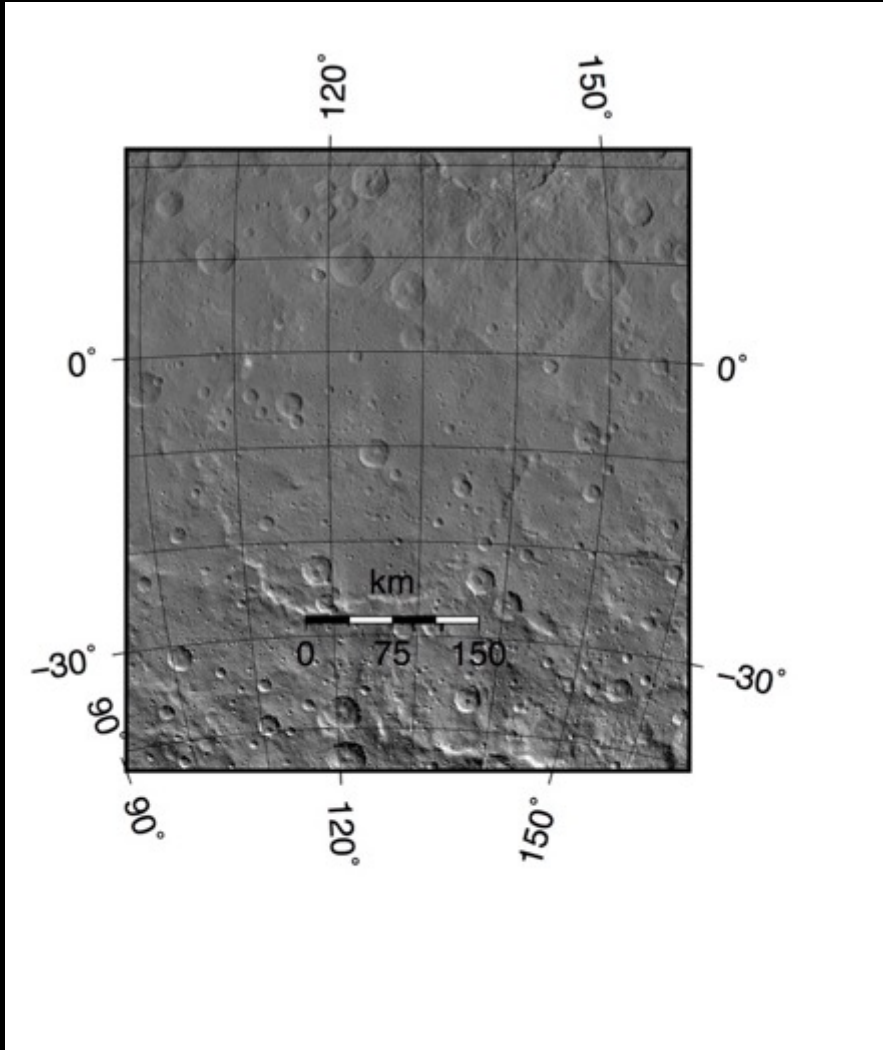
B=1230/574 m

G=3198/1558 m

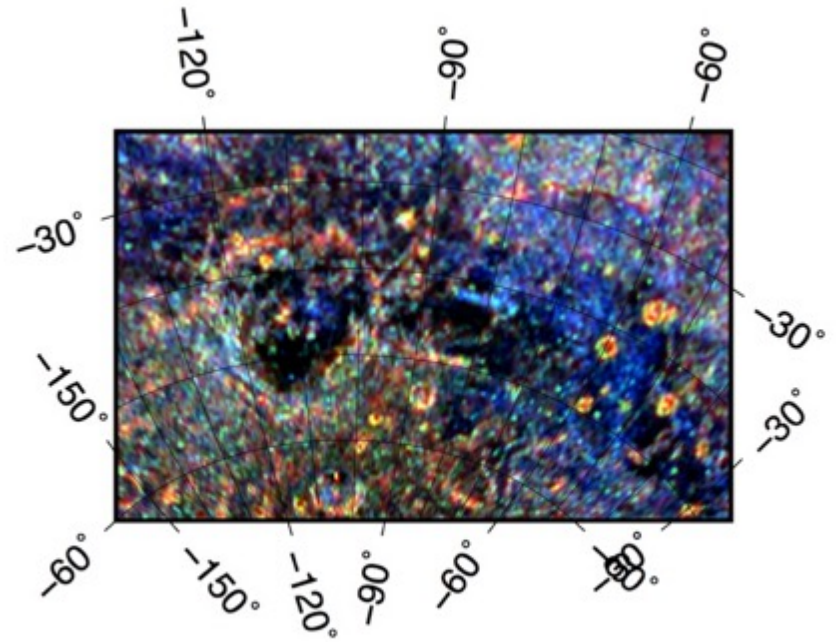
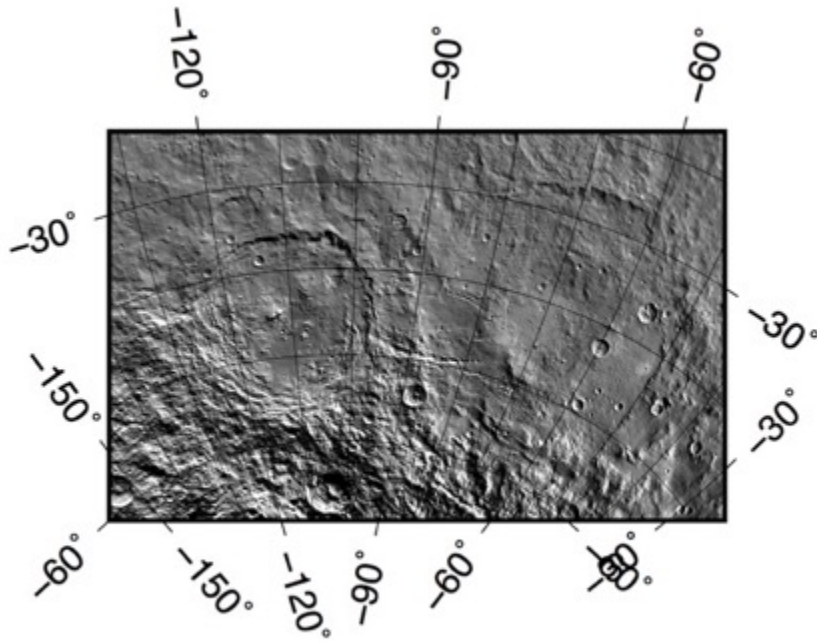
R=7134/3526 m



# Kerwan

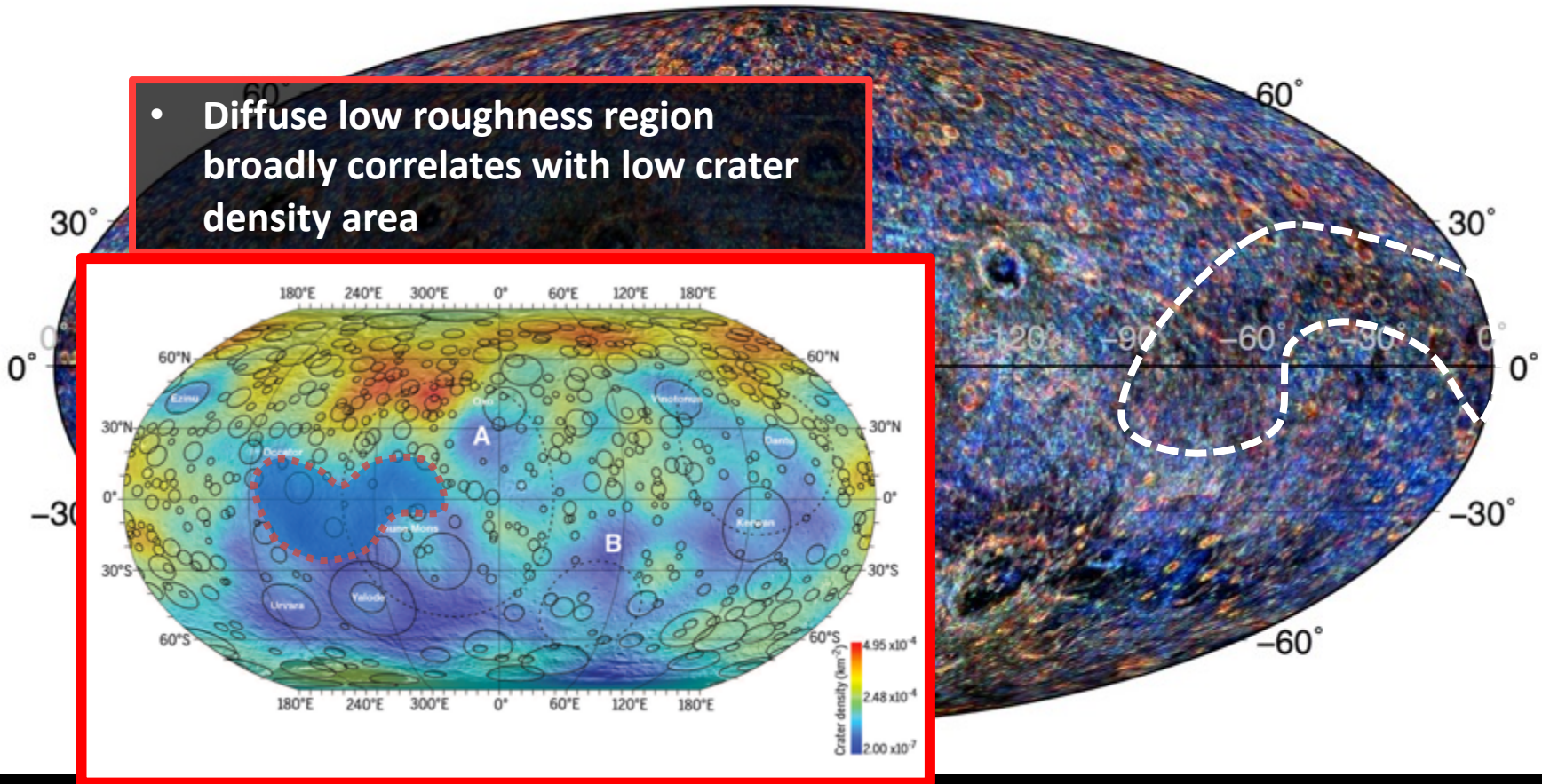


# Urvara and Yalode



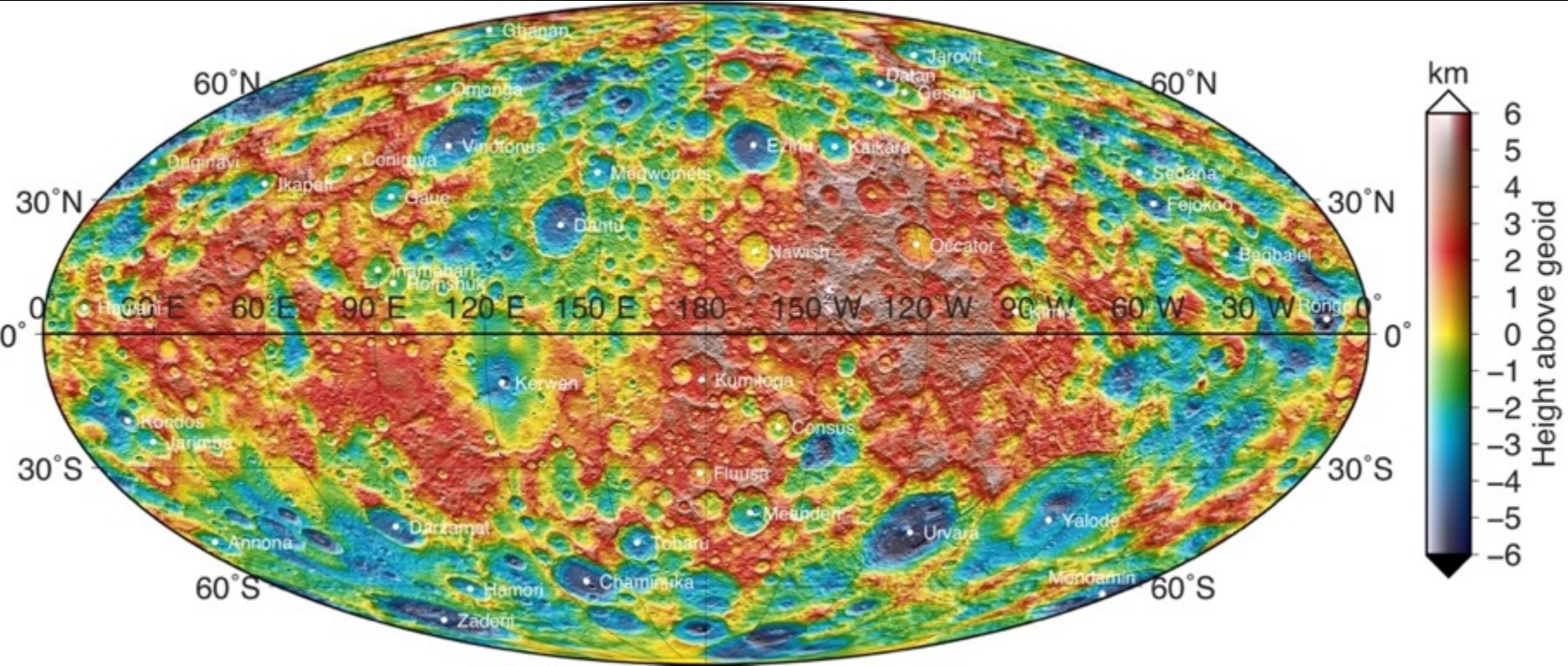
# Diffuse low roughness region

- Diffuse low roughness region broadly correlates with low crater density area

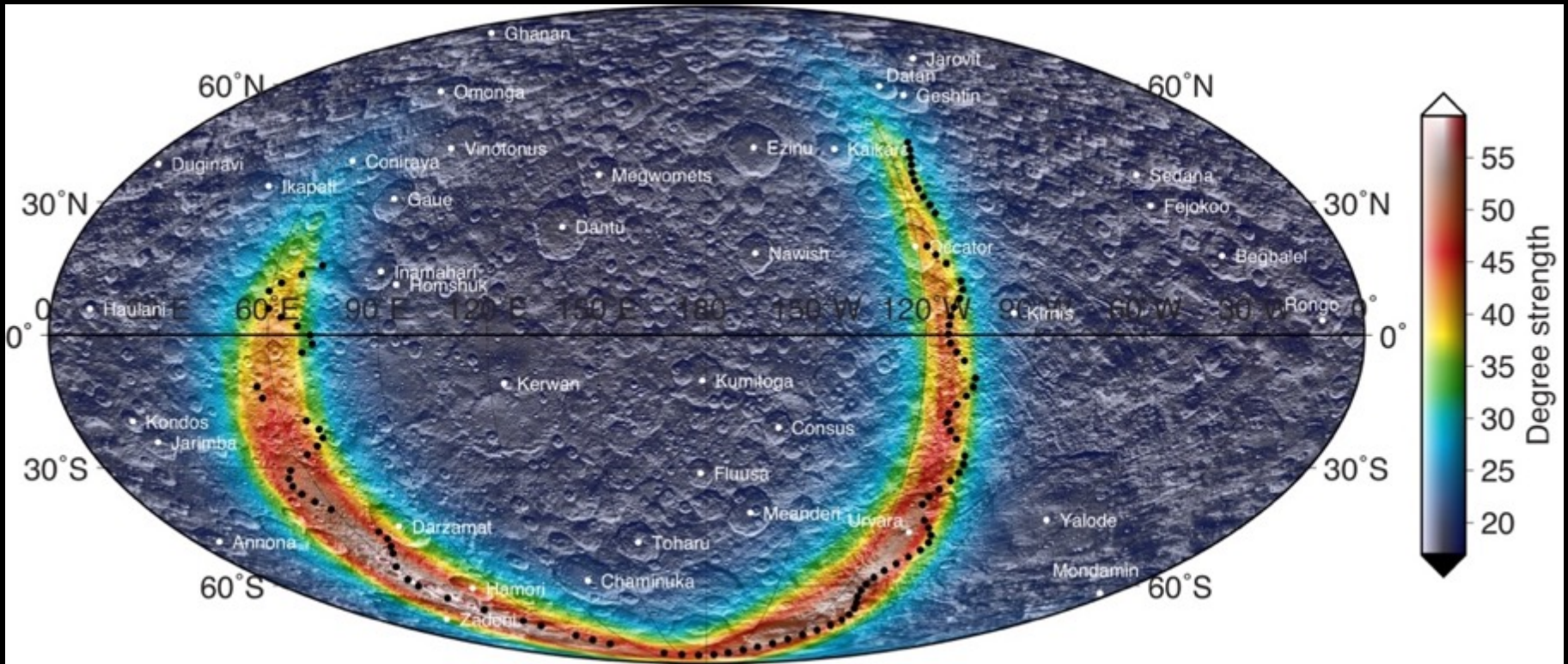


- 
- **Vesta and Ceres may have a higher angle of repose ( $\phi$ ) than Mars and the Moon**
    - $\phi_{\text{Vesta}}=35^\circ$ ;  $\phi_{\text{Ceres}}=34^\circ$ ;  $\phi_{\text{Mars}}=31^\circ$ ;  $\phi_{\text{Moon}}=30^\circ$
    - If interpreted as the dynamic angle of repose, contradicts experiments by Kleinhans et al., 2011
    - Surface gravity? Composition? Particle shape?
  - **Roughness dichotomy on Vesta and only regional scale variations on Ceres**
  - **Smooth ejecta blankets on Vesta and Ceres as opposed to rough ejecta blankets on Moon and Mercury**
  - **Abundant ejecta rays on Ceres and absence thereof on Vesta**
    - Easier to produce topographically-expressed secondaries on Ceres?
    - Could be caused by different surface composition and/or different impact velocity of the secondaries ( $v_{\text{esc,vesta}}=0.36$  km/s,  $v_{\text{esc,ceres}}=0.51$  km/s)
    - Curving ejecta rays due to rotation on Ceres
  - **Produced roughness maps could aid geologic mapping of Vesta and Ceres**

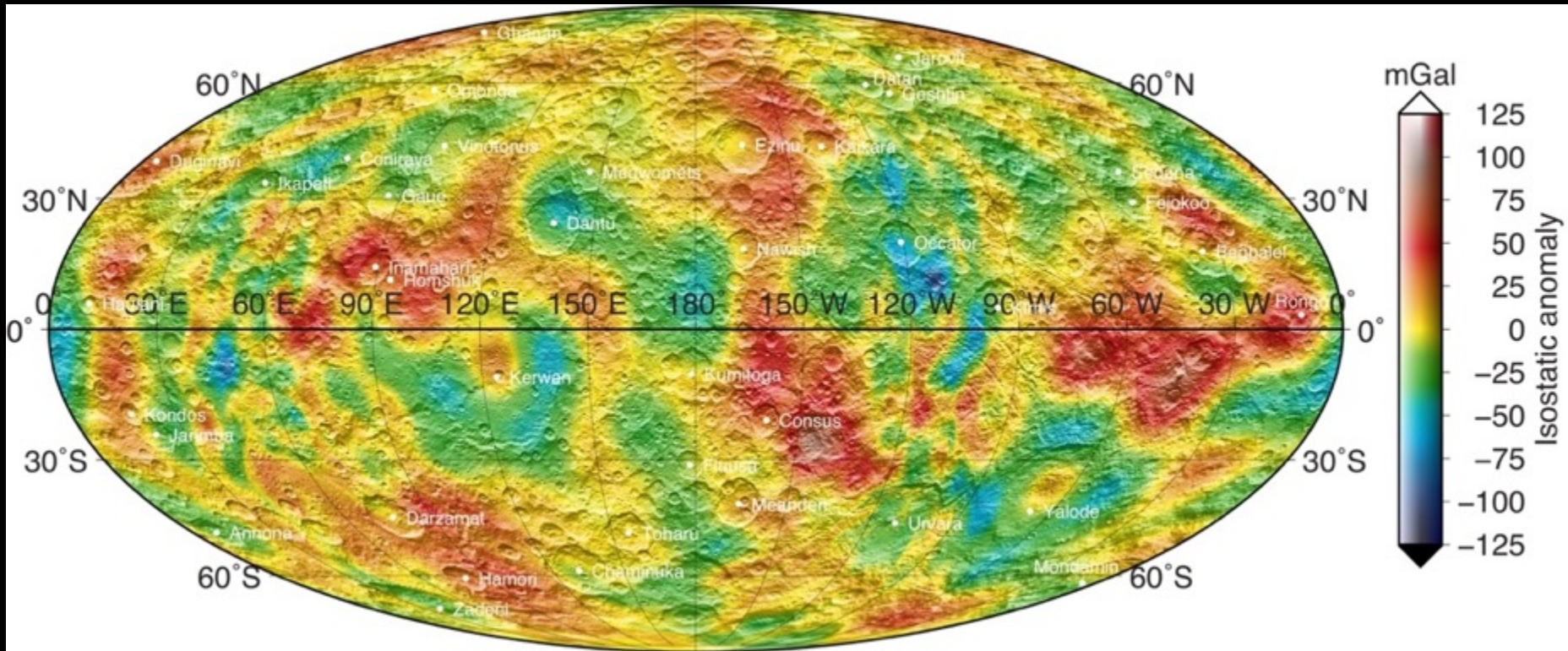
# XM2 results



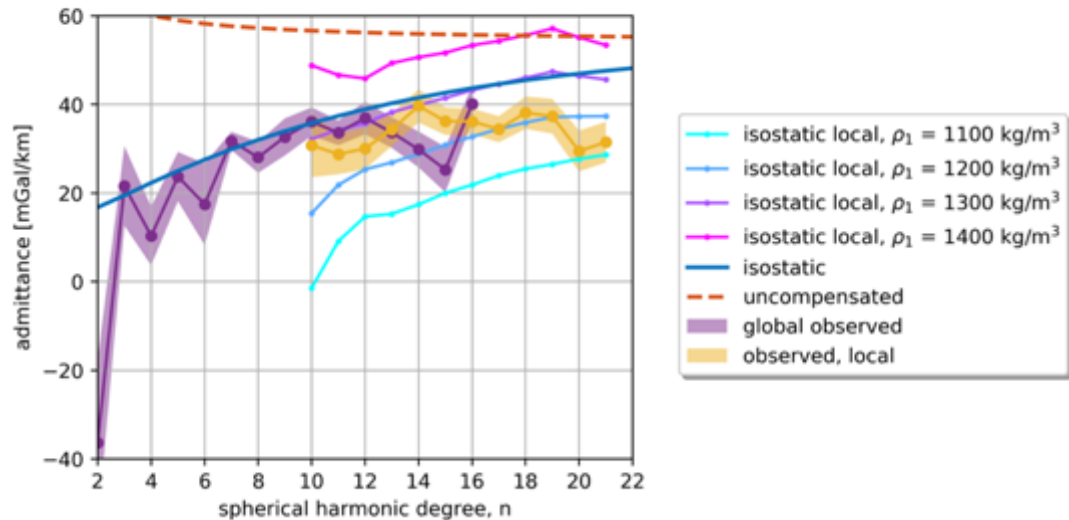
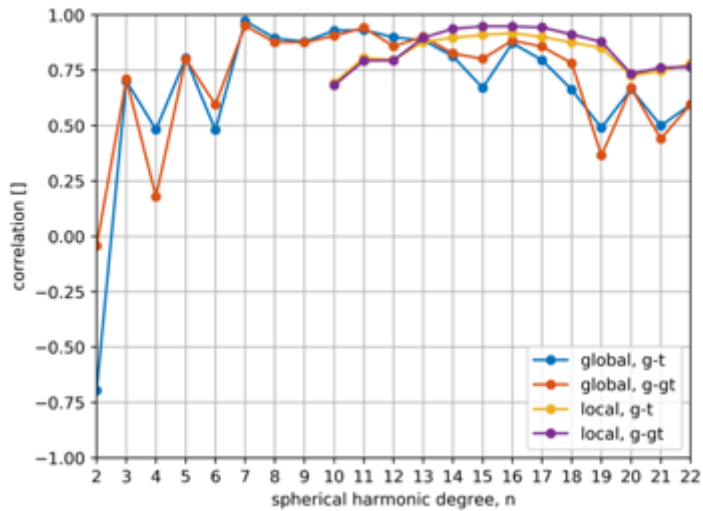
# XM2 results: degree strength



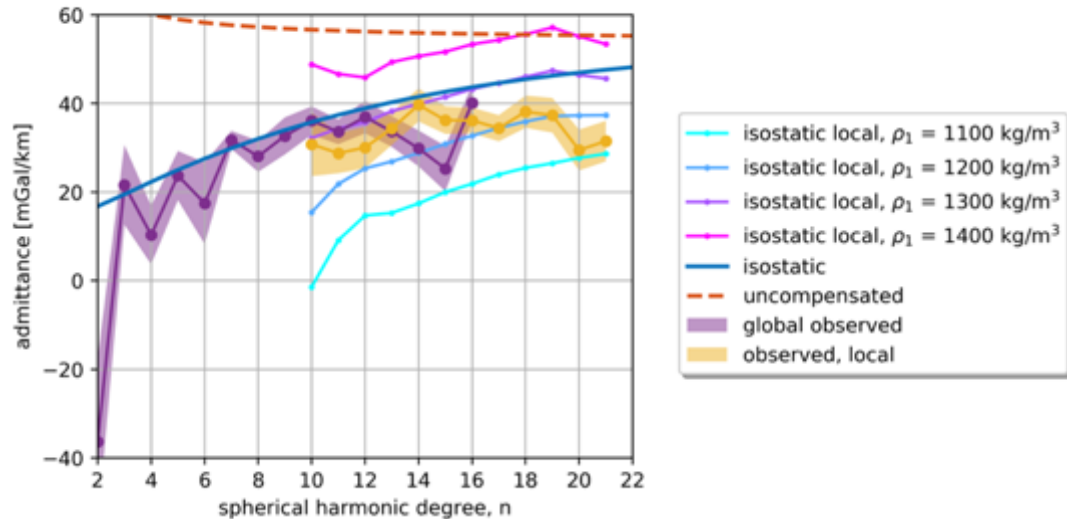
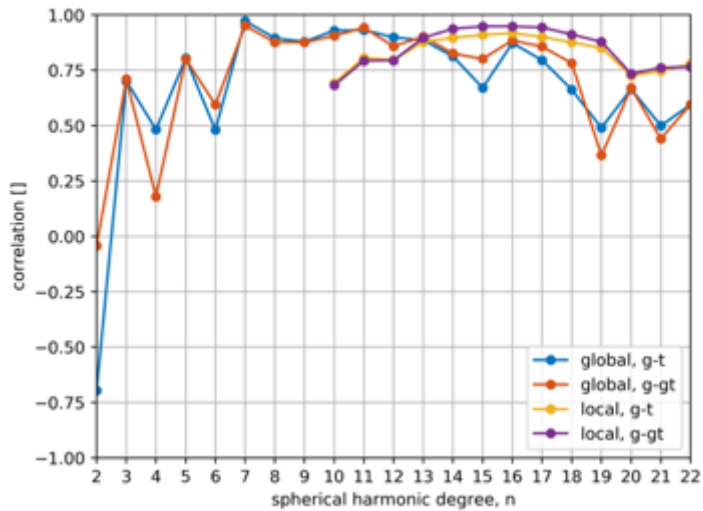
# XM2 results: isostatic anomaly



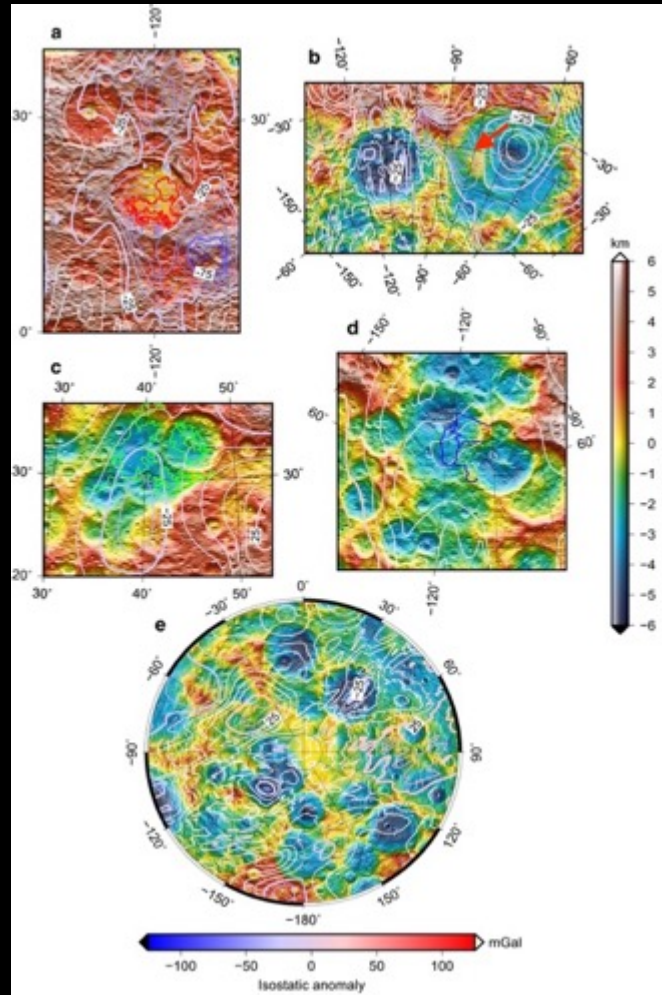
# XM2 results: Correlation and admittance



# XM2 results: Correlation and admittance



# XM2 results: Isostatic anomaly

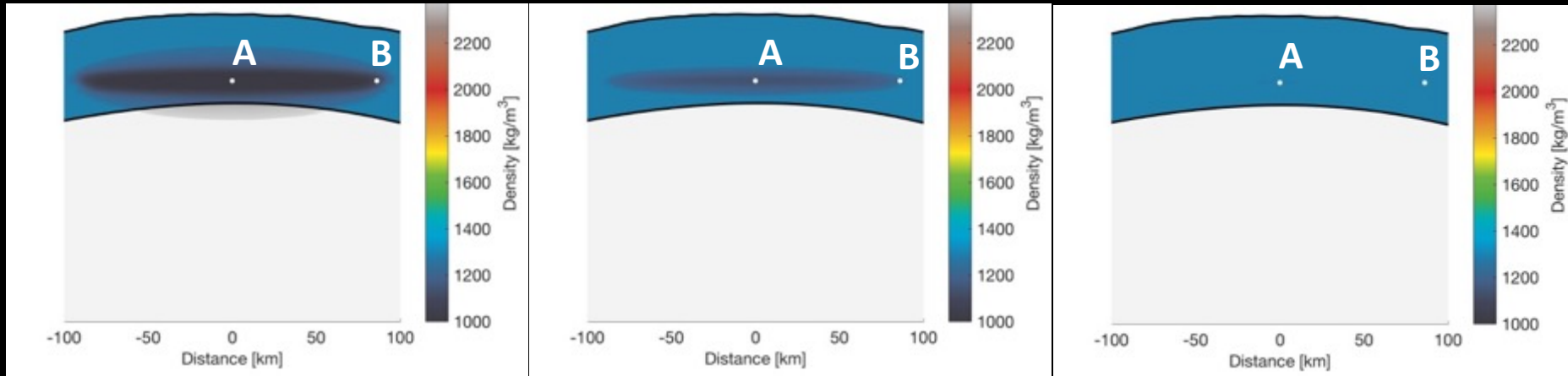


# XM2 results: MCMC inversions Occator

16<sup>th</sup> percentile

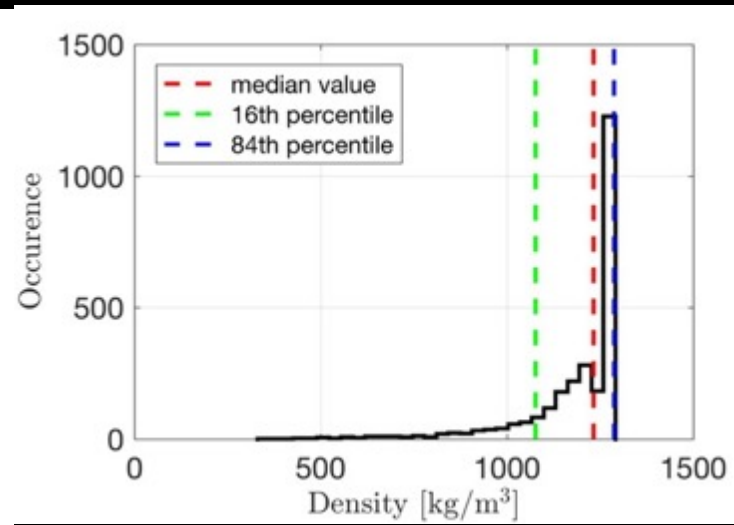
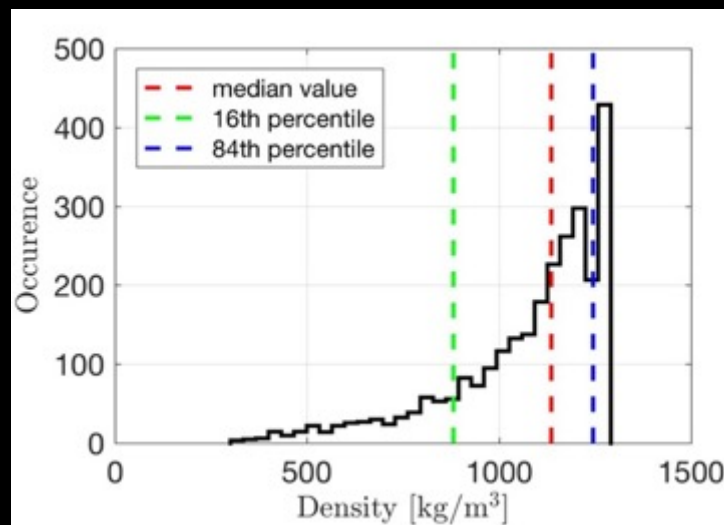
50<sup>th</sup> percentile

84<sup>th</sup> percentile



A

B

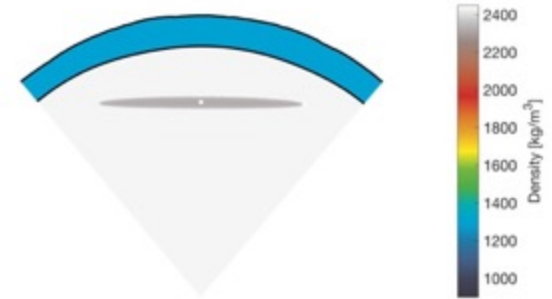
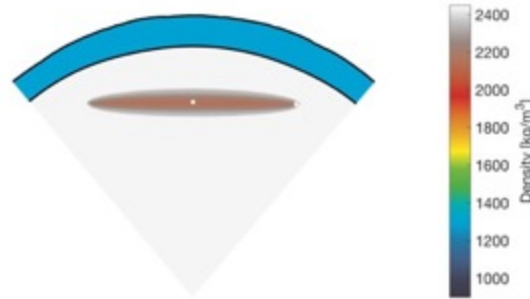
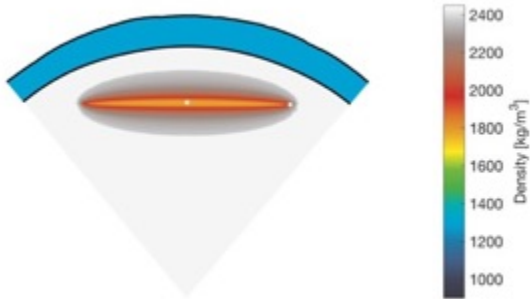


# XM2 results: MCMC inversions Hanami

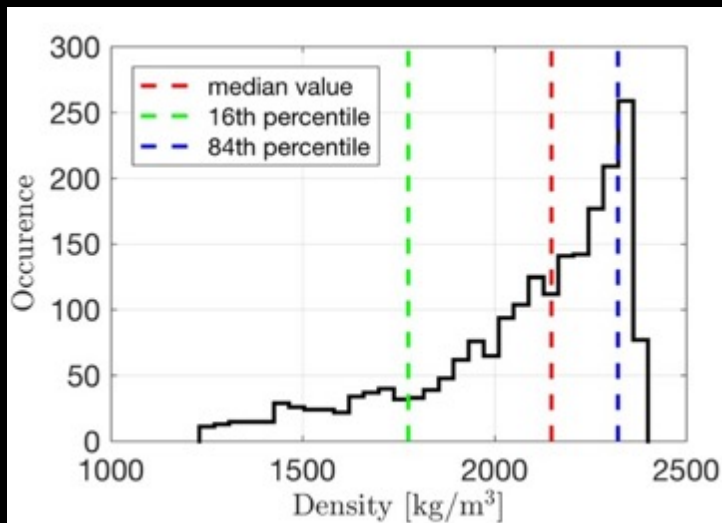
16<sup>th</sup> percentile

50<sup>th</sup> percentile

84<sup>th</sup> percentile



A



B

